Document Front Sheet

nalcor energy
LOWER CHURCHILL PROJECT

NE-LCP Contractor/Supplier

Contract or Purchase Number and Description:	Contractor/Supplier Name: SNC Lavalin
Document Title: CH0008- NORTH SPUR STABILIZATION WORK North Spur Stabilization Works Dynamic Analysis Study	Total Number of Pages Incl. Front Sheet: 150
Contractor Document Number: 505573-3281-4GER-0005	Revision Number: 01
Supplier Document Number:	Revision Number:

NE-LCP Document Number: MFA-SN-CD-2800-GT-RP-0007-01	NE-LCP Issue Number: B2

Approver's Signature:	Date (dd-mmm-yyyy): 11-Dec-2015	Review Class:
Comments:		Equipment Tag or Model Number:

NE-LCP

REVIEW DOES NOT CONSTITUTE APPROVAL OF DESIGN DETAILS, CALCULATIONS, TEST METHODS OR MATERIAL DEVELOPED AND/OR SELECTED BY THE CONTRACTOR, NOR DOES IT RELIEVE THE CONTRACTOR FROM FULL COMPLIANCE WITH CONTRACTUAL OR OTHER OBLIGATIONS.

- [x] 01 – REVIEWED AND ACCEPTED – NO COMMENTS
- [ ] 02 – REVIEWED – INCORPORATE COMMENTS, REVISE AND RESUBMIT
- [ ] 03 – REVIEWED - NOT ACCEPTED
- [ ] 04 – INFORMATION ONLY
- [ ] 05 – NOT REVIEWED

Lead Reviewer:	Date (dd-mmm-yyyy): 14-DEC-2015	Project Manager:	Date (dd-mmm-yyyy): 15-Dec-2015
NE-LCP Management:	Date (dd-mmm-yyyy): 11-Dec-2015		

General Comments:

SNC·LAVALIN

nalcor energy

Lower Churchill Project

ENGINEERING REPORT
North Spur Stabilization Works
Dynamic Analysis Study

SLI Document No. 505573-3281-4GER-0005-01

Nalcor Reference No. MFA-SN-CD-2800-GT-RP-0007-01 Rev. B2

Date: 08-Dec-2015

Prepared by: for.
Denise Leahy
Geotechnical Engineer

Verified by:
Regis Bouchard
Lead Engineer-Geotechnical

Approved by:
Greg Snyder
Engineering Manager

REVISION INDEX

Revision					
N^{o}	By	Verif.	Appr.	Date	Remarks
B2	DL	RB	GS	8-Dec-2015	Re-issued for use.
B1	DL	RB	GS	05-Oct-2015	Issued for use.

NOTICE TO READER

TABLE OF CONTENTS

Page No.

LIST OF FIGURES

LIST OF TABLES

LIST OF APPENDICES

1 CONTEXT OF THE STUDY

Forming part of the Lower Churchill Project (LCP) in Newfoundland and Labrador, Canada, the Muskrat Falls Hydroelectric Development is located on the Churchill River, about 291 km downstream of the Churchill Falls Hydroelectric Development which was developed in the early 1970's. The installed capacity of the Muskrat Falls facility will be 824 MW (4 units of 206 MW each).

The North Spur is a deposit of marine and estuarine sediments which naturally provides a partial closure of the Churchill River valley at the Muskrat Falls site. This natural closure is one of the economically attractive features of this site and needs to be maintained for the life of the project.

The North Spur is about one kilometre long between the rock knoll in the south and the Kettle Lakes in the north which represent natural boundaries to the North Spur, in terms of both seepage and stability (Figure 1-1).

The early studies for the Muskrat Falls site recognized the importance of the North Spur as part of the reservoir retention works. A major slide on the downstream face of the Spur, in November 1978 (Figure 1-1), revealed the fragility of this natural deposit and its susceptibility to toe erosion and ice accumulation in the bay downstream. Maintaining the integrity of the Spur is fundamental to the viability of the project and this fact has been understood from the outset.

The raising of the headpond and the change in the downstream flow regime for the Muskrat Falls hydro-electric project could adversely affect the stability and integrity of the North Spur. Stabilization works to address this have been considered from 1965 to date and the design has been modified and adapted over the decades to arrive at the current 2015 design.

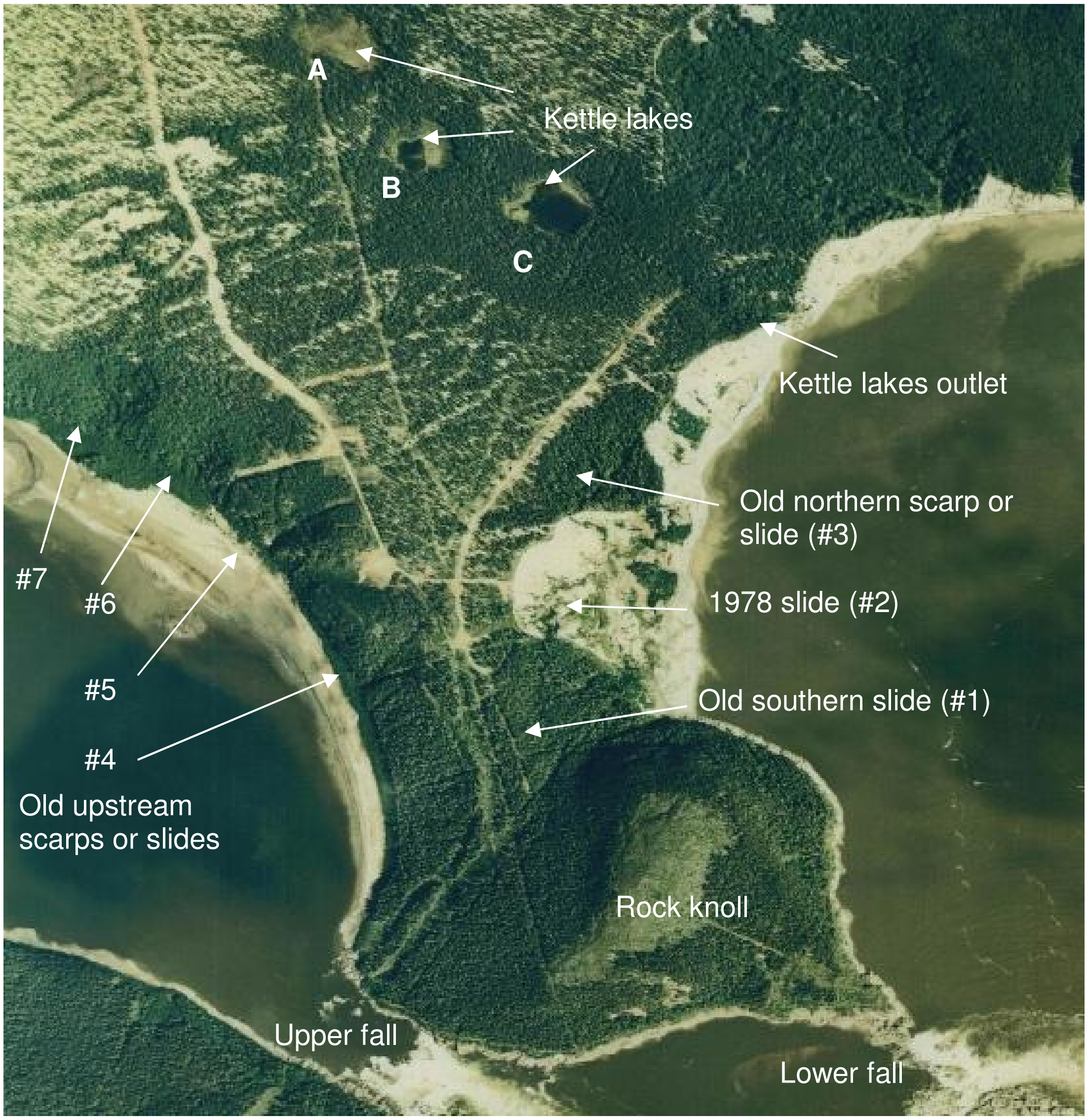

Figure 1-1: Aerial photo of the North Spur (1988)

1.1 PRELIMINARY DYNAMIC STUDY

As part of the engineering design, a one-dimensional dynamic analysis was performed to assess the stability of the Spur in case of an earthquake. Based on this preliminary analysis, there was no issue for this aspect. However, an external review performed on the entire project recommended, apart from the dynamic analysis already performed, that the project should perform a detailed analysis to examine the impact of topographic effects and assess cyclic strains. A workshop with external international experts Prof. Serge Leroueil and Prof. I.M. Idriss was held in December 2013. Their main recommendations are presented below.

1.2 RECOMMENDATIONS BY PROF. SERGE LEROUEIL

Based on the stability analyses presented, Prof. Leroueil noted that the factor of safety of about 1.0 for the existing slopes confirms the validity of the strength parameters used, and that all the stabilized slopes seem to have a satisfactory factor of safety, as recommended by CDA (2013) Guidelines. Based on the investigation reports of the North Spur (in particular SNC-Lavalin NL, 1980), Prof. Leroueil made the following remarks:

- *Salinity of the pore water is above 5 g/l at elevations lower than 5 m. Above 5 m, salinity slightly increases with depth from 0 g/l at an elevation of 45 m to about 1 g/l at the elevation + 5 m.*
- *This change in salinity is reflected in both the plasticity index and the liquidity index. Below an elevation of about 12 m, the plasticity index is about 15% on average and the liquidity index is less than 1.0. Above the elevation 12 m, the plasticity index is smaller, between 7 and 12%, and the liquidity index is greater, generally between 1.0 and 2.2.*
- *From the grain size distributions performed, none of them shows clean silt. Also, there are no measured plasticity index values less than 5 or 7%.*

1.3 RECOMMENDATIONS BY PROF. I.M. IDRISS

Based on the presentations made during the workshop and on the review of analyses performed to assess the liquefaction potential of cohesionless layers and the cyclic softening of the upper sensitive clays, Prof. Idriss made the following recommendations:

- *Ask Dr. Atkinson to conduct a deaggregation of the results for the 10,000-year return period to obtain values of magnitude M, distance R and at a number of periods, e.g., T = 0.01, 0.05, 0.2, and 1 sec.*
- *Ask Dr. Atkinson to provide an estimate for the range of effective duration for the M and R scenario events that she would get from deaggregating the results of the probabilistic seismic hazard analysis (PSHA).*
- *Re-examine all the previously selected seed time histories and possibly replace some of them, as appropriate*
- *Reconstruct the modified time histories using a program that includes a base-line correction*
- *Repeat site-response calculations*
- *Repeat the evaluation of the potential for triggering liquefaction in the sand layers*
- *Complete the documentation of the strength of the Upper Sensitive Clay*
- *Repeat the examination of the potential for cyclic softening*
- *In addition, once a final (or near-final) design is established for the North Spur, a dynamic nonlinear analysis should be conducted to assess the pattern of deformations that may be induced by the postulated earthquake ground motions. The computer program FLAC is probably the most useful to use for this purpose. It is critical, however, that the appropriate shear strength parameters for each critical soil layer be properly established and properly constructed input time histories are used.*

1.4 SCOPE OF THE COMPLEMENTARY DYNAMIC STUDY

Based on Prof. Idriss recommendations and taking into account Prof. Leroueil remarks, a complementary dynamic study was conducted to assess the dynamic stability of the North Spur in the long term, after the implementation of the recommended stabilization measures and after reservoir impoundment. This study can be divided into 6 parts:

1. Selection of the most critical site (Section 2)
2. Revision of the seismic hazard analysis and selection of an updated Design Response Spectrum (Section 3)
3. Updated selection of representative input motions (Section 4)
4. 1D equivalent-linear dynamic response analyses for uphill and downhill vertical soil profiles (Section 5.3)
5. 2D equivalent-linear dynamic response analyses for a cross-section representative of the most critical site conditions (Section 5.4)
6. 2D non-linear dynamic response analyses for a cross-section representative of the most critical site conditions (Section 5.5).

2 MOST CRITICAL SITE CONDITIONS

2.1 SITE DESCRIPTION

The Muskrat Falls site is located on the Churchill River, about 30 km upstream from Happy Valley-Goose Bay in Labrador. The two falls, about 1 km apart, cause a drop of about 14 m in the Churchill River water level from 17 m at the upstream side to 3 m at the downstream side of the falls. A rock knoll with a top elevation of 142 m is located at the North side of the falls and is connected to the left bank (north) of the river by a spur of land which is referred to as the “North Spur”.

The Churchill River actually flows in a bedrock channel south of the rock knoll. Past continental glaciations followed by marine, glacial and fluvio-glacial deposition formed the overburden in the Muskrat Falls area.

Detailed topographical, geological and geotechnical information based on past investigation was presented in SLI (2015a). The location of the boreholes and in situ tests and the main stratigraphic interpretation are indicated on the drawings of Appendix A:

- MFA-SN-CD-2800-GT-PL-0012-01: Plan View
- MFA-SN-CD-2800-GT-SE-0004-01 to -03 : Sections

2.2 STRATIGRAPHIC CONDITIONS

The geological conditions including the stratigraphy and material properties of different layers of overburden, the ground water regime within the North Spur, and the effects of existing dewatering system were reviewed in SLI (2015a) design report. The main stratigraphic information is summarized below.

After de-glaciations, the Churchill River valley was submerged as far upstream as the Gull Island. Marine sediments deposited in the Muskrat Falls region constituted the marine clay and silty sand layers. Following gradual recession of the sea, superficial fine sand layers, that likely represent former estuarine sand beaches, were deposited on top of the marine sediments.

The stratigraphy of the overburden layers, from ground surface to bedrock level, was interpreted based on available data from geotechnical investigation campaigns. Continuous logs obtained from CPTs and sonic drillings during the 2013 investigations along with conventional boreholes drilled during various investigations provided more information on the stratified nature of the soil. Different correlations between tests and physical properties were used to interpret the stratrigraphy of the North Spur and comprehensive stratigraphic cross sections of the North Spur were prepared and are presented in the design report (SLI, 2015a).

Based on this information and as illustrated on Figure 2-1, four distinct sedimentary units have been identified in and underlying the Spur:

1. Upper Sand, generally from the crest of the Spur down to about elevation 45 m to 50 m;
2. Stratified Drift, including two major deposits of silty sand/sandy silt and silty clay materials, generally from elevation 45 m to 50 m to elevation 5 m to 15 m;
3. Lower Marine Clay, generally from elevation 5 m to 15 m to elevation -70 m;
4. Lower Aquifer, consisting of glacial sand, gravel and boulder infill of the preglacial valley, generally bellow elevation -70 m to bedrock.

The description of the different layers is reported below. Stratigraphy is heterogeneous on the North Spur and can change locally.

2.2.1 UPPER SAND LAYER

The upper sand layer covers the surface on the North Spur generally from elevation 60 m to 45 m. This layer mainly consists of compact to very dense, grey fine to medium sand with low fines content.

Grain size analyses on the samples recovered from this layer resulted in a range of fines content (percent passing sieve # 200 or 0.075 mm) from 1 to 9 percent, except for some samples from a thin layer of silty sand/sandy silt, within the upper sand layer, which had higher fines contents.

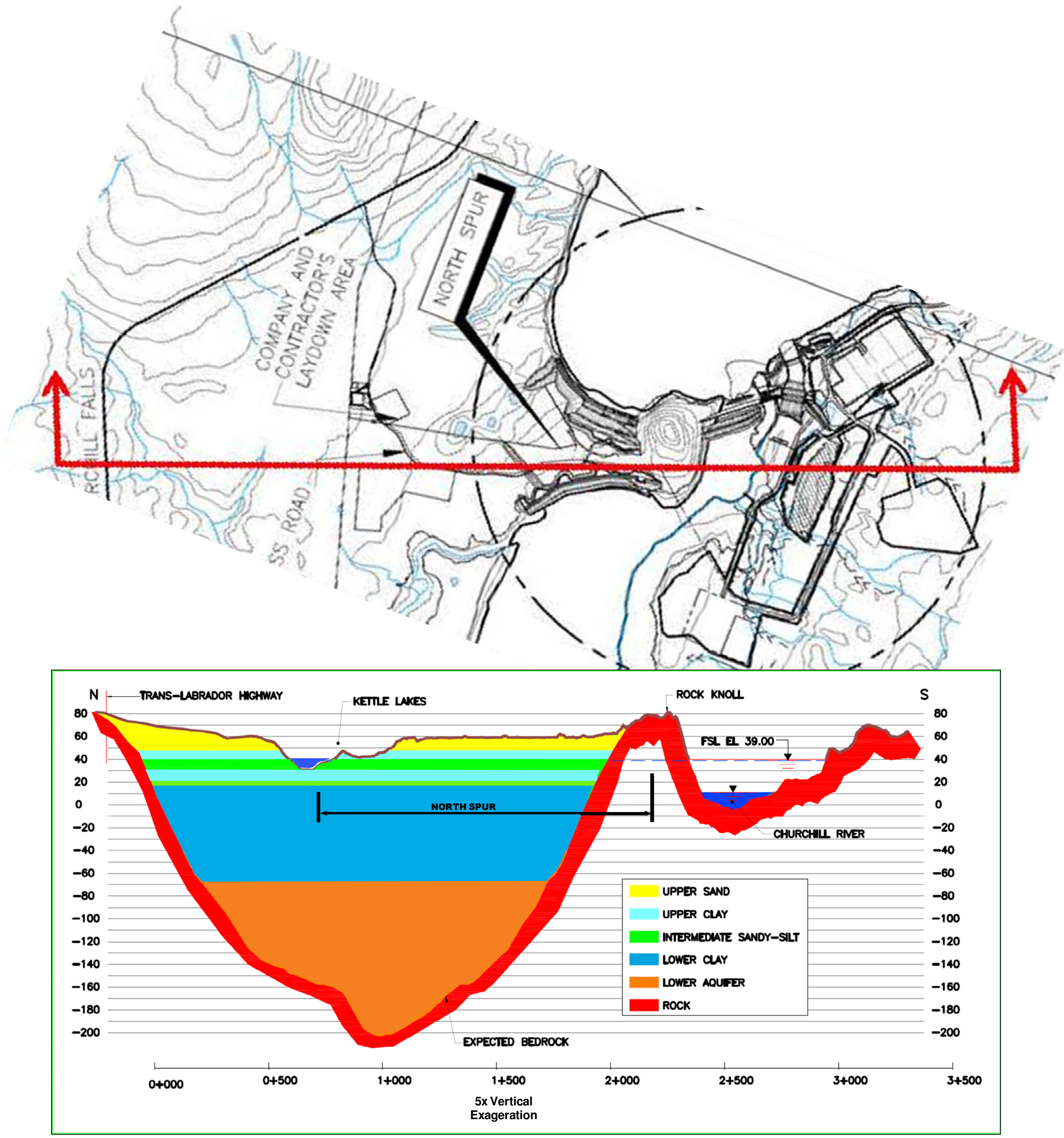

Figure 2-1 : North Spur Schematic Stratigraphy for North-South Cross-Section

The standard penetration tests (SPT) carried out in this layer resulted in N values varying from 12 to more than 100 with an average value of 44. The compacity of this sand layer can be qualified as a compact to very dense.

This layer is mostly dry and well drained except for a perched water table observed at the contact between upper sand layer and the more impervious clayey silt underlying layer. No permeability tests were performed in this layer. Using grain size distribution curves and empirical relationships, a value of 1×10^{-4} m/s was estimated as the hydraulic conductivity for this layer.

2.2.2 STRATIFIED DRIFT

The stratified drift is a heterogeneous mix of clays, silts and sands with sub-horizontal layering from the marine and estuarine deposition. It has been observed approximately from elevation 45 m to 15 m. This unit consists of alternating layers of silty clay of low to medium plasticity which is referred to as “upper silty clay”, and silty sand and occasional cleaner sand seams which is called “intermediate silty sand”.

2.2.2.1 Upper Silty Clay Layer

A low to medium plastic, sensitive, stiff to very stiff silty clay to clayey silt material has been observed within the stratified drift. A summary of material properties for this upper clay layer is presented in Table 2-1. The Liquidity Index values are above unity. The in-situ undrained shear strength obtained by vane shear tests ranged from 35 to 135 kPa which indicates clay material of firm to very stiff consistencyin an intact condition. The average shear strength parameters of ϕ'=31° and c'=6 kPa were interpreted from the triaxial and Direct Shear Test (DST) test results.

Table 2-1: Upper Silty Clay Layer – Physical and Mechanical Properties

Property	General Range	Average	Number of tests
Percent finer than 2 microns	35 – 45	_	19
Water content, w %	17 – 43	31	199
Liquid limit, LL %	17 – 43	30	168
Plastic limit, PL %	13 – 32	19	168
Plasticity Index, PI %	2 – 22	11	168
Liquidity Index, LI	0.6 – 2.8	1.3	168
Intact Undrained shear strength, S_u kPa	35 – 135	_	_
Remoulded Undrained shear strength, S_u kPa	60 – 2	_	_
Sensitivity, in-situ, S_t	1 – 36	10	43
Large strain friction angle, ϕ'_{cv} º	30 – 32	_	_
Effective cohesion, c', kPa	0 – 10	_	_
Unit weight, γ kN/m^3	18.4 – 19.7	_	11
Initial void ratio, e_0	0.93 – 1.06	_	_
Compression index, c_c	0.32 – 0.5	_	_
Recompression index, c_r	0.03 – 0.06	_	_
Hydraulic Conductivity, k, m/s	$10^{-7} – 10^{-9}$	_	_
Salt content, g/l	0.8 – 1.5	_	_

2.2.2.2 Intermediate Silty Sand/Sandy Silt Layer

The results of sieve analyses on samples recovered from the intermediate silty sand/sandy silt layers indicated a generally fine silty sand material with an average of 27% fines content. The standard penetration tests carried out in this layer resulted in N values generally higher than 50 which indicate the silty sand/sandy silt layers are in a very dense condition. Three consolidated undrained triaxial tests were conducted on samples from intermediate sand layers, during the 1979 investigations, which resulted in an average effective friction angle of 35° to 37° and effective cohesion of 0 kPa under large strain conditions. Two direct shear tests were completed on silty sand and sandy silt samples from borehole NS-1-13, between elevations 28 to 38 m, which resulted in average values of ϕ'=35° and c'=0.

The presence of silty clay or clayey silt strata interbedded within the intermediate silty sand layer influences permeability test results with values from 10^{-7} to 10^{-9} m/s with an average of 10^{-8} m/s within stratified drift. Main physical and mechanical properties of the intermediate silty sand layer are presented in Table 2-2.

Table 2-2: Intermediate Silty Sand Layer – Physical and Mechanical Properties

Property	General Range	Average
Fine contents	55 – 5	_
Unit weight, γ kN/m^3	18.4 – 19.7	_
Large strain friction angle, ϕ'_{cv} º	35 – 37	36
Effective cohesion, c', kPa	0	_
Hydraulic Conductivity, k, m/s	10^{-7} – 10^{-9}	_

2.2.3 LOWER MARINE CLAY LAYER

The lower clay layer is located below the stratified drift (generally below the stratified drift and above the lower aquifer (lower sand and gravel layer). This layer consists of silty clay of low to medium plasticity which exhibits lower values of liquidity index than the upper clay layer and can be classified as slightly sensitive.

The consistency of clay is stiff to very stiff with in-situ undrained shear strength of 53 to 200 kPa. A summary of material properties for the lower clay layer is presented in Table 2-3.

Table 2-3: Lower Marine Clay Unit – Physical and Mechanical Properties

Property	General Range	Average	Number of tests
Percent finer than 2 microns	15 – 35		
Water content, w %	17 – 45	29	201
Liquid limit, LL %	22 – 48	37	123
Plastic limit, PL %	13 – 27	21	123
Plasticity Index, PI %	7 – 25	16	123
Liquidity Index, LI	0.1 – 2	0.6	123
Intact Undrained shear strength, S_u, kPa	53 – 200	_	_
Remoulded Undrained shear strength, S_u, kPa	8 – 96	_	_
Sensitivity in-situ, s_t	2 – 11	4	35
Large strain friction angle, ϕ'_{cv} º	33	_	_
Effective cohesion, c', kPa	6	_	_
Salt content, g/l	8 – 22	_	8
Unit weight, γ , kN/m^3	19.2 – 19.5	_	3
Hydraulic Conductivity, k, m/s	10^{-7} – 10^{-9}	_	_

As can be seen on Figure 2-2, based on CPT data, the undrained shear strength at a given elevation is generally similar throughout the North Spur with the OCR at about 1.0 below the crest and between 3 and 15 below the downstream toe. It should be noted that some of the material at shallow depth below the toe in areas subjected to previous slides can be remoulded.

2.2.4 LOWER AQUIFER UNIT

The lower aquifer is located below the lower clay layer and above the bedrock. It is generally observed from elevation -70 m to bedrock level and consists of sand and gravel with some cobbles and boulders.

A representative value of the hydraulic conductivity of 10^{-4} m/s was retained for this layer from the obtained values coming from the pumping tests performed in 1979.

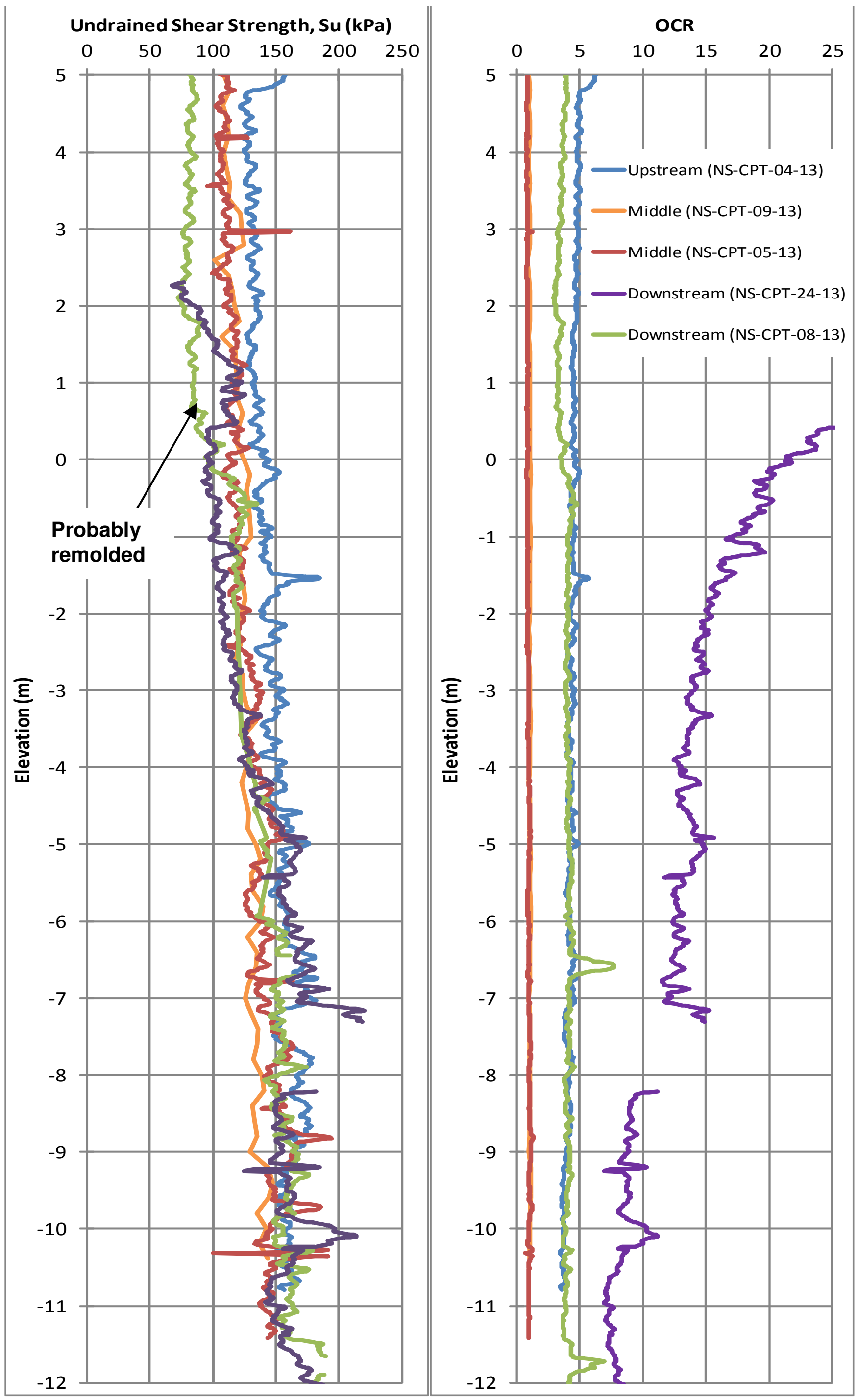

Figure 2-2: Undrained Shear Strength and OCR estimated based on CPT

2.2.5 BEDROCK FORMATION

The bedrock has been reached and sampled in 7 boreholes. The type of bedrock is generally granite gneiss with pegmatite intrusions. The RQD values in boreholes D2-79 and D3-79 (close to rock knoll) are generally between 55 and 89 (average of 72) except for a lower value of 17 at the rock surface in D3-79. These RQD values measured at relatively shallow depth might not be representative of the deeper bedrock.

2.3 REPRESENTATIVE SECTIONS

2.3.1 Most Critical Slope

Based on topographic and stratigraphic information, the most critical slope of the North Spur has been identified on the downstream side of the spur, about 200 m south-west of Kettle Lakes outlet, where the steep slope is still intact as shown on Figure 2-3 (Section 13). The stratigraphic information at Section 13 is summarized on Figure 2-4.

Short-term stability analyses for the static conditions performed in the SLI (2015a) study have shown that the present factor of safety would be about 1.0 as illustrated on Figure 2-5-a, i.e. the current stability of this slope would be only marginal. After proposed re-grading and stabilization works (see Figure 2-5-b), the factor of safety is expected to be about 1.6. The normal water level below the crest is expected to be at an elevation of 15 m after the completion of the stabilization works.

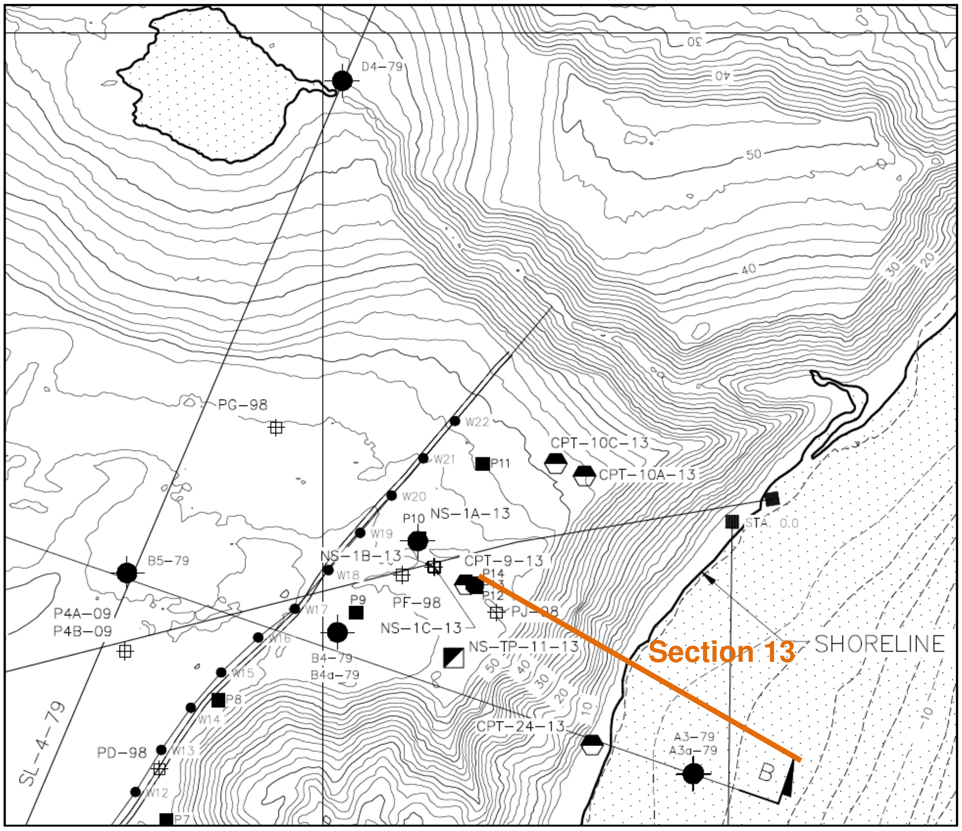

Figure 2-3: Present Conditions – Location Plan of Critical Section 13

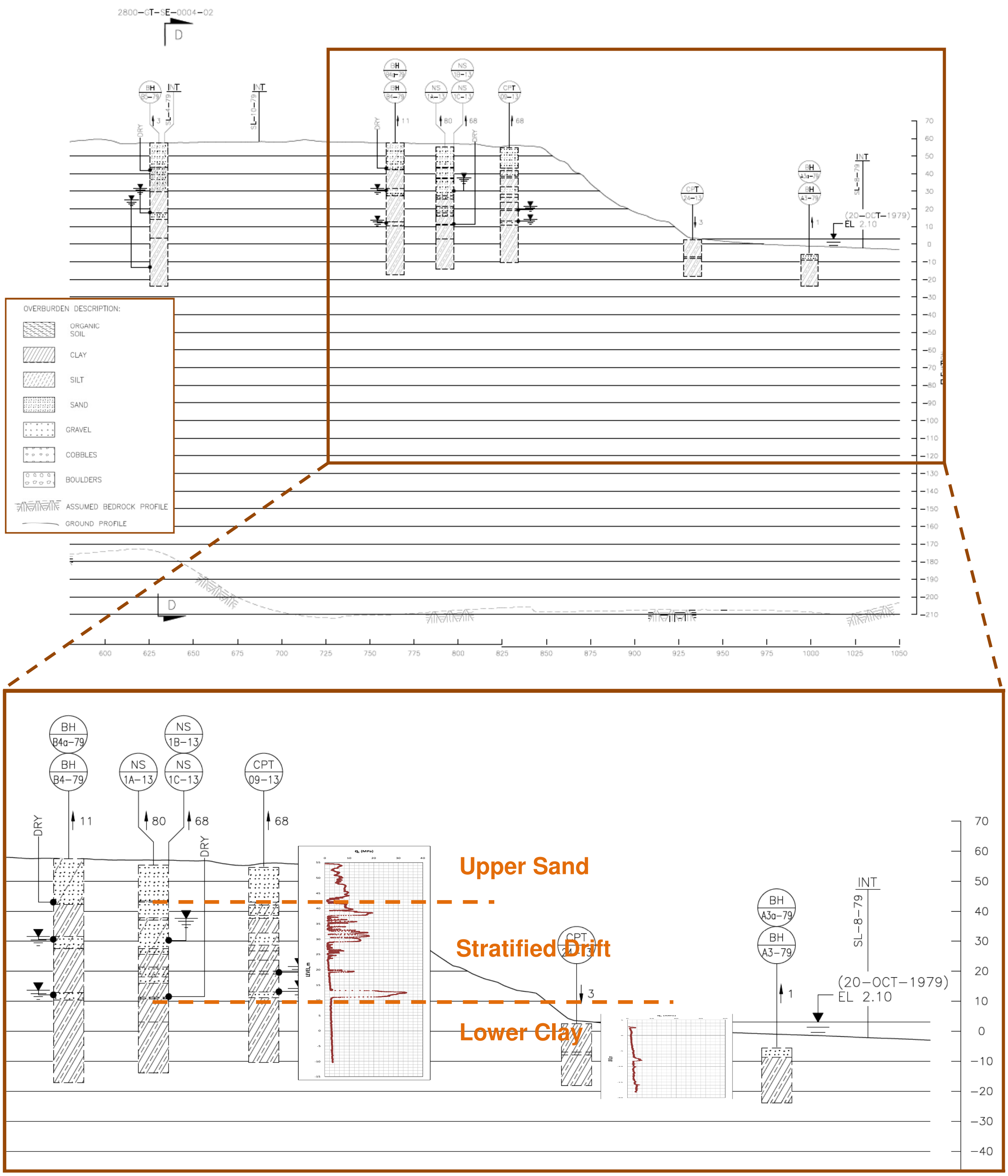

Figure 2-4: Section 13 - Stratigraphic Data and Typical CPT Profiles

2.3.2 Other Conditions

The conditions elsewhere on the slopes of the spur are less critical:

- On the upstream side of the spur, the height of the slope is less and the presence of the reservoir will have a stabilizing effect. After the completion of the stabilization works, the normal water level below the crest is expected to be at an elevation of 25 m at a distance of 20 m from the crest as illustrated on Figure 2-6; a conservative water table elevation of 30 m was assumed for the dynamic analyses.
- On the southern part of the downstream side where landslides have already occurred (see Figure 1-1), the slope is gentler and the presence of slide debris in the toe area has a stabilizing effect as illustrated on Figure 2-7.

The purpose of the stabilization works is mainly to protect the banks against further erosion of the slope surface and of the toe area and, where needed, to add weight in the toe area to act as a stabilization berm.

2.3.3 Selection of Section and Profiles for Dynamic Analyses

The dynamic stability will be analysed for three vertical 1D profiles and one 2D section:

- P1: 1D profile for top of the hill conditions of Section 13;
- P2: 1D profile for toe conditions of Section 13;
- S1: 1D profile for top of the hill conditions of Section 9 (see Figure 2-8 for location);
- Section 13: 2D section for stabilized conditions (Figure 2-9).

Two water table elevation conditions will be considered: the downstream conditions at 15 m and the upstream conditions at 30 m.

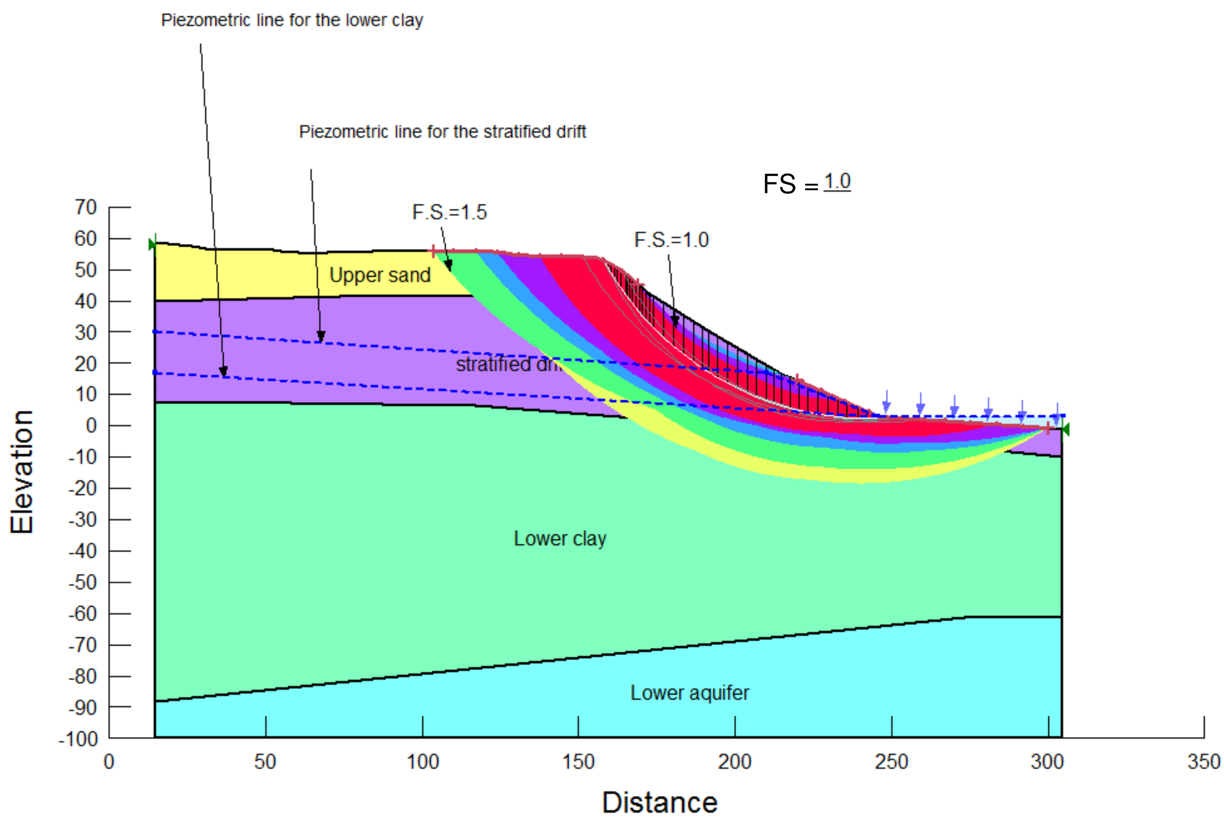

a) Section 13 - Before Stabilization Works

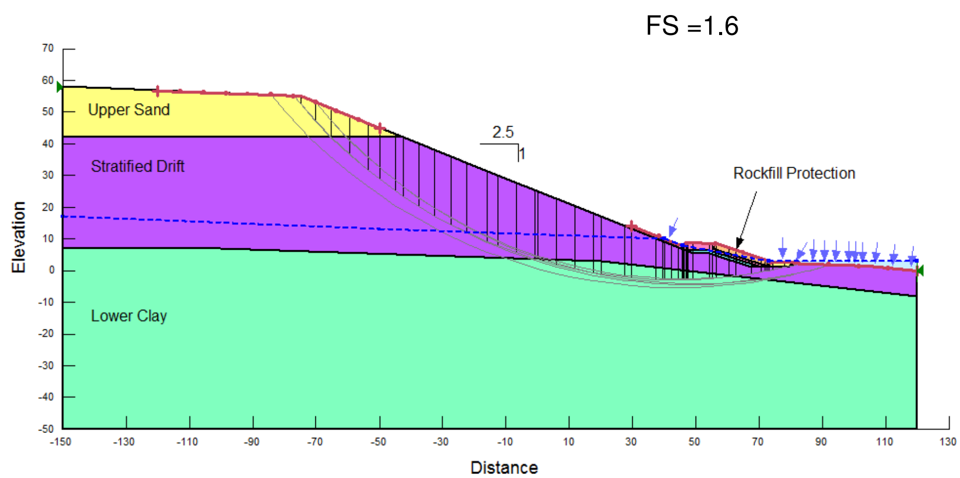

b) Section 13 - After Stabilization Works

Figure 2-5: Stability Conditions of Downstream Section 13 a) Before and b) After Stabilization Works

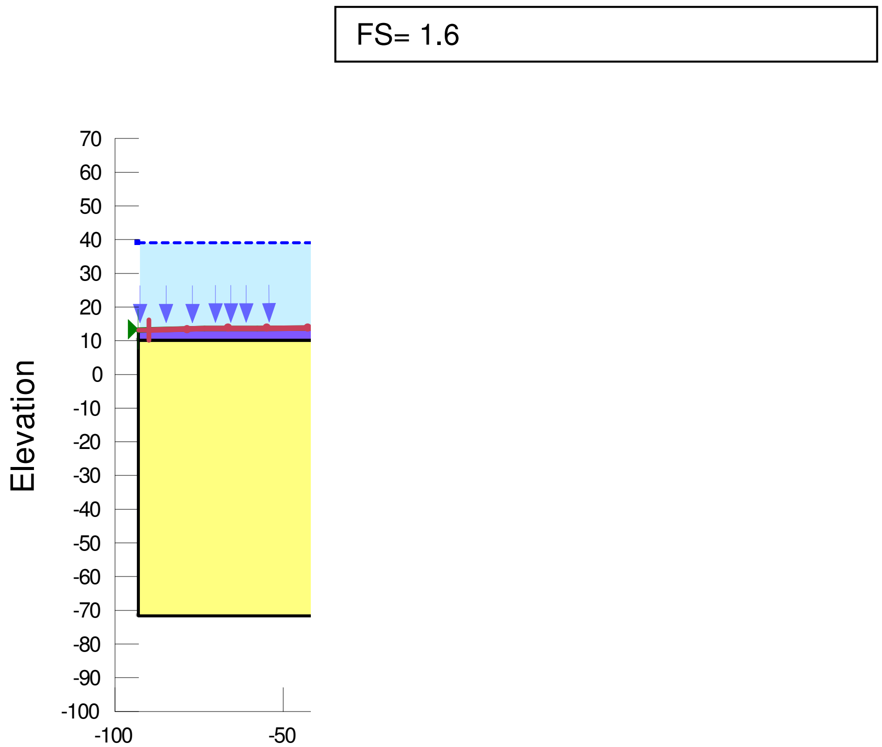

Figure 2-6: Conditions of the Upstream Section 4 after Stabilization Works

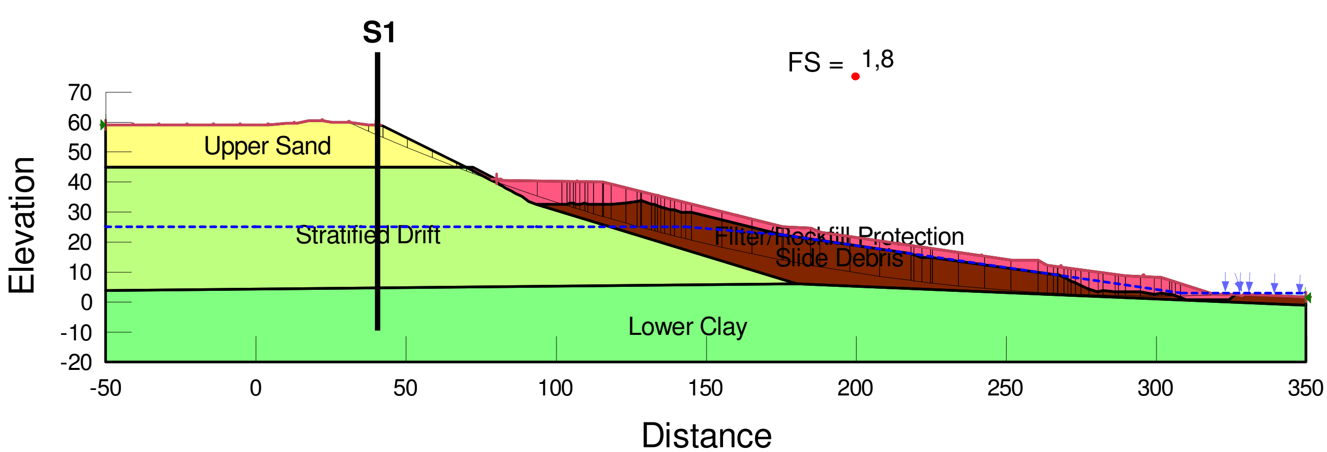

Figure 2-7: Stability Conditions of the Downstream Section 9 after Stabilization Works

Figure 2-8: Layout of Stabilization Works and Sections Location

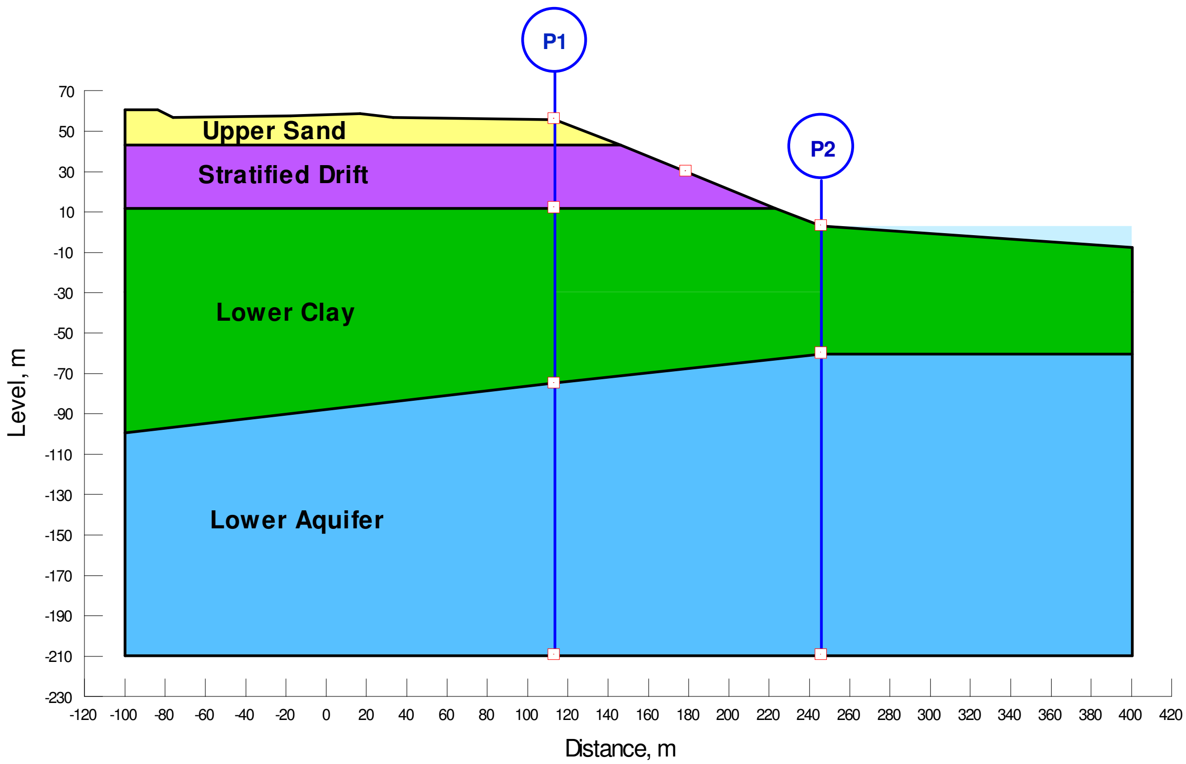

Figure 2-9: Section 13 - 2D Stratigraphic Model

3 SEISMIC PARAMETERS

Prof. Gail Atkinson was asked to update her 2008 Earthquake Hazard Analysis for the Muskrat Falls site at coordinates 53.25N 60.77W (the coordinates of the previous 2008 study were 52.5N 61.0W, half-way between the Gull Island and Muskrat Falls sites). She was also asked to provide deaggregation of the hazard for the 1: 10 000 year spectrum.

As stated by Prof. Atkinson (2014), *"...the results of this study consider the effects of major uncertainties on the hazard at Muskrat, and incorporate up-to-date information on seismicity and ground motion prediction equations (GMPEs), which have evolved considerably over the last 10 years (e.g. see Atkinson and Goda, 2011 for discussion)." "The analysis assumes that there are no such local features that would affect the overall regional hazard estimates; (...) such features are very rare in eastern Canada, and it is thus very unlikely that they will be* *identified in the site area. The analysis addresses natural seismicity, and does not address the probability of reservoir-induced seismicity or other potential induced seismicity sources, if any."*

3.1 DESIGN RESPONSE SPECTRA

The Atkinson (2014) study report provides the mean-hazard UHS (Uniform Hazard Spectra) for a range of annual probabilities (1/1000, 1/2475, 1/5000 and 1/10 000) and for different site conditions as reported in Table 3-1. The mean-hazard UHS for Hard-rock site condition (Class A) is shown in Figure 3-1 (on log-log and semi-log plots) to compare with the previous UHS from Atkinson 2008. It can be seen that the amplitude of the spectral acceleration in the 2014 UHS is somewhat lower than the 2008 UHS. The main differences are due to different site coordinates and to an updated seismicity database, methodology and GMPEs.

Table 3-1: Mean-Hazard Ground Motions for Muskrat Falls

53.25N 60.77W		PSA, PGA (cm/s^2) and PGV (cm/s) (1)							
Freq. (Hz)	Period (s)	1:1 000 year		1:2 475 year		1:5 000 year		1:10 000 year	
		Class B/C(2)	Class A(3)	Class B/C	Class A	Class B/C	Class A	Class B/C	Class A
0.2	5	1.3	1.1	2.4	2.1	3.6	3.1	4.9	4.3
0.5	2	5.6	4.5	9.6	7.8	13.5	11	18.1	14.7
1	1	11.4	8.9	18.8	14.6	26.0	20.2	34.2	26.6
2	0,5	20.3	14.7	32.6	23.6	43.5	31.5	57.5	41.6
5	0,2	31.7	24	50.5	38.3	73.6	55.8	101.0	76.6
10	0,1	31.5	29.4	53.6	50.1	79.3	74.1	115.2	107.5
20	0,05	20.6	25.9	36.7	46.2	55.6	70	84.3	106.1
PGA		16.8	14.9	28.3	26.3	40.7	40.1	59.4	60.2
PGV		1.4	1.2	2.5	2.0	3.7	3.0	4.9	4.0

Notes :

1. Ground motions for 5% damped horizontal-component Pseudo-acceleration (PSA), Peak ground acceleration (PGA) and Peak ground velocity (PGV); PSA and PGA are in cm/s^2 and PGV in cm/s.
2. Ground motions for NEHRP B/C site conditions (near-surface shear-wave velocity, Vs_{30}, of 760 m/s)
3. Ground motions for NEHRP A site conditions (Hard Rock, Vs_{30} greater than 1500 m/s)

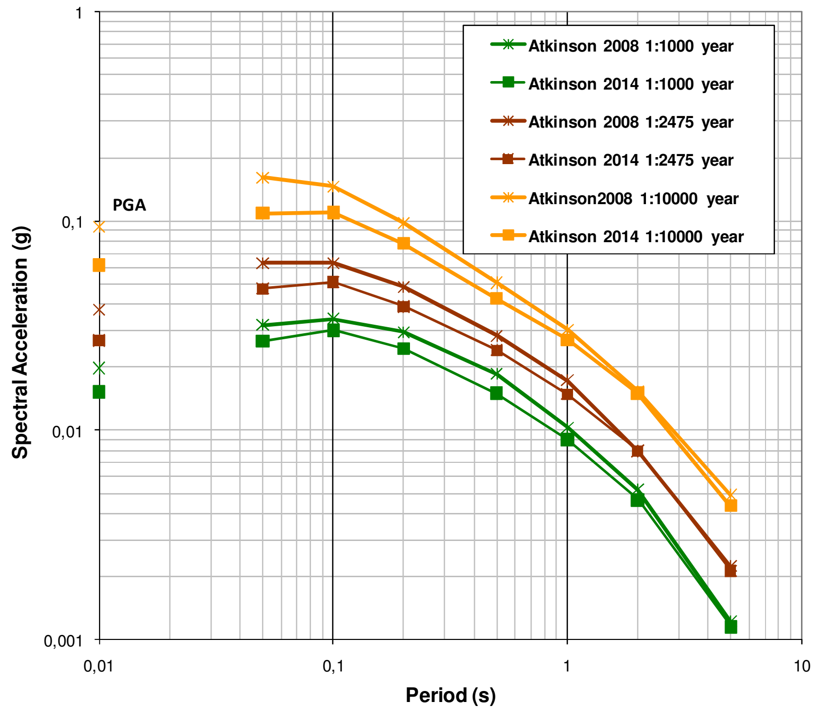

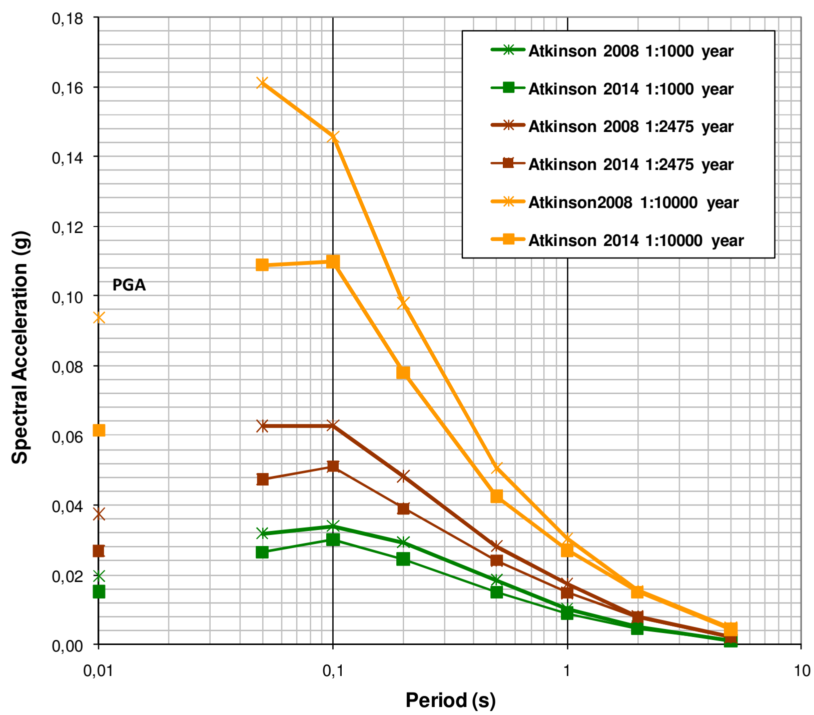

Figure 3-1: Mean-hazard UHS for Hard-rock Site Conditions

3.2 DEAGGREGATION RESULTS

The results of the deaggregation for the 1/10 000 motions performed by Atkinson (2014) are presented in Figure 3-2.

Table 5 – Mean deaggregation results for 1/10,000 motions

	M	R[km]	Epsilon	Duration[s]
PGA	6.1	90	1.0	9.8
PSA(5.0Hz)	6.2	98	1.1	10
PSA(1.0Hz)	7.0	294	1.7	38
PSA(0.2Hz)	7.3	377	1.4	51

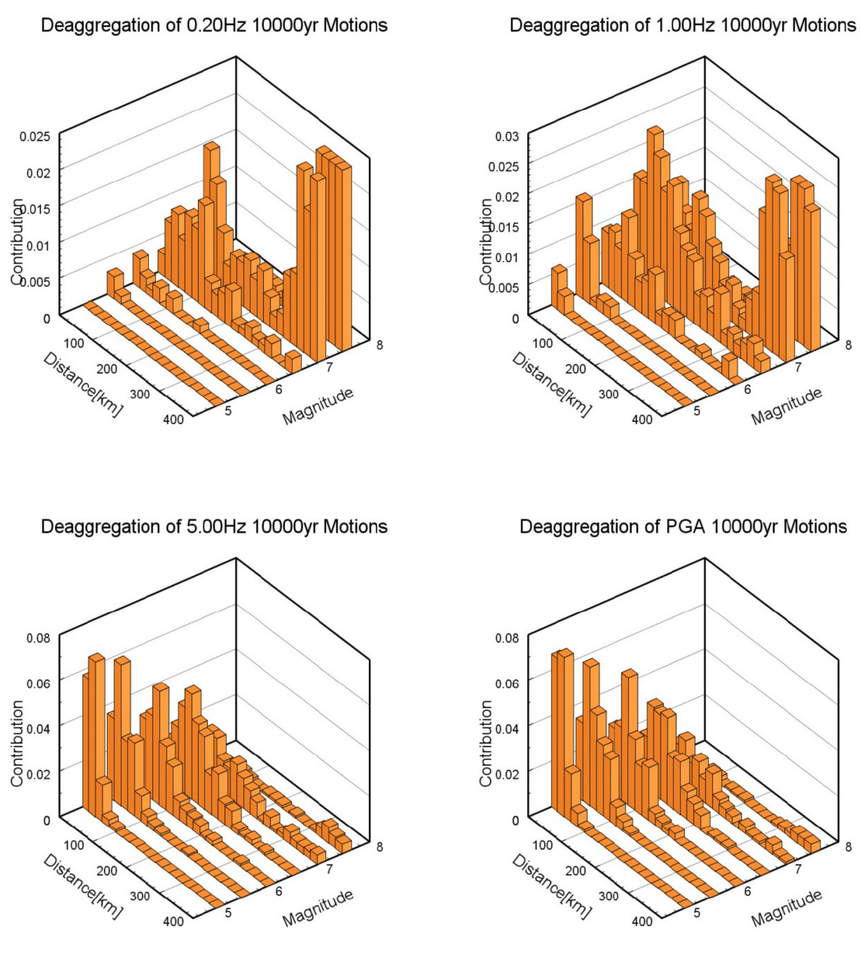

Figure 10. Deaggregation plots of 10000yr return period motion at Muskrat.

Figure 3-2: Deaggregation Results (from Atkinson, 2014)

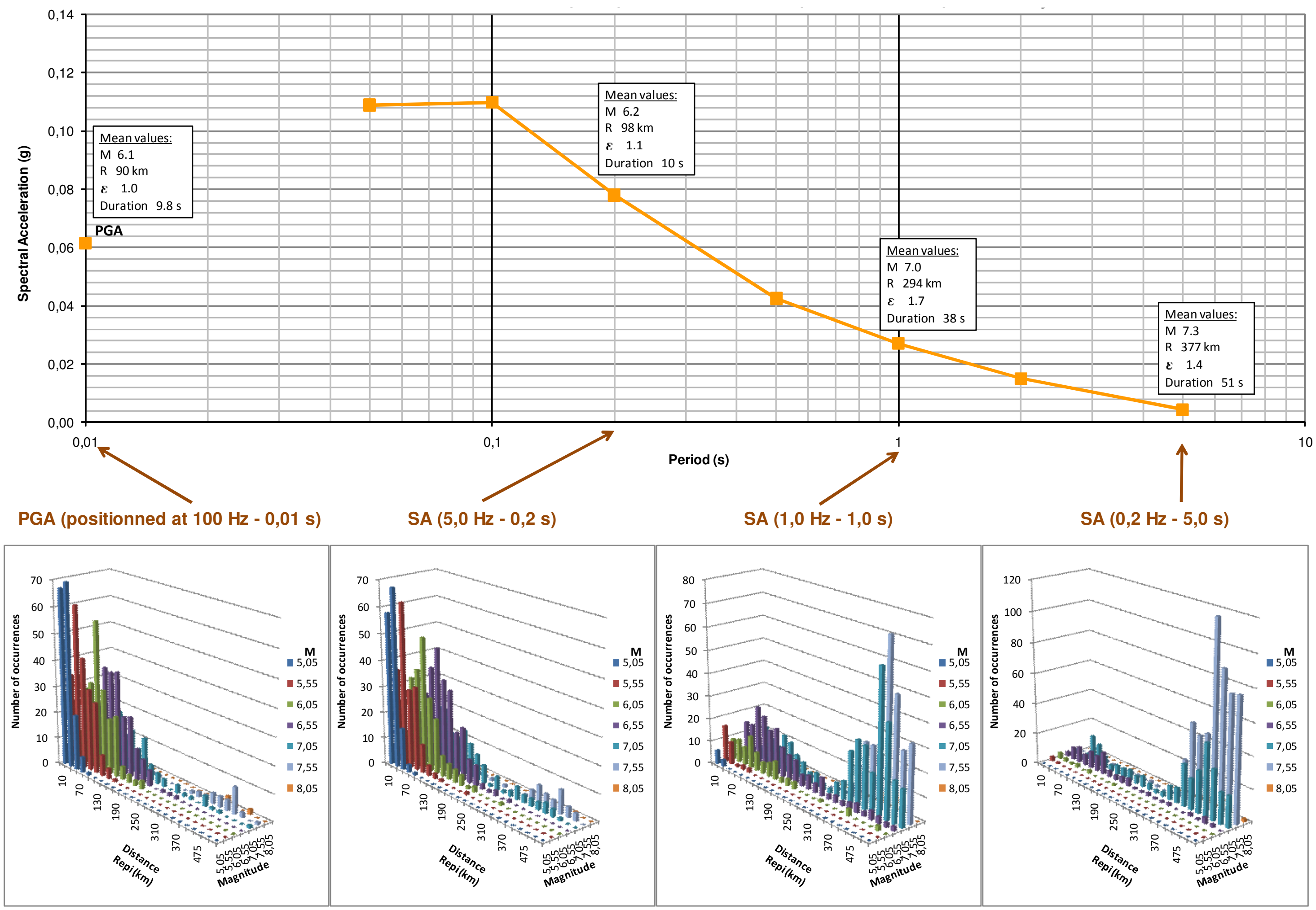

Figure 3-3: Class A (Hard Rock) UHS and Deaggregation Results for 1/10 000 Annual Exceedance Probability

The results of the deaggregation are defined as:

- M or M_W, Moment magnitude
- R, Distance from the epicenter
- ε, the number of standard deviations with respect to the median ground motion prediction equation (GMPE)
- Duration, significant duration calculated as the sum of the source duration and path duration components

They are associated to the data of the Design Response Spectrum on Figure 3-3. The deaggregation plot for SA (1 Hz or 1 s) shows that there are very few contributions in the bins around the mean scenario values of M 7.0 and 294 km. Based on the detailed deaggregation data provided with the Atkinson (2014) report, the contributions for SA (1 Hz or 1 s) were divided in two groups with the following average values:

- Short distances (< 250 km): M 6.5, R 103 km and ε 1.3
- Long distances (> 250 km): M 7.3, R 425 km and ε 1.9

3.3 ARIA'S INTENSITY

The Aria's Intensity, I_A, is a measure of the energy content of an input motion. The Aria's intensity, I_A, to be expected from the design earthquake was estimated for the mean scenario events contributing to the hazard based on the deaggregation results; the average relationship proposed by Lee (2009) for Central/Eastern US motions (see Figure 3-4) was used and the results are presented in Table 3-2. The values obtained have an I_A less than 0.1 m/s in accordance with the low seismicity of the site.

3.4 REPRESENTATIVE SCENARIOS

Based on the deaggregation results and assuming that the North Spur is mostly sensitive to frequencies between 0.5 and 5 Hz (periods between 2 and 0.2 s), two scenarios were identified and their characteristics are summarised on Table 3-3.

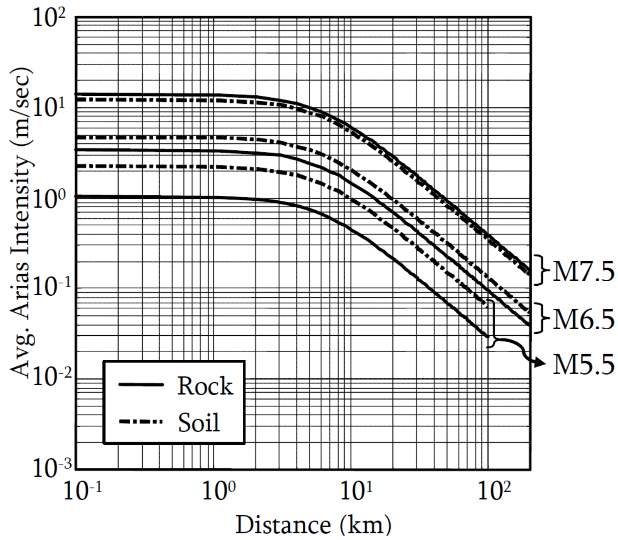

Figure 3-4: Average I_A Relation for Central/Eastern US Soil and Rock Motions - Lee (2009)

Table 3-2: Estimation of Arias Intensity

1:10 000 year	PGA	SA (0,2 s)	SA (1,0 s)			SA (5,0 s)
Spectral Acceleration (g)	0.06	0.08		0.03		0.004
			< 250 km		> 250 km	
Magnitude M_W	6.1	6.2	6.5	7.0	7.3	7.3
Distance (m)	90	98	103	294	425	377
Duration (s)	9.8	10		38		51
I_A (m/s)	**0.085**	**0.090**	**0.090**	**0.035**	**0.036**	**0.042**
	Near Events				**Far Events**	

Table 3-3: Selected Representative Scenarios

Representative Scenarios (Annual Probability of 1/10 000)		
	Near Field Event	**Far Field Event**
Magnitude, M_W	6.5	7.3
Distance, R	100 km	400 km
Aria Duration	10 s	50 s
Aria's Intensity, I_A	0.09 m/s	0.04 m/s

4 REPRESENTATIVE INPUT MOTIONS

Representative input motions for Muskrat Falls for a 1/10 000 annual probability were selected and treated based on the UHS (Uniform Hazard Spectrum) and on the deaggregation results provided by Atkinson (2014) and summarized on Figure 3-3 above.

4.1 METHODOLOGY

The selection and treatment of representative input motions were performed using the “Spectral Matching” module of EZ-FRISK™ (version 7.62, Fugro, 2011), a computer program for Earthquake ground motion estimation. The spectral matching code is based on the RspMatch 2009 time-domain spectral matching code as documented in:

> "An Improved Method for Nonstationary Spectral Matching", Linda Al Atik and Norman Ambrahamson, *Earthquake Spectra*, Volume 26, No. 3, pages 601-617, August 2010.

This improved method does not induce any drift in the modified input motion so that an additional baseline correction is not required.

The Spectral matching module also provides access to different databases of earthquake recordings with the possibility of filtering the data based on different criteria (magnitude, distance, duration, etc…). The representative duration is estimated by the so-called Aria’s duration, defined as the time interval between 5% and 95% of the final intensity.

<u>Treatment of Accelerograms</u>

Since it is not possible to find enough real ground motions representative of the design spectrum, recordings are treated by scaling and/or spectral matching. As discussed in Al Atik and Abrahamson (2010):

> *Design time series are developed by modifying initial time series that consist of empirical recordings from past earthquakes representative of the design event or numerical simulations of the ground motion for the design event. Two approaches exist for modifying the time series to be consistent with the design response spectrum: scaling and spectral matching. Scaling involves multiplying the initial time series by a constant factor so that*

the spectrum of the scaled time series is equal to or exceeds the design spectrum over a specified period range. Spectral matching involves modifying the frequency content of the time series to match the design spectrum at all spectral periods. Although spectral matching is commonly used in engineering practice, the concept of using spectrum compatible time series in the seismic design of structures remains controversial for two reasons. First, a time series that matches the entire design spectrum represents more than one earthquake at a time since the design spectrum may be an envelope of multiple earthquakes. As a result, it is generally believed that such time series overestimate the structural response. Second, spectrum compatible time series have smooth response spectra and are considered unrealistic when compared to typical earthquake response spectra that tend to have large peaks and troughs.

This issue was discussed with Prof. Idriss during the December 2013 Workshop. Prof. Idriss pointed out that while simply scaling different real ground motions to match different parts of the UHS should produce input motions that are more realistic, many more such input motions are required to insure that all potential scenarios are taken care of. He estimated that around 6-7 spectral matched input motions should be adequate in most situations while around 20 scaled-only input motions would be required. For situations where the outcome of the dynamic analyses is controlling the design and where less over-conservatism is preferred, he proposed to perform spectral matching on so-called Conditional Mean Spectra prepared with the method proposed by Prof. Jack W. Baker in

"Conditional Mean Spectrum: Tool for Ground-Motion Selection", Jack W. Baker, *Journal of Structural Engineering,* Vol. 137, No. 3, pages 322-331, March 1, 2011.

Given the very low seismicity of the Muskrat Falls site and the results of the preliminary dynamic analyses, the new dynamic analyses are not expected to control the design and the use of Conditional Mean Spectra is not judged necessary.

Therefore for this study, the input motions selected were spectral matched following the methodology proposed by Al Atik and Abrahamson (2010) and then the resulting input motions were examined as to identify the best candidates based on Husid plot (normalised

Aria's intensity as a function of time). If necessary, these were then base-line corrected to eliminate any drift in velocity or displacement.

4.2 INPUT GROUND MOTION SELECTION

The accelerograms from the initial selection are presented in Appendix B; for each one the initial magnitude, distance, Aria's intensity and duration are given. Different groups of accelerograms were selected from the databases available through the EZ-Frisk software:

1. Representative accelerograms from the PEER and the CEUS databases were requested based on the two scenario events identified in Section 3.4:
   - Near field event with M_W 6.5, R 100 km and Aria duration of 10 s;
   - Far field event with M_W 7.3, R 400 km and Aria duration of 50 s;
2. Recordings of the Saguenay 1988 earthquake from stations located in the Saguenay region: especially given the relative proximity of the Saguenay region;
3. Recordings of the Nahanni 1985 earthquake;
4. Accelerograms used in the preliminary dynamic study.

For each group, the response spectra of the original recordings were compared to the design UHS on Figure B-1. The main characteristics of the spectral matched input motions are shown on figures B-2 to B-6.

1D Profile P1 (top of the hill conditions at Section 13, near SCPT-09-13) was submitted to 1D equivalent-linear analyses using all the initially selected input motions. Then a first selection of 18 input motions was done keeping candidates showing the best fit to the two scenario events together with those showing the strongest response in the 1D analyses of Profile P1. These were used for the remaining 1D analyses. Their main characteristics are summarized on Figure B-7. Based on these, a short list of eight (8) accelerograms was selected for 2D Equivalent-linear analyses. These are described in detail on the figures of Appendix E.

5 LIQUEFACTION AND CYCLIC SOFTENING

5.1 TYPE OF SITE RESPONSE ANALYSES AND SOFTWARE

Different types of analyses were performed in this complementary program:

- Empirical methods for liquefaction and cyclic mobility assessment
- 1D Equivalent-linear method (Shake type analyses using EZ-Frisk)
  Site Response module of EZ-Frisk, version 7.62, Fugro (2011a)
- 2D Equivalent-linear method (Quake/W similar to Quad4Mu)
  Quake/W module of GeoStudio Suite, version 8.12.3.7901, Geo-Slope Inc., 2013;
- 2D non-linear method (Finite differences model using FLAC)
  FLAC 2D, version 7.0.411, Itasca, 2011.

5.1.1 EMPIRICAL METHODS

In the empirical methods, the imposed seismic loading is compared to the loading to which the material can resist without undergoing liquefaction (for granular materials) or cyclic softening (for clay-like materials).

The imposed seismic loading is represented by the Cyclic Stress Ratio (CSR) estimated using site specific dynamic response analyses. The site is represented by either a one-dimensional vertical soil column (1D) or a two-dimensional section (2D) using equivalent-linear total stress analyses or non-linear effective stress analyses, as described below.

The Cyclic Resistance Ratio (CRR) is estimated based on SPT or CPT tests for granular material and plasticity and undrained shear strength for clay-like material.

The methods that were used:

- CRR for liquefaction (granular materials) and CRR for cyclic mobility (clay): relationships proposed by Idriss and Boulanger (2008).

This estimation is generally conservative as it represents a lower bound of the liquefaction cases of an important case history database.

In the procedure proposed by Idriss and Boulanger (2008), CRR and CSR are normalised relative to the effective overburden stress, σ'_{vc} as:

$$\mathrm{CSR} = 0.65 \frac{\tau_{\max}}{\sigma'_{vc}}$$

CRR for liquefaction (granular materials)

Figures 5.1 and 5.2 illustrate the estimation of $CRR_{7.5}$ based on respectively the SPT Normalised Index $(N_1)_{60cs}$ and the CRR from CPT Normalised Tip Resistance q_{c1N}.

CRR is normalised to clean sand taking into account the fines content, to a moment magnitude M_W = 7.5, to an effective vertical stress of 1 atm or 100 kPa and apply to flat or gently sloping ground.

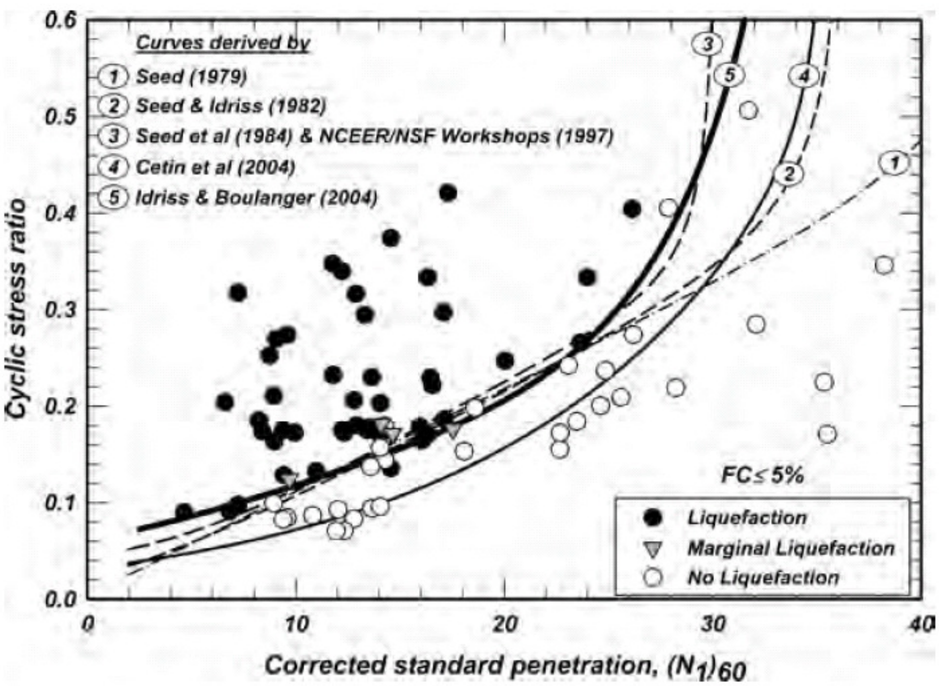

Figure 66. Curves relating the CRR to $(N_1)_{60}$ for clean sands with $M = 7.5$ and $\sigma'_{vc} = 1$ atm.

Figure 5-1: $CRR_{7.5}$ from SPT Normalised Index $(N_1)_{60cs}$ (from Idriss and Boulanger, 2008)

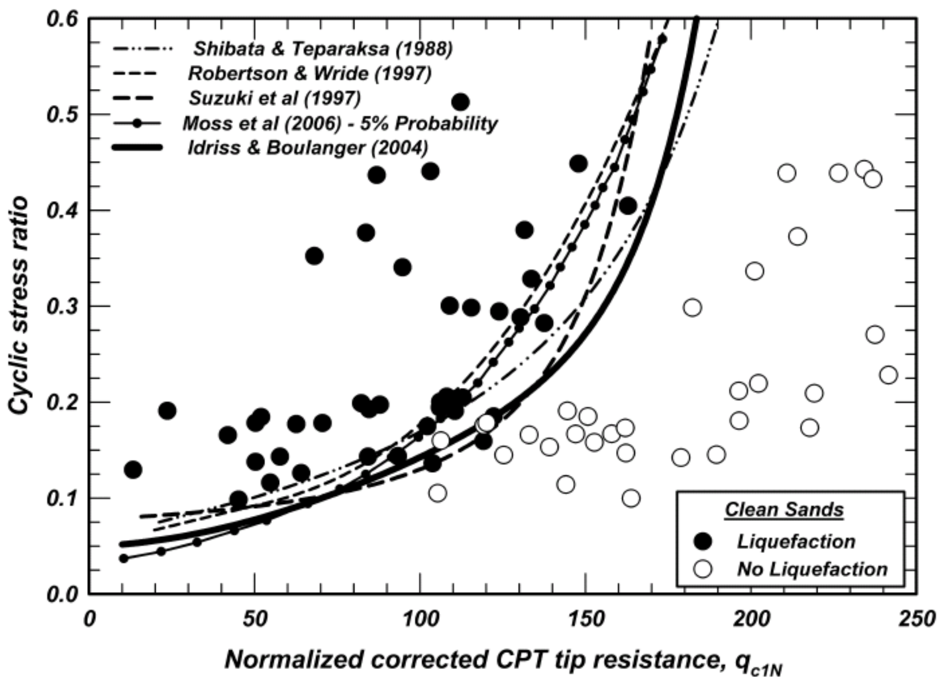

Figure 67. Curves relating the CRR to q_{c1N} for clean sands with M = 7.5 and σ'_{vc} = 1 atm.

Figure 5-2: CRR$_{7.5}$ from CPT Normalised Tip Resistance q$_{c1N}$ (from Idriss and Boulanger, 2008)

<u>CRR for cyclic softening (clay-like material)</u>

Cohesive materials are not prone to liquefaction but can be subject to cyclic softening. The criterion proposed by Idriss and Boulanger (2008) to identify clay-like material is illustrated on Figure 5-3. According to this criteria, fine grained material with a plasticity index, I_P greater than 7 is best analysed as clay-like material.

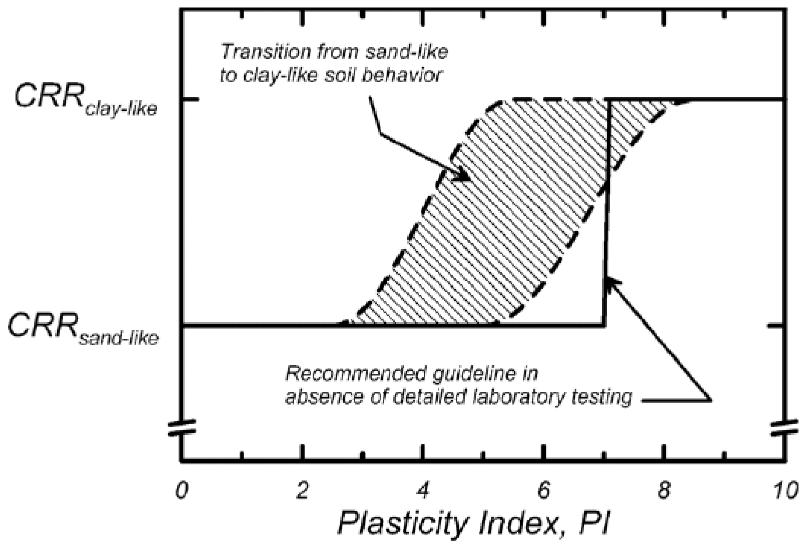

Figure 5-3: Liquefaction susceptibility criteria (Idriss and Boulanger, 2008)

Once a material has been identify as clay-like, its susceptibility to cyclic softening can be assessed based on its undrained shear strength. According to Idriss and Boulanger (2008), the normalised $CRR_{7.5}$ against cyclic softening (3% shear strain) can be estimated as:

$$CRR_{M=7.5} = C_{2D}\left(\frac{\tau_{cyc}}{s_u}\right)_{N=30}\frac{s_u}{\sigma'_{vc}} = 0.8\cdot\frac{s_u}{\sigma'_{vc}}$$

- *Vane shear test* $\quad (s_u)_{field} = \mu\cdot(s_u)_{VST}$
- *Cone penetration* $\quad s_u = \dfrac{q_{cT} - \sigma_v}{N_k}$
- *Lab tests or correlation* $\quad \dfrac{s_u}{\sigma'_{vc}} = S\cdot OCR^m \approx 0.22\cdot OCR^{0.8}$

$$(CRR)_M = (CRR)_{M=7.5}\cdot MSF\cdot K_\alpha$$

CRR is normalised to a moment magnitude M_W = 7.5 and to flat or gently sloping ground.

Magnitude Scaling Factor, MSF

The magnitude scaling factor MSF recommended by Idriss and Boulanger (2008) to take into account the Magnitude different than 7.5 is illustrated on Figure 5-4. Given the magnitude specified for the scenario events of 6.5 for near events and 7.3 for far events (see Table 3-3), a conservative value of MSF = 1.0 was considered in all analyses.

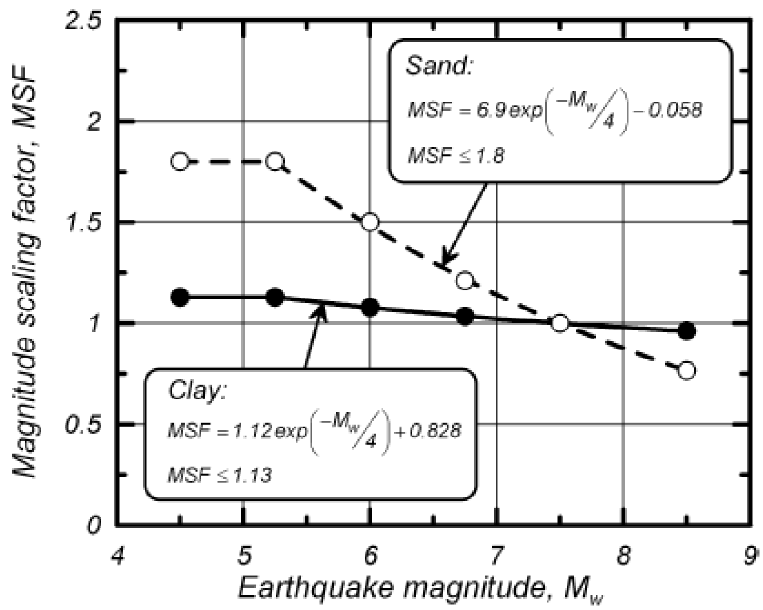

Figure 130. MSF relationship for clays and plastic silts (Boulanger and Idriss 2007, with permission from ASCE).

Figure 5-4: Magnitude Scaling Factor, MSF (Idriss and Boulanger, 2008)

Static Shear Stress Correction Factor, Kα

The Kα correction factor proposed by Idriss and Boulanger (2008) for liquefaction assessment to take into account the effect of static shear stresses is illustrated on Figure 5-5 for different values of SPT - $(N_1)_{60}$ and CPT - q_{c1N}. Given the uncertainty of this correction factor and the representative $(N_1)_{60cs}$ of 13-14 (see Figure C-13 of Appendix C), a value of 1.0 was considered for Kα for sand-like materials.

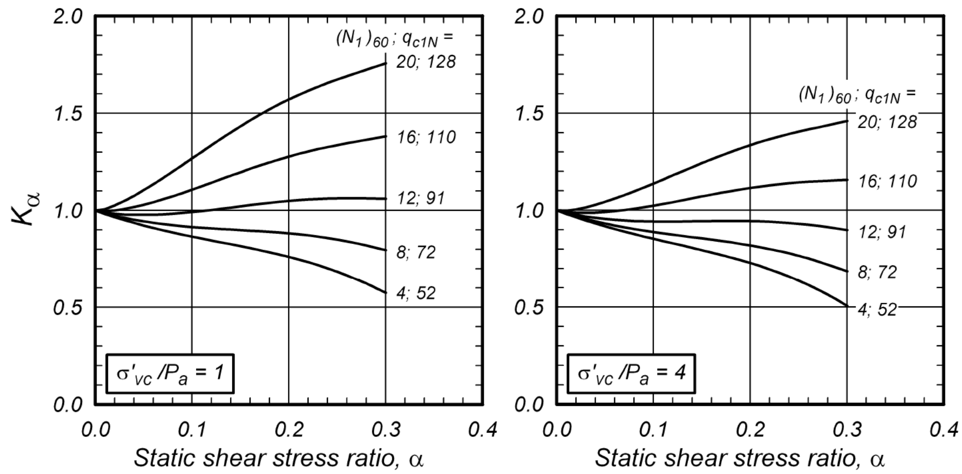

Figure 65. Variations of K_α with SPT and CPT penetration resistances at effective overburden stresses of 1 and 4 atm.

Figure 5-5: Static Shear Stress Correction Factor, Kα, for Sand-like Material (Idriss and Boulanger, 2008)

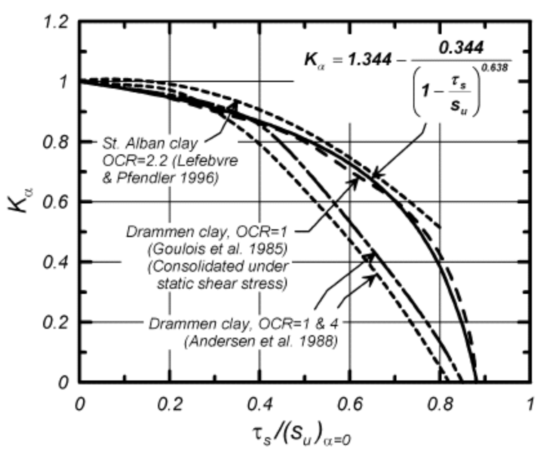

Figure 131. K_α versus $(\tau_s/s_u)_{\alpha=0}$ relationships for clays (Boulanger and Idriss 2007, with permission from ASCE). Note that the specimens were not consolidated under the applied static shear stresses, except as otherwise labeled.

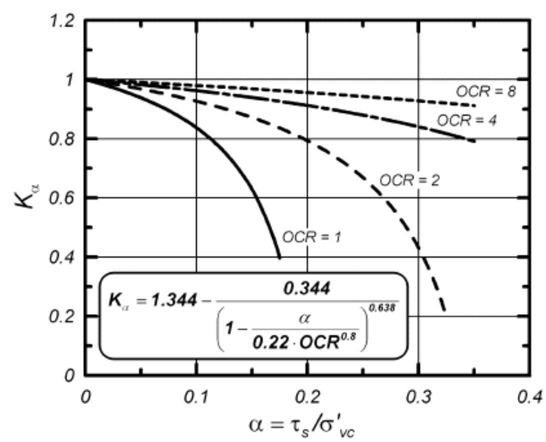

Figure 132. The K_α versus τ_s/σ'_{vc} relationship for clay at different overconsolidation ratios.

Figure 5-6: Static Shear Stress Correction Factor, Kα, for Clay-like Material (Idriss and Boulanger, 2008)

For the clay-like materials, the Kα correction factor proposed by Idriss and Boulanger (2008) for cyclic softening assessment is illustrated on Figure 5-6. This factor was first neglected for 1D analyses and then estimated to be about 0.9 based on static shear stresses estimated in 2D analyses.

5.1.2 1D EQUIVALENT-LINEAR DYNAMIC RESPONSE ANALYSES

1D Equivalent-linear Dynamic Response Analyses have been conducted using EZ-Frisk Site Response module, version 7.62, (Fugro, 2011). This software is a Windows implantation of Shake91+, an enhanced version of the industry-standard Shake91. It allows the definition of a soil or soft-rock column by specifying soil properties such as maximum shear wave velocity and density. Then, Shake91+ propagates an input motion applied to the bedrock (or any other layer) through the soil or soft-rock column to produce a site-specific ground motion time history. The analyses are performed in the frequency domain using the total density of each sub-layer.

An equivalent-linear procedure is used to account for the non-linearity of the soil using an iterative procedure to obtain values of modulus and damping that are compatible with the equivalent uniform strain induced in each sub-layer (of the vertical profile) (Idriss and Sun, 1992).

The degradation of the material properties due to shear strain were estimated based on degradation curves proposed in Shake91:

- For Sand - Seed & Idriss 1970:
    - G/Gmax and Damping Average curves
- For Clay - Sun et al 1988:
    - G/Gmax proposed for IP of 10-20%
    - Damping average curve

They are illustrated in figures 5-6 and 5-7 and compared to other curves proposed in the literature.

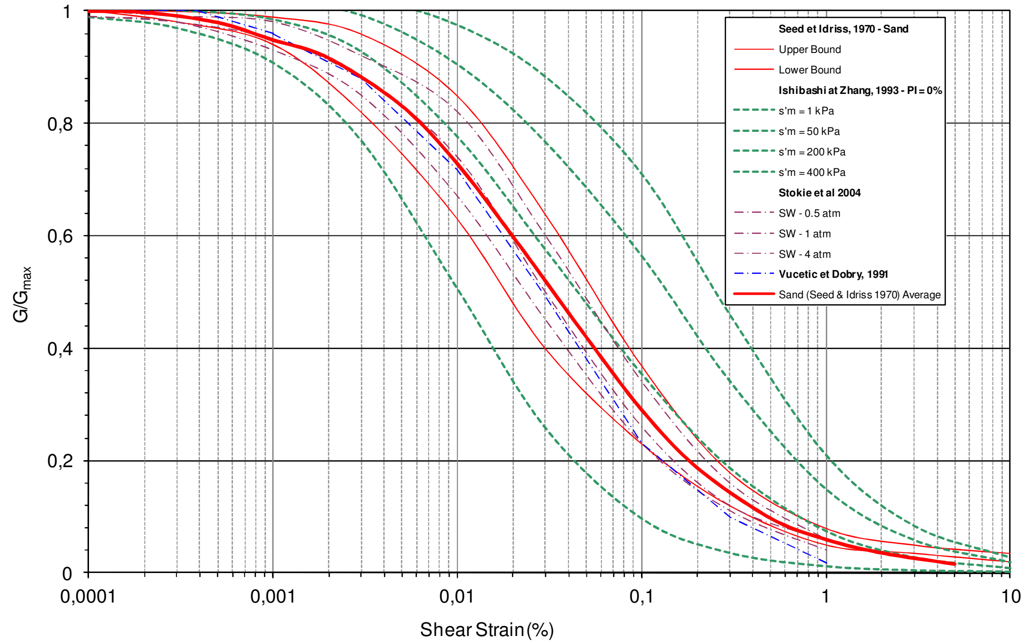

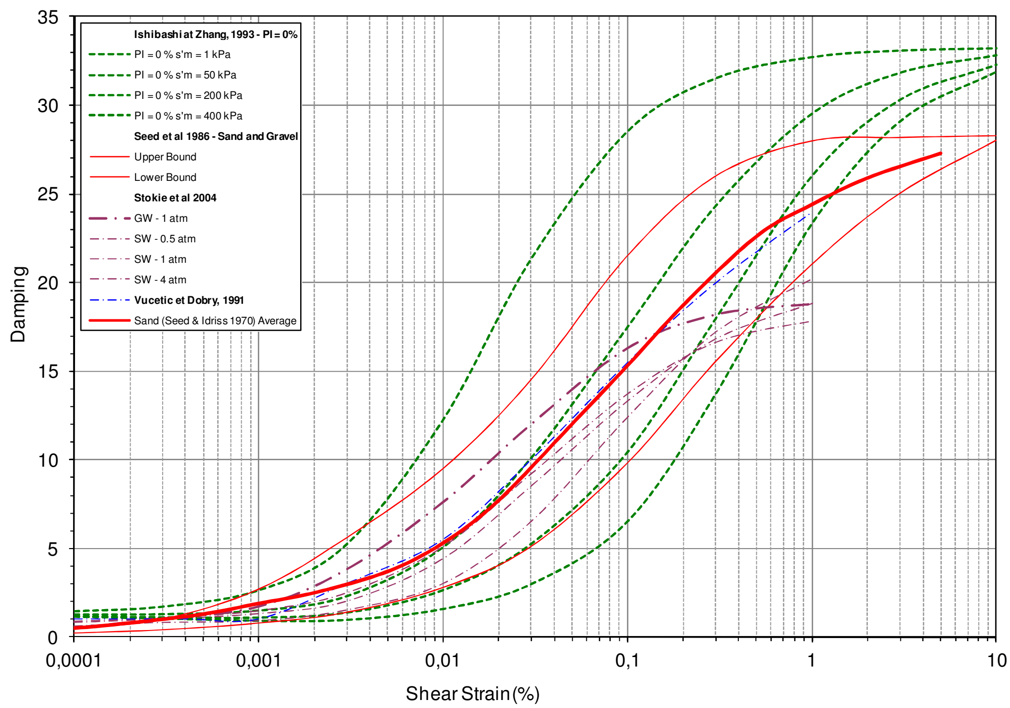

Figure 5-7: Degradation Curve for Sand Material

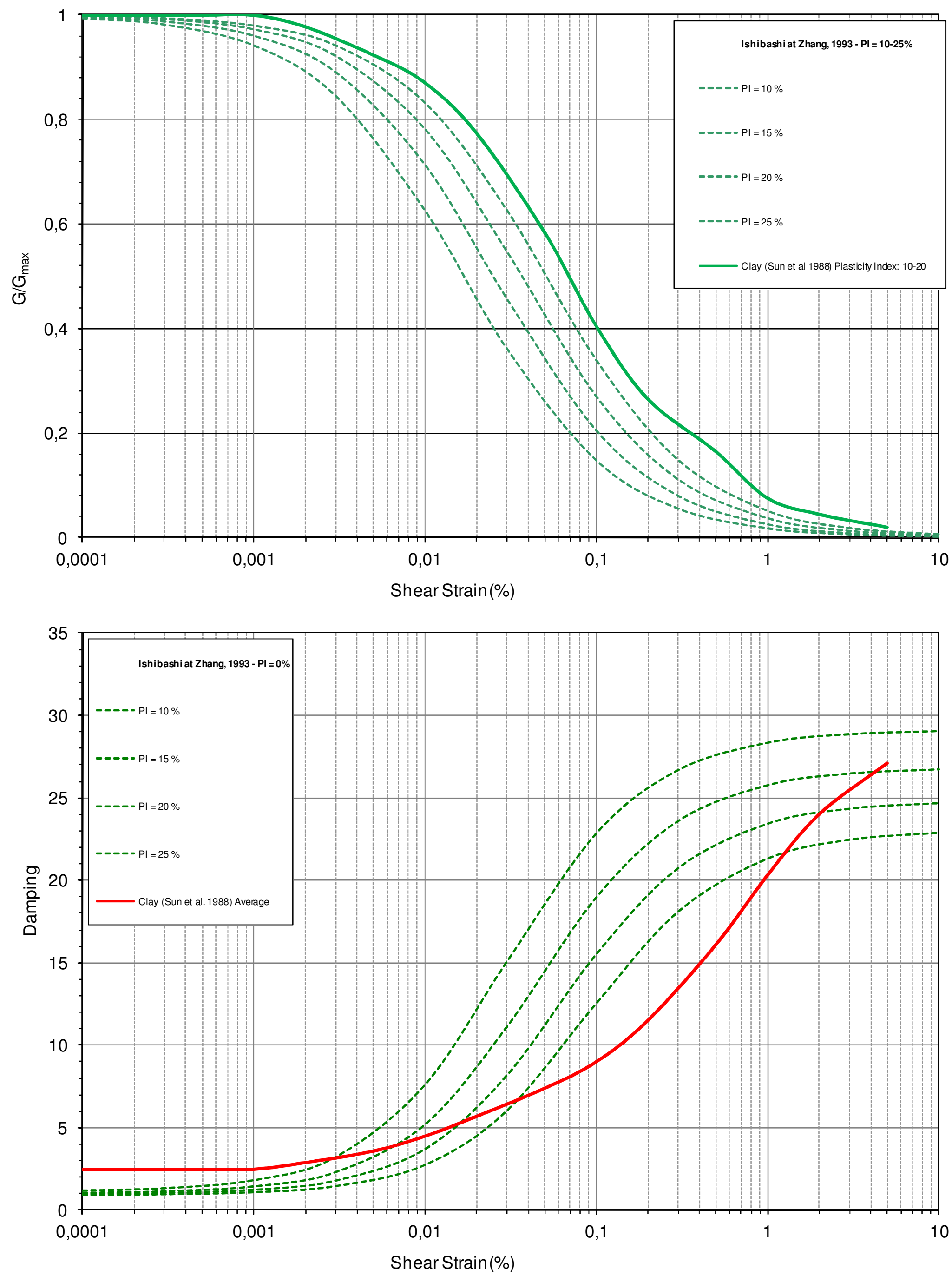

Figure 5-8: Degradation Curves for Clay

5.1.3 2D EQUIVALENT-LINEAR DYNAMIC RESPONSE ANALYSES

GeoStudio Quake/W Site Response module was used to perform 2D equivalent-linear analyses. A similar equivalent-linear iterative procedure to the 1D analysis is used. However, the software is a finite element model solving in the time domain. The same degradation curves as for 1D analyses were used in the 2D Equivalent-linear analyses (see figures 5-6 and 5-7 above). As a validation, the same software was used to perform 1D equivalent-linear analyses for comparison with analyses performed using Shake91+ implemented in EZ-Frisk Site Response module. The results indicated that although Quake/W uses a different formulation, the Quake/W results are similar but somewhat more conservative (higher CSR profile).

5.1.4 2D NON-LINEAR DYNAMIC RESPONSE ANALYSES

2D non-linear Dynamic Response Analyses have been conducted using version 7.0.4011 of the FLAC two-dimensional, finite difference software program by the Itasca Consulting Group (Itasca 2011) with the dynamic and user-defined constitutive model options. The main characteristics of this model are:

- Solving in the time domain;
- Damping and shear modulus reduction are function of the shear strain in each element.
- Excess porewater generation modeled and considered in analysis.
- Deformation and stresses induced by earthquake shaking considered in the dynamic response.

Two constitutive models of material behavior were used in the modeling, the Mohr-Coulomb model as implemented in FLAC for the materials not susceptible to liquefaction and the UBCSand model (version 904aR) developed by Beaty and Byrne (2011) for potentially liquefiable materials. The generic version of the UBCSand model as a function of $(N_1)_{60cs}$ was used and the model generates modulus reduction and damping. For the other materials, hysteretic damping is added and adjusted to fit the modulus reduction and damping curves used in the 1D and 2D Equivalent-linear Analyses.

5.2 SOIL RESISTANCE TO DYNAMIC LOADING – EMPIRICAL METHODS

5.2.1 CRR based on CPT

All the CPT profiles performed at the North Spur were analysed to estimate the CRR profile. CRR for liquefaction was estimated based on measured CPT tip resistance. CRR for cyclic softening was estimated based on undrained shear strength, Su, interpreted from CPT tip resistance with a Nkt factor of 15 based on correlations with undrained shear strength measured in vane field tests.

The investigation data and the interpreted CRR profiles are shown in detail on figures C-1 to C-6 of Appendix C for the three representative profiles, P1, P2 and S1:

- Figures C-1 and C-2: P1 (SCPT-09-13)
  1D profile for top of the hill conditions of Section 13 (see location on Figure 2-3);
- Figures C-3 and C-4: P2 (CPT-24-13)
  1D profile for toe conditions of Section 13;
- Figures C-5 and C-6: S1 (SCPT-11-13)
  1D profile for top of the hill conditions of Section 9 (see location on Figure 2-3).

The CRR profiles estimated for all the CPT tests are summarised on the following figures:

- Figures C-7 and C-8 - CRR Estimated based on CPT - Upstream Toe
- Figures C-9 and C-10 - CRR Estimated based on CPT - Crest of North Spur
- Figure C 11 - CRR Estimated based on CPT - Downstream Toe

In all cases, CRR is either the CRR for liquefaction (sand-like material) or CRR for cyclic softening (clay-like material). The fine grained material is generally considered as clay-like material based on CPT pore pressure response that has been correlated with IP greater than 7 in the associated boreholes as can been seen in figures C-1 to C-4 for SCPT-09-13 and SCPT-11-13.

The toe profiles show that the material at the toe is generally clay-like with only non-continuous layers of granular material. The weaker material indicated by CPT-06-13 is located in a landslide area and is believed to be remoulded material not representative of the intact clay. CRR for clay-like material for the toe profile is generally greater than that of Crest profiles because of the higher OCR.

The profiles selected as representative of sand-like and clay-like materials for the vertical profile at the downstream crest of the North Spur (profile P1) are indicated on Figure C-9. They will be used in the estimation of the liquefaction and cyclic softening potential respectively.

5.2.2 CRR based on SPT

SPT indices measured in the Upper Sand and in the silty sand of the Stratified Drift were revised and normalised to $(N_1)_{60cs}$ as recommended in Idriss and Boulanger (2008). The results and the estimated CRR profiles are summarised on the following figures:

- Figure C-12 - Estimated CRR based on SPT - Upstream Toe
- Figure C-13 - Estimated CRR based on SPT – Crest of North Spur
- Figure C-14 - Estimated CRR based on SPT - Downstream Toe

Generally, the estimated CRR based on $(N_1)_{60cs}$ are greater than 0.1 and greater than the lowest CRR values estimated based on CPT-qc1N.

For the crest profile, the values have been correlated with grain size and consistency indexes measured in laboratory on the same samples. Weak SPT values associated with samples of plastic clay have been removed from Figure C-13. These results show $(N_1)_{60cs}$ values generally greater than 30 for the Upper Sand and the granular layers of the Stratified Drift indicating non-liquefiable material. The weaker SPT indexes could be associated with the presence of layers of clay-like material. The $(N_1)_{60cs}$ profile used in the non-linear analyses to represent the sand-like material using the UBCSand model (see section 5.5.1) is also shown on Figure C-13. This profile was considered to be representative of the zones that could be susceptible to liquefaction based on CPT tip resistance and on Vs profiles (from Seismic CPT SCPT-09-13 and SCPT-11-13). This profile is consistent with the weaker $(N_1)_{60cs}$ values from SPT tests.

For the toe profiles, many of the weaker SPT indices are believed to have been affected by the presence of interlayers of clay-like material. In addition, interpretation of the stratigraphic data in a 3D Catia model has not shown a horizontal continuity of the sand-like material layers. The surface layers are in many locations associated with toe deposition of eroded material.

SPT indexes measured in 2013 boreholes were not retained because they were judged non-representative. As noted AMEC (2013) report, the rig was modified to accommodate a safety hammer while no measurement of the transmitted energy was performed.

The selected CRR profile for vertical profile P1 based on CPT (from Figure C-9) is compared on Figure C-15 to the CRR values based on $(N_1)_{60cs}$. As can be observed, the selected profile is lower than the SPT CRR values.

5.3 1D EQUIVALENT-LINEAR ANALYSES

5.3.1 DYNAMIC PROPERTIES

The material properties assumed for the 1D equivalent-linear analyses are listed on figures D-1, D-2 and D-3 of Appendix D for respectively vertical profiles P1 (crest profile for Section 13), P2 (toe profile for Section 13) and S1 (crest profile for Section 9). The V_S and G_{max} profiles were estimated based on the two seismic CPT profiles and on triaxial seismometer measurements as presented on the Figures C-16 to C-18 of Appendix C:

- Profile P1: Figure C-16 shows the Vs profile measured in SCPT-09-13 and its extension to fit the fundamental period of 1.85 sec estimated based on nearby triaxial seismometer measurements: the extrapolated Vs profile is also based on the stratigraphy observed in B5-79, the nearest borehole reaching bedrock. The fundamental period is estimated using the “Approximate Rayleigh Method”, method no 7 proposed by Dobry et al. (1976) and the Vs profile for the deep layers was adjusted by iteration.
- Profile S1: in the same manner, Vs profile from SCPT-11-13 was extended based on triaxial seismometer results using data from borehole NS-2-13. However in this case, the

exact calibration to the fundamental period of 0.95 sec was not possible probably due to the sloping bedrock surface as shown on Figure C-17. To be on the conservative side, the extrapolated Vs profile was selected with values greater than the linear extrapolation of measured values.

- Profile P2: no triaxial seismometer test and no deep borehole were performed near CPT-24-13 for P2 downstream toe profile at Section 13. Based on P1 and S1 profiles, a Gmax distribution as a function of the effective overburden stress was estimated and the results were extrapolated to section P2 as illustrated on Figure C-18. Such a common Gmax – σ'_v relationship was required for the 2D analyses for a smooth transition between the crest P1 profile to the toe P2 profile. This extrapolation takes into an account that, a given elevation, measured Vs values for granular material are characterised by higher Vs values than for clay material.

5.3.2 RESULTS OF ANALYSES

The results of the 1D equivalent-linear dynamic response analyses are shown on the figures of Appendix D.

P1 Downstream Crest Profile (Deep bedrock)

Figure D-4 shows the CRR and CSR for P1 Downstream (WL 15 m) Profile at Section 13 (deep bedrock at elevation -210 m):

- CRR profiles are based on SCPT-09-13 Tip Resistance for Sand-like material (liquefaction) and Interpreted Undrained Shear Strength for Clay-like material (cyclic softening);
- CSR Profiles were obtained from 1D Equivalent-linear Analyses with all the initially selected Input Motions from a) Far Field Event Scenario; b) Near Field Event Scenario; c) Saguenay 1988 Recordings; d) Nahanni 1985 Recordings; e) Accelerograms Used in Preliminary Dynamic Study; f) Maximum CSR Profiles for Each Group of Input Motions.

  See Figures B-2 to B-6 of Appendix B for details on input motion characteristics.

Selection of Input Motions for 1D Analyses

Based on these results, 17 input motions (see Figure B-7) were selected for the analyses of the cases representative of the following conditions:

- Upstream conditions:

  These conditions were modeled using the same stratigraphic profile as the P1 Downstream (WL 15 m) analyses but assuming a normal reservoir elevation of 39 m and a water level of 30 m in the slope below the crest.

  Figure D-5 compares the CRR and CSR for P1 Downstream (WL 15 m) and Upstream (WL 30 m) profiles: the upstream conditions are more severe because the water table elevation is higher; the saturated zone is reaching higher in the stratified drift and the effective vertical stress is lower; therefore the CSR is higher.

- Shallow bedrock (-55 m) conditions:

  S1 profile (crest profile for Section 9) was analysed and the results are presented in Figure D-6 for the upstream water table elevation (WL 30 m). CRR profiles are based on SCPT-11-13 Tip Resistance for Sand-like material (liquefaction) and Interpreted Undrained Shear Strength for Clay-like material (cyclic softening).

  These analyses show that the shallower S1 profile is on average more severe than profile P1 with deep bedrock. However, everywhere CRR is greater than CSR indicating no significant risk of liquefaction or cyclic softening under the design earthquake.

Selection of Input Motions for 2D Analyses

Based on the characteristics of the scenarios to be considered (see Table 3-3) and on the results of the 1D equivalent-linear analyses, eight input motions were selected for the 2D Analyses (see Figure B-7). Figure D-7 shows the CRR and CSR from 1D analyses for P1 (deep bedrock) and S1 (shallow bedrock) profiles with Upstream WL of 30 m for these eight input motions.

Downstream Toe Profile

The same input motions have been applied to the P2 Downstream toe profile (deep bedrock) with the following data:

- CRR profile are based on CPT-24-13 and CPT-08-13; the thin sand layers do not seem to be continuous;
- CSR Profiles from 1D equivalent-linear analyses with input motions selected for 2D analyses (see Figure B-7).

  The results are illustrated on Figure D-8: they indicate that the clay below the toe of the North Spur offers good resistance relative to cyclic softening under the design earthquake.

The 1D equivalent-linear analyses indicate adequate provision against liquefaction for granular material and cyclic softening for clay material.

5.4 2D EQUIVALENT-LINEAR ANALYSES

2D equivalent-linear analyses were performed to study the 2D propagation of the selected input motions.

5.4.1 Representative section

A 2D representation of Section 13 was developed based on the 3D Catia model. The vertical profile for P1 (crest profile) is somewhat different from what was assumed in 1D analyses based only on SCPT-09-13 and nearby D5-79 borehole: the clay layer reaches deeper. However, this has little influence on the results of equivalent-linear analyses that are sensitive mainly to the Gmax profile that was estimated based on Vs measurements. The water table in the profile is based on a 3D seepage model and 2D seepage analyses performed. The normal water level below the crest is expected to be at an elevation of 15 m after the completion of the stabilization works. The normal water level at the toe is expected to still be at about 3 m.

5.4.2 DYNAMIC PROPERTIES

The material properties assumed for the 2D equivalent-linear analyses are shown in Figure F-1. They are generally similar to those used in the 1D equivalent-linear analyses. As illustrated on Figure C-18, Gmax was correlated to the effective vertical stress in order to obtain a relationship applicable for each soil layer.

5.4.3 Input motions

Eight input motions were selected for the 2D Equivalent-linear analyses based on the specifications of the scenarios (see Table 3-3) and on the results of the 1D equivalent-linear analyses (see Figure D-7). Their properties are summarised on Figure B-7 and presented in details on the figures of Appendix E: Husid plots are provided together with acceleration, velocity and displacement history plots.

5.4.4 RESULTS OF ANALYSES

The results of the 2D equivalent-linear dynamic response analyses are shown on the figures of Appendix F. Two cases were analysed: the base case with the deep bedrock assumed at an elevation of -210 m for Section 13 (see results on Figure F-2 for P1 crest profile and Figure F-4 for P2 toe profile); a case with a shallower bedrock at -55 m to represent the conditions assumed near Section 9 in the southern portion of the Spur (see results on Figure F-5 for S1 crest profile).

In both cases, the analyses indicate that CSR for all the input motions are lower than the selected CRR profiles for liquefaction of sand-like material and for cyclic softening of clay-like material (see selection of CRR profiles on Figure C-9) except for the sand-like material on P2 toe profile; as noted above, many of the weaker SPT indices are believed to have been affected by the presence of interlayers of clay-like material and these sand-like material layers are not continuous. This indicates that liquefaction and cyclic softening should not be an issue for Section 13 and Section 9.

As complementary information, for the analysis of the first case (Section 13) submitted to input motion SAG-16T, Figure F-3 shows the Arias' Intensity and Husid Plots. It indicates that the energy is transmitted and amplified from the base of the model to the top of the stratified drift but is somewhat attenuated in the surface layers.

5.5 2D NON-LINEAR DYNAMIC RESPONSE ANALYSES (FLAC)

Even if the 1D and 2D equivalent-linear analyses indicated no potential for liquefaction of the granular materials or potential for cyclic softening for the clay, Section 13 was submitted to 2D non-linear dynamic response analyses *to assess the pattern of deformations that may be induced by the postulated earthquake ground motions* as proposed by Prof. Idriss (see section 1.3). These analyses were performed using FLAC version 7.0.411 (Itasca, 2011).

5.5.1 Representative section

A 2D representation of Section 13 was developed based on the 3D Catia model. The vertical profile for P1 (crest profile) is somewhat different from what was assumed in 1D analyses based only on SCPT-09-13 and nearby D5-79 borehole: the clay layer reaches deeper. The section developed for non-linear analyses is very similar to the section submitted to 2D Equivalent-linear analyses. The geometry of the model, the stratigraphy and the location of the control points are shown on Figure G-1 of Appendix G.

5.5.2 DYNAMIC PROPERTIES

The material properties assumed for the 2D non-linear analyses are listed in Table G-1 of Appendix G. The properties are generally similar to those of the equivalent-linear analyses. They are based on the investigation data presented above in sections 2.2 and 5.2, and otherwise on typical values for these kinds of materials. The relationship of Gmax as a function of the effective vertical stress developed for 2D equivalent-linear analyses was maintained in order to obtain a relationship applicable for each soil layer with a smooth variation horizontally.

As can be seen on Figure G-2, two constitutive models of material behavior were used in the modeling: the Mohr-Coulomb model as implemented in FLAC and the UBCSand model (version 904aR) developed by Beaty and Byrne (2011). The UBCSand model was used for the Upper Sand and the granular part of the Stratified Drift. The other materials were represented using the Mohr-Coulomb model.

The generic version of the UBCSand model is based on $(N_1)_{60cs}$. A representative $(N_1)_{60cs}$ profile was developed based on CPT qc1N profiles and on $(N_1)_{60cs}$ from 1979 SPT tests. The profile shown on figure C-13 was selected to produce, in the generic UBCSand model, a Gmax profile consistent with the Vs values measured in 1979 SCPT tests.

The generic version of the UBCSand model generates modulus reduction and damping. For the other materials, hysteretic damping is added and adjusted to fit the modulus reduction and damping curves used in the 1D and 2D Equivalent-linear Analyses.

5.5.3 Input motions

Three input motions matched to the Design Response Spectrum were selected for the 2D non-linear analyses based on the specifications of the scenarios (see Table 3-3): Their properties are summarised on Table 5-1 and presented in detail on the figures of Appendix E: Husid plots are provided together with acceleration, velocity and displacement history plots.

Input motion TAP035-N is representative of the Far Field Events Scenario and input motions Sag-16T and S2330 of the Near Field Events Scenario.

Table 5-1: Input Motions Selected for 2D Non-linear Dynamic Response Analyses

CASE	**TAP035-N**	**Sag-16T**	**S2330**
DATA BASE	USGS	USCS	PEER
Mw	7,6	5,9	6,76
Distance (km)	96,8	51,9	4,9
USGS Code	A		
Campbell's GEOCODE	---		**D**
SITE TYPE	ROCK	ROCK	
LOCATION	Chi-Chi, Taiwan	SAGUENAY 1988	Nahanni 1985
dT (s) =	0,005	0,005	0,005
a_{max} (m/s^2) =	0,50	0,45	0,52
a_{max} (g) =	0,05	0,05	0,05
I_{Af} (m/s) =	**0,03**	**0,03**	**0,02**
Husid Time (s) =	**50,9**	**16,0**	**10,7**

5.5.4 ANALYSES RESULTS

The results of the 2D non-linear dynamic response analyses are shown on the figures of Appendix G. Each case includes the following steps:

- Analysis of the static conditions, ensuring both mechanical and seepage equilibrium; the effective vertical stress distribution and the pore pressure distribution at the end of the static analysis are shown on Figure G-3 and G-4.
- Dynamic response analysis: the model was submitted to one of the three selected input motions. The results of the three dynamic analyses along the P1 vertical crest profile are summarised on Figure G-5.

  The detailed results are presented on figures G-6 to G-15 for input motion Sag-16T, G-16 to G-25 for Nahanni S2330 and G-26 to G-35 for TAP035-N. In each case, the pore pressure distribution and the effective vertical stress distribution at the end of shaking is presented and can be compared to the end of static analysis distributions. The distribution at the end of shaking of horizontal and vertical displacement and of pore overpressure ratio, $r_u = {\Delta\sigma'_{vo}}/{\sigma'_{vo}}$ are also shown. It should be noted that this definition of r_u allows the parameter to follow changes in the effective vertical stress due to stress redistribution as well as excess porewater pressure variation.

  Finally, the variation in time of the Cyclic Stress Ratio (CSR), the horizontal displacement, the shear strain and the shear stress are provided for some of the control points located on Figure G-1.

In general, the results indicate displacements of the crest of less than 3 cm both horizontally and vertically, very little porewater pressure increase and conditions at the end of shaking very similar to those at the end of the static analysis.

5.6 DISCUSSION

5.6.1 Maximum Acceleration near Ground Surface

The results from 2D non-linear analyses are generally in accordance with the results from 1D and 2D equivalent-linear analyses. However, some 2D non-linear analyses have resulted in unrealistically high a_{max} values near the ground surface as can be seen on Figure G-5 on the a_{max} profile.

Some verification analyses were performed for profile P1, water level at 15 m and the Sag-16T input motion. The results are presented on Figure G-26 and compared with 1D and 2D equivalent-linear analyses. First, a 2D non-linear analysis was carried without the UBCSand model, using instead the Mohr-Coulomb constitutive model. The results are very similar to those obtained in 1D equivalent-linear analyses using EZ-Frisk.

Then, the same case was run using for the Upper Sand and the Stratified Drift version 2 of the PM4-Sand model developed by Boulanger and Ziotopoulou (2012) and recently implemented for FLAC. For these analyses performed as an indication only, relative density Dr and Go were estimated with generic relationships based on constant values of SPT $(N_1)_{60}$:

PM4Sand Model	**$(N_1)_{60}$**	**Relative Density Dr**	**G_o**
Upper Sand	14	0,56	678
Stratified Drift	13	0,54	657

The results of these analyses confirm that the a_{max} values near the ground surface obtained with the UBCSand model are unrealistic. It is also confirmed that these acceleration spikes near the surface do not affect significantly the profiles of maximum shear stress τ_{max} and cyclic stress ratio CSR: these profiles for the UBCSand and PM4-Sand analyses are very similar.

5.6.2 Crest Displacement

In general, the 2D non-linear analyses indicate displacements of the crest of less than 3 cm both horizontally and vertically. It can be noted that these results are of the same order of magnitude as the amplitude of the crest displacement history in 1D equivalent-linear analyses as can be seen on Figure D-9 for the three input motions used for 2D non-linear analyses.

As an indication, the crest displacement was also estimated using the simplified procedure proposed by Bray and Travasarou (2007) for estimating seismic slope displacements. In this method, the crest displacement is estimated taking into account the following parameters:

Parameter	**Estimation**	**Value estimated for North Spur Profile P1**
Yield coefficient k_y	From pseudostatic stability analyses	k_y = 0,12
Initial fundamental period T_s	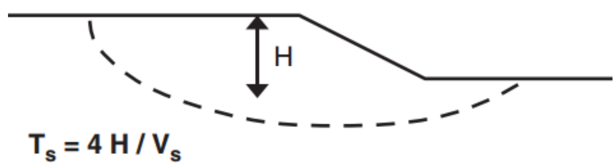	T_s = 0.5 – 1.0 s 1.5 T_s = 0.8 – 1.5 s
Spectral acceleration (Sa) of the sliding mass for 1.5 T_s	From the amplified response spectrum in the sliding mass estimated in 2D equivalent-linear analyses	0.09 – 0.18 g

For a magnitude Mw of 7.3 (deaggregation results for low frequency events, see Section 3.2), the predicted crest displacement is between 0,2 and 2,9 cm for an exceedance probability of 84 to 16% (+/- one standard deviation).

6 CONCLUSION

Based on recommendations by Prof. Idriss and taking into account Prof. Leroueil's remarks, a complementary dynamic study of the long term conditions of the North Spur was undertaken. The seismic hazard analysis of the site was revised by Prof. Atkinson based on updated seismic source database and attenuation relationships. Seismic scenarios were selected based on deaggregation of the hazard. Input motions were selected to represent these scenarios and spectrally matched to the Uniform Hazard Spectrum (UHS) for a return period of 10 000 years.

Uphill and downhill vertical soil profiles and a cross-section representative of the most critical site conditions were submitted to the selected input motions using 1D and 2D equivalent-linear dynamic response modelling. The results were compared to the resistance of the different soil layers based on investigation data from boreholes, SPT, CPT and SCPT tests performed at the site. The resistance to liquefaction for granular materials and to cyclic softening for clay was estimated using the methods proposed by Idriss and Boulanger (2008).

The results indicate no potential for liquefaction of the granular materials or potential for cyclic softening of the clay. As proposed by Prof. Idriss, a cross-section was also submitted to indicative 2D non-linear dynamic response analyses. These analyses confirmed the findings of the equivalent-linear analyses.

In conclusion, based on the findings of this complementary dynamic study, the North Spur integrity is not expected to be affected by the occurrence of the design seismic event (probability of 1/10 000). This applies to the conditions that were considered and that are described in the report.

Limitations and Sensitivity

The validity of these conclusions are limited by the representativity of the conditions assumed that can differ from the site conditions: it should be noted that little information is known on the dynamic properties of the material below elevation -10 m and the data available were extrapolated to greater depth. However, it was observed from the index tests that the lower clay layer is significantly less sensitive than the upper clays. The behavior of the granular material can be very sensitive to their saturation. It was assumed that the design earthquake would occur under normal seepage conditions. The normal elevation of the water table in the North Spur was estimated based the conditions predicted by previous seepage analyses. The actual seepage conditions will have to be confirmed by monitoring at the various stages of construction and of reservoir filling.

7 REFERENCES

Al Atik, L. And Ambrahamson, N. (2010) An Improved Method for Nonstationary Spectral Matching, *Earthquake Spectra*, Volume 26, No. 3, pages 601-617, August 2010.

AMEC (2013) Geotechnical Investigations Report - 2013 Field Investigations – North Spur, Muskrat Falls Hydroelectric Development, Lower Churchill Project. AMEC Project No. TF13104118. November 2013.

Atkinson, G. (2014) *Earthquake Hazard Analysis: Muskrat Damsite, Lower Churchill, Labrador.* Draft Report to SNC-Lavalin, May 22, 2014.

Beaty, M. and Byrne, P.M. (2011) *UBCSAND Constitutive Model, Version 904aR*. Beaty Engineering LLC and University of British Columbia. February, 2011

Boulanger, R. W., and Ziotopoulou, K. (2012). “PM4Sand (version 2): A sand plasticity model for earthquake engineering applications.” Report No. UCD/CGM-12/01, Center for Geotechnical Modeling, Department of Civil and Environmental Engineering, University of California, Davis, CA, May, 100 pp. (Revision 1 posted July 2012 – Boulanger_Ziotopoulou_Sand_Model_CGM-12-01_2012_rev1)

Bray, J. D., and Travasarou, T. (2007) “Simplified procedure for estimating earthquake-induced deviatoric slope displacements.” J. Geotech. Geoenviron. Eng., 1334, 381–392.

Canadian Dam Association (CDA, 2013) Dam Safety Guidelines and Technical Bulletins. 2013 Revision of 2007 Version.

Dobry, R., Oweis, I. And Urzua, A. (1976) Simplified Procedures for Estimating the Fundamental Period of a Soil Profile. Bulletin of the Seismological Society of America, Vol.66, No.4, pp. 1293 1321.August 1976

Fugro’s Risk Engineering group (Fugro, 2011a) Site Response module of EZ-Frisk, 1D Equivalent-linear method using Shake91+, version 7.62.

Fugro's Risk Engineering group (Fugro, 2011b) Spectral Matching module of EZ-FRISK, Earthquake ground motion estimation, version 7.62.

Geo-Slope International (2013) Quake/W module of GeoStudio Suite, 2D Equivalent-linear method, version 8.12.3.7901.

Idriss, I.M. (2014) *Appendix 4 to SNC-Lavalin's Report - Review of Seismic Performance of the North Spur - Lower Churchill Project.* Draft Report, 31-Jan-2014.

Idriss, I.M. and Boulanger, R.W. (2008). Soil Liquefaction during Earthquakes. MNO-12, Earthquake Engineering Research Institute, Oakland, CA.

Idriss, I.M. and Sun, J.I. (1992). « SHAKE91: a computer program for conducting equivalent linear seismic response analyses of horizontally layered soil deposits." User's Guide, University of California, Davis.

Itasca Consulting Group (Itasca) (2011). FLAC – Fast Langrangian Analysis of Continua: two-dimensional explicit finite difference program for engineering mechanics computation, version 7.0.411.

Lee (2009) *Engineering Characterization of Earthquake Ground Motions*. Ph.D. Dissertation University of Michigan, 2009.

Leroueil, S. (2013) *Dynamic Study Workshop, North Spur, Muskrat Falls project.* Report, 13-Dec-2013.

Seed H.B. and Idriss, I.M. (1970). Soil moduli and damping factors for dynamic response analyses. Report EERC 70-10, Earthquake Engineering Research Center, University of California, Berkeley.

Seed, R.B., Wong, R.T., Idriss, I.M. and Tokimatsu, K. (1986). Moduli and Damping Factors for Dynamic Analyses of Cohesionless Soils, Journal of Geotechnical Engineering Division, ASCE, Vol. 112, No. GT11, pp 1016-1032.

SNC-Lavalin Newfoundland Ltd (SNC-Lavalin NL, 1980) Engineering Report and 1979 Field Investigation Program. Volumes I to IV, March 1980.

SNC-Lavalin (SLI, 2015a) *Lower Churchill Project - Engineering Report - North Spur Stabilization*. Draft Report no 505573-3281-4GER-0001-PA, April 2015.

SNC-Lavalin (SLI, 2015b) Technical Specifications and drawings.

APPENDICES

NOTE – APPENDICES NOT CHANGED FROM PREVIOUS REVISION

APPENDIX A – DRAWINGS – GEOLOGICAL AND GEOTECHNICAL INFORMATION

APPENDIX B – INPUT MOTION INITIAL SELECTION

APPENDIX C – SELECTED PIEZOCONE TESTS AND ASSOCIATED BOREHOLES – INVESTIGATION DATA AND INTERPRETED CRR AND VS PROFILES

APPENDIX D – 1D EQUIVALENT-LINEAR ANALYSES

APPENDIX E – INPUT MOTION SELECTION FOR 2D ANALYSES

APPENDIX F – 2D EQUIVALENT-LINEAR ANALYSES

APPENDIX G – 2D NON-LINEAR ANALYSES

APPENDIX A

DRAWINGS – GEOTECHNICAL INFORMATION

A. DRAWINGS – GEOTECHNICAL INFORMATION

Drawing MFA-SN-CD-2800-GT-PL-0012-01

Drawing MFA-SN-CD-2800-GT-SE-0004-01

Drawing MFA-SN-CD-2800-GT-SE-0004-02

Drawing MFA-SN-CD-2800-GT-SE-0004-03

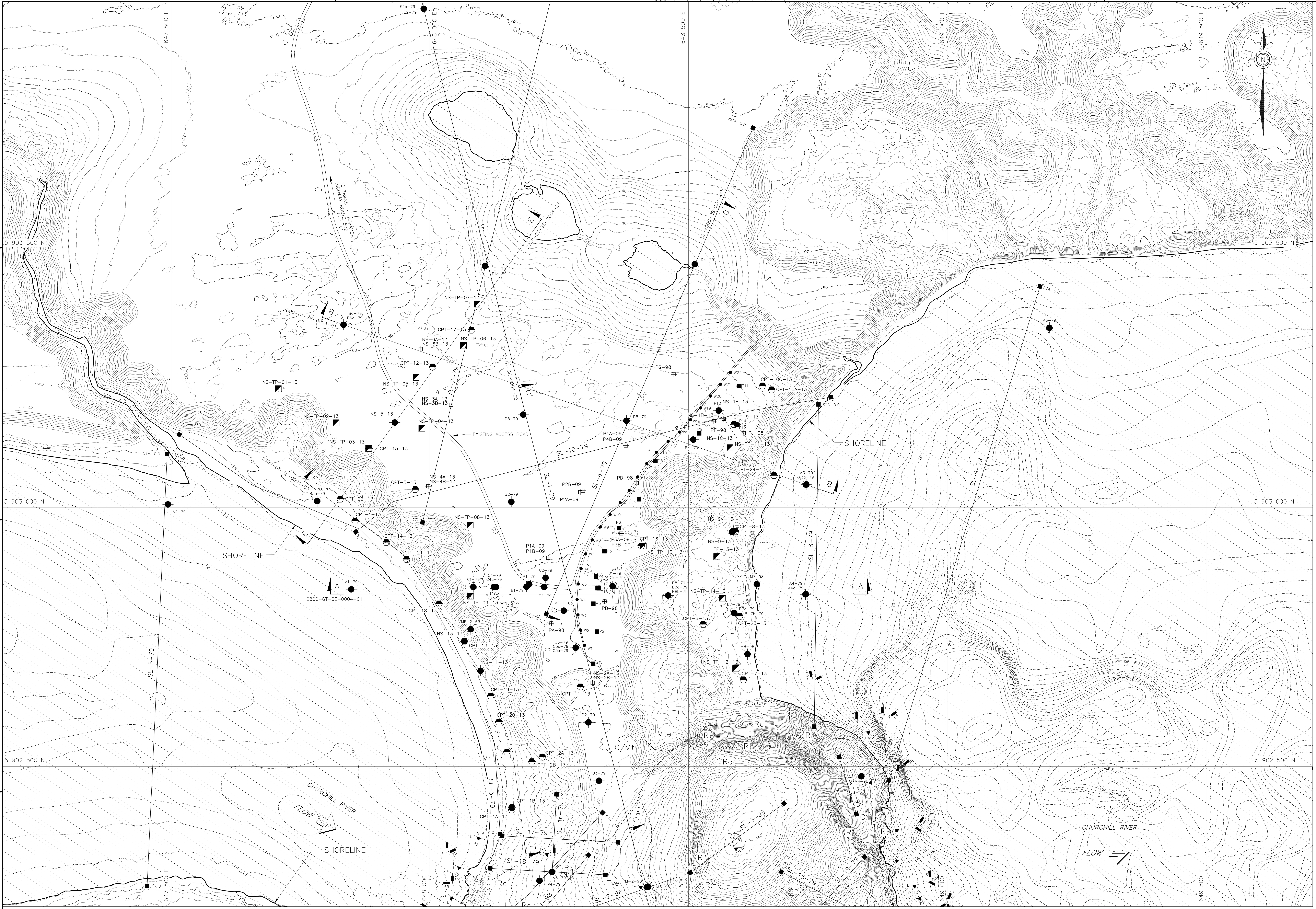

PLAN

NOTES:

1. ALL COORDINATES ARE REFERENCED TO UTM NAD83, ZONE 20.
2. THE GROUND TOPOGRAPHY CONTOURS ARE BASED ON A SITE-SPECIFIC LIDAR SURVEY COMPLETED IN 2006.
3. THE RIVER BATHYMETRY CONTOURS ARE BASED ON AN AIRBORNE BATHYMETRIC SURVEY COMPLETED IN 1998.
4. THE CONTOUR INTERVAL OF THE GROUND TOPOGRAPHY AND THE RIVER BATHYMETRY IS 2 METRES.
5. ELEVATIONS AND DIMENSIONS ARE IN METRES UNLESS NOTED OTHERWISE.

LEGEND:

TOPOGRAPHIC CONTOUR
BATHYMETRIC CONTOUR
SPRING FLOOD WATER LEVEL
SSSSSSSSS SHEAR ZONE
SSS SSS ASSUMED SHEAR ZONE
GEOLOGICAL BOUNDARY
SEISMIC LINE
EXPOSED ROCK
ANGLE INCLINED JOINT
VERTICAL JOINT
ANGLE INCLINED FOLIATION
VERTICAL BOREHOLE
INCLINED BOREHOLE
W9 PUMPING WELL
P6 LOST PIEZOMETER
no-YEAR EXISTING PIEZOMETER
NS-no-13 2013 BOREHOLE
CPT-no-13 2013 CPT TEST
NS-TP-no-13 2013 TEST PIT
EL ELEVATION
INT INTERSECTION

SURFICIAL GEOLOGY:

C	COLLUVIAL
A	AEOLIAN
G	GLACIOFLUVIAL
M	MARINE
T	GLACIAL TILL
O	BOG
R	ROCK
c	CONCEALED BY VEGETATION
e	ERODED AND DISSECTED
p	PLAIN
r	RIDGE
t	TERRACE
v	VENEER

PROVINCE OF NEWFOUNDLAND PERMIT HOLDER CLASS "A"
This Permit Allows
SNC-LAVALIN Inc.
To practice Professional Engineering in Newfoundland and Labrador. Permit No. as issued by PEGNL N0458 which is valid for the year 2013.

0 50 100 150 200 m
SCALE 1:2500

ISSU.	REV.	DATE	DISTRIBUTION & STATUS	ISSU.	REV.	DATE	DISTRIBUTION & STATUS
1	C1	07-NOV-2013	ISSUED FOR INFORMATION				

ISSUE REGISTER

No.	REFERENCE DRAWING
MFA-SN-CD-2800-GT-SE-0004-03	EXISTING GEOLOGICAL AND GEOTECHNICAL INFORMATION - NORTH SPUR SECTIONS - SHEET 3 OF 3
MFA-SN-CD-2800-GT-SE-0004-02	EXISTING GEOLOGICAL AND GEOTECHNICAL INFORMATION - NORTH SPUR SECTIONS - SHEET 2 OF 3
MFA-SN-CD-2800-GT-SE-0004-01	EXISTING GEOLOGICAL AND GEOTECHNICAL INFORMATION - NORTH SPUR SECTIONS - SHEET 1 OF 3

No.	REFERENCE DRAWING	No.	DATE	REVISION	MOD.	VER.	APP.

* * * * * * * * * FOR INTERNAL USE ONLY * * * * * * * * *

REVIEW CLASS: | EQUIPMENT TAG NUMBER:

REVIEW DOES NOT CONSTITUTE APPROVAL OF DESIGN DETAILS, CALCULATIONS, TEST METHODS OR MATERIAL DEVELOPED AND/OR SELECTED BY THE CONTRACTOR, NOR DOES IT RELIEVE THE CONTRACTOR FROM FULL COMPLIANCE WITH CONTRACTUAL OR OTHER OBLIGATIONS.

- ☐ 1. REVIEWED AND ACCEPTED NO COMMENTS
- ☐ 2. REVIEWED - INCORPORATE COMMENTS, REVISE & RESUBMIT
- ☐ 3. REVIEWED - NOT ACCEPTED
- ☐ 4. INFORMATION ONLY
- ☐ 5. NOT REVIEWED

LEAD REVIEWER: Date (dd-mmm-yyyy):
NE-LCP MANAGEMENT: Date (dd-mmm-yyyy):
PROJECT MANAGER: Date (dd-mmm-yyyy):

PROFESSIONAL STAMP
REGISTERED PROFESSIONAL ENGINEER PEG Newfoundland and Labrador
NASSER DAIYAN
SIGNATURE
07-NOV-2013
DATE
NEWFOUNDLAND & LABRADOR

SNC·LAVALIN

DESIGNED BY N. DAIYAN
DRAWN BY R. MERRI
VERIFIED BY A. CEBALLOS
DATE 22 SEP 2012
APPROVED Discipline Lead Engineer R. BOUCHARD
APPROVED Engineering Manager G. SNYDER
SCALE 1:2500

CLIENT nalcor energy LOWER CHURCHILL PROJECT

PROJECT LOWER CHURCHILL PROJECT

TITLE MUSKRAT FALLS
NORTH SPUR STABILIZATION WORKS
EXISTING GEOLOGICAL AND GEOTECHNICAL INFORMATION
PLAN

File No. 505573-3281-4GDD-0008-01
MFA-SN-CD-2800-GT-PL-0012-01 Rev. C1
FORMAT A0 (mm)

SUB-PKG: 0008-4G03 PLATE G04

2013.11.21/10:40am

NOTE:

1. FOR NOTES AND LEGEND SEE DRAWING MFA-SN-CD-2800-GT-SE-0004-03.

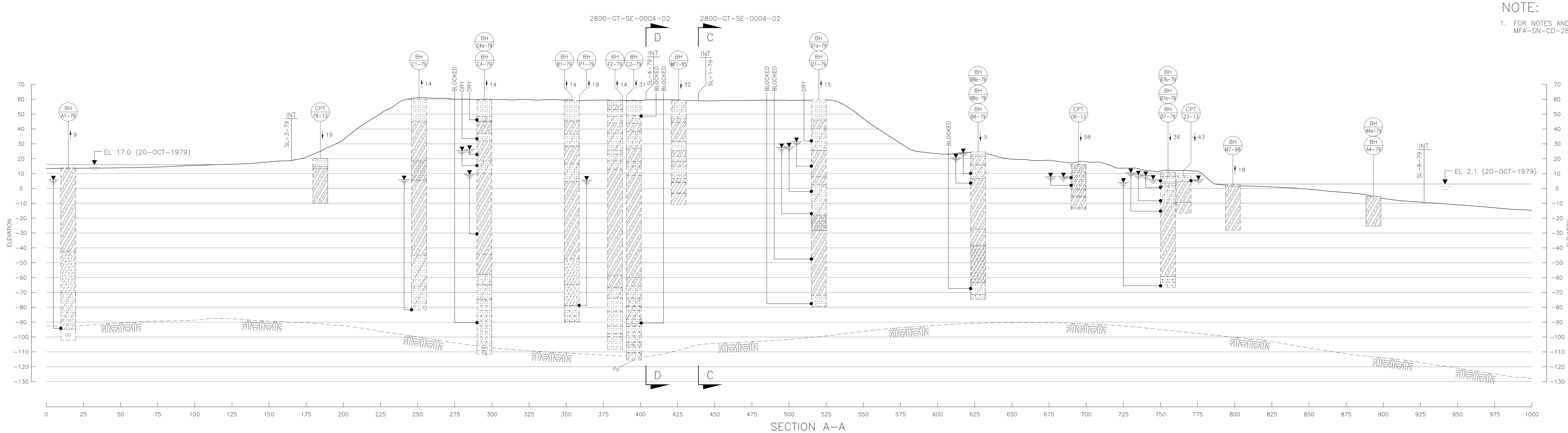

SECTION A-A

2800-GT-PL-0012-01

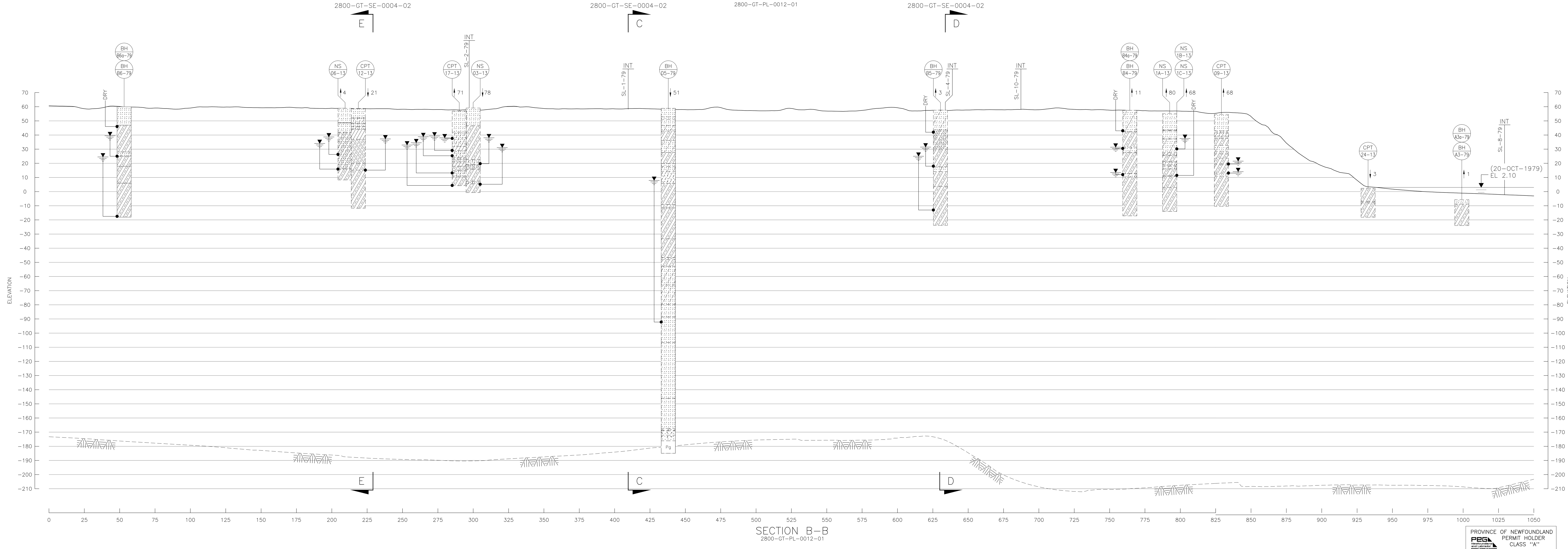

SECTION B-B

2800-GT-PL-0012-01

SCALE 1:1000

PROVINCE OF NEWFOUNDLAND PERMIT HOLDER CLASS "A"
This Permit Allows
SNC-LAVALIN Inc.
To practice Professional Engineering in Newfoundland and Labrador.
Permit No. as issued by PEGNL N0458 which is valid for the year 2013.

ISSU.	REV.	DATE	DISTRIBUTION & STATUS	ISSU.	REV.	DATE	DISTRIBUTION & STATUS
1	C1	07-NOV-2013	ISSUED FOR INFORMATION				

ISSUE REGISTER

No.	REFERENCE DRAWING
MFA-SN-CD-2800-GT-SE-0004-03	EXISTING GEOLOGICAL AND GEOTECHNICAL INFORMATION – NORTH SPUR SECTIONS – SHEET 3 OF 3
MFA-SN-CD-2800-GT-SE-0004-02	EXISTING GEOLOGICAL AND GEOTECHNICAL INFORMATION – NORTH SPUR SECTIONS – SHEET 2 OF 3
MFA-SN-CD-2800-GT-PL-0012-01	EXISTING GEOLOGICAL AND GEOTECHNICAL INFORMATION – NORTH SPUR PLAN

No.	REFERENCE DRAWING	No.	DATE	REVISION	MOD.	VER.	APP.

* * * * * * * * * FOR INTERNAL USE ONLY * * * * * * * * *

REVIEW CLASS: | EQUIPMENT TAG NUMBER:

REVIEW DOES NOT CONSTITUTE APPROVAL OF DESIGN DETAILS, CALCULATIONS, TEST METHODS OR MATERIAL DEVELOPED AND/OR SELECTED BY THE CONTRACTOR, NOR DOES IT RELIEVE THE CONTRACTOR FROM FULL COMPLIANCE WITH CONTRACTUAL OR OTHER OBLIGATIONS.

- ☐ 1. REVIEWED AND ACCEPTED NO COMMENTS
- ☐ 2. REVIEWED - INCORPORATE COMMENTS, REVISE & RESUBMIT
- ☐ 3. REVIEWED - NOT ACCEPTED
- ☐ 4. INFORMATION ONLY
- ☐ 5. NOT REVIEWED

LEAD REVIEWER: Date (dd-mmm-yyyy):

NE-LCP MANAGEMENT: Date (dd-mmm-yyyy):

PROJECT MANAGER: Date (dd-mmm-yyyy):

PROFESSIONAL STAMP

REGISTERED PROFESSIONAL ENGINEER PEG Newfoundland and Labrador NASSER DAIYAN SIGNATURE 07-NOV-2013 DATE NEWFOUNDLAND & LABRADOR

SNC·LAVALIN

DESIGNED BY N. DAIYAN | APPROVED Discipline Lead Engineer R. BOUCHARD

DRAWN BY R. MERRI

VERIFIED BY A. CEBALLOS | APPROVED Engineering Manager G. SNYDER

DATE 22-SEP-2012 | SCALE 1:1000

CLIENT: nalcor energy LOWER CHURCHILL PROJECT

PROJECT: LOWER CHURCHILL PROJECT

TITLE: MUSKRAT FALLS NORTH SPUR STABILIZATION WORKS EXISTING GEOLOGICAL AND GEOTECHNICAL INFORMATION SECTIONS – SHEET 1 OF 3

SLI DOC No. 505573-3281-4GDD-0018-SH1-01

NE DOC No. MFA-SN-CD-2800-GT-SE-0004-01 Rev. C1

FORMAT A0 (mm)

G:\505573\4L_Drafting\Drawings\Civil\Issued\3281\F_C1_07-NOV-2013\BOUND\
MFA-SN-CD-2800-GT-SE-0004-01.dwg

2013.11.20/12:10pm

NOTE:

1. FOR NOTES AND LEGEND SEE DRAWING MFA-SN-CD-2800-GT-SE-0004-03.

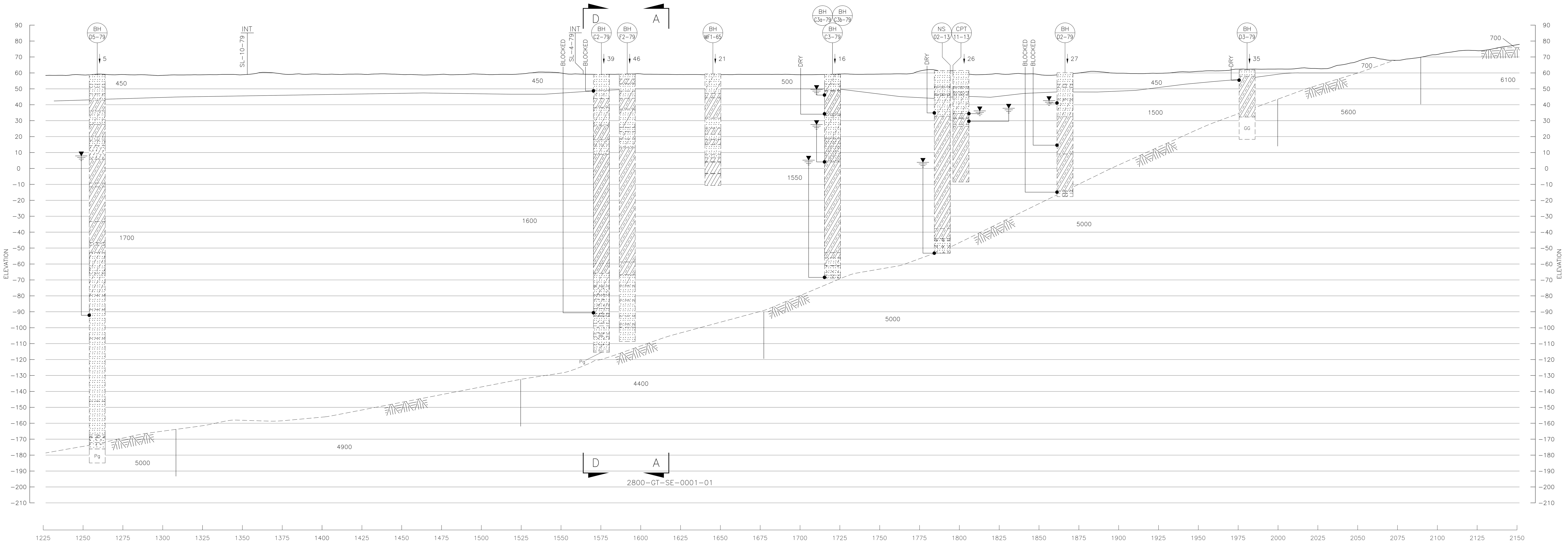

SECTION C–C SEISMIC LINE SL–1–79

2800–GT–PL–0012–01

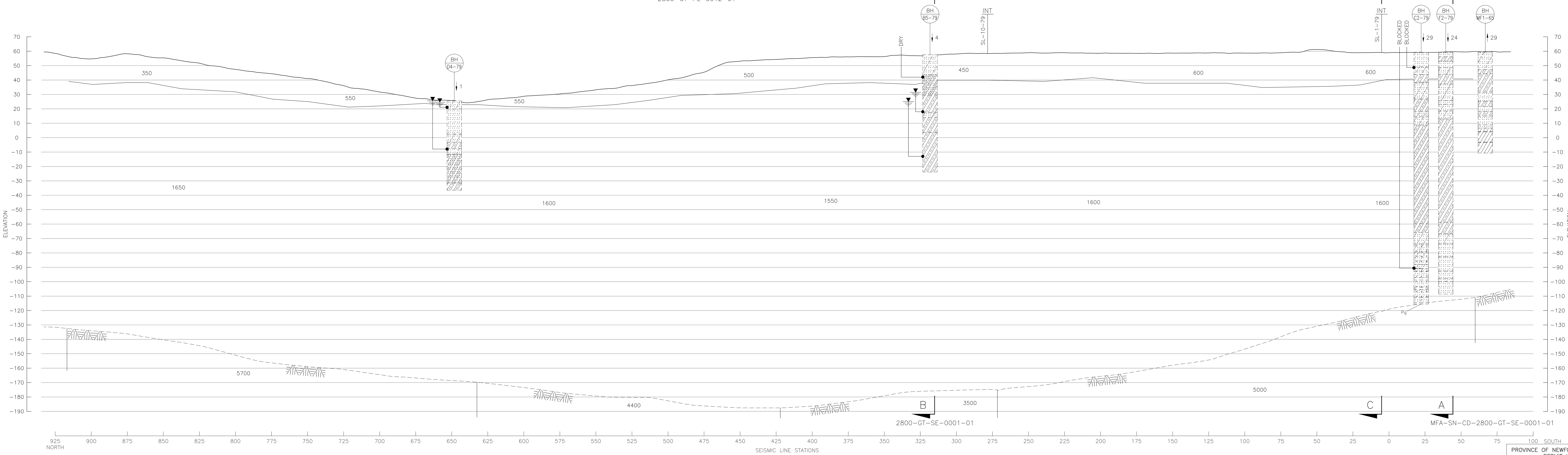

SECTION D–D SEISMIC LINE SL–4–79

2800–GT–PL–0012–01

0 10 20 30 40 50 100 m

SCALE 1:1000

PROVINCE OF NEWFOUNDLAND PERMIT HOLDER CLASS "A"
This Permit Allows
SNC–LAVALIN Inc.
To practice Professional Engineering in Newfoundland and Labrador.
Permit No. as issued by PEGNL N0458 which is valid for the year 2013.

ISSU.	REV.	DATE	DISTRIBUTION & STATUS	ISSU.	REV.	DATE	DISTRIBUTION & STATUS
1	C1	07–NOV–2013	ISSUED FOR INFORMATION				

ISSUE REGISTER

No.	REFERENCE DRAWING
MFA–SN–CD–2800–GT–SE–0004–03	EXISTING GEOLOGICAL AND GEOTECHNICAL INFORMATION – NORTH SPUR SECTIONS – SHEET 3 OF 3
MFA–SN–CD–2800–GT–SE–0004–01	EXISTING GEOLOGICAL AND GEOTECHNICAL INFORMATION – NORTH SPUR SECTIONS – SHEET 1 OF 3
MFA–SN–CD–2800–GT–PL–0012–01	EXISTING GEOLOGICAL AND GEOTECHNICAL INFORMATION – NORTH SPUR PLAN

No.	DATE	REVISION	MOD.	VER.	APP.

* * * * * * * * * FOR INTERNAL USE ONLY * * * * * * * * *

REVIEW CLASS: EQUIPMENT TAG NUMBER:

REVIEW DOES NOT CONSTITUTE APPROVAL OF DESIGN DETAILS, CALCULATIONS, TEST METHODS OR MATERIAL DEVELOPED AND/OR SELECTED BY THE CONTRACTOR, NOR DOES IT RELIEVE THE CONTRACTOR FROM FULL COMPLIANCE WITH CONTRACTUAL OR OTHER OBLIGATIONS.

- ☐ 1. REVIEWED AND ACCEPTED NO COMMENTS
- ☐ 2. REVIEWED - INCORPORATE COMMENTS, REVISE & RESUBMIT
- ☐ 3. REVIEWED - NOT ACCEPTED
- ☐ 4. INFORMATION ONLY
- ☐ 5. NOT REVIEWED

LEAD REVIEWER: Date (dd-mmm-yyyy):

NE-LCP MANAGEMENT: Date (dd-mmm-yyyy):

PROJECT MANAGER: Date (dd-mmm-yyyy):

PROFESSIONAL STAMP

REGISTERED PROFESSIONAL ENGINEER PEG Newfoundland and Labrador
NASSER DAIYAN
SIGNATURE
07–NOV–2013
DATE
NEWFOUNDLAND & LABRADOR

SNC·LAVALIN

DESIGNED BY N. DAIYAN

DRAWN BY R. MERRI

VERIFIED BY A. CEBALLOS

DATE 22–SEP–2011

APPROVED Discipline Lead Engineer R. BOUCHARD

APPROVED Engineering Manager G. SNYDER

SCALE 1:1000

CLIENT nalcor energy LOWER CHURCHILL PROJECT

PROJECT LOWER CHURCHILL PROJECT

TITLE MUSKRAT FALLS NORTH SPUR STABILIZATION WORKS EXISTING GEOLOGICAL AND GEOTECHNICAL INFORMATION SECTIONS – SHEET 2 OF 3

SLI DOC No. 505573–3281–4GDD–0018–SH2–01

NE DOC No. MFA–SN–CD–2800–GT–SE–0004–02

Rev. C1

FORMAT A0 (mm)

2013.11.20/12:11pm

SUB-PKG: 0008-4G03 PLATE G06

2800-GT-SE-0004-01

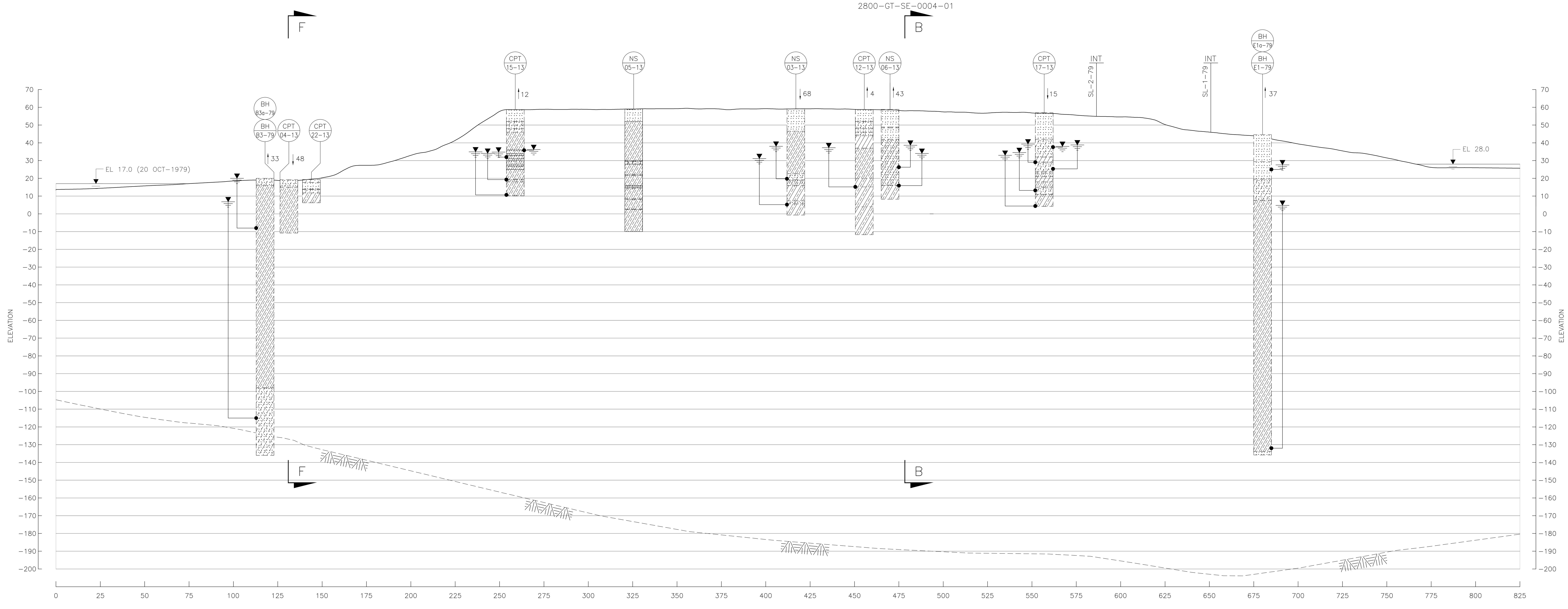

SECTION E-E

2800-GT-PL-0003-01
1:100

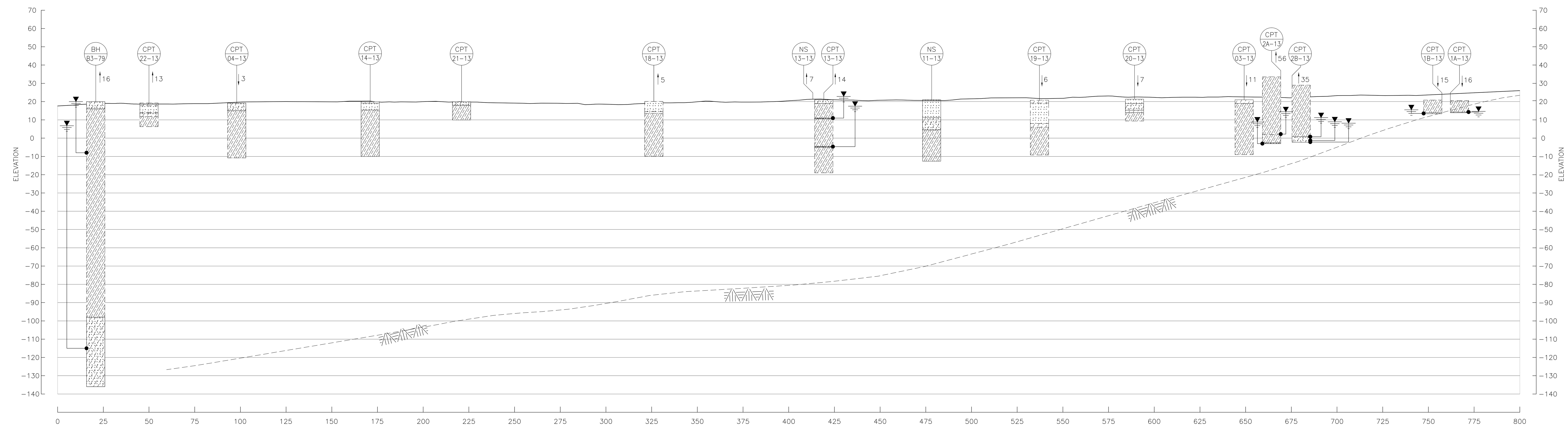

SECTION F-F

2800-GT-PL-0003-01
1:100

NOTES:

1. ROCK PROFILES HAVE BEEN GENERATED FROM THE 2010, 1998 AND 1979 BOREHOLES DATA, SEISMIC REFRACTION DATA AND THE 2006 ROCK OUTCROPS TOPOGRAPHY SURVEY DATA.
2. THE ASSUMED BEDROCK PROFILE IS ILLUSTRATED AS BEING A SMOOTH SURFACE. THE ACTUAL ROCK PROFILE MAY BE JAGGED AND IRREGULAR.
3. ELEVATIONS AND DIMENSIONS ARE IN METRES.
4. DATA CONCERNING THE STRATIGRAPHY HAS BEEN OBTAINED AT THE BOREHOLE LOCATIONS ONLY AND MAY BE DIFFERENT FROM THE STRATIGRAPHY BETWEEN BOREHOLES.
5. THE STRATIGRAPHY SHOWN IN THE BOREHOLE SECTIONS HAS BEEN SIMPLIFIED. FOR A DETAILED DESCRIPTION OF STRATIGRAPHY, REFER TO THE BOREHOLE LOGS IN EXHIBIT 11.
6. DATA CONCERNING THE BOREHOLE AND THE CPT FROM THE 2013 INVESTIGATION WORK ARE PRELIMINARY.

LEGEND:

BOREHOLE/CPT PERFORMED 5 m IN FRONT OF THE SECTION

BOREHOLE/CPT PERFORMED 4 m BEHIND THE SECTION

OVERBURDEN

ROCK

ROCK DESCRIPTION:

- Gn GNEISS
- GG GRANITIC GNEISS
- Gr GRANITE
- Am AMPHIBOLITE
- Pg PEGMATITE
- Sc SCHIST

OVERBURDEN DESCRIPTION:

- ORGANIC SOIL
- CLAY
- SILT
- SAND
- GRAVEL
- COBBLES
- BOULDERS

ASSUMED BEDROCK PROFILE

GROUND PROFILE

SHEAR WAVE VELOCITY LIMIT

6100 SHEAR WAVE VELOCITY IN m/SEC

BH X-79 PIEZOMETER LOCATION AND WATER LEVEL ON 1-NOV-1979

NS X-13 PIEZOMETER LOCATION AND WATER LEVEL ON JUL-2013

CPT X-13 DISSIPATION TEST LOCATION AND WATER LEVEL ON JUN AND JUL-2013

PROVINCE OF NEWFOUNDLAND
PEGNL PERMIT HOLDER
CLASS "A"
This Permit Allows
SNC-LAVALIN Inc.
To practice Professional Engineering in Newfoundland and Labrador.
Permit No. as issued by PEGNL N0458 which is valid for the year 2013.

0 10 20 30 40 50 100 m
SCALE 1:1000

ISSU.	REV.	DATE	DISTRIBUTION & STATUS	ISSU.	REV.	DATE	DISTRIBUTION & STATUS
1	C1	07-NOV-2013	ISSUED FOR INFORMATION				

ISSUE REGISTER

No.	REFERENCE DRAWING
MFA-SN-CD-2800-GT-SE-0004-02	EXISTING GEOLOGICAL AND GEOTECHNICAL INFORMATION – NORTH SPUR SECTIONS – SHEET 2 OF 3
MFA-SN-CD-2800-GT-SE-0004-01	EXISTING GEOLOGICAL AND GEOTECHNICAL INFORMATION – NORTH SPUR SECTIONS – SHEET 1 OF 3
MFA-SN-CD-2800-GT-PL-0012-01	EXISTING GEOLOGICAL AND GEOTECHNICAL INFORMATION – NORTH SPUR PLAN

No.	DATE	REVISION	MOD.	VER.	APP.

* * * * * * * * * * FOR INTERNAL USE ONLY * * * * * * * * * *

REVIEW CLASS: | EQUIPMENT TAG NUMBER:

REVIEW DOES NOT CONSTITUTE APPROVAL OF DESIGN DETAILS, CALCULATIONS, TEST METHODS OR MATERIAL DEVELOPED AND/OR SELECTED BY THE CONTRACTOR, NOR DOES IT RELIEVE THE CONTRACTOR FROM FULL COMPLIANCE WITH CONTRACTUAL OR OTHER OBLIGATIONS.

☐ 1. REVIEWED AND ACCEPTED NO COMMENTS
☐ 2. REVIEWED - INCORPORATE COMMENTS, REVISE & RESUBMIT
☐ 3. REVIEWED - NOT ACCEPTED
☐ 4. INFORMATION ONLY
☐ 5. NOT REVIEWED

LEAD REVIEWER: Date (dd-mmm-yyyy):
NE-LCP MANAGEMENT: Date (dd-mmm-yyyy):
PROJECT MANAGER: Date (dd-mmm-yyyy):

PROFESSIONAL STAMP
REGISTERED PROFESSIONAL ENGINEER – PEGNL Newfoundland and Labrador – NASSER DAIYAN – SIGNATURE – 07-NOV-2013 – DATE – NEWFOUNDLAND & LABRADOR

SNC·LAVALIN

DESIGNED BY N. DAIYAN
DRAWN BY R. MERRI
VERIFIED BY A. CEBALLOS
DATE 17-JUL-2013
APPROVED Discipline Lead Engineer R. BOUCHARD
APPROVED Engineering Manager G. SNYDER
SCALE 1:1000

CLIENT nalcor energy LOWER CHURCHILL PROJECT

PROJECT LOWER CHURCHILL PROJECT

TITLE MUSKRAT FALLS
NORTH SPUR STABILIZATION WORKS
EXISTING GEOLOGICAL AND GEOTECHNICAL INFORMATION
SECTIONS – SHEET 3 OF 3

SLI DOC No. 505573-3281-4GDD-0018-SH3-01
NE DOC No. MFA-SN-CD-2800-GT-SE-0004-03
Rev. C1
FORMAT A0 (mm)

SUB-PKG: 0008-4G03 PLATE G07

2013.11.20/12:13pm

APPENDIX B

INPUT MOTION INITIAL SELECTION

B. INPUT MOTION INITIAL SELECTION

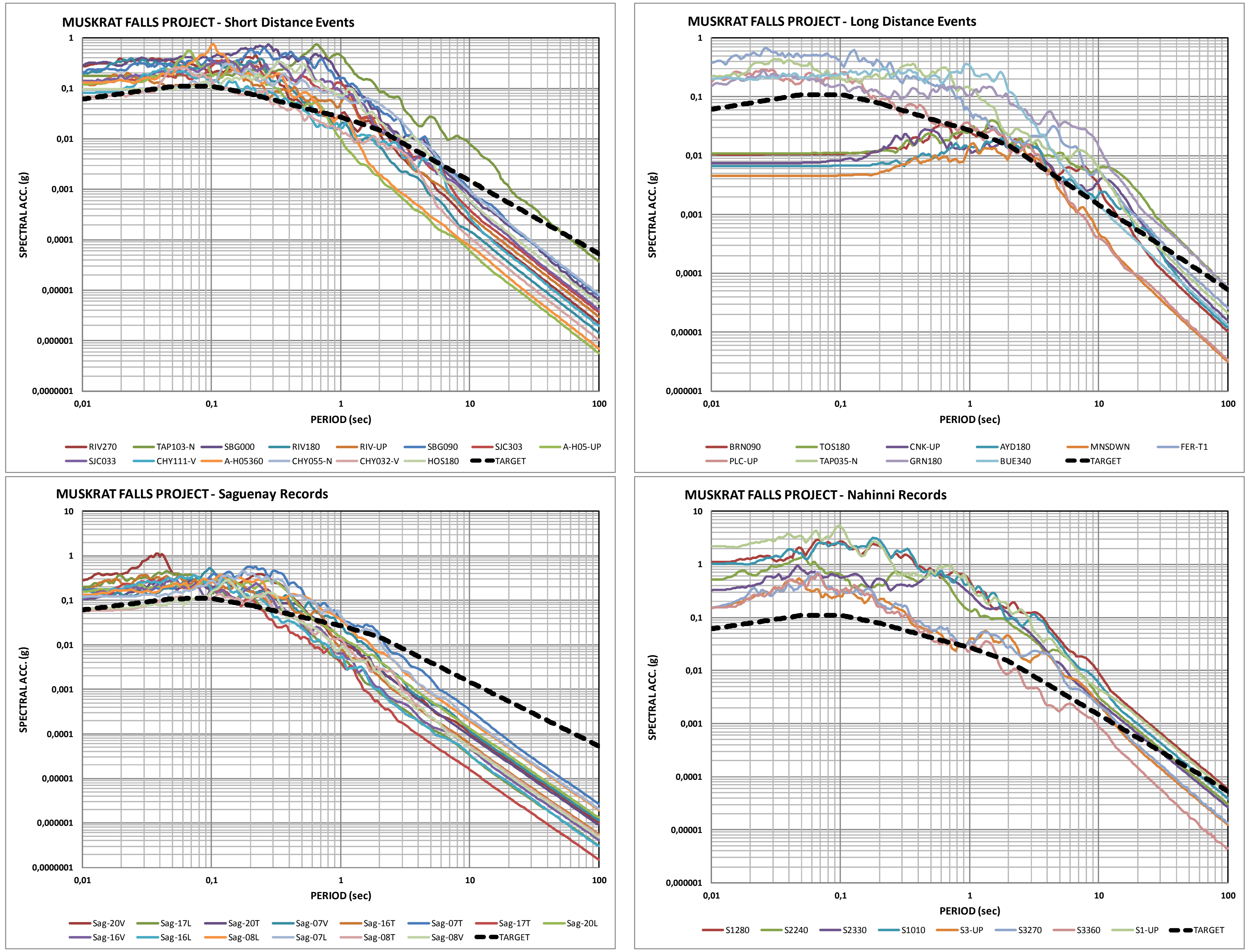

Figure B-1 - Input Motion – Initial Selection from PEER and CEUS Databases

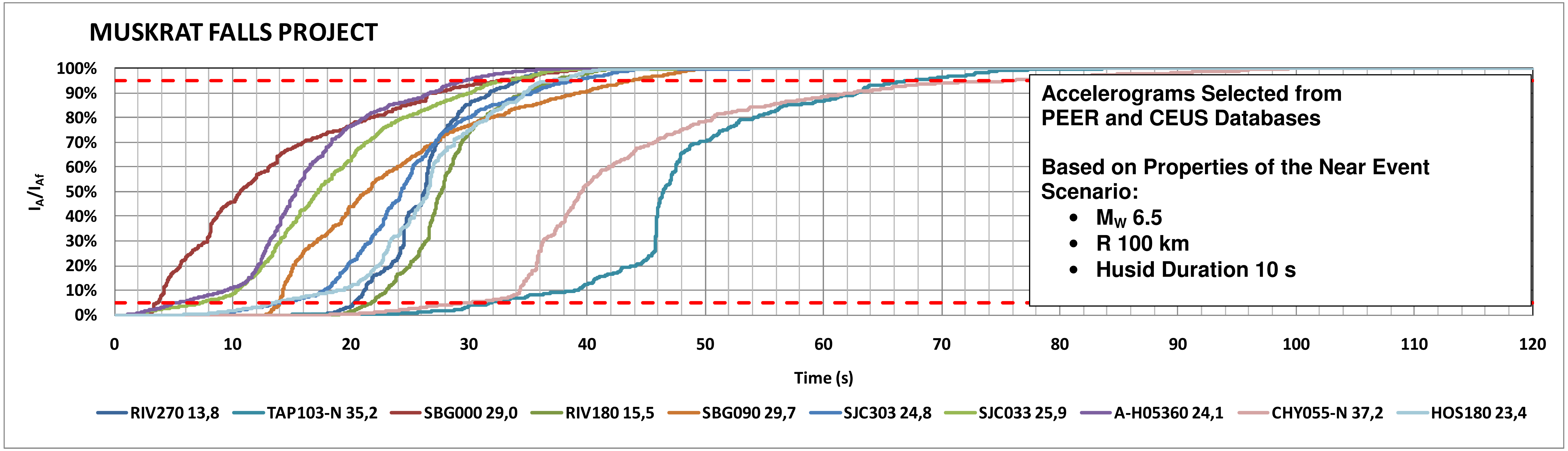

DATA BASE	USGS	PEER	USGS	USGS	USGS	USGS	USGS	USGS	PEER	PEER
Mw	6,7	6,2	6,7	6,7	6,7	6,6	6,6	6	6,2	6,69
Distance (km)	101,3	116,2	111,3	101,3	111,3	104	104	105	97,72	108,29
USGS Code	B	---	---	B	---	---	---	C	---	---
Campbell's GEOCODE	---	C	---	---	---	---	---	---	A	A
SITE TYPE	ROCK	---	SOIL	ROCK	SOIL	SOIL	SOIL	SOIL	---	
LOCATION	Northridge	Chi-Chi, Taiwan-05	Northridge	Northridge	Northridge	San Fernando	San Fernando	Whittier Narrows	Chi-Chi, Taiwan-05	Northridge-01
CASE	RIV270	TAP103-N	SBG000	RIV180	SBG090	SJC303	SJC033	A-H05360	CHY055-N	HOS180
dT (s) =	0,005	0,005	0,005	0,005	0,005	0,005	0,005	0,005	0,004	0,005
amax (m/s2) =	0,61	0,56	0,56	0,59	0,55	0,46	0,52	0,56	0,49	0,49
amax (g) =	0,06	0,06	0,06	0,06	0,06	0,05	0,05	0,06	0,05	0,05
I_{Af} (m/s) =	**0,02**	**0,01**	**0,03**	**0,03**	**0,03**	**0,03**	**0,04**	**0,03**	**0,02**	**0,02**
Husid Time (s) =	**13,8**	**35,2**	**29,0**	**15,5**	**29,7**	**24,8**	**25,9**	**24,1**	**37,2**	**23,4**

Figure B-2 - Input Motions - Near Events – Spectral Matched

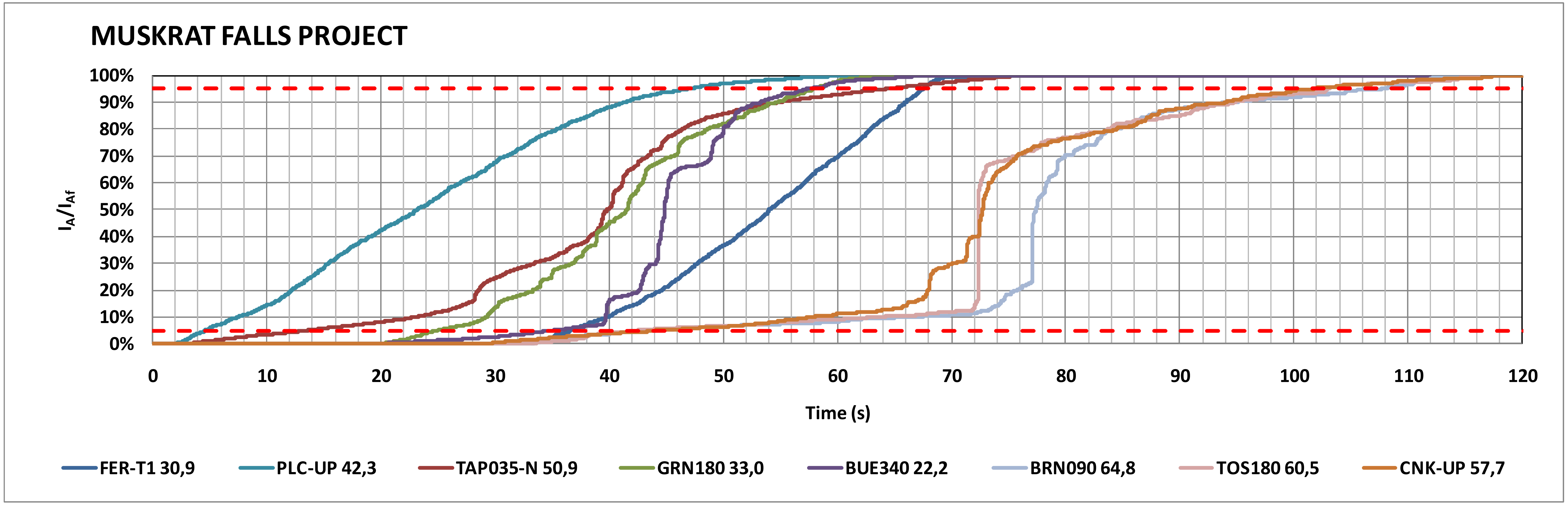

DATA BASE	USGS	USGS	USGS	USGS	USGS	PEER	PEER
Mw	7,4	7,3	7,6	7,3	7,3	7,51	7,51
Distance (km)	94,4	95,9	96,8	141,6	162,1	315,9	256,94
USGS Code	---	B	A	A	C	---	---
Campbell's GEOCODE	---	---	---	---	---	A	---
SITE TYPE	ROCK	ROCK	ROCK	ROCK	SOIL	---	---
LOCATION	Tabas, Iran	Landers	Chi-Chi, Taiwan	Landers	Landers	Kocaeli, Turkey	Kocaeli, Turkey
CASE	FER-T1	PLC-UP	TAP035-N	GRN180	BUE340	BRN090	TOS180
dT (s) =	0,005	0,005	0,005	0,005	0,005	0,005	0,005
amax (m/s2) =	0,49	0,56	0,50	0,58	0,53	0,77	0,79
amax (g) =	0,05	0,06	0,05	0,06	0,05	0,08	0,08
I_{Af} (m/s) =	**0,10**	**0,11**	**0,03**	**0,03**	**0,01**	**0,01**	**0,01**
Husid Time (s) =	**30,9**	**42,3**	**50,9**	**33,0**	**22,2**	**64,8**	**60,5**

Accelerograms Selected from PEER and CEUS Databases

Based on Properties of the Far Event Scenario:

- **M_W 7.3**
- **R 400 km**
- **Husid Duration 50 s**

Figure B-3 - Input Motions - Far Events – Spectral Matched

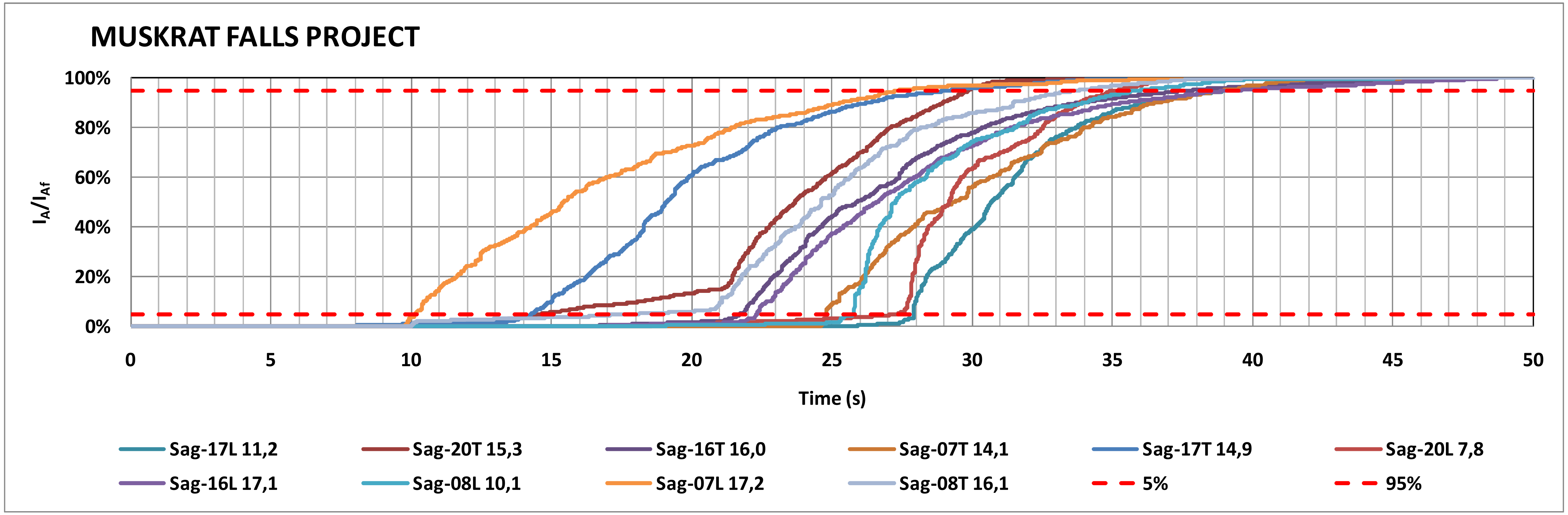

DATA BASE	USCS									
Mw	5,9									
Distance (kM)	70,3	95	51,9	95,6	70,3	95	51,9	97,5	95,6	97,5
USGS Code										
SITE TYPE	ROCK	ROCK	ROCK	SOIL	ROCK	ROCK	ROCK	ROCK	SOIL	ROCK
LOCATION	SAGUENAY									
CASE	Sag-17L	Sag-20T	Sag-16T	Sag-07T	Sag-17T	Sag-20L	Sag-16L	Sag-08L	Sag-07L	Sag-08T
dT (s) =	0,005	0,005	0,005	0,005	0,005	0,005	0,005	0,005	0,005	0,005
amax (m/s2) =	0,50	0,47	0,45	0,57	0,49	0,59	0,48	0,49	0,50	0,56
amax (g) =	0,05	0,05	0,05	0,06	0,05	0,06	0,05	0,05	0,05	0,06
IAf (m/s) =	0,02	0,03	0,03	0,02	0,03	0,01	0,03	0,02	0,03	0,03
CASE	Sag-17L	Sag-20T	Sag-16T	Sag-07T	Sag-17T	Sag-20L	Sag-16L	Sag-08L	Sag-07L	Sag-08T
Husid Time (s) =	11,2	15,3	16,0	14,1	14,9	7,8	17,1	10,1	17,2	16,1

Accelerograms Selected from PEER and CEUS Databases

Saguenay 1988 – Recordings from the Saguenay Region

- **M_W 5,9**

Figure B-4 - Input Motions - Saguenay 1988 Recordings – Spectral Matched

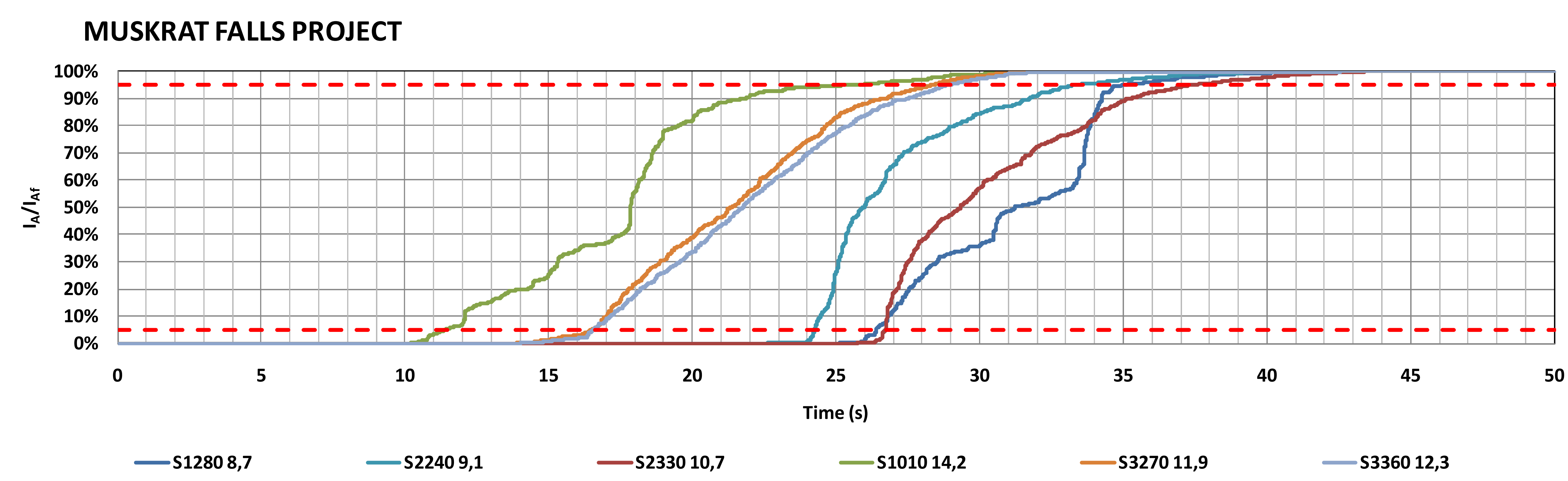

DATA BASE	PEER					
Mw	6,76					
Distance (km)	9,6	4,93	4,93	9,6	16	16
USGS Code						
Campbell's GEOCODE	D					
SITE TYPE						
LOCATION	Nahanni, Canada					
CASE	S1280	S2240	S2330	S1010	S3270	S3360
dT (s) =	0,005	0,005	0,005	0,005	0,005	0,005
amax (m/s2) =	0,51	0,51	0,52	0,53	0,46	0,42
amax (g) =	0,05	0,05	0,05	0,05	0,05	0,04
I_{Af} (m/s) =	**0,01**	**0,01**	**0,02**	**0,01**	**0,04**	**0,04**
Husid Time (s) =	**8,7**	**9,1**	**10,7**	**14,2**	**11,9**	**12,3**

Accelerograms Selected from PEER and CEUS Databases

Nahanni 1985 Recordings

- **M_W 6.76**

Figure B-5 - Input Motions - Nahanni 1985 Recordings – Spectral Matched

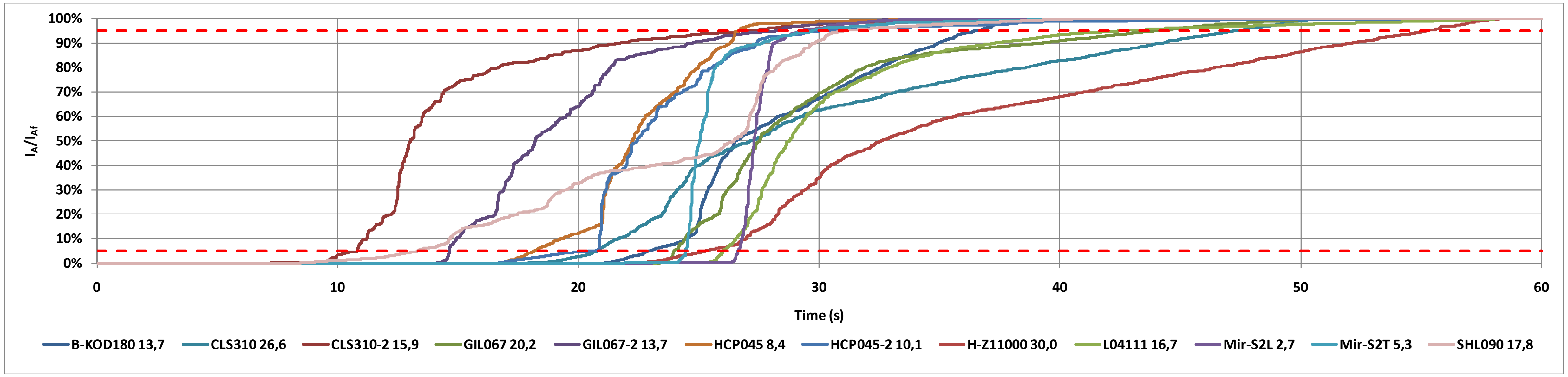

DATA BASE	USGS	USGS	PEER	USGS	PEER	USGS	PEER	USGS	USGS			USGS
Mw	5,4	6,2	6,19	6,2	6,19	6	6,06	6,4	6,6			7,1
Distance (km)	22,02	22,7	23,24	16,2	14,84	34,9	29,83	28,4	28,52			33,8
USGS Code	C	B		B		B	A		B			B
Campbell's GEOCODE			C		E							
SITE TYPE	ROCK	ROCK		ROCK		ROCK		ROCK	ROCK			ROCK
LOCATION	Livermore	Morgan Hill	Morgan Hill	Morgan Hill	Morgan Hill	N. Palm Springs	N. Palm Springs	Coalinga	San Fernando	Miramichi		Cape Mendocino
CASE	B-KOD180	CLS310	CLS310-2	GIL067	GIL067-2	HCP045	HCP045-2	H-Z11000	L04111	Mir-S2L	Mir-S2T	SHL090
dT (s) =	0,005	0,005	0,005	0,005	0,005	0,005	0,005	0,005	0,005	0,005	0,005	0,005
amax (m/s2) =	0,52	0,54	0,30	0,44	0,62	0,57	0,58	0,44	0,58	0,46	0,48	0,45
amax (g) =	0,05	0,05	0,03	0,05	0,06	0,06	0,06	0,05	0,06	0,05	0,05	0,05
I_{Af} (m/s) =	0,02	0,03	0,01	0,02	0,02	0,02	0,01	0,04	0,02	0,01	0,01	0,02
Husid Time (s) =	13,7	26,6	15,9	20,2	13,7	8,4	10,1	30,0	16,7	2,7	5,3	17,8

Accelerograms Selected from PEER and CEUS Databases

Recordings Used in the Preliminary Dynamic Study, Matched to Atkinson 2014 UHS

Figure B-6 - Input Motions - Accelerograms Used in Preliminary Dynamic Study – Spectral Matched

Far Events

DATA BASE	PEER	USGS	USGS	USGS	PEER
Mw	7,51	7,4	7,6	7,3	7,51
Distance (km)	256,94	94,4	96,8	95,9	315,9
USGS Code	---	---	A	B	---
Campbell's GEOCODE	---	---	---	---	A
SITE TYPE	---	ROCK	ROCK	ROCK	---
LOCATION	Kocaeli, Turkey	Tabas, Iran	Chi-Chi, Taiwan	Landers	Kocaeli, Turkey
CASE	TOS180	FER-T1	TAP035-N	PLC-UP	BRN090
dT (s) =	0,005	0,005	0,005	0,005	0,005
amax (m/s2) =	0,79	0,49	0,50	0,56	0,77
amax (g) =	0,08	0,05	0,05	0,06	0,08
I_{Af} (m/s) =	**0,01**	**0,10**	**0,03**	**0,11**	**0,01**
Husid Time (s) =	**60,5**	**30,9**	**50,9**	**42,3**	**64,8**

Near Events

DATA BASE	PEER	USGS	USGS	PEER
Mw	6,2	6,6	6	6,2
Distance (km)	116,2	104	105	83,42
USGS Code	---	---	C	---
Campbell's GEOCODE	C	---	---	A
SITE TYPE	---	SOIL	SOIL	---
LOCATION	Chi-Chi, Taiwan-05	San Fernando	Whittier Narrows	Chi-Chi, Taiwan-05
CASE	TAP103-N	SJC303	A-H05-UP	CHY111-V
dT (s) =	0,005	0,005	0,005	0,004
amax (m/s2) =	0,56	0,46	0,45	0,45
amax (g) =	0,06	0,05	0,05	0,05
IAf (m/s) =	**0,01**	**0,03**	**0,03**	**0,04**
Husid Time =	**35,2**	**24,8**	**24,5**	**21,2**

Saguenay and Nahanni

DATA BASE	USCS			PEER	
Mw	5,9			6,76	
Distance (kM)	70,3	51,9	97,5	4,93	16
USGS Code					
Campbell's GEOCODE				D	
SITE TYPE	ROCK	ROCK	ROCK		
LOCATION	SAGUENAY 1988			Nahanni 1985	
CASE	Sag-17L	Sag-16T	Sag-08V	S2330	S3360
dT (s) =	0,005	0,005	0,005	0,005	0,005
amax (m/s2) =	0,50	0,45	0,42	0,52	0,42
amax (g) =	0,05	0,05	0,04	0,05	0,04
IAf (m/s) =	**0,02**	**0,03**	**0,01**	**0,02**	**0,04**
Husid Time (s) =	**11,2**	**16,0**	**17,2**	**10,7**	**12,3**

NOTE: INPUT MOTIONS MARKED IN RED ARE FOR 2D ANALYSES

Previous Study

DATA BASE	USGS	USGS	USGS
Mw	6,6	6,2	6,4
Distance (km)	28,52	16,2	28,4
USGS Code	B	B	
Campbell's GEOCODE			
SITE TYPE	ROCK	ROCK	ROCK
LOCATION	San Fernando	Morgan Hill	Coalinga
CASE	L04111	GIL067	H-Z11000
dT (s) =	0,005	0,005	0,005
amax (m/s2) =	0,58	0,44	0,44
amax (g) =	0,06	0,05	0,05
I_{Af} (m/s) =	**0,02**	**0,02**	**0,04**
Husid Time (s) =	**16,7**	**20,2**	**30,0**

Figure B-7 - Input Motions - Spectral Matched Accelerograms Selected for 1D and 2D Equivalent-linear Analyses

APPENDIX C

SELECTED PIEZOCONE TESTS AND ASSOCIATED BOREHOLES - INVESTIGATION DATA AND INTERPRETED CRR AND VS PROFILES

C. SELECTED PIEZOCONE TESTS AND ASSOCIATED BOREHOLES - INVESTIGATION DATA AND INTERPRETED CRR AND VS PROFILES

SNC·LAVALIN	NORTH SPUR STABILIZATION WORKS – DYNAMIC ANALYSIS STUDY – PHASE 2	Revision		
	Nalcor Doc. No. MFA-SN-CD-2800-GT-RP-0007-01	B2	Date	Page
	SLI Doc. No. 505573-3281-4GER-0005	01	08-Dec-2015	C-2

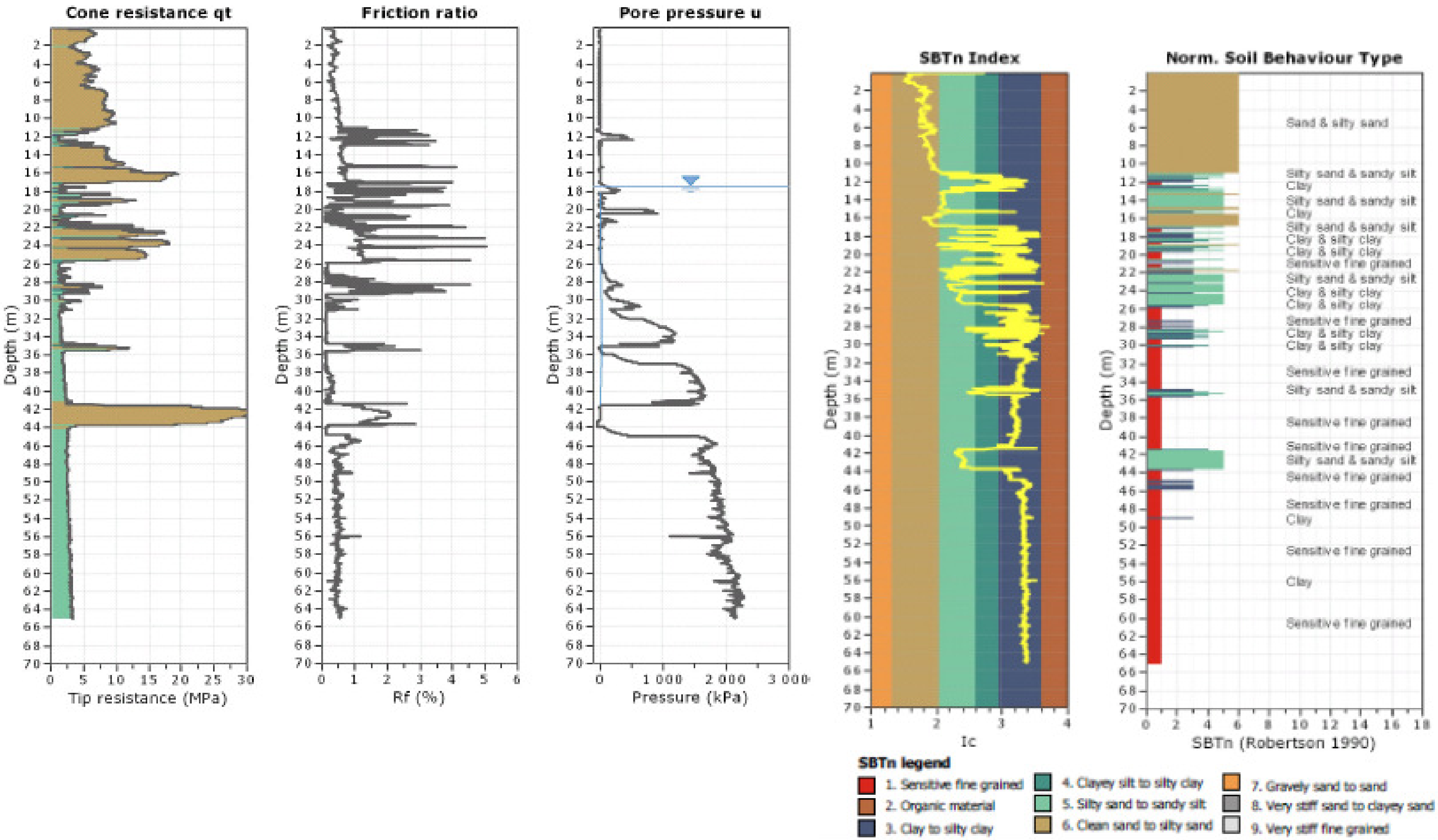

Figure C-1 - P1 (SCPT-09-13) – Investigation Data

SNC·LAVALIN	NORTH SPUR STABILIZATION WORKS – DYNAMIC ANALYSIS STUDY – PHASE 2	Revision		
	Nalcor Doc. No. MFA-SN-CD-2800-GT-RP-0007-01	B2	Date	Page
	SLI Doc. No. 505573-3281-4GER-0005	01	08-Dec-2015	C-3

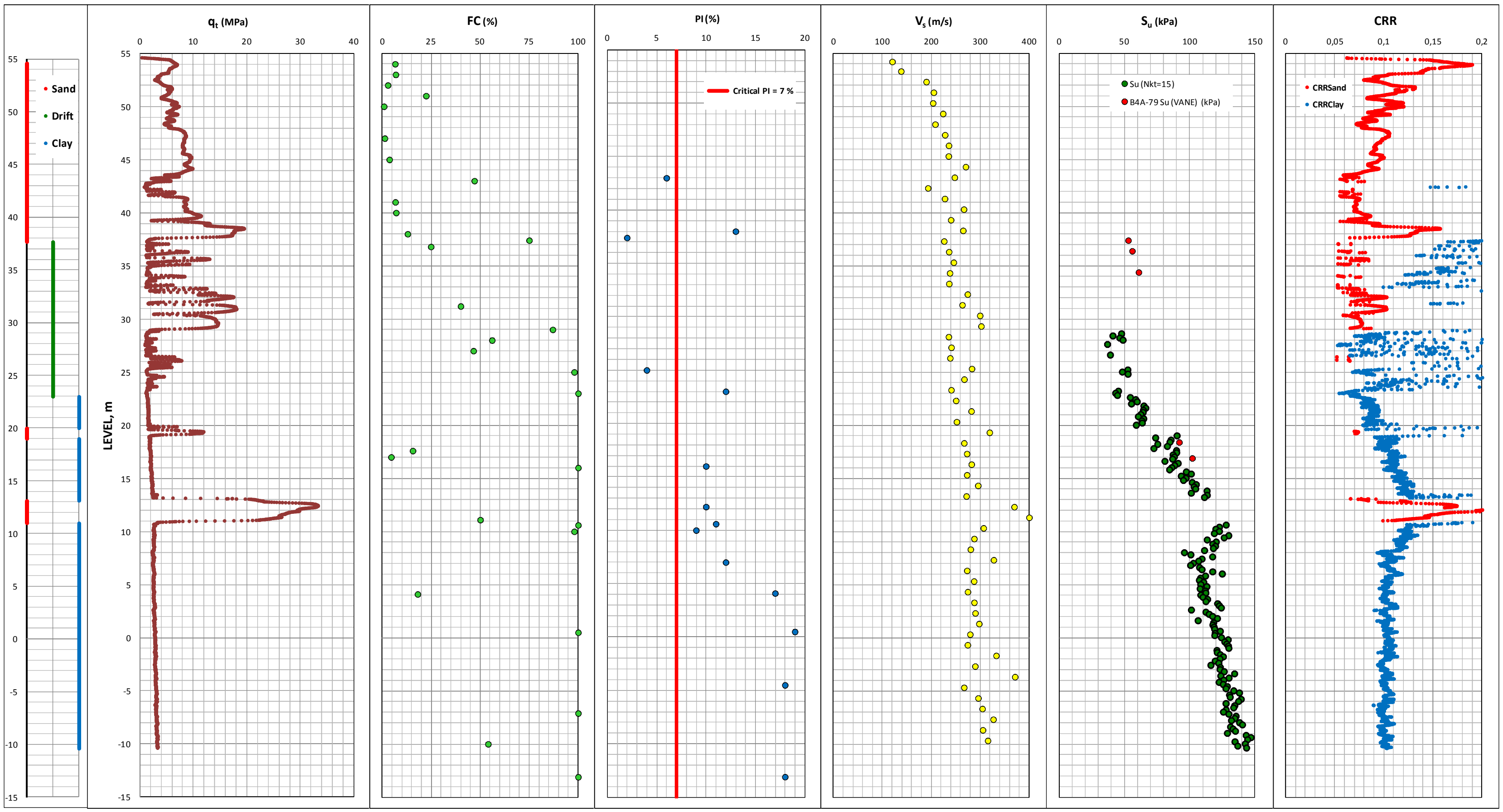

Figure C-2 - P1 (SCPT-09-13) – Data from Associated B4-79 Borehole and Interpreted Vs and CRR Profiles

SNC·LAVALIN	NORTH SPUR STABILIZATION WORKS – DYNAMIC ANALYSIS STUDY – PHASE 2	Revision		
	Nalcor Doc. No. MFA-SN-CD-2800-GT-RP-0007-01	B2	Date	Page
	SLI Doc. No. 505573-3281-4GER-0005	01	08-Dec-2015	C-4

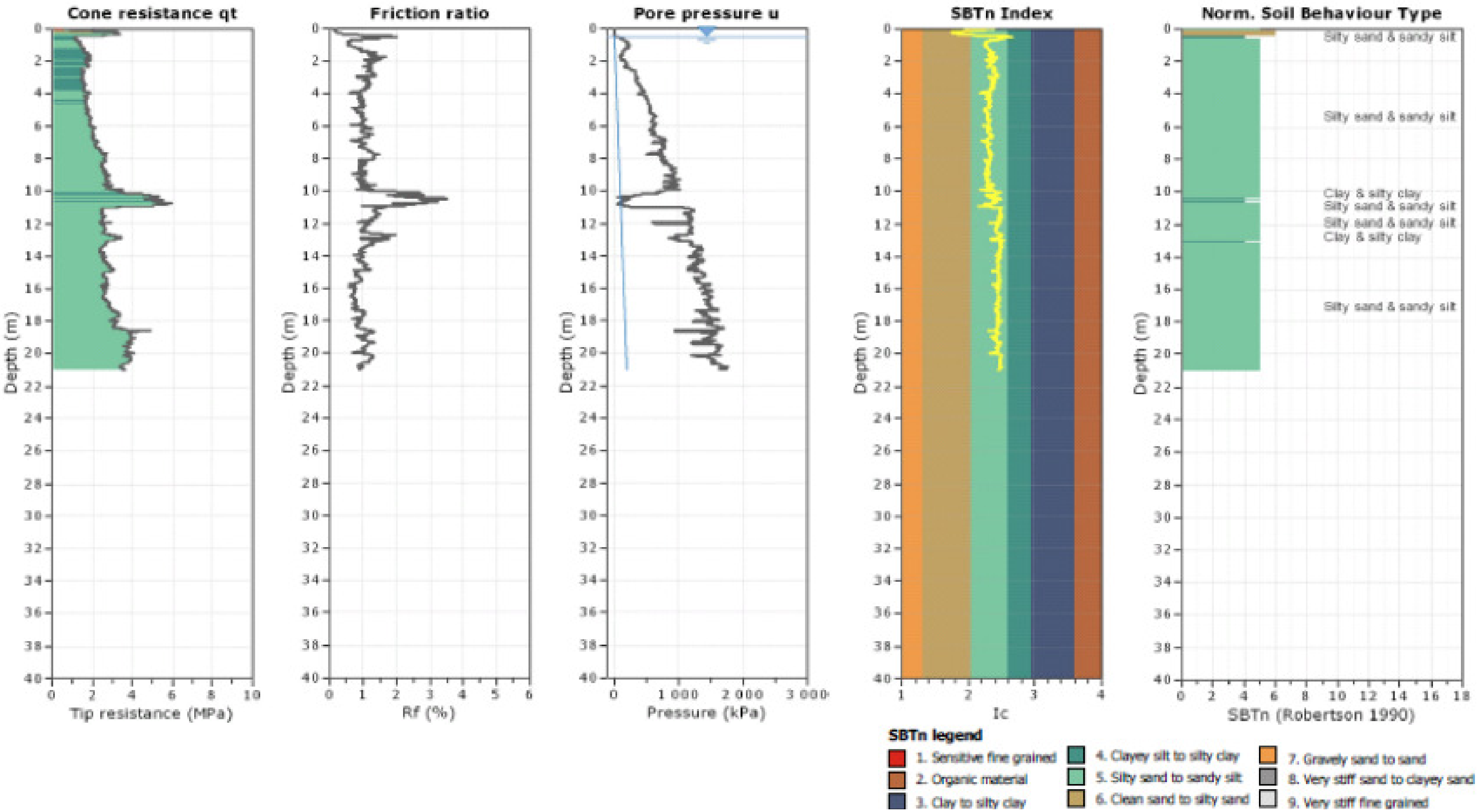

Figure C-3 - P2 (CPT-24-13) – Investigation Data

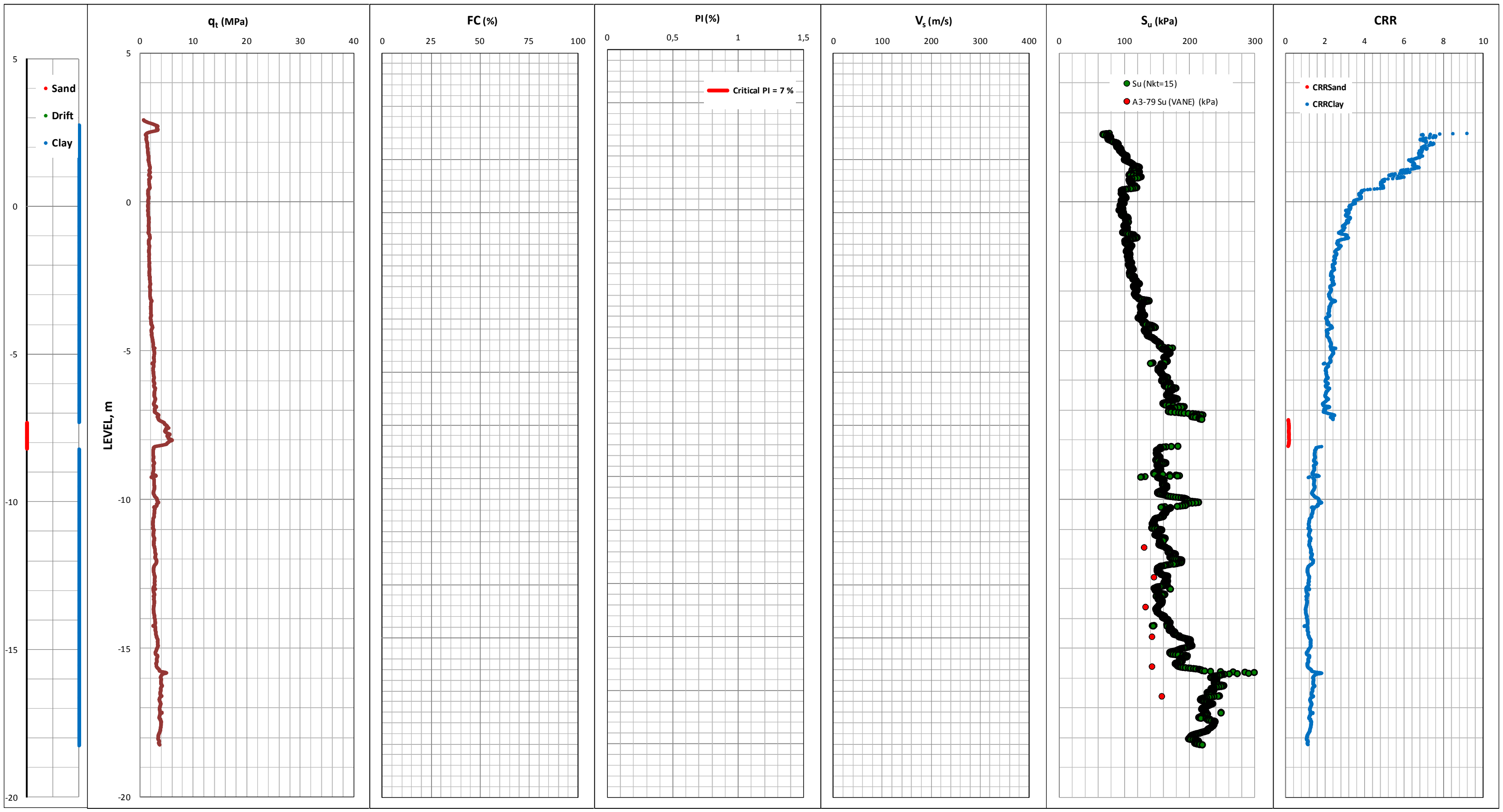

Figure C-4 - P2 (CPT-24-13) – Data from Associated A3-79 Borehole and Interpreted Vs and CRR Profiles

SNC·LAVALIN	NORTH SPUR STABILIZATION WORKS – DYNAMIC ANALYSIS STUDY – PHASE 2	Revision		
	Nalcor Doc. No. MFA-SN-CD-2800-GT-RP-0007-01	B2	Date	Page
	SLI Doc. No. 505573-3281-4GER-0005	01	08-Dec-2015	C-6

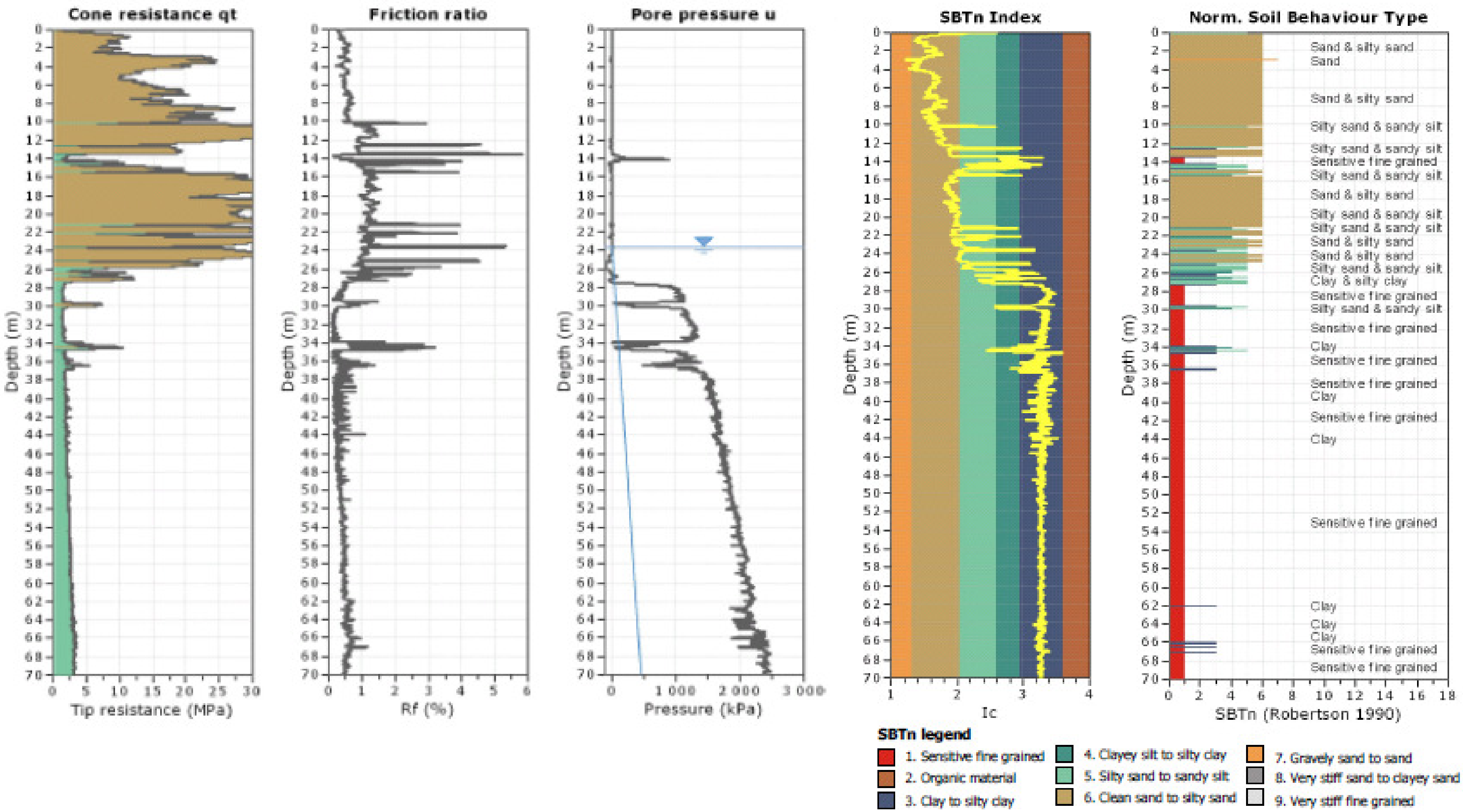

Figure C-5 - S1 (SPTU - 11-13) – Investigation Data

SNC·LAVALIN	NORTH SPUR STABILIZATION WORKS – DYNAMIC ANALYSIS STUDY – PHASE 2	Revision		Page
	Nalcor Doc. No. MFA-SN-CD-2800-GT-RP-0007-01	B2	Date	
	SLI Doc. No. 505573-3281-4GER-0005	01	08-Dec-2015	C-7

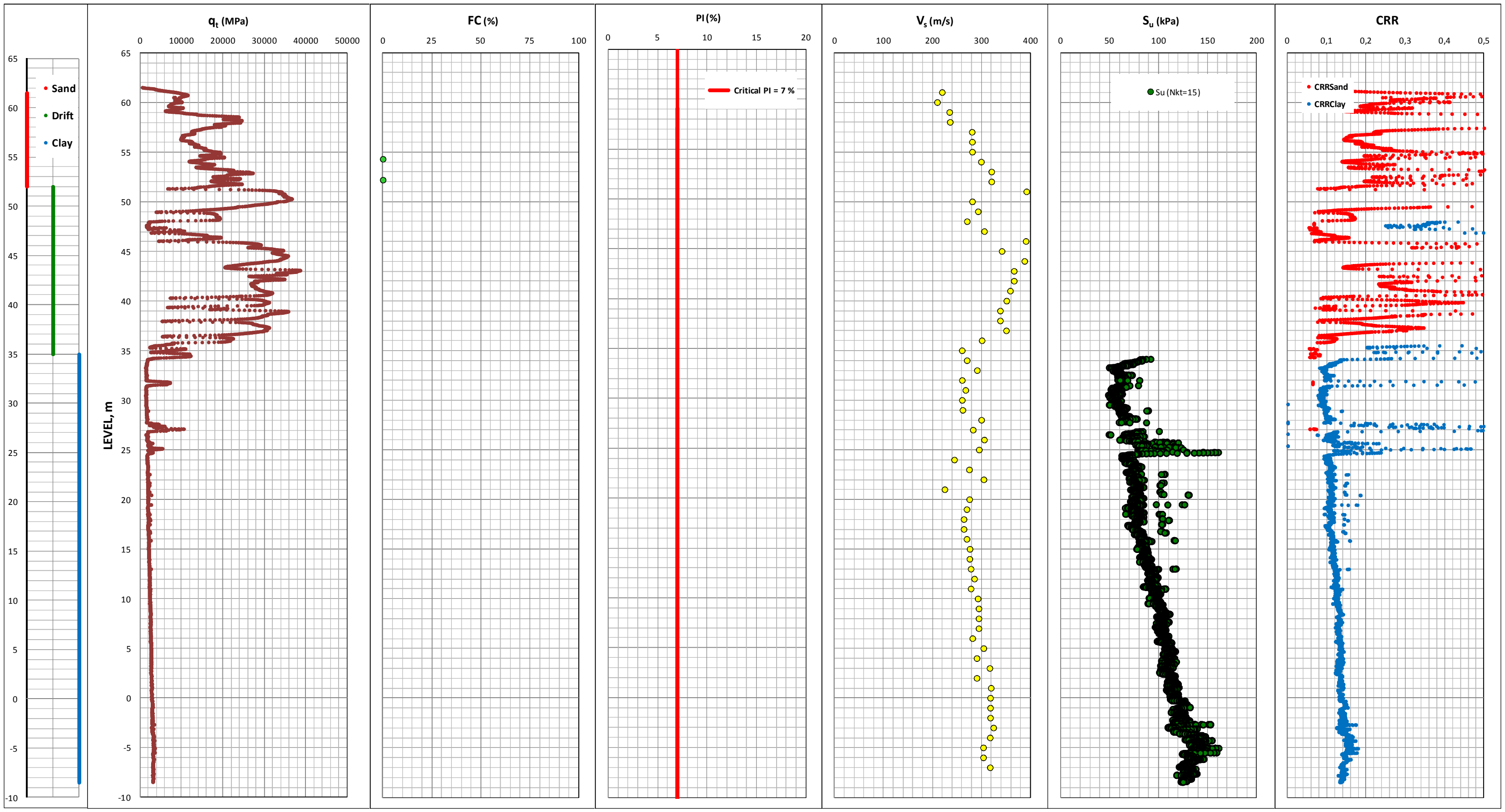

Figure C-6 – S1 (SCPTU-11-13) – Data from Associated NS-2-13 Borehole and Interpreted Vs and CRR Profiles

SNC·LAVALIN	NORTH SPUR STABILIZATION WORKS – DYNAMIC ANALYSIS STUDY – PHASE 2	Revision		Page
	Nalcor Doc. No. MFA-SN-CD-2800-GT-RP-0007-01	B2	Date	
	SLI Doc. No. 505573-3281-4GER-0005	01	08-Dec-2015	C-8

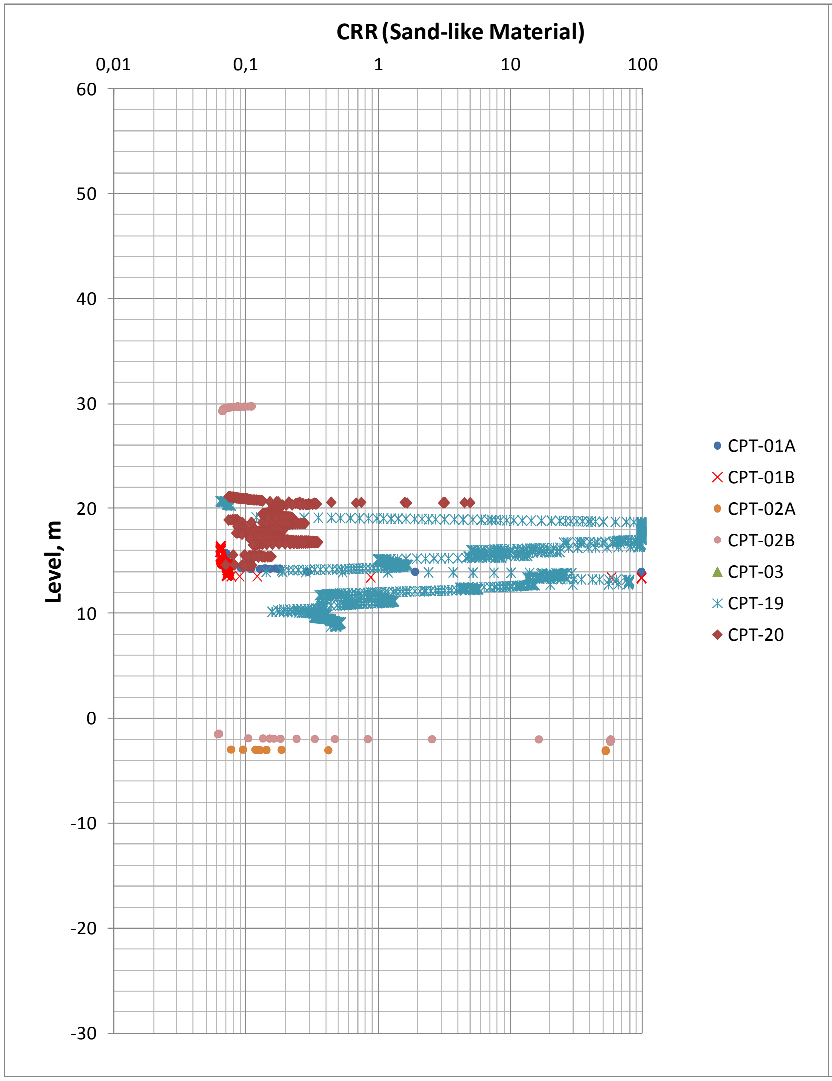

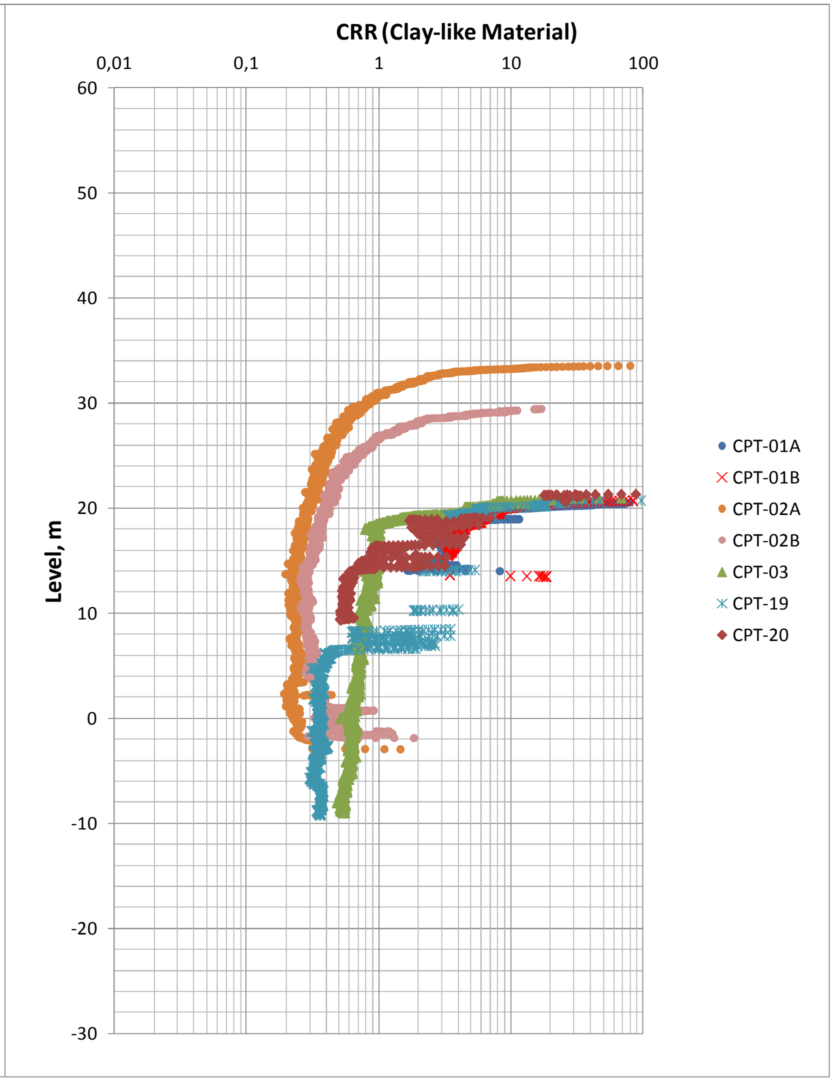

Figure C-7 - CRR Estimated based on CPT - Upstream Toe (South)

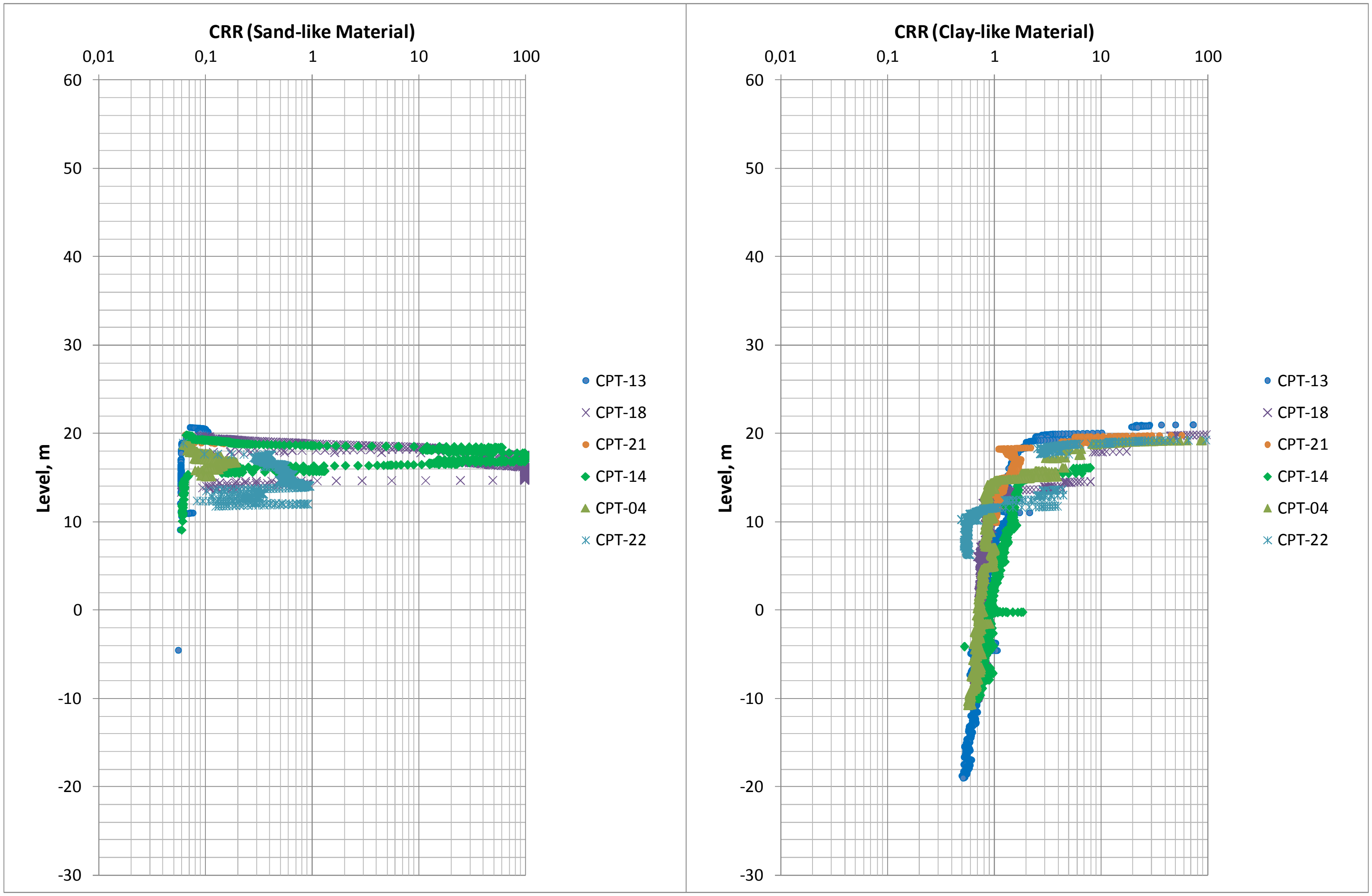

Figure C-8 - CRR Estimated based on CPT - Upstream Toe (North)

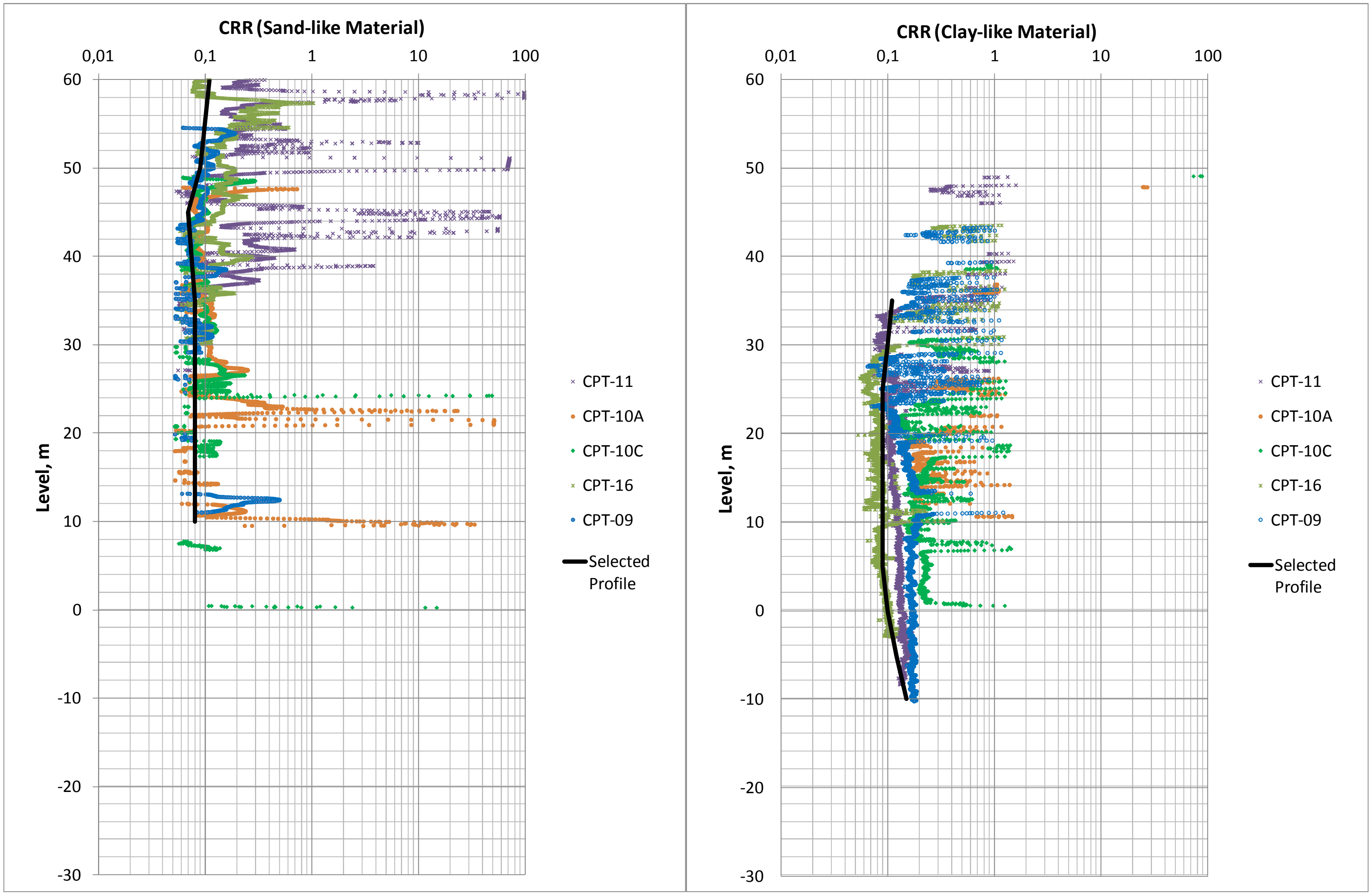

Figure C-9 - CRR Estimated based on CPT and Selected CRR Profiles - Crest of North Spur (East)

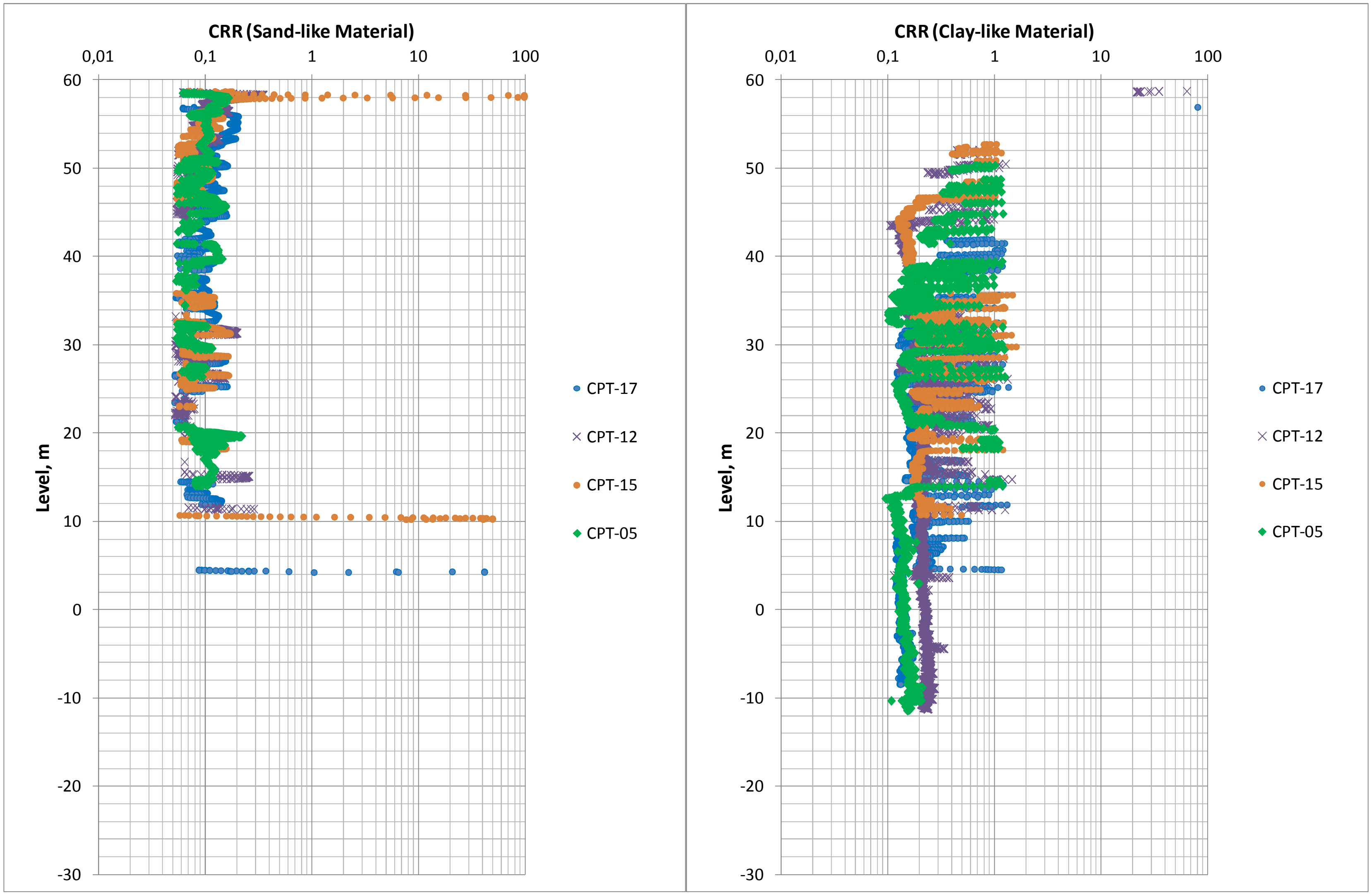

Figure C-10 - CRR Estimated based on CPT – Crest of North Spur (West)

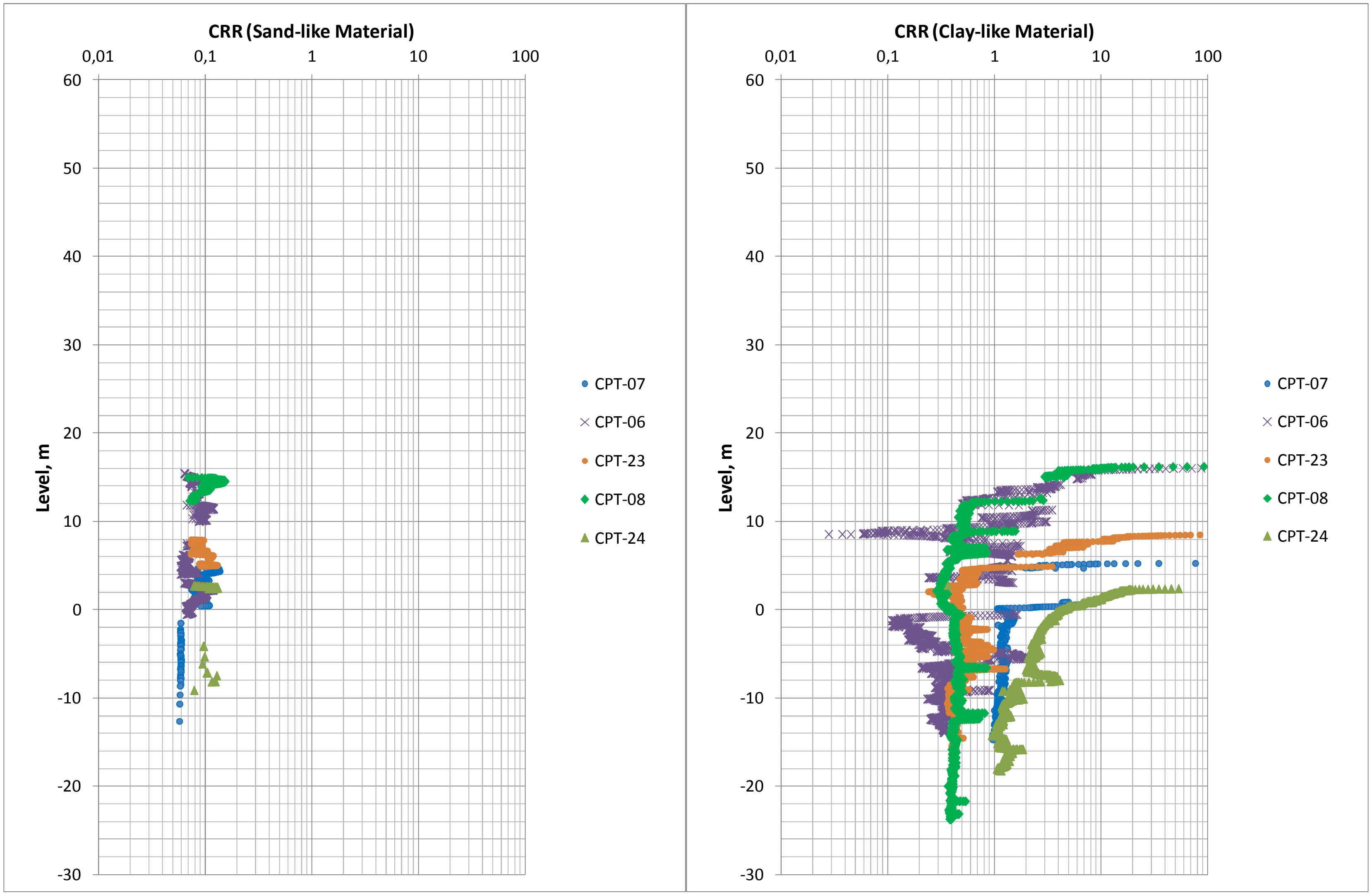

Figure C-11 - CRR Estimated based on CPT - Downstream Toe

SNC·LAVALIN	NORTH SPUR STABILIZATION WORKS – DYNAMIC ANALYSIS STUDY – PHASE 2	Revision		
	Nalcor Doc. No. MFA-SN-CD-2800-GT-RP-0007-01	B2	Date	Page
	SLI Doc. No. 505573-3281-4GER-0005	01	08-Dec-2015	C-13

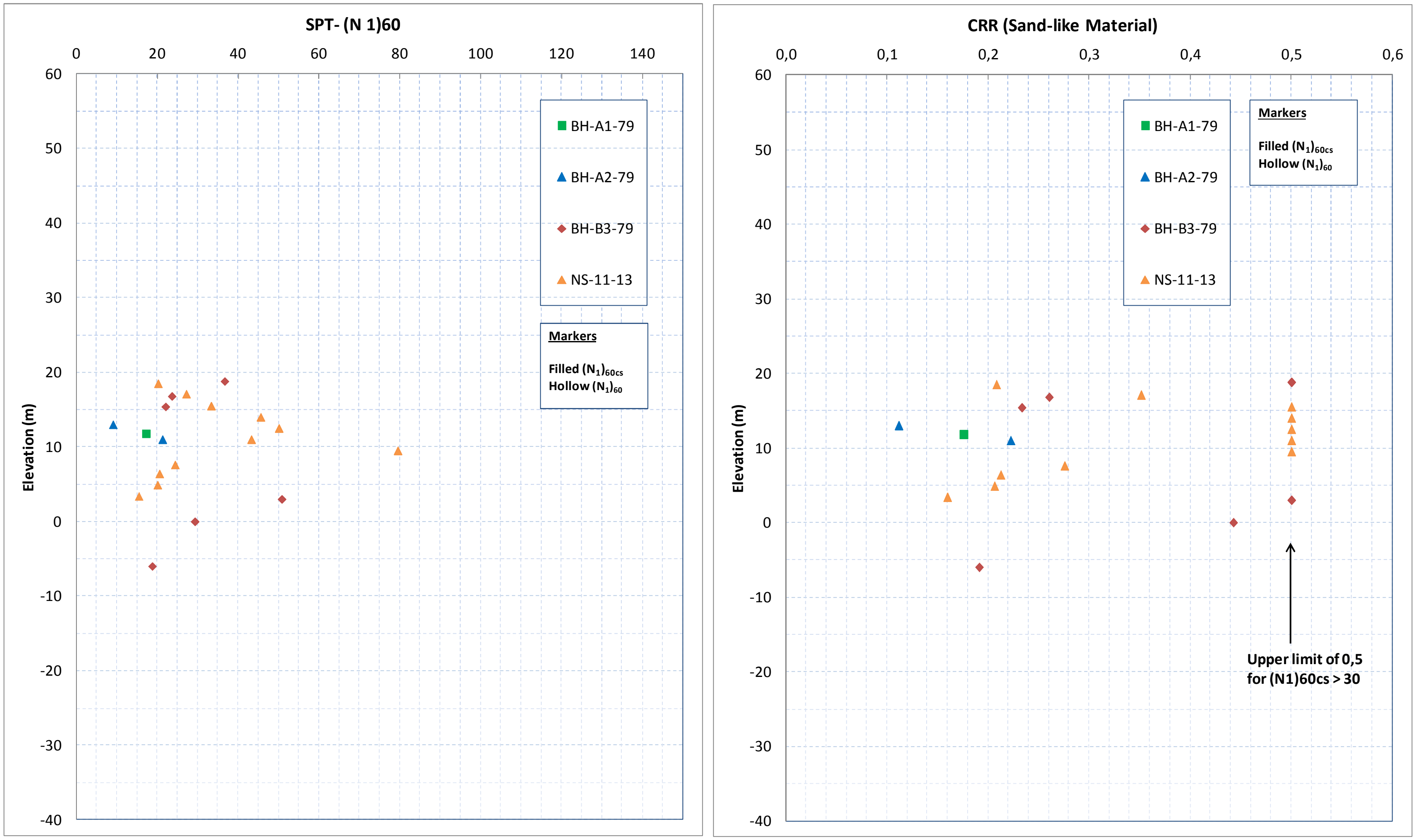

Figure C-12 - CRR Estimated based on SPT - Upstream Toe

SNC·LAVALIN	NORTH SPUR STABILIZATION WORKS – DYNAMIC ANALYSIS STUDY – PHASE 2	Revision		Page
	Nalcor Doc. No. MFA-SN-CD-2800-GT-RP-0007-01	B2	Date	
	SLI Doc. No. 505573-3281-4GER-0005	01	08-Dec-2015	C-14

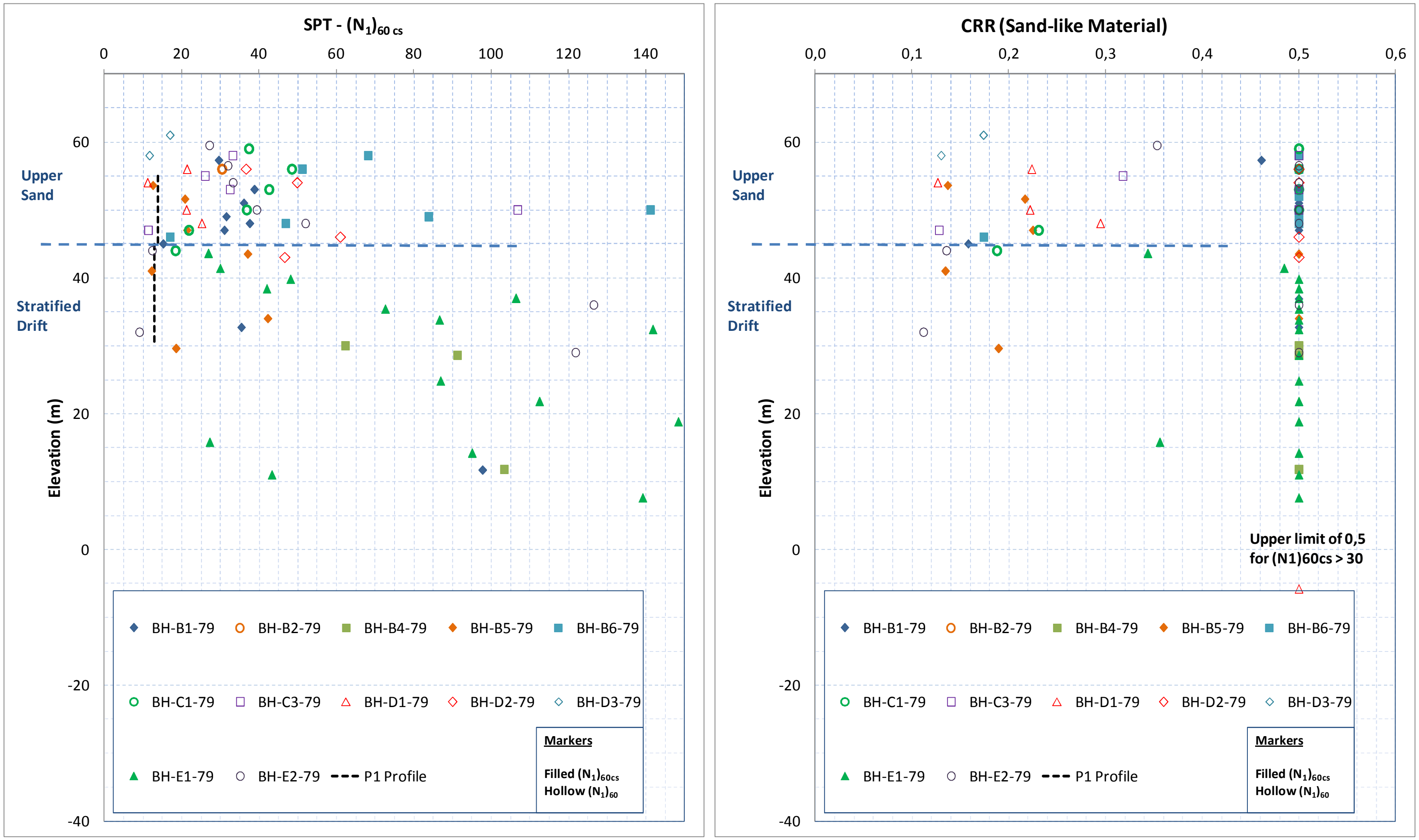

Figure C-13 - CRR Estimated based on SPT – Crest of North Spur

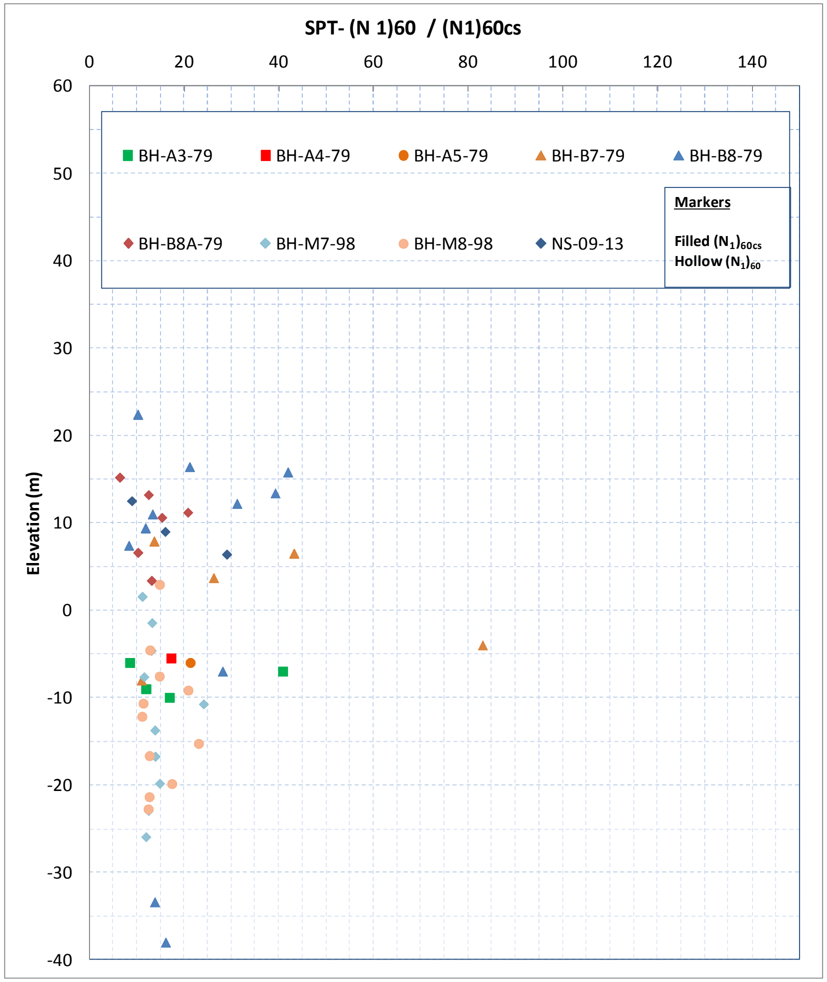

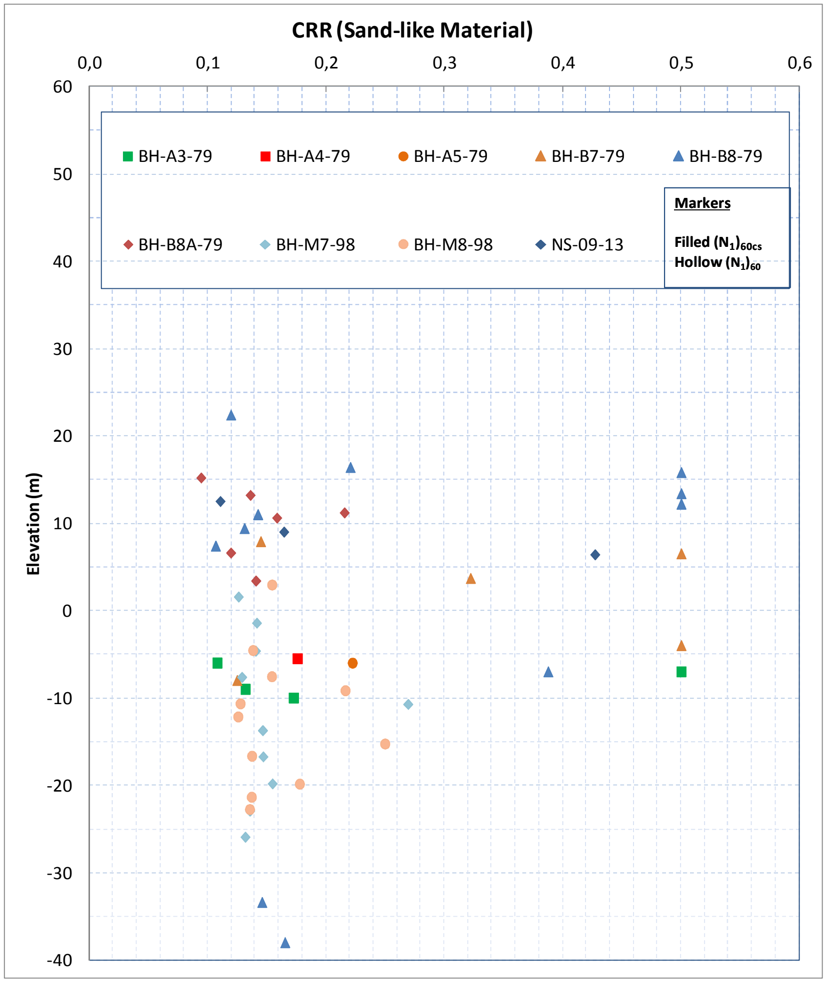

Figure C-14 - CRR Estimated based on SPT - Downstream Toe

SNC·LAVALIN	NORTH SPUR STABILIZATION WORKS – DYNAMIC ANALYSIS STUDY – PHASE 2	Revision		Page
	Nalcor Doc. No. MFA-SN-CD-2800-GT-RP-0007-01	B2	Date	
	SLI Doc. No. 505573-3281-4GER-0005	01	08-Dec-2015	C-16

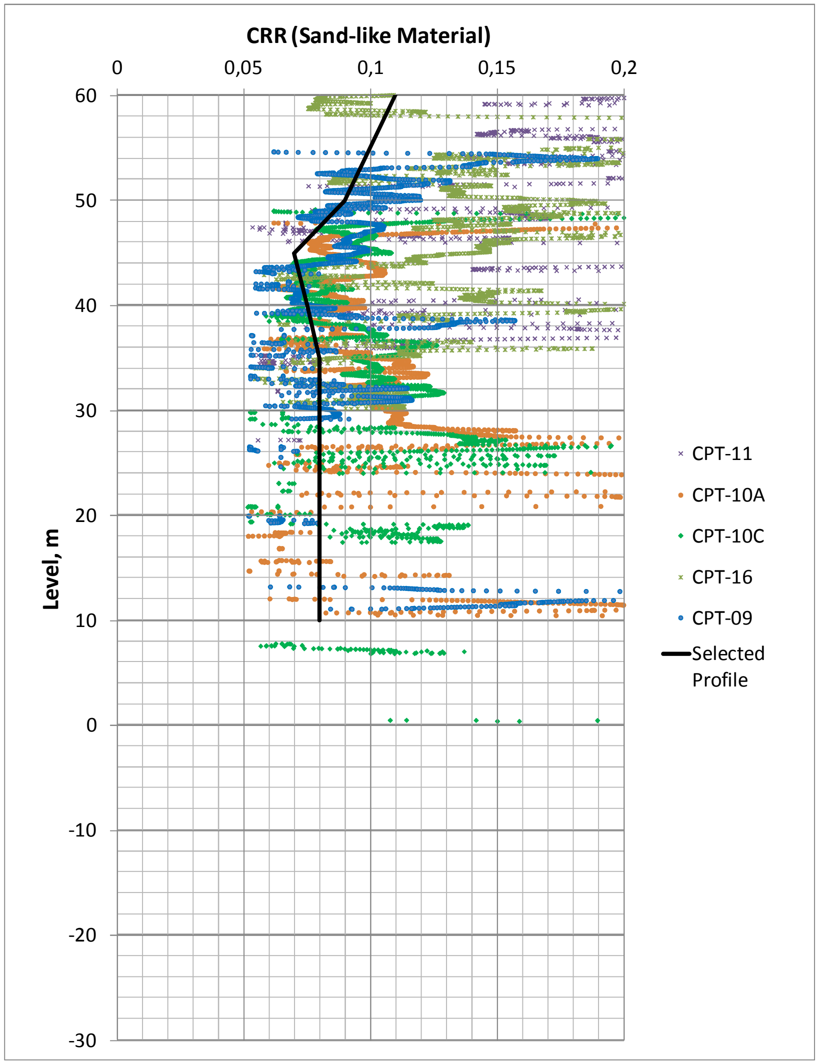

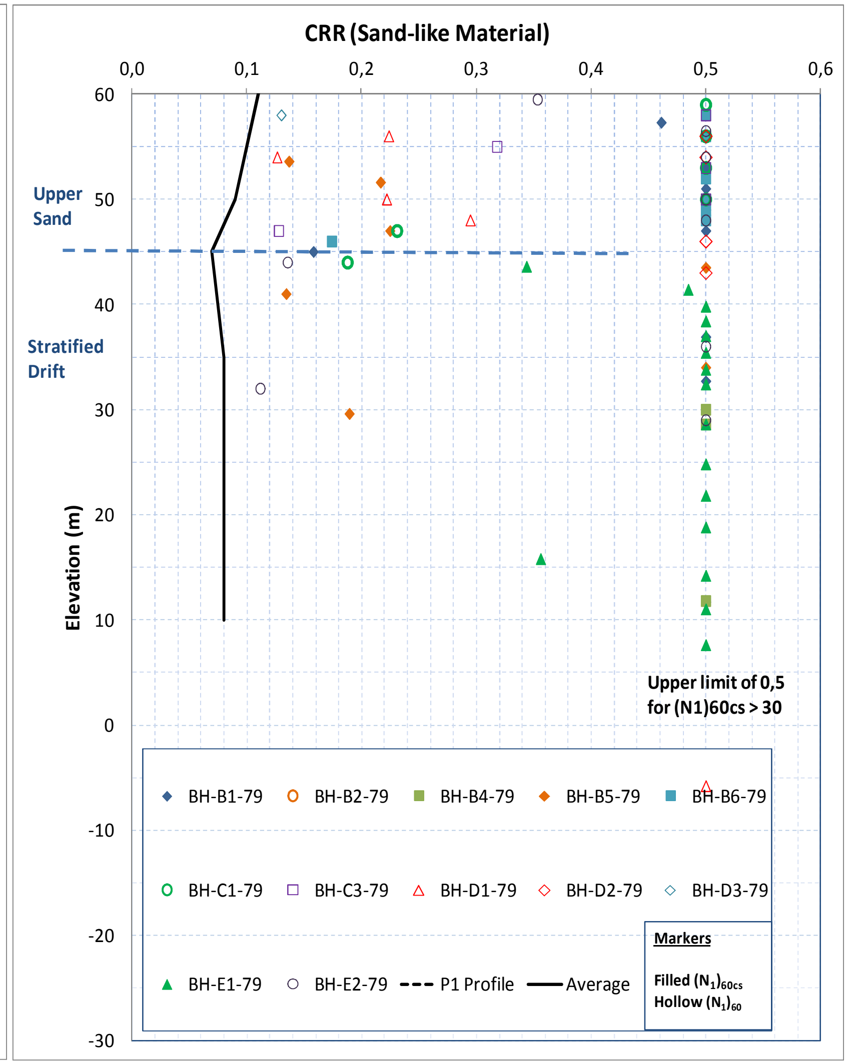

Figure C-15 – Selected Profile - CRR based on CPT and SPT - Crest

Triaxial Seismometer		
Tromino	To =	1,85 s
SCPTU-09-13 Extended		
Estimated Fundamental Period		
	To =	1,84 s

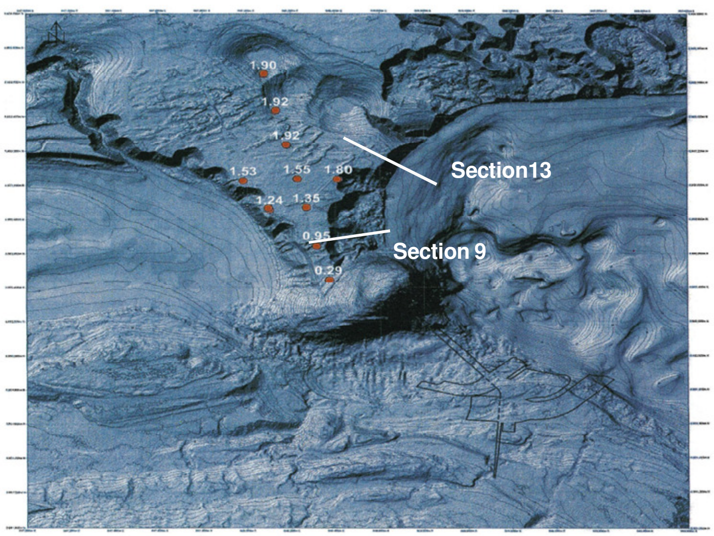

Figure 1: Average Period (T_0) Readings at the North Spur

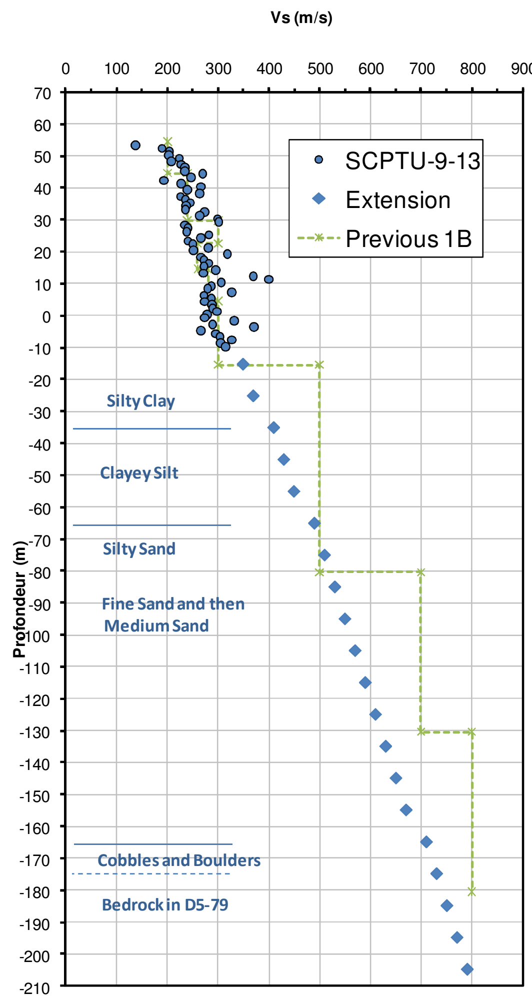

Figure C-16 - P1 (SCPT-09-13) - Vs Profile Based on SCPT-09-13 Extended Profile

Triaxial Seismometer		
Tromino	To =	0,95 s
SCPTU-11-13 Extended		
Estimated Fundamental Period		
	To =	1,19 s

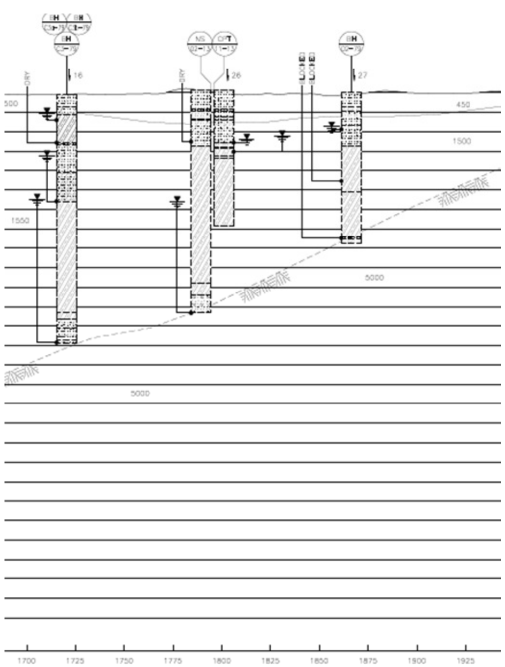

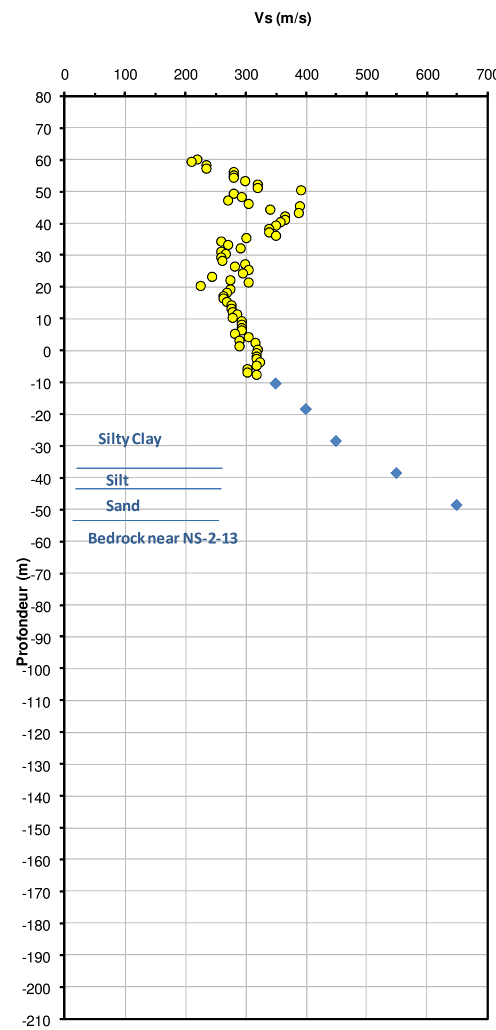

Figure C-17 - S1 (SCPT-11-13) - Vs Profile Based on SCPT-11-13 Extended Profile

SNC·LAVALIN	NORTH SPUR STABILIZATION WORKS – DYNAMIC ANALYSIS STUDY – PHASE 2	Revision		Page
	Nalcor Doc. No. MFA-SN-CD-2800-GT-RP-0007-01	B2	Date	
	SLI Doc. No. 505573-3281-4GER-0005	01	08-Dec-2015	C-19

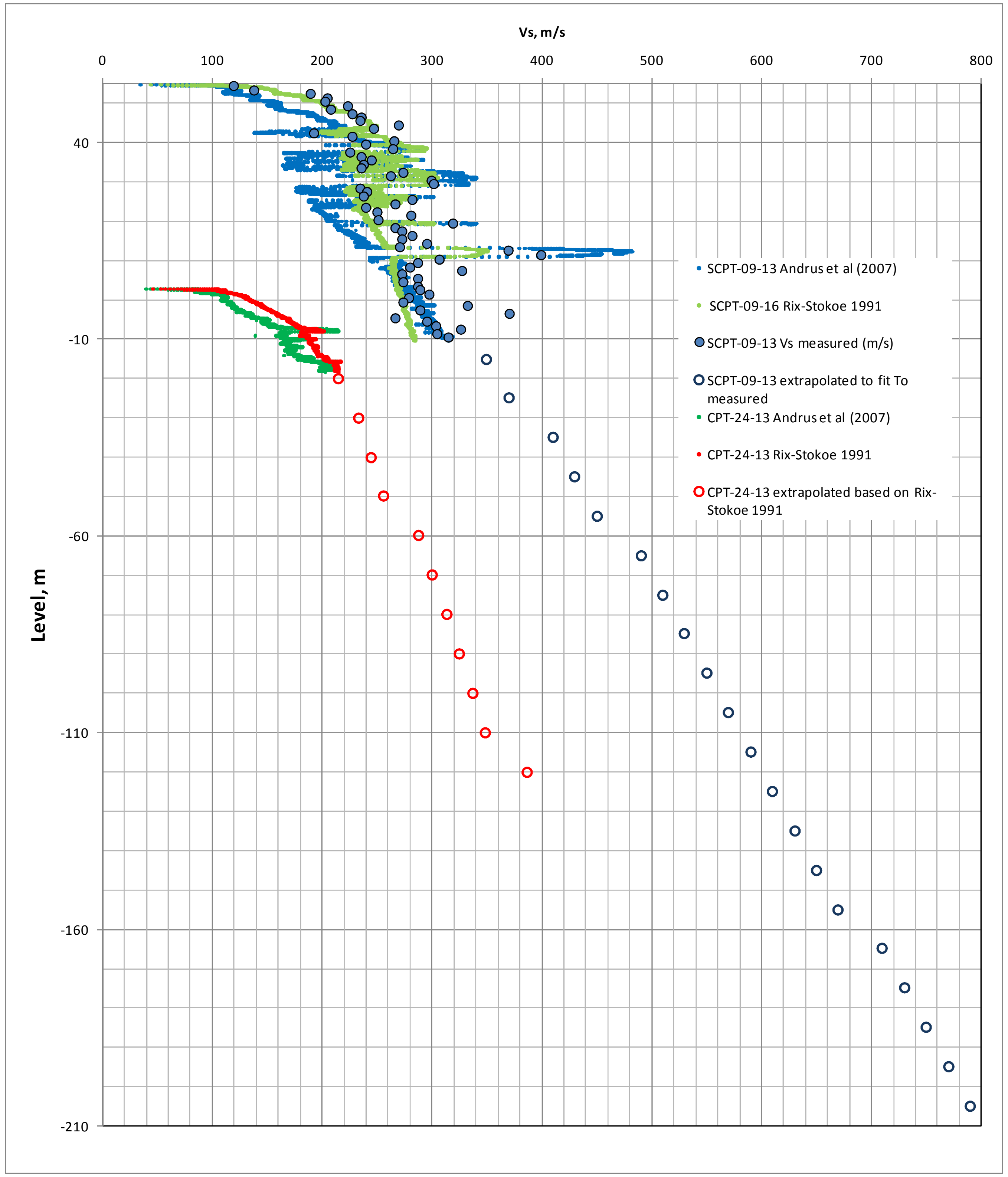

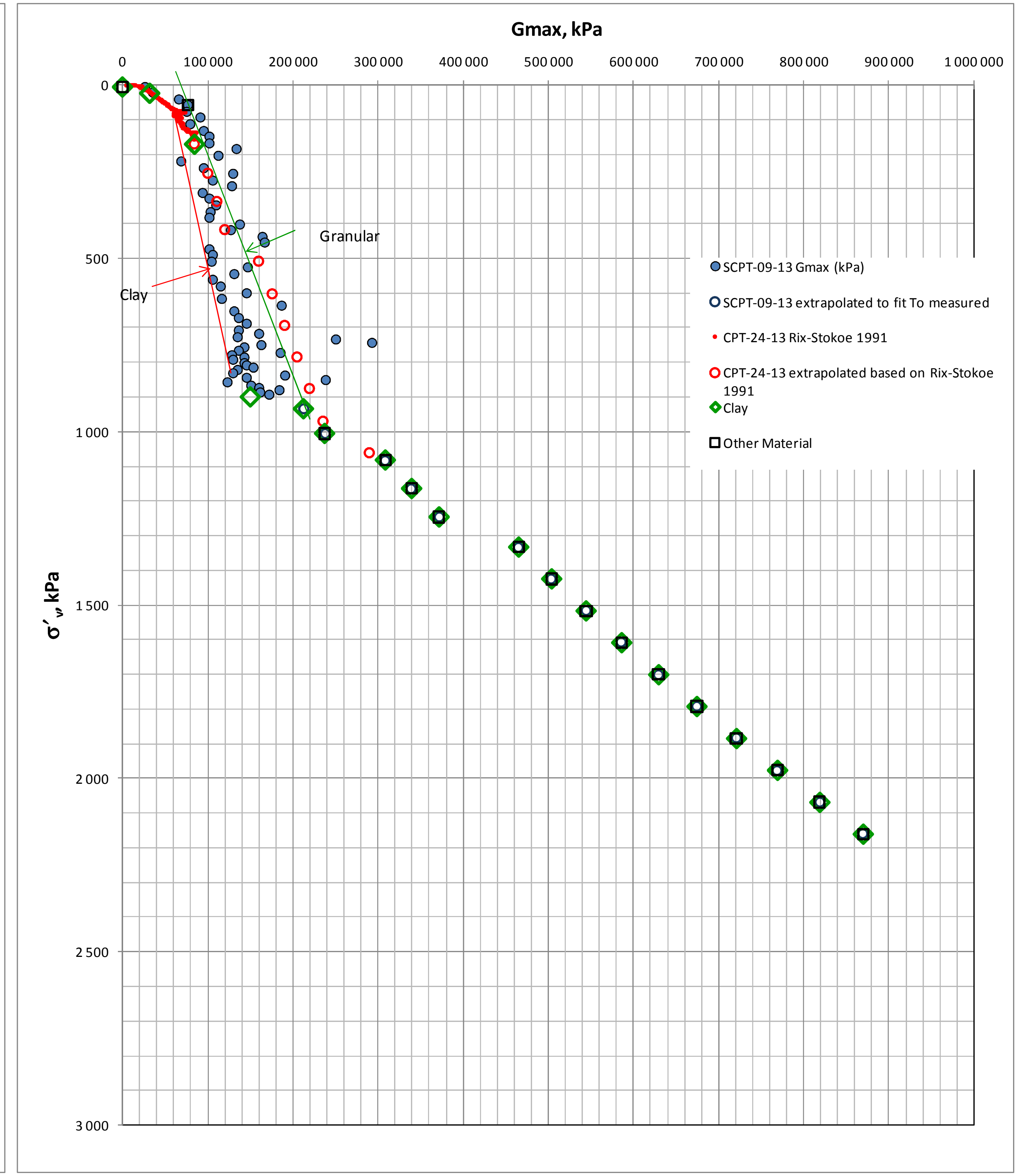

Figure C-18 - P2 (CPT-24-13) - Vs Profile based on Extrapolation from SCPT-09-13 Extended Profile

APPENDIX D

1D EQUIVALENT-LINEAR ANALYSES

D. 1D EQUIVALENT-LINEAR ANALYSES

Layer		Thickness (m)	Unit Weight (kN/m^3)	G Reduction Fn	Daming Ratio Fn	Vs (m/s)
UPPER SAND		43.80	18	Seed & Idriss 1970	Seed & Idriss Average	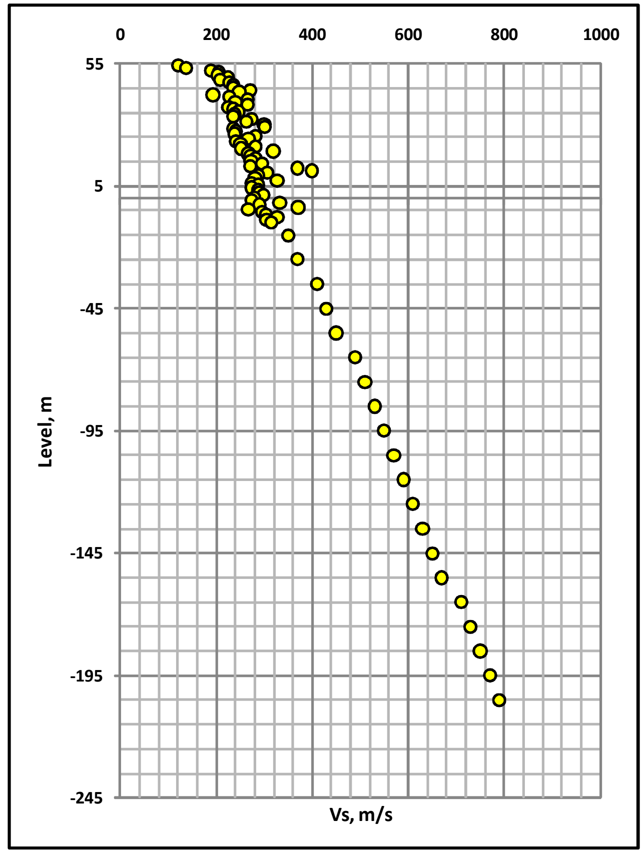
LOWER CLAY		40.80	17	Sun et al. PI 10-20	Sun et al. 1988 Average	
Lower Acquifer	SILT	30.00	18	Seed & Idriss 1970	Seed & Idriss Average	
	SAND	100.00	19	Seed & Idriss 1970	Seed & Idriss Average	
	COBLES, BOULDERS	50.00	20	Seed & Idriss 1970	Seed & Idriss Average	
Rock		3.05	26	Schnabel et al., 1972	Schnabe, Lysmer, Seed & Bolton, 1972	2500

Figure D-1 - Material Properties - Profile P1

SNC·LAVALIN	NORTH SPUR STABILIZATION WORKS – DYNAMIC ANALYSIS STUDY – PHASE 2	Revision		
	Nalcor Doc. No. MFA-SN-CD-2800-GT-RP-0007-01	B2	Date	Page
	SLI Doc. No. 505573-3281-4GER-0005	01	08-Dec-2015	D-3

Layer		Thickness (m)	Unit Weight (kN/m^3)	G Reduction Fn	Daming Ratio Fn	Vs (m/s)
LOWER CLAY		32.80	17	Sun et al. PI 10-20	Sun et al. 1988 Average	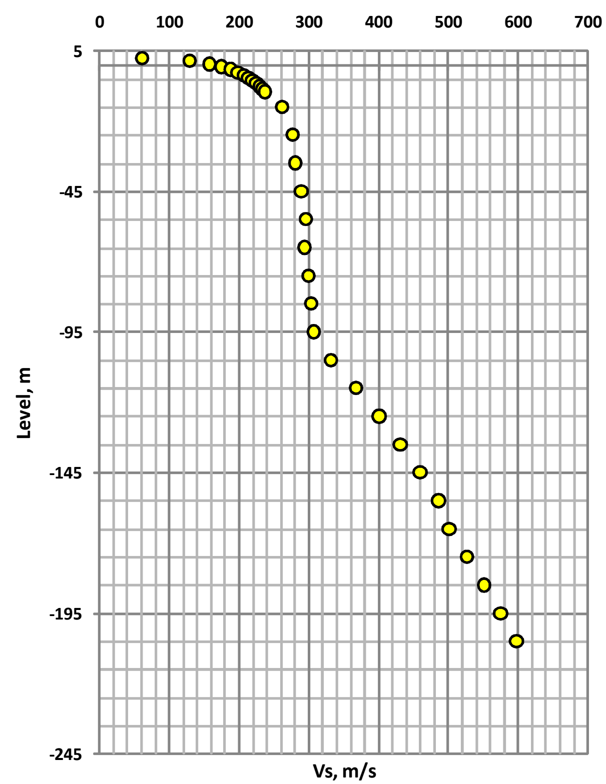
Lower Acquifer	SILT	30.00	18	Seed & Idriss 1970	Seed & Idriss Average	
	SAND	100.00	19	Seed & Idriss 1970	Seed & Idriss Average	
	COBLES, BOULDERS	50.00	20	Seed & Idriss 1970	Seed & Idriss Average	
Rock		3.05	26	Schnabel et al., 1972	Schnabe, Lysmer, Seed & Bolton, 1972	2500

Figure D-2 - Material Properties - Profile P2

SNC·LAVALIN	NORTH SPUR STABILIZATION WORKS – DYNAMIC ANALYSIS STUDY – PHASE 2	Revision		
	Nalcor Doc. No. MFA-SN-CD-2800-GT-RP-0007-01	B2	Date	Page
	SLI Doc. No. 505573-3281-4GER-0005	01	08-Dec-2015	D-4

Layer		Thickness (m)	Unit Weight (kN/m^3)	G Reduction Fn	Daming Ratio Fn	Vs (m/s)
UPPER SAND		27.00	18	Seed & Idriss 1970	Seed & Idriss Average	
LOWER CLAY		68.00	17	Sun et al. PI 10-20	Sun et al. 1988 Average	
Lower Acquifer	SILT	10.00	18	Seed & Idriss 1970	Seed & Idriss Average	
	SAND	10.00	19	Seed & Idriss 1970	Seed & Idriss Average	
Rock		3.05	26	Schnabel et al., 1972	Schnabe, Lysmer, Seed & Bolton, 1972	2500

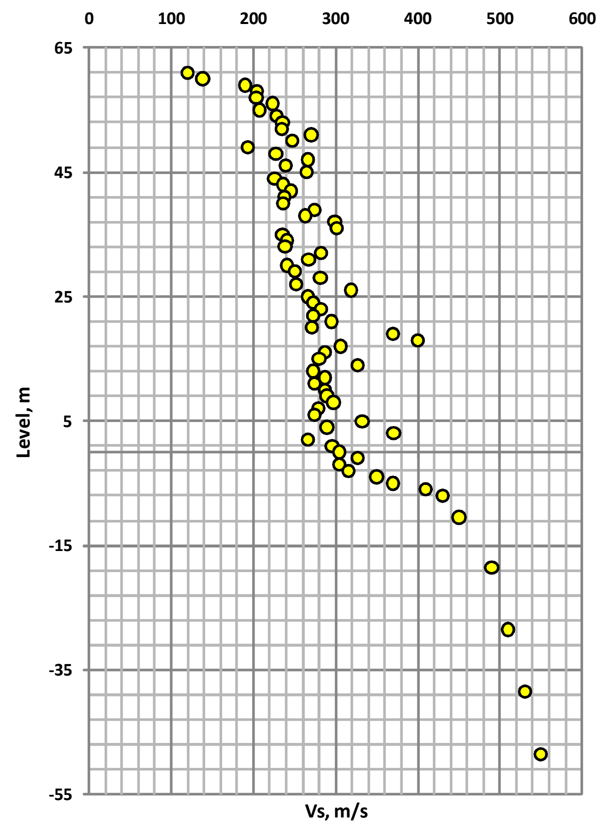

Figure D-3 - Material Properties - Profile S1

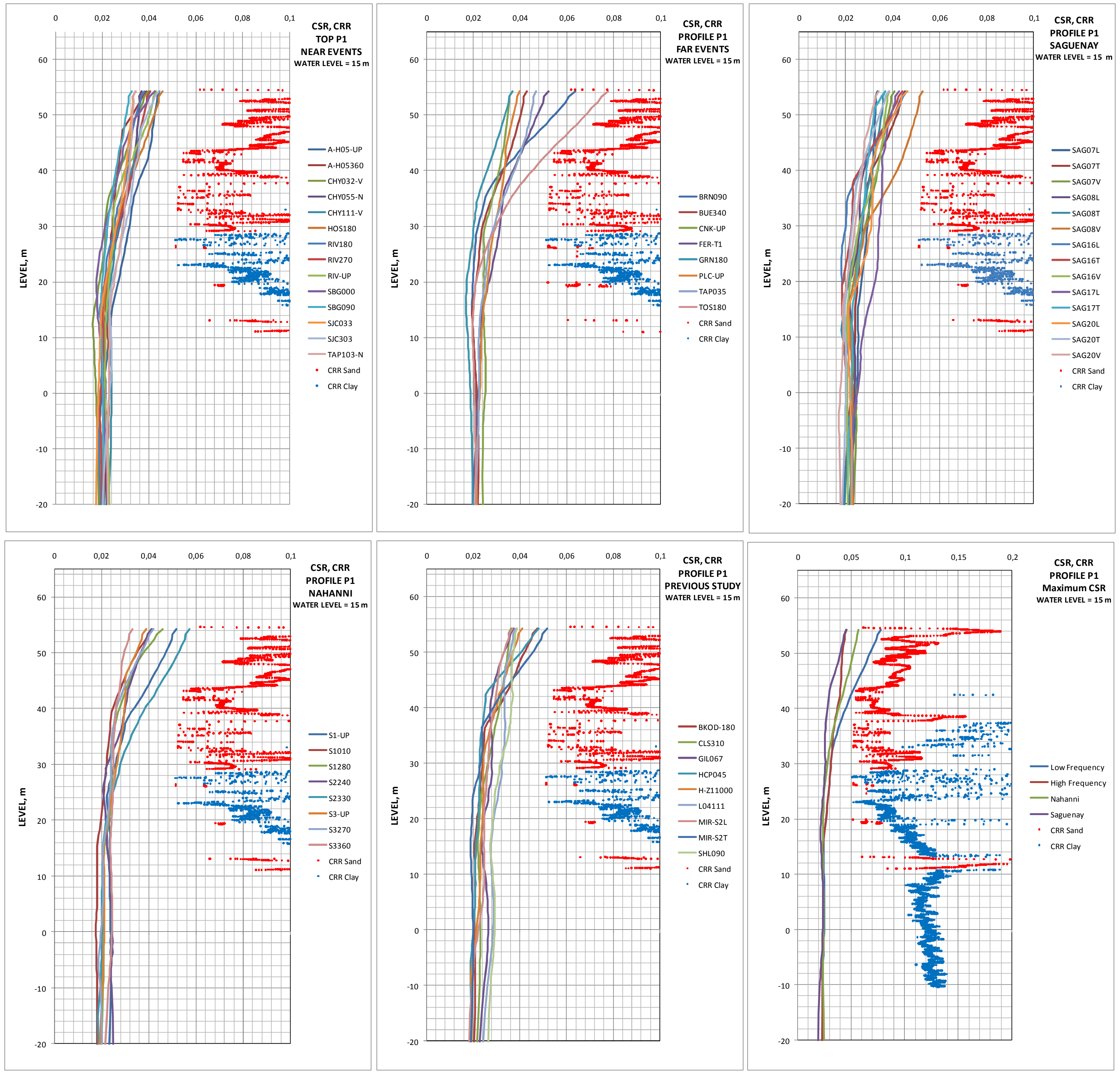

Figure D-4 - CRR and CSR for P1 Downstream (WL 15 m) Profile

CRR Profiles based on SCPT-09-13 Tip Resistance for Sand and Interpreted Undrained Shear Strength for Clay.

CRR Profiles from 1D Equivalent-linear Analyses with Input Motions Selected from a) Far Event Scenario; b) Near Event Scenario; c) Saguenay 1988 Recordings; d) Nahanni 1985 Recordings; e) Accelerograms Used in Preliminary Dynamic Study; f) Maximum CSR Profiles for Each Group of Input Motions.

See Figures of Appendix C for details on input motions characteristics.

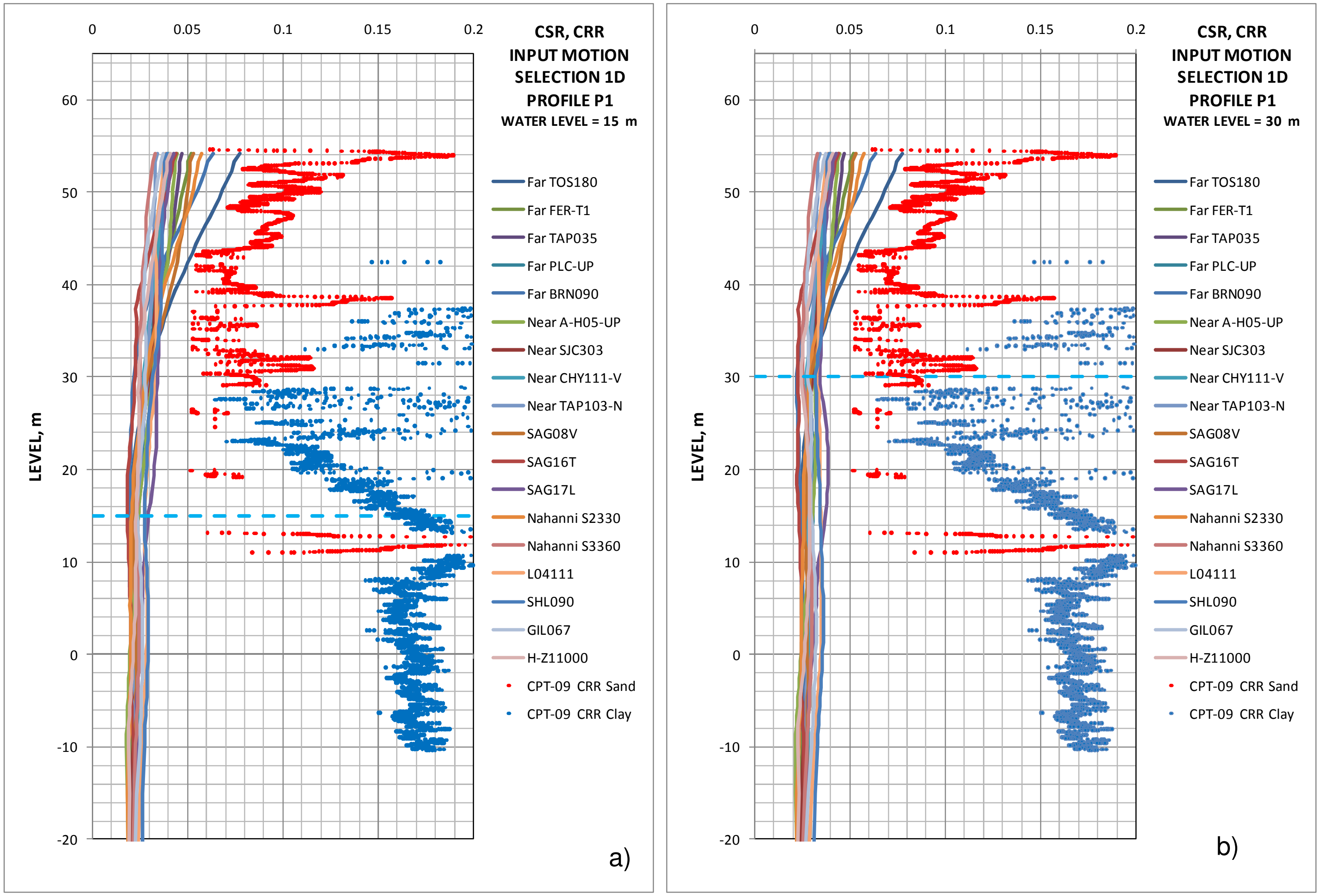

Figure D-5 - CRR and CSR for P1 Profile – Selection of Input Motions for 1D Analyses
a) Downstream (WL 15 m); b) Upstream (WL 30 m)

SNC·LAVALIN	NORTH SPUR STABILIZATION WORKS – DYNAMIC ANALYSIS STUDY – PHASE 2	Revision		Page
	Nalcor Doc. No. MFA-SN-CD-2800-GT-RP-0007-01	B2	Date	
	SLI Doc. No. 505573-3281-4GER-0005	01	08-Dec-2015	D-7

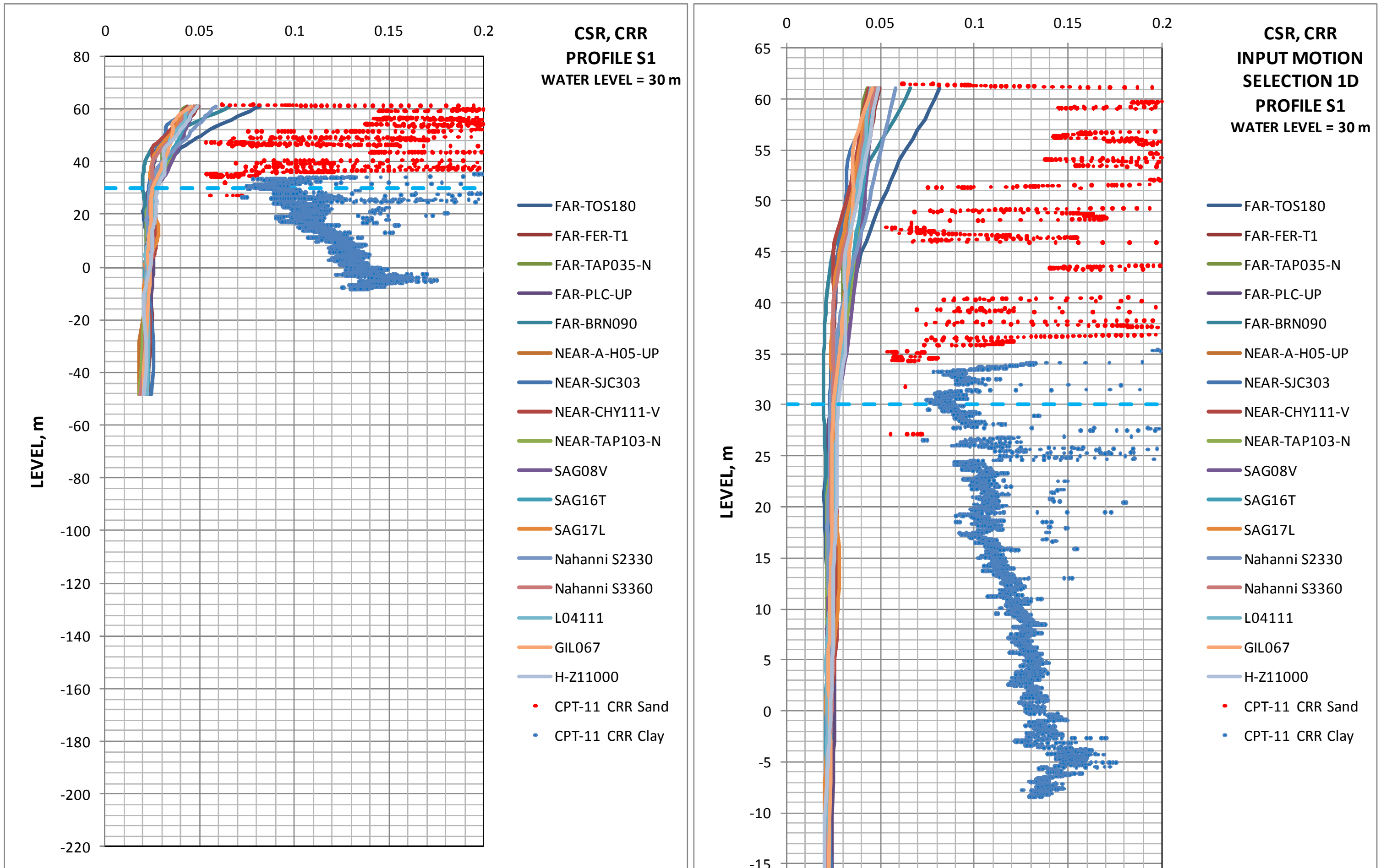

CRR Profiles based on SCPT-11-13 Tip Resistance for Sand and Interpreted Undrained Shear Strength for Clay

Figure D-6 - CRR and CSR for S1 Upstream (WL 30 m) Profile – Input Motions Selected for 1D Analyses

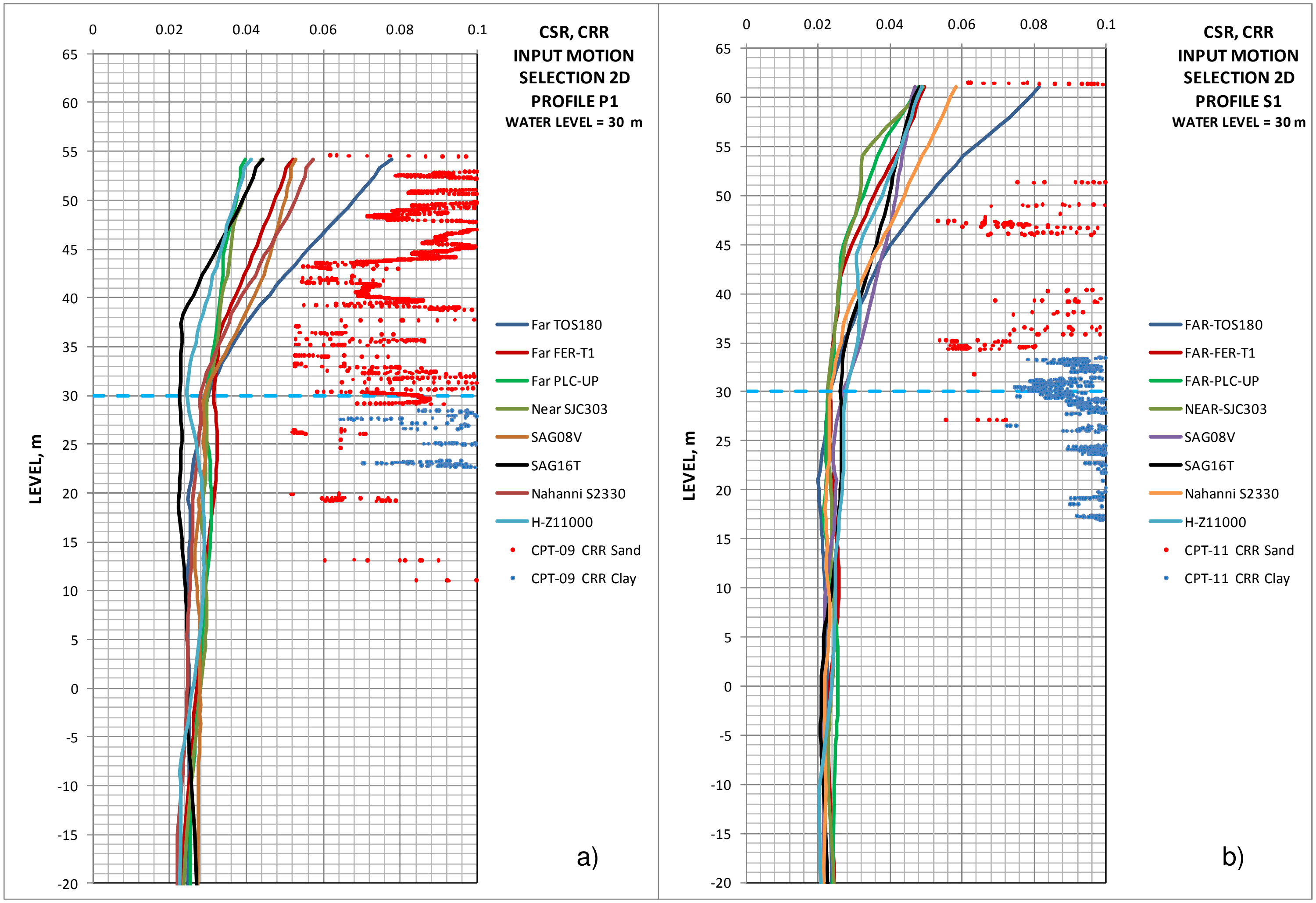

Figure D-7 - CRR and CSR– 1D Analyses for Input Motions Selected for 2D Analyses

a) P1 Profile (WL 30 m); b) S1 Profile (WL 30 m)

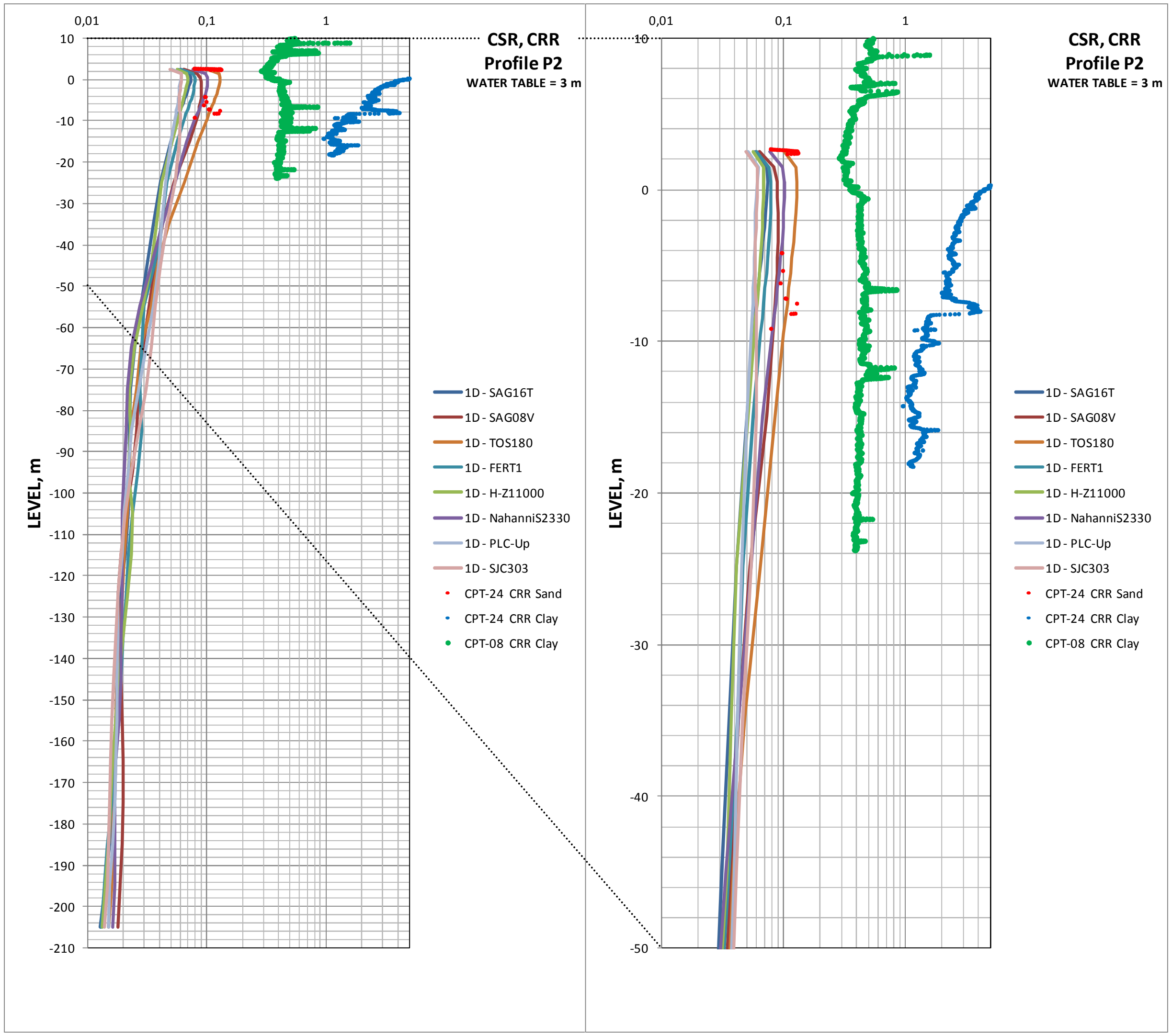

Figure D-8 - CRR and CSR for P2 Downstream (WL 3 m) Profile – 1D Analyses for Input Motions Selected for 2D Analyses

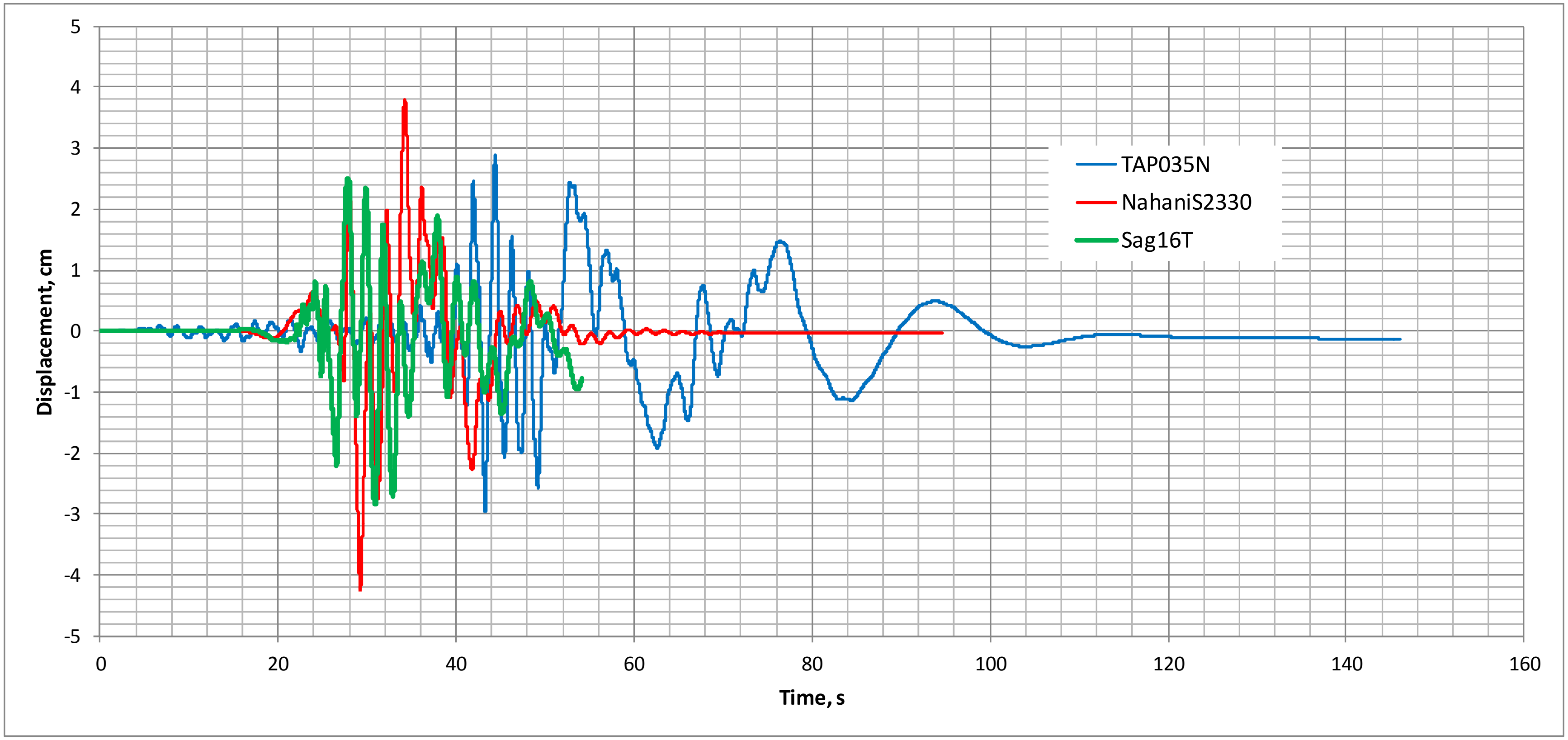

Figure D-9 – Crest Displacement History for P1 Downstream (WL 15 m) Profile – 1D Equivalent-Linear Analyses for Input Motions Selected for 2D Non-Linear Analyses

APPENDIX E

INPUT MOTION SELECTION FOR 2D ANALYSES

E. INPUT MOTION SELECTION FOR 2D ANALYSES

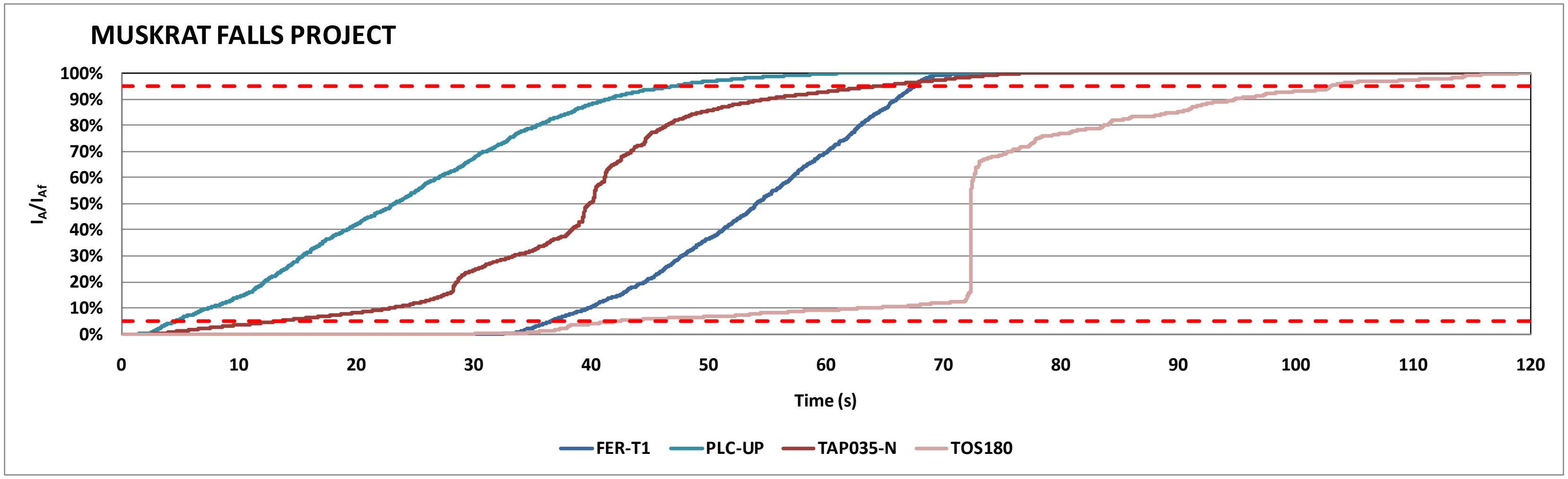

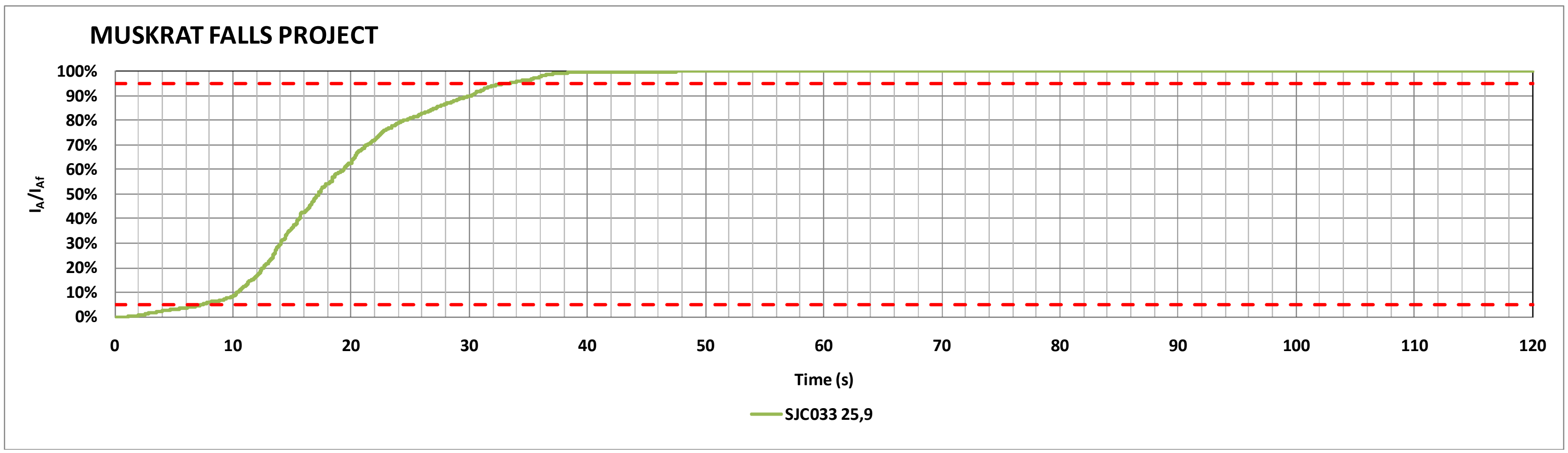

Figure E-1 - Spectral Matched Input Motions - Selection for 2D Analyses – Husid Plots
a) Far Events Scenario; b) Near Events Scenario

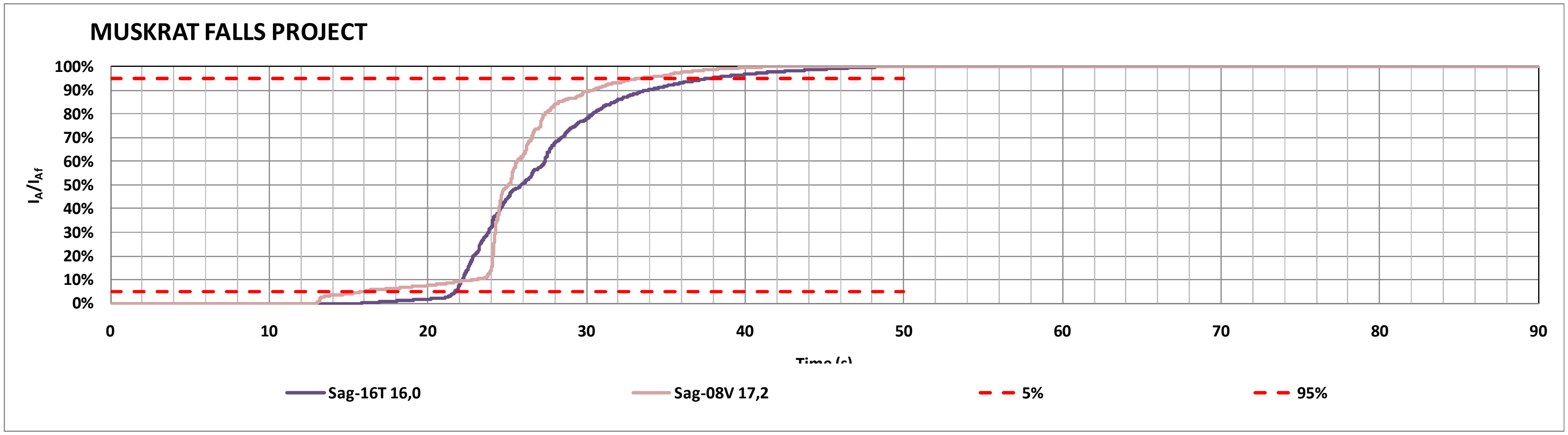

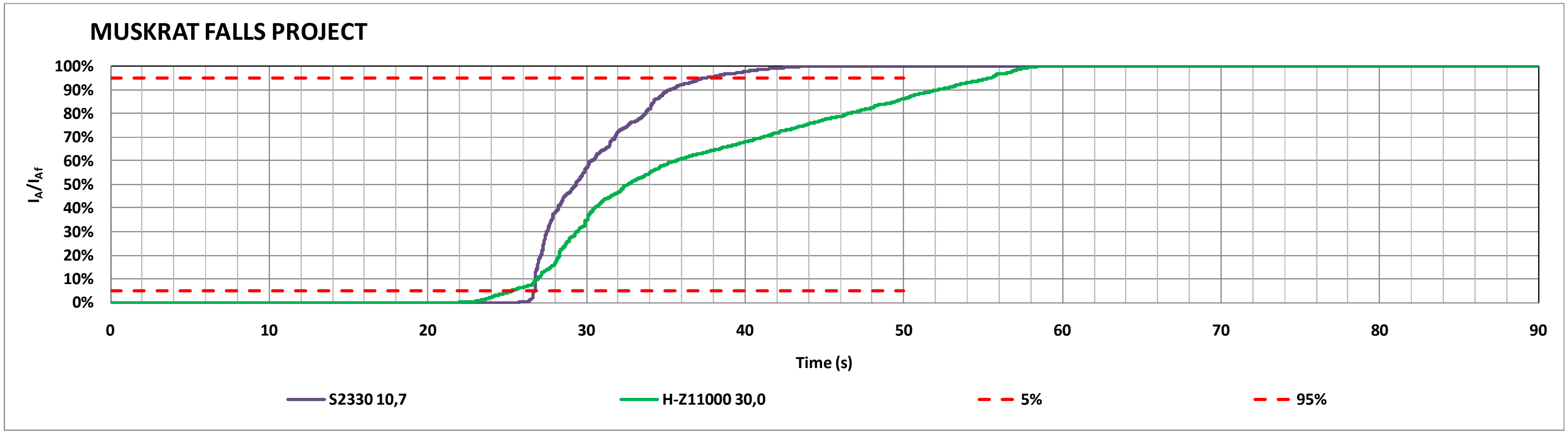

Figure E-1 - Spectral Matched Input Motions - Selection for 2D Analyses – Husid Plots

c) Saguenay 1988; d) Nahanni 1985 and Previous Study

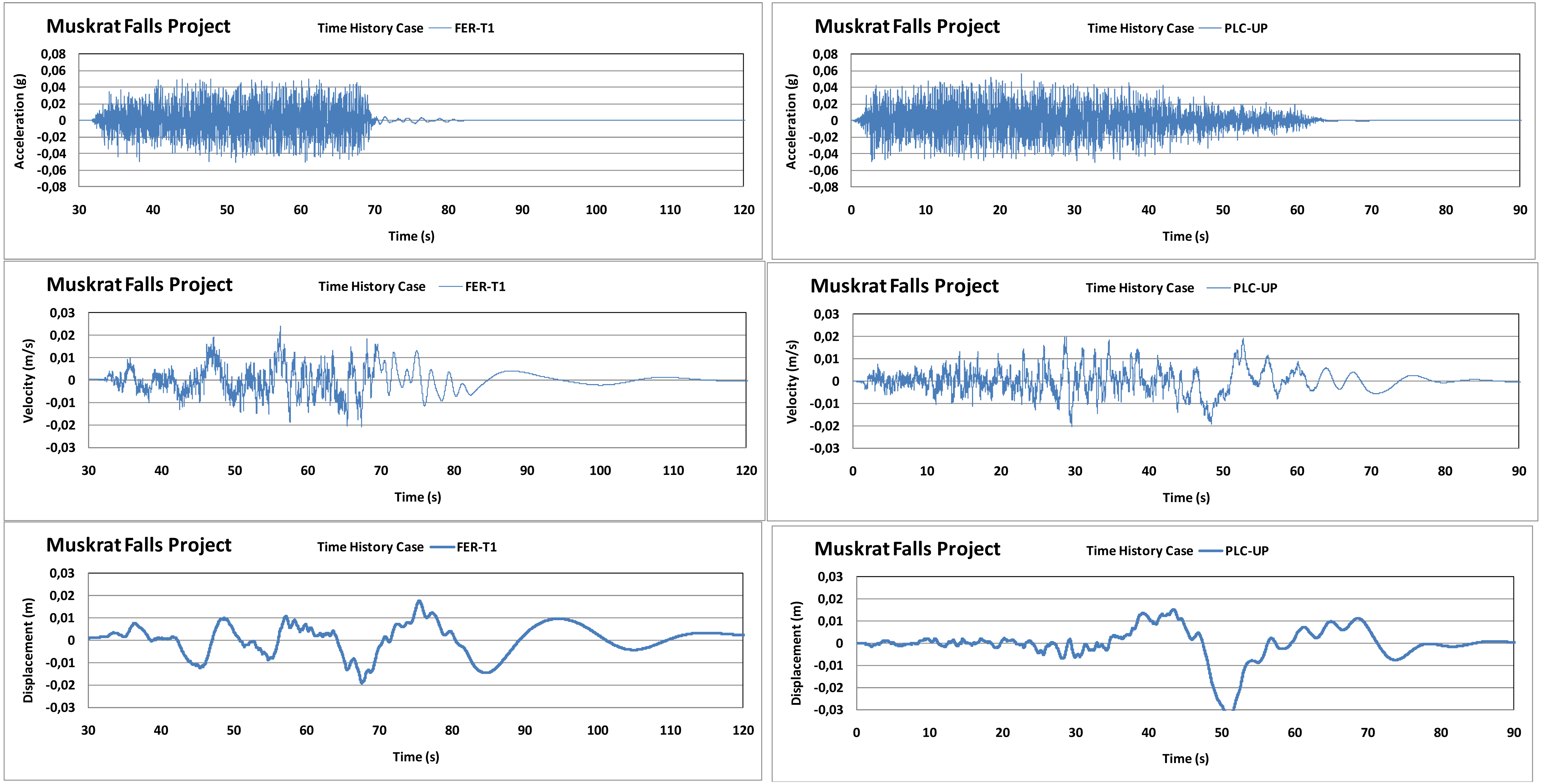

Figure E-2 - Spectral Matched Input Motions - Selection for 2D Analyses – Acceleration, Velocity and Displacement

a) **FER-T1 and PLC-UP**

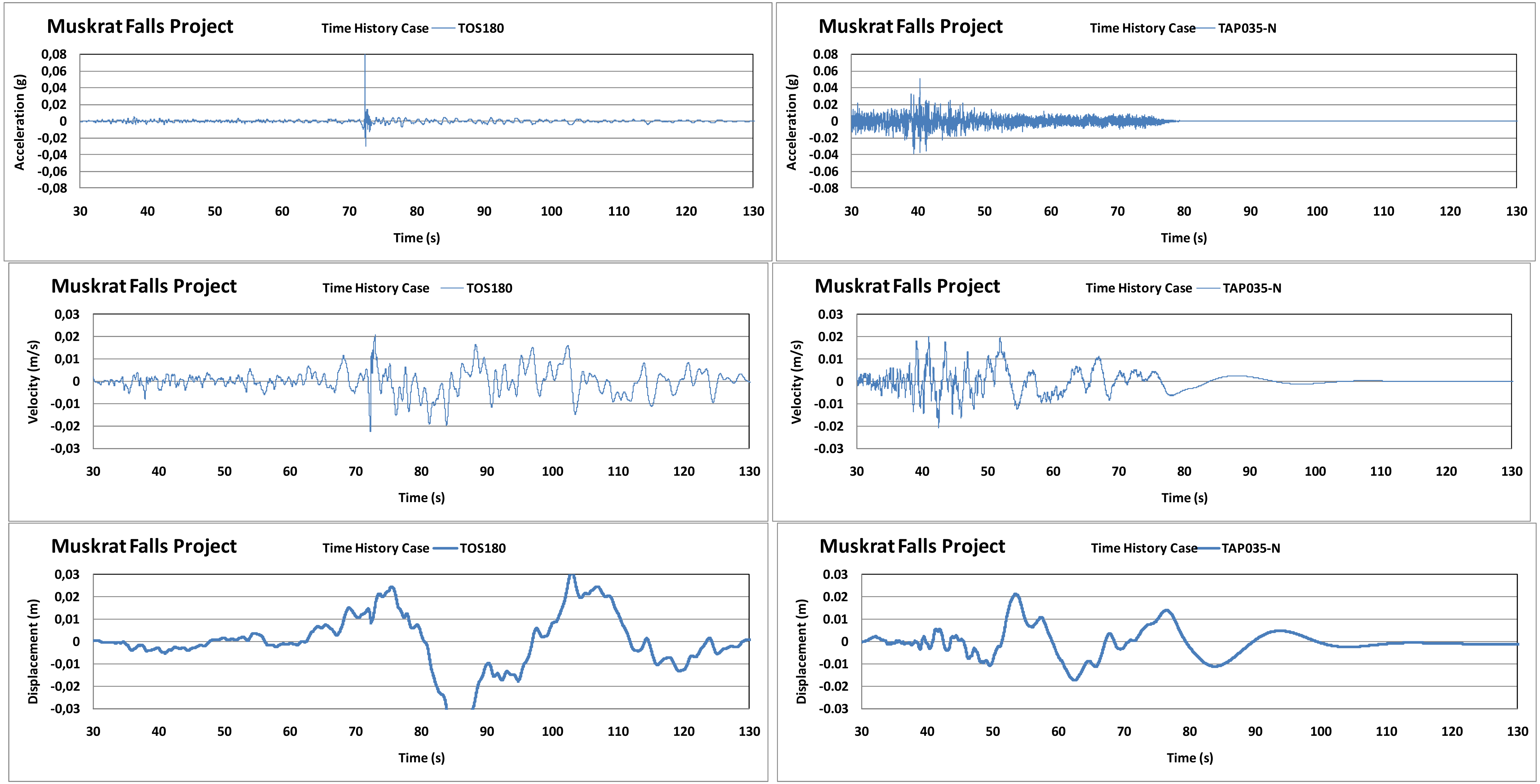

Figure E-2 – Spectral Matched Input Motions - Selection for 2D Analyses – Acceleration, Velocity and Displacement

b) TOS-180 and TAP035-N

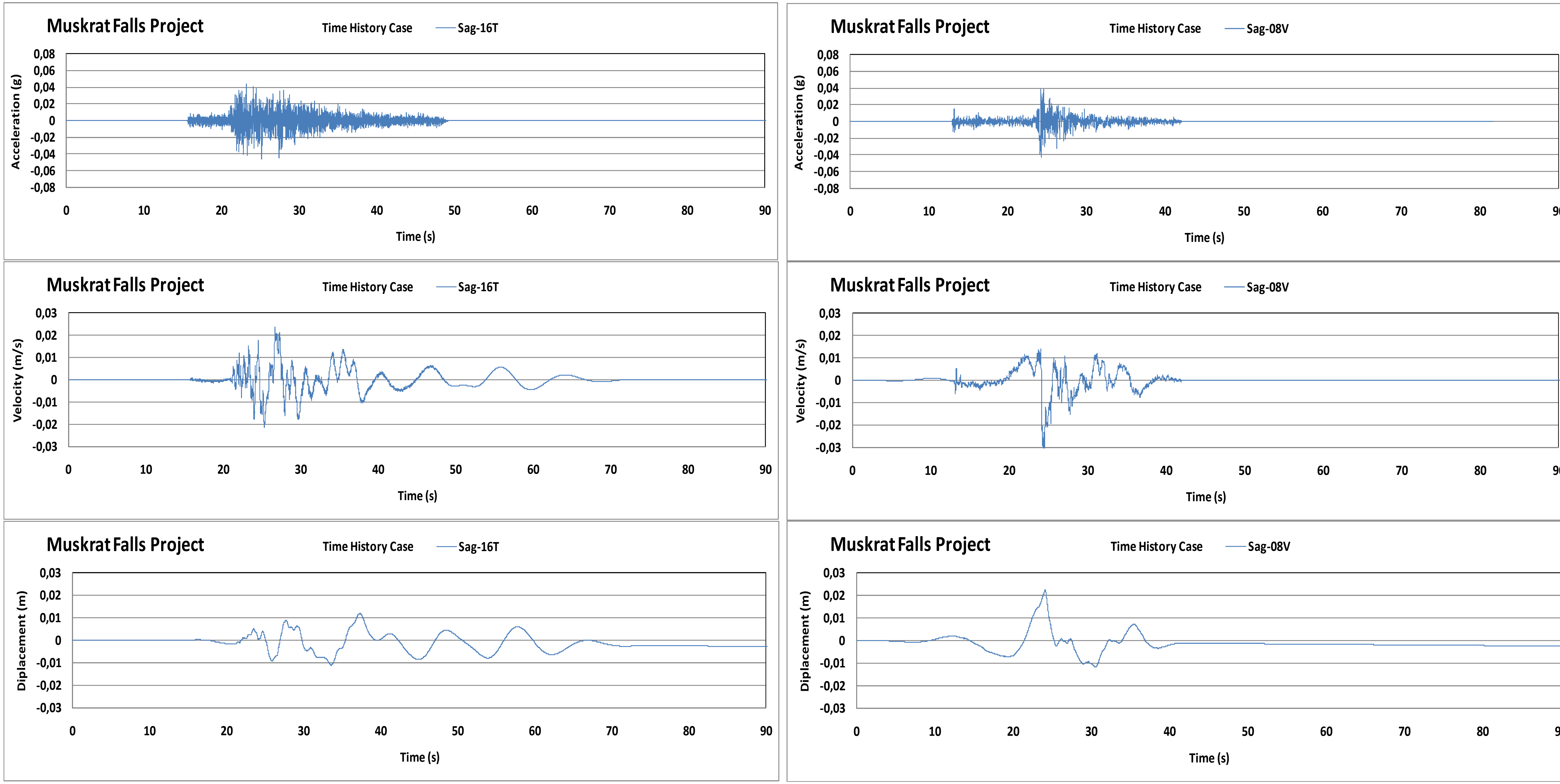

Figure E-2 – Spectral Matched Input Motions - Selection for 2D Analyses – Acceleration, Velocity and Displacement

c) SAG-16T and SAG-08V

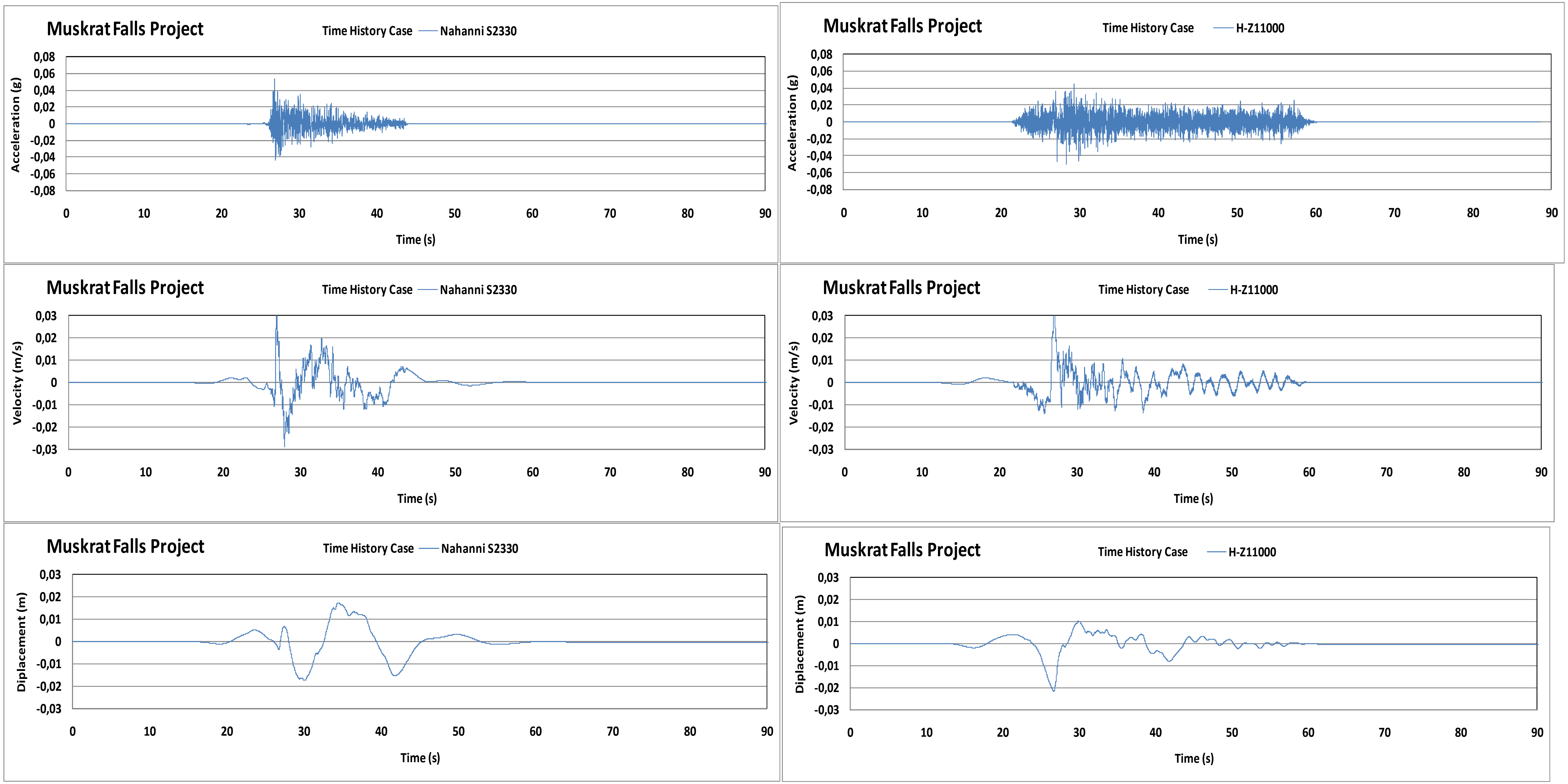

Figure E-2 – Spectral Matched Input Motions - Selection for 2D Analyses – Acceleration, Velocity and Displacement

d) Nahanni S2330 and H-Z11000

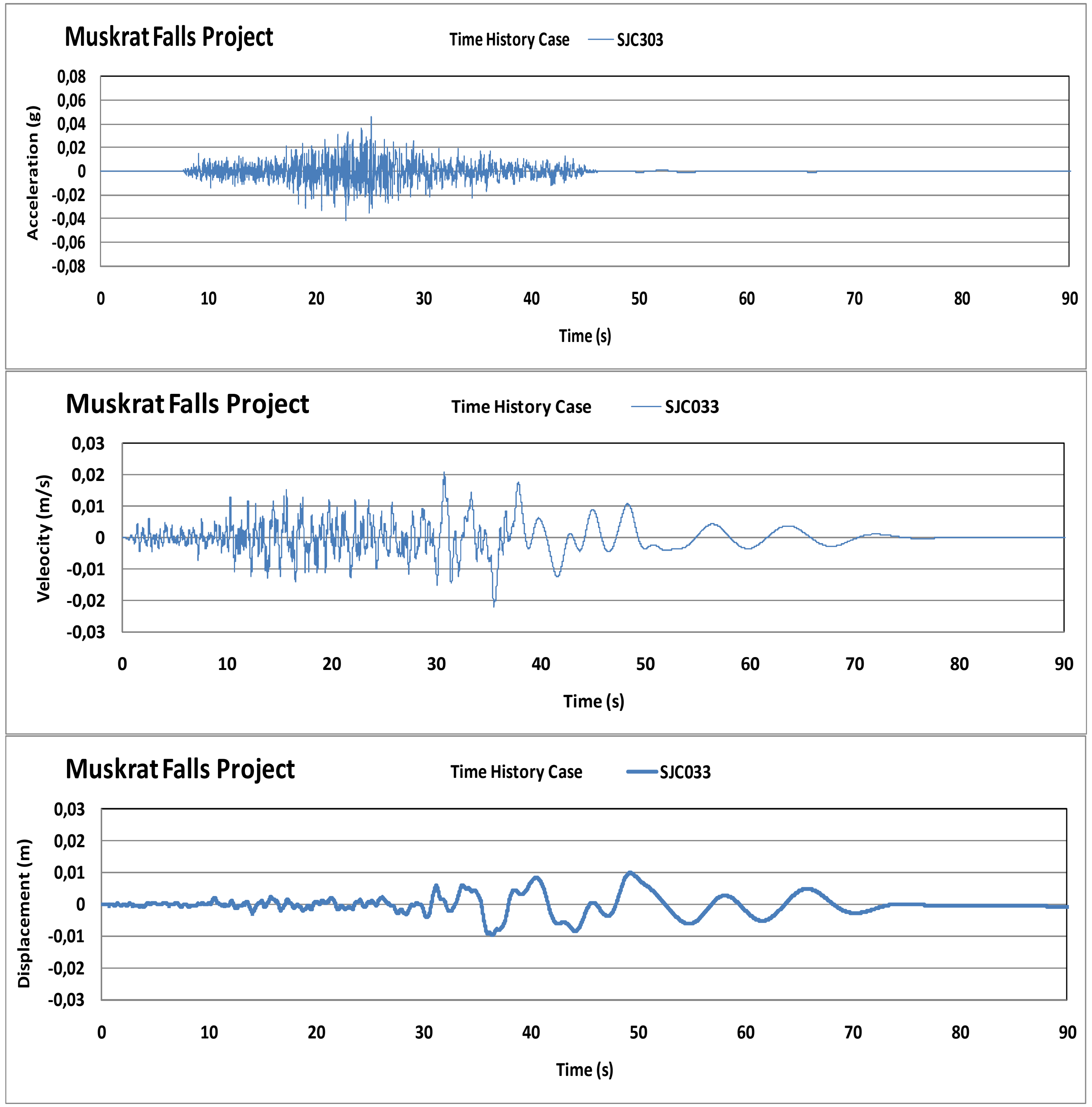

Figure E-2 – Spectral Matched Input Motions - Selection for 2D Analyses – Acceleration, Velocity and Displacement

e) SJC033

APPENDIX F

2D EQUIVALENT-LINEAR ANALYSES

F. 2D EQUIVALENT-LINEAR ANALYSES

Layer	Unit Weight (kN/m^3)	G Reduction Fn	Daming Ratio Fn	G_{max} (kPa) = f(σ'_{vo})
UPPER SAND	18	Seed & Idriss 1970	Seed & Idriss Average	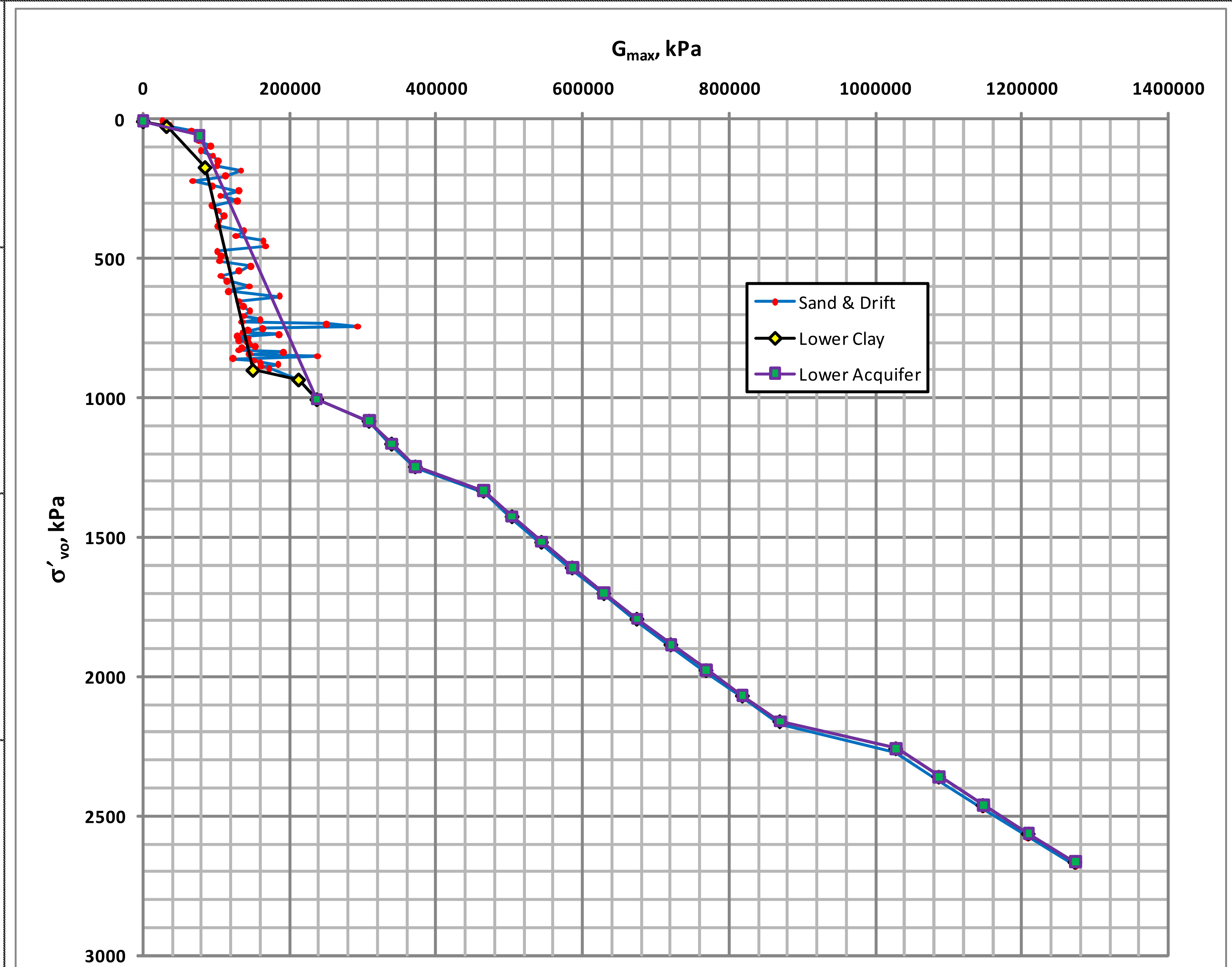
Stratified Drift	17	Seed & Idriss 1970	Seed & Idriss Average	
LOWER CLAY	17	Sun et al. PI 10-20	Sun et al. 1988 Average	
Lower Acquifer	20	Seed & Idriss 1970	Seed & Idriss Average	

Figure F-1 - Material Properties for 2D Equivalent-linear Analyses

SNC·LAVALIN	NORTH SPUR STABILIZATION WORKS – DYNAMIC ANALYSIS STUDY – PHASE 2	Revision		Page
	Nalcor Doc. No. MFA-SN-CD-2800-GT-RP-0007-01	B2	Date	
	SLI Doc. No. 505573-3281-4GER-0005	01	08-Dec-2015	F-3

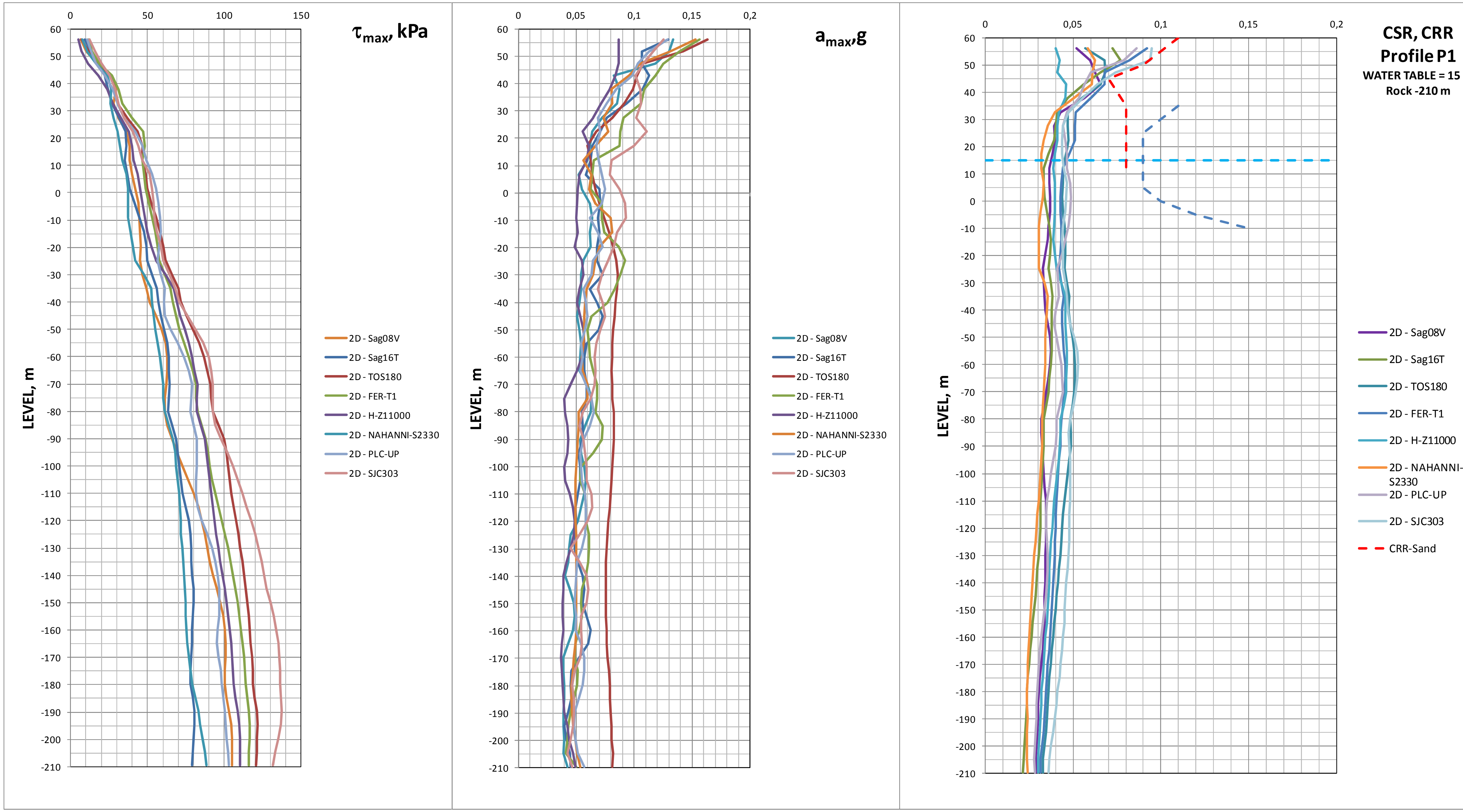

Figure F-2 - 2D Equivalent-linear Analyses - 8 Selected Input Motions -– Section 13 (Bedrock at -210 m) for Downstream Water Table Elevation (15 m) – Results at P1 Crest Profile

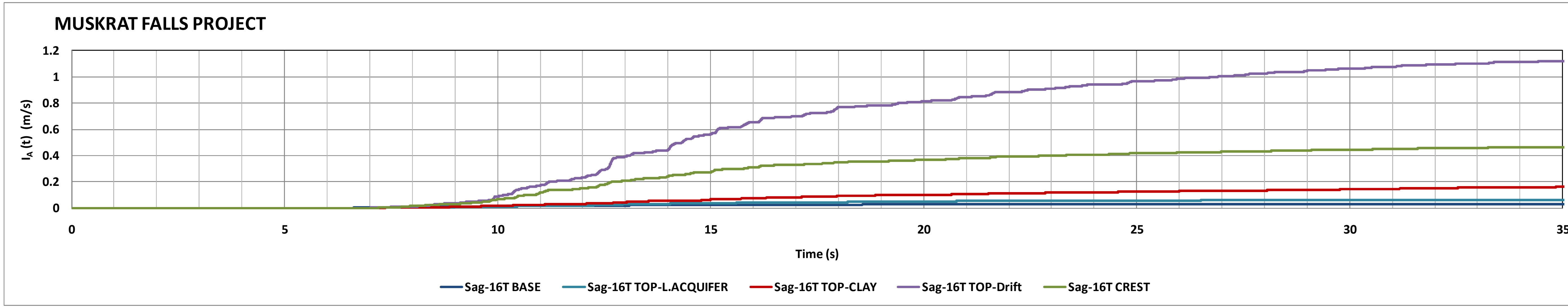

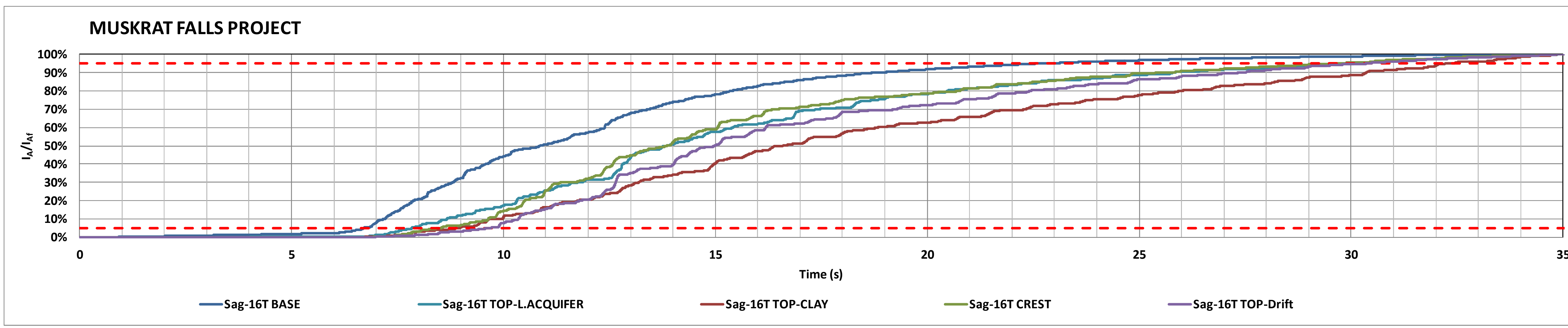

Figure F-3 – 2D Equivalent-linear Analyses – Section 13 (Bedrock at -210 m) Submitted to SAG-16T - Arias' Intensity and Husid Plots for Different Control Points on P1 Crest Profile

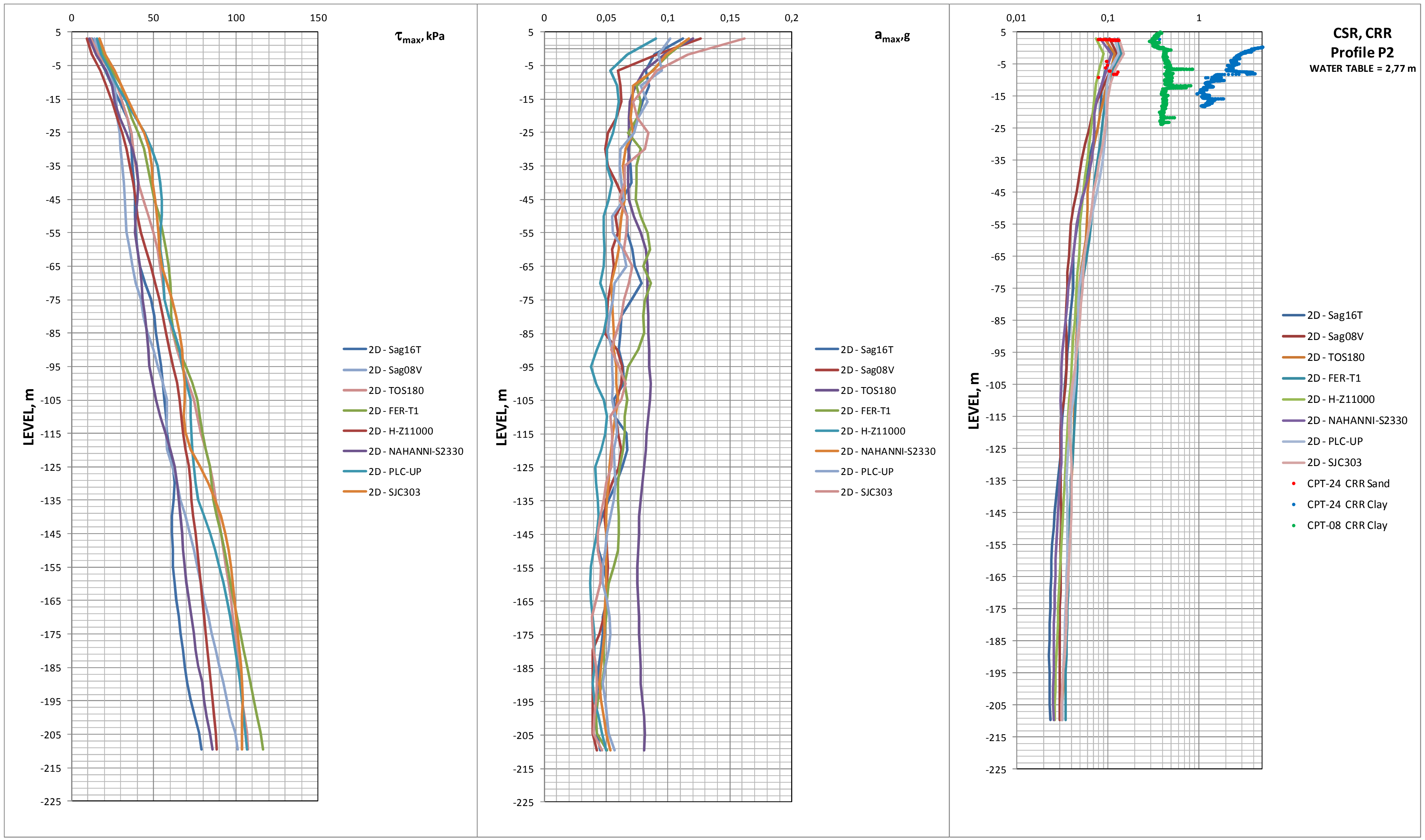

Figure F-4 - 2D Equivalent-linear Analyses - 8 Selected Input Motions -– Section 13 (Bedrock at -210 m) for Downstream Water Table Elevation (15 m) – Results at P2 Toe Profile

SNC·LAVALIN	NORTH SPUR STABILIZATION WORKS – DYNAMIC ANALYSIS STUDY – PHASE 2	Revision		Page
	Nalcor Doc. No. MFA-SN-CD-2800-GT-RP-0007-01	B2	Date	
	SLI Doc. No. 505573-3281-4GER-0005	01	08-Dec-2015	F-6

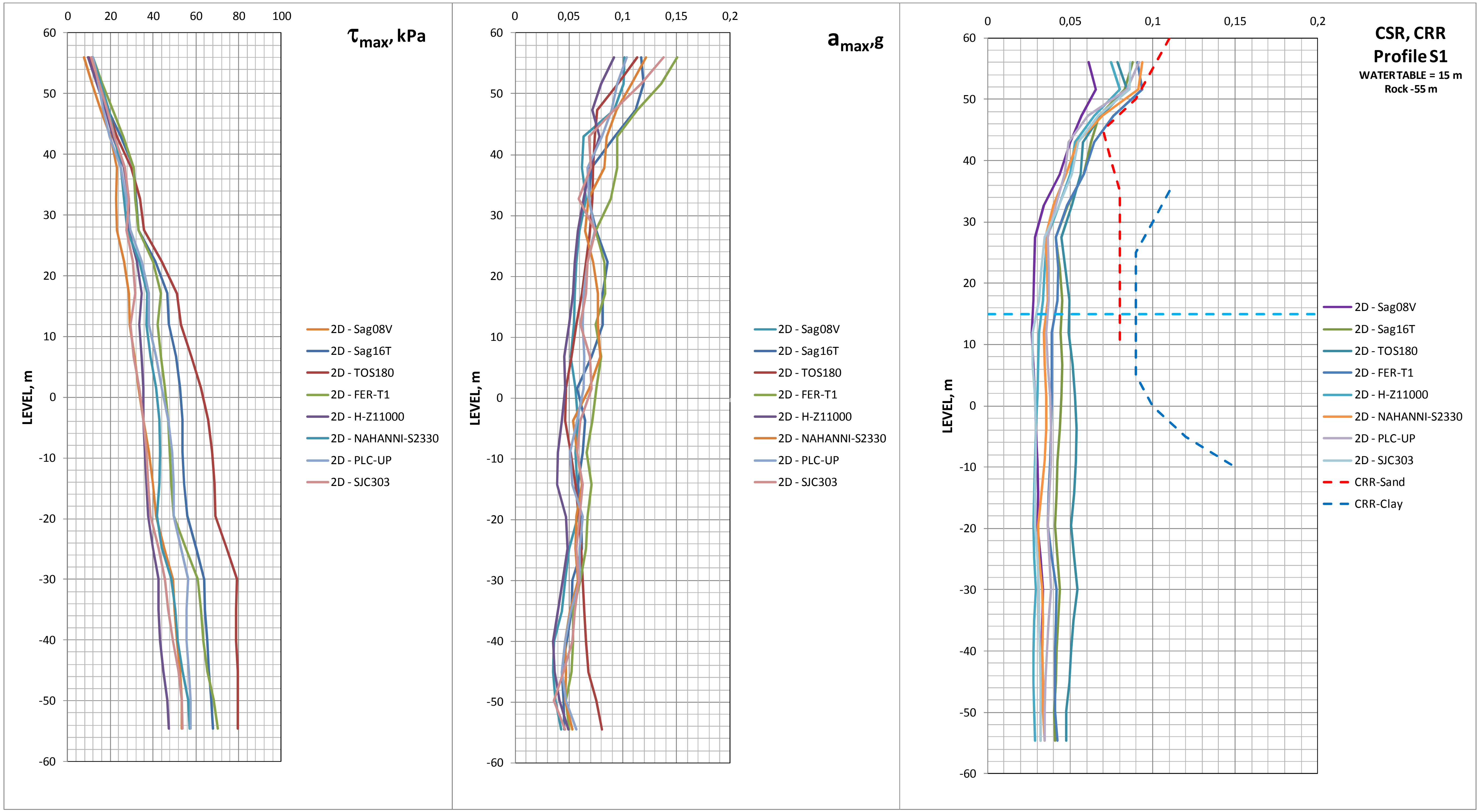

Figure F-5 - 2D Equivalent-linear Analyses - 8 Selected Input Motions -– Section 9 (Bedrock at -55 m) for Downstream Water Table Elevation (15 m) – Results at S1 Crest Profile

APPENDIX G

2D NON-LINEAR ANALYSES

G. 2D NON-LINEAR ANALYSES

Table G-1 – 2D Non-Linear Dynamic Response Analyses - Material Properties

Material	Dry Unit Mass	Water Content	Porosity	Cohesion	Internal Friction Angle	Dilation Angle	SPT Index	Constant volume friction angle (deg)	Poisson's Ratio	Shear Modulus	Bulk Modulus	Hydraulic Conductivity	Mobility Coefficient
	ρ_{DRY}[1]	w[2]	n	c'	ϕ'	ψ'	$(N_1)_{60-CS}$	ψ'_{cv}[2]	ν	G[3]	K[3]	k_H (m/s)	k (m^2/kPa-sec)
	(Mg/m^3)	%		(kPa)	(°)	(°)	(blows/m)	(°)		(kPa)	(kPa)		
Upper Sand	1.79	20	0.36	0	35	0	14	33.6	0.33	8.29E+04	2.16E+05	1.00E-05	1.02E-06
Stratified Drift - Sand	1.65	25	0.41	0	35	0	13	33.7	0.33	1.17E+05	3.05E+05	1.00E-05	1.02E-06
Stratified Drift - Upper Clay	1.46	33	0.48	6	31	0	--	--	0.45	2.04E+05	1.97E+06	1.00E-05	1.02E-06
Lower Clay	1.46	33	0.48	6	31	0	--	--	0.45	2.04E+05	1.97E+06	1.00E-08	1.02E-09
Lower Acquifer	1.79	20	0.36	0	35	0	--	--	0.33	8.73E+05	2.28E+06	1.00E-04	1.02E-05

Note:

1- The values of dry unit mass are calculated based on average water content measured in boreholes.

2- In the UBCSand model, the constant volume friction angle, ψ'_{cv}, is a function of the corrected standard penetration blow count, $(N_1)_{60-CS}$ and the effective internal friction angle, ϕ': $\psi'_{cv}=\phi'-(N_1)_{60-CS}/10$; Gmax and K values are calculated based on $(N_1)_{60-cs}$ and σ'_m of each element.

3- The values shown in this column are used during initial static state in FLAC. A profile of Gmax in function of σ'_{vo} is applied during the dynamic analysis as follows:

$$G_{max}(Granular\ Materials) = \begin{cases} G_{max} = 39241\ln(\sigma'_{vo}) - 81679 & \sigma'_{vo} \leq 900\ kPa \\ G_{max} = 530.77(\sigma'_{vo}) - 287692 & \sigma'_{vo} > 900\ kPa \end{cases}$$

$$G_{max}\quad(Clay\ Materials) = \begin{cases} G_{max} = 26153\ln(\sigma'_{vo}) - 52839 & \sigma'_{vo} \leq 900\ kPa \\ G_{max} = 576.92(\sigma'_{vo}) - 389231 & \sigma'_{vo} > 900\ kPa \end{cases}$$

Damping:

- Low level of Rayleigh damping to remove high frequency noise
- Hysteretic damping for Mohr-Coulomb material: Sig3 model provided in FLAC was calibrated to fit the degradation curves used in 1D and 2D equivalent-linear analyses.
- Damping included in UBCSand model

SNC·LAVALIN	NORTH SPUR STABILIZATION WORKS – DYNAMIC ANALYSIS STUDY – PHASE 2	Revision		
	Nalcor Doc. No. MFA-SN-CD-2800-GT-RP-0007-01	B2	Date	Page
	SLI Doc. No. 505573-3281-4GER-0005	01	08-Dec-2015	G-4

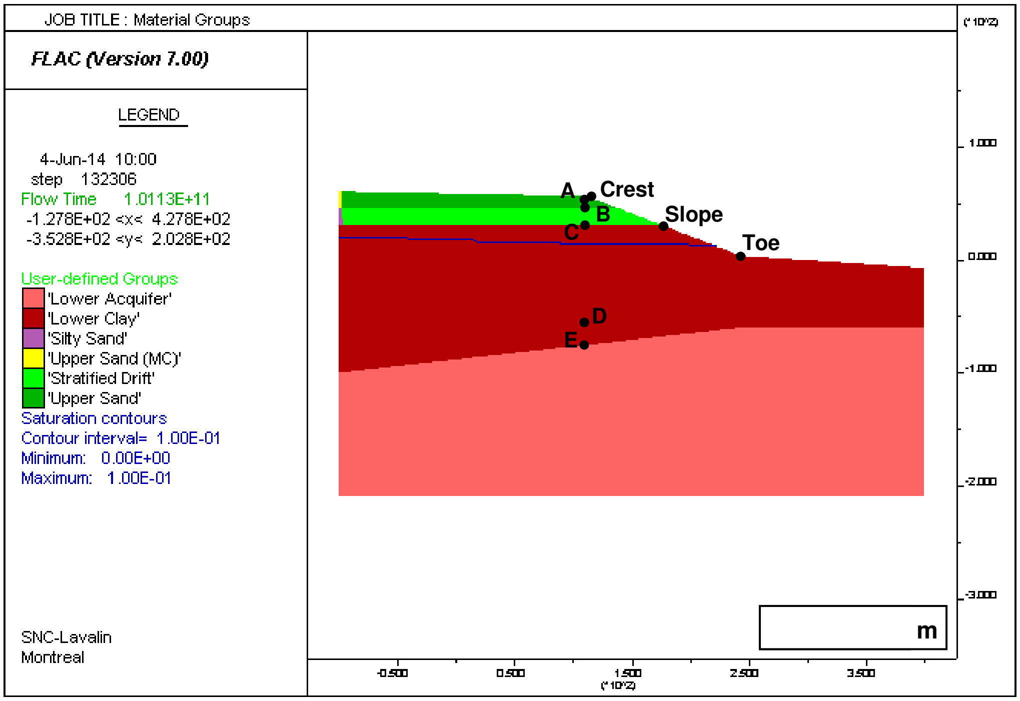

Figure G-1 - Geometry, Material Groups and Water Table

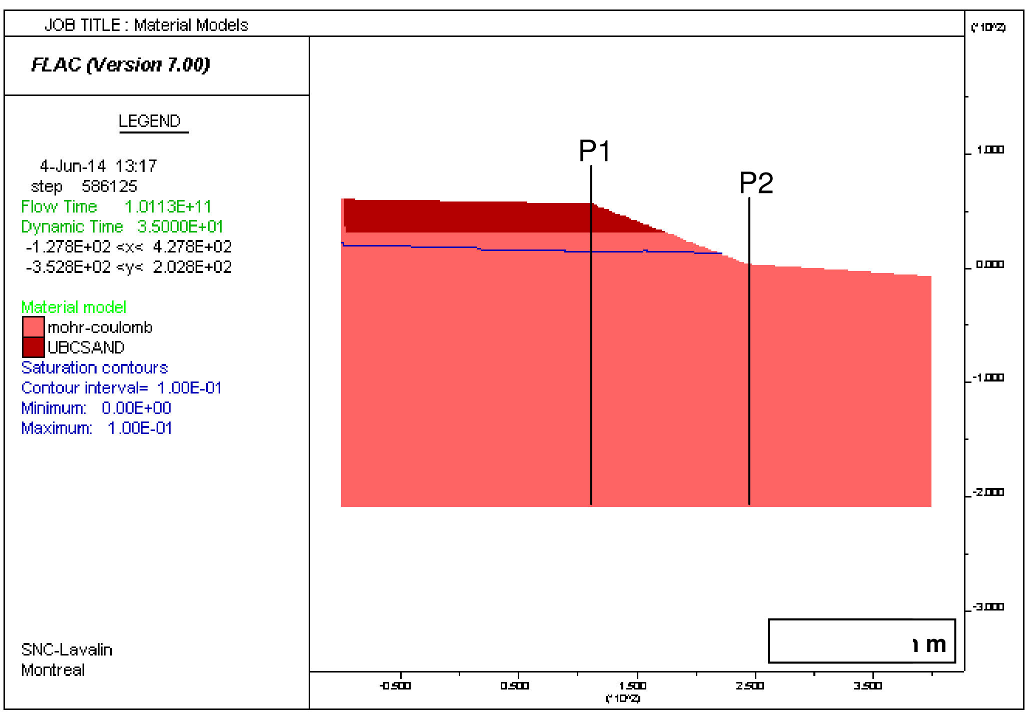

Figure G-2 - Material Models and Water Table

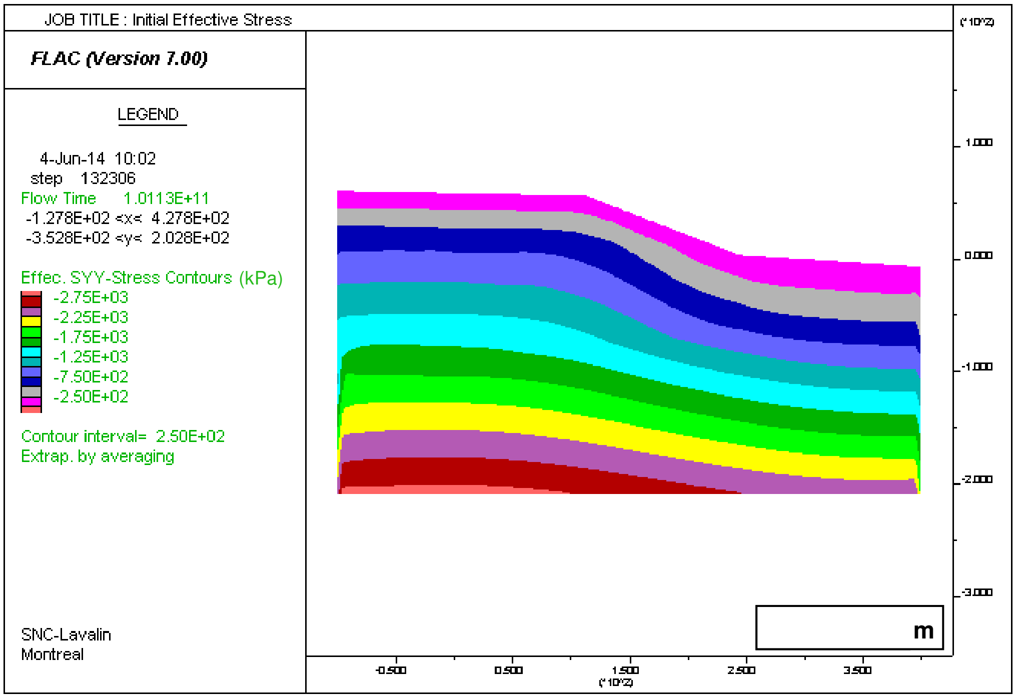

Figure G-3 - Initial Vertical Effective Stress

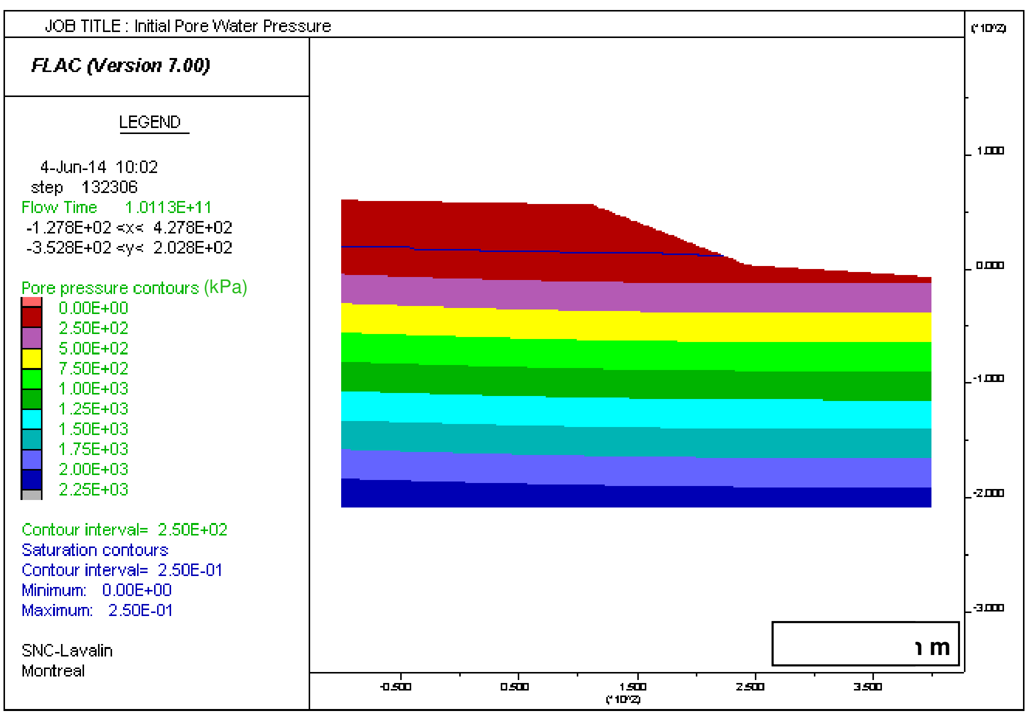

Figure G-4 - Initial Pore Water Pressure

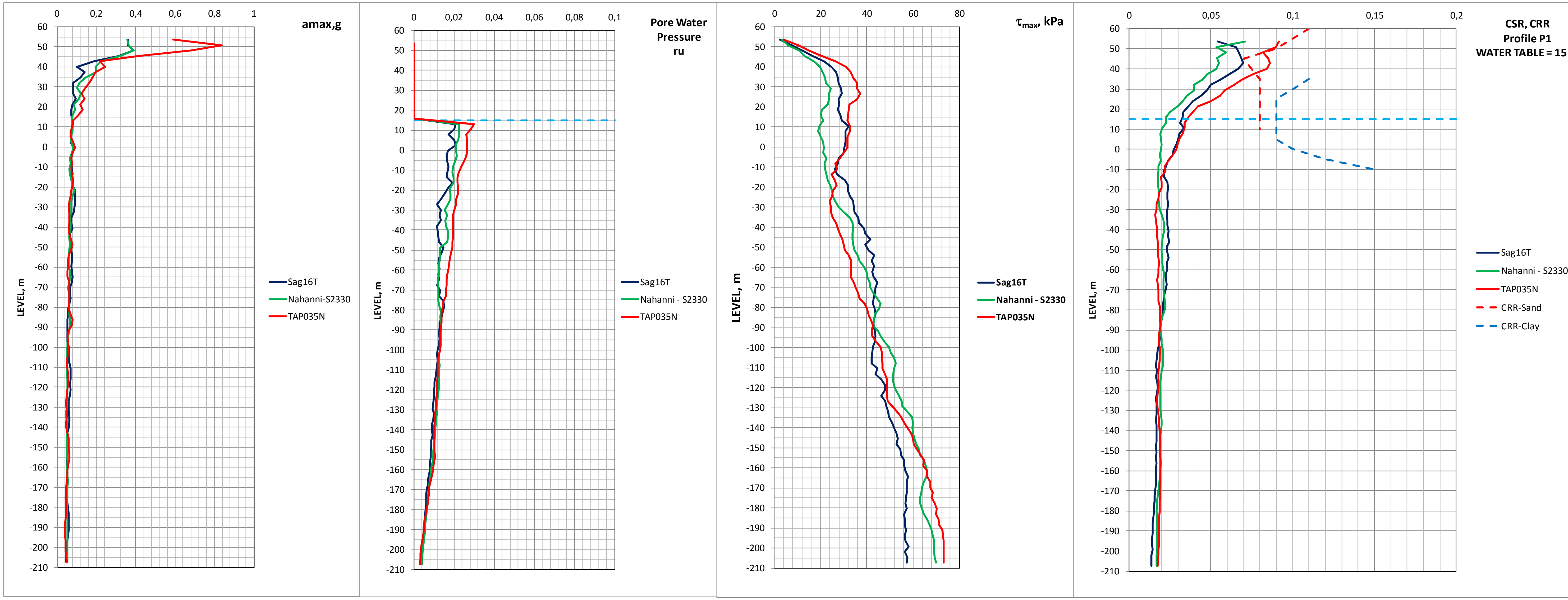

Figure G-5 – FLAC Analyses – Summary for P1 Profile

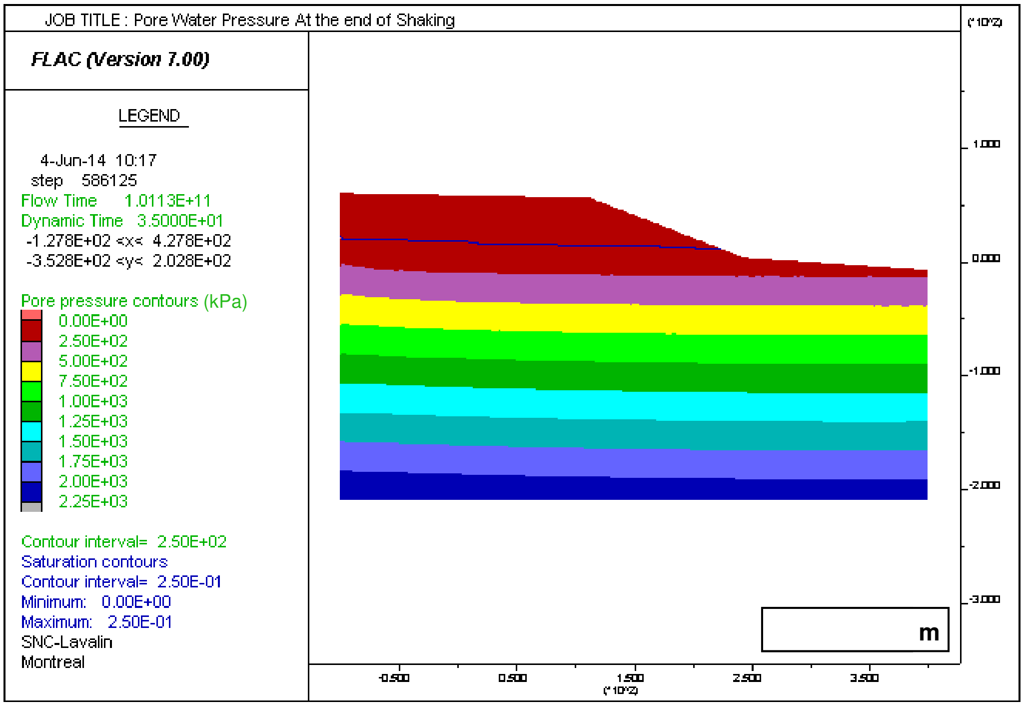

Figure G-6 - Sag16T - Pore Water Pressure at the End of Shaking

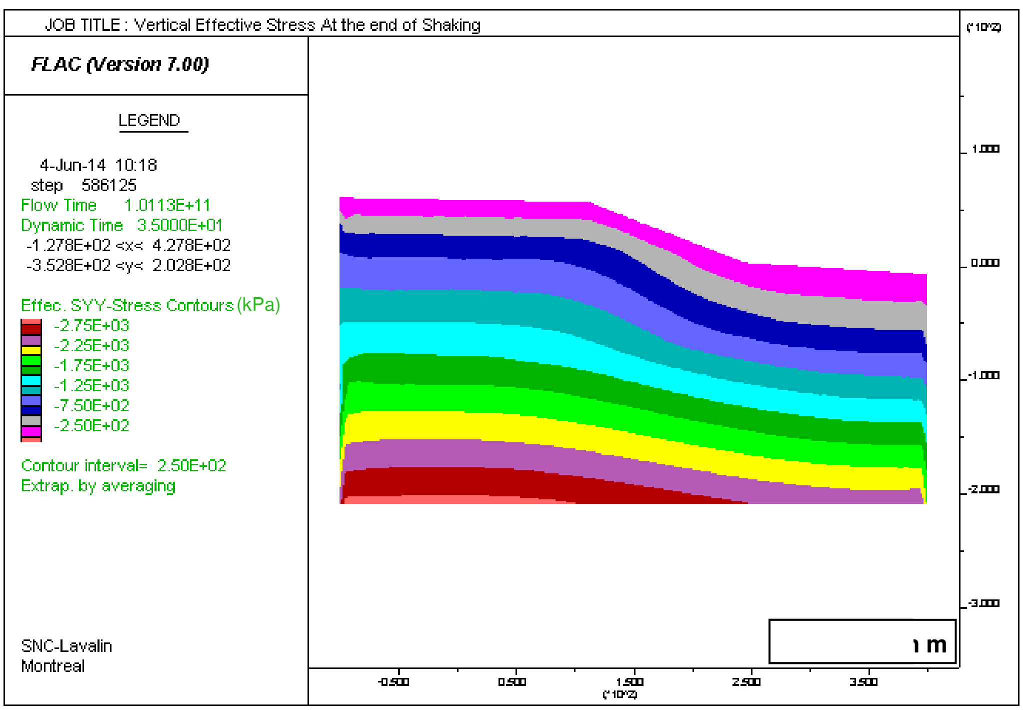

Figure G-7 - Sag16T – Effective Vertical Stress at the End of Shaking

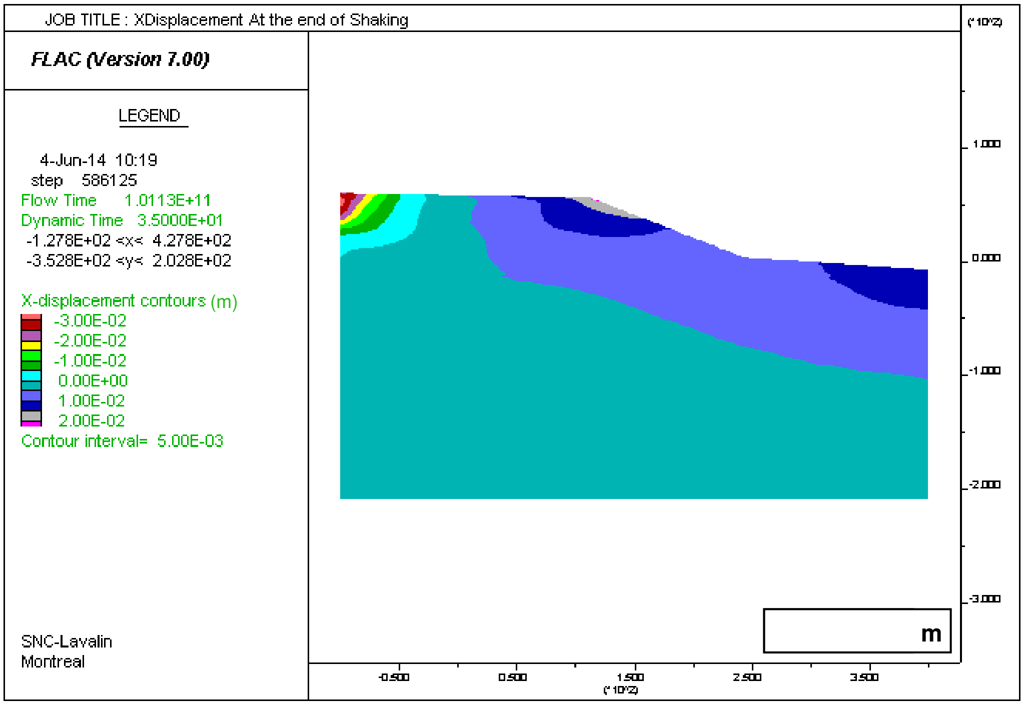

Figure G-8 - Sag16T – X-Displacement at the End of Shaking

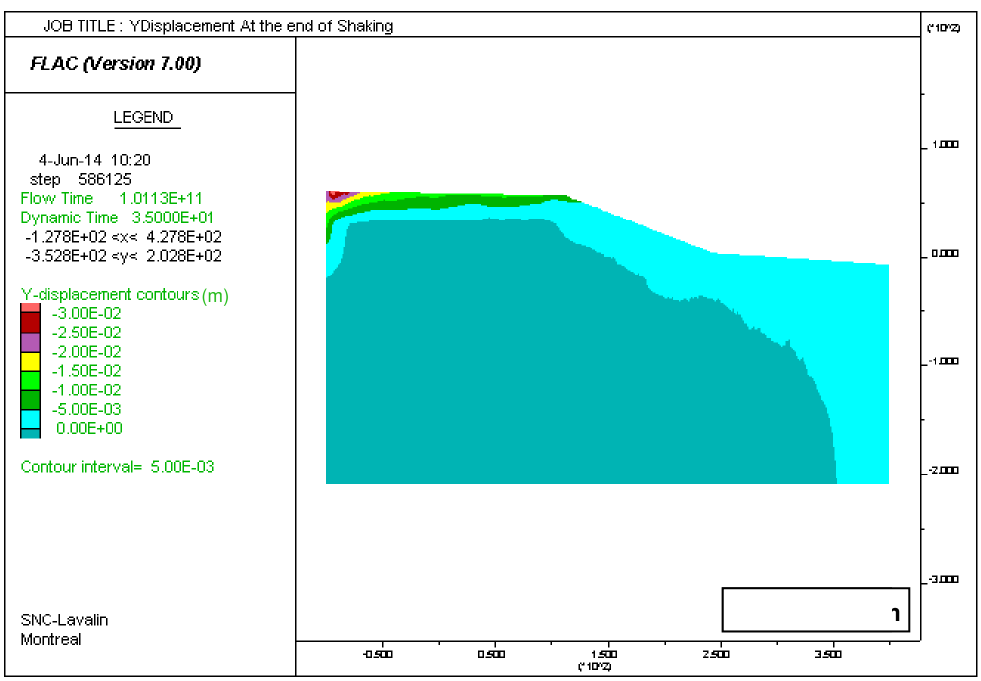

Figure G-9 - Sag16T – Y-Displacement at the End of Shaking

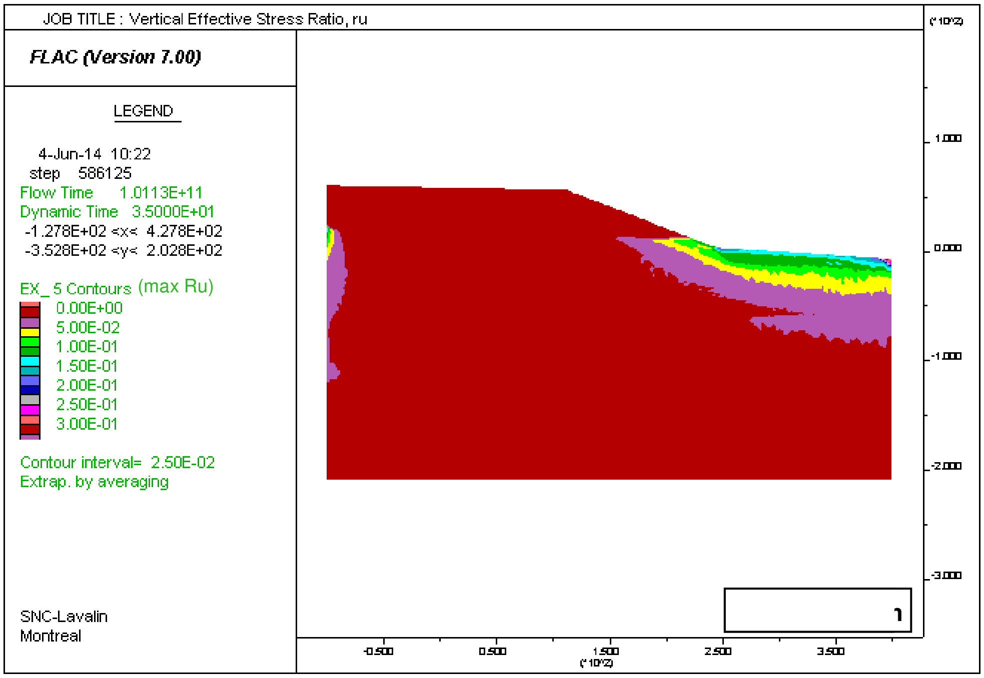

Figure G-10 - Sag16T – Maximum Ru[1] at the End of Shaking

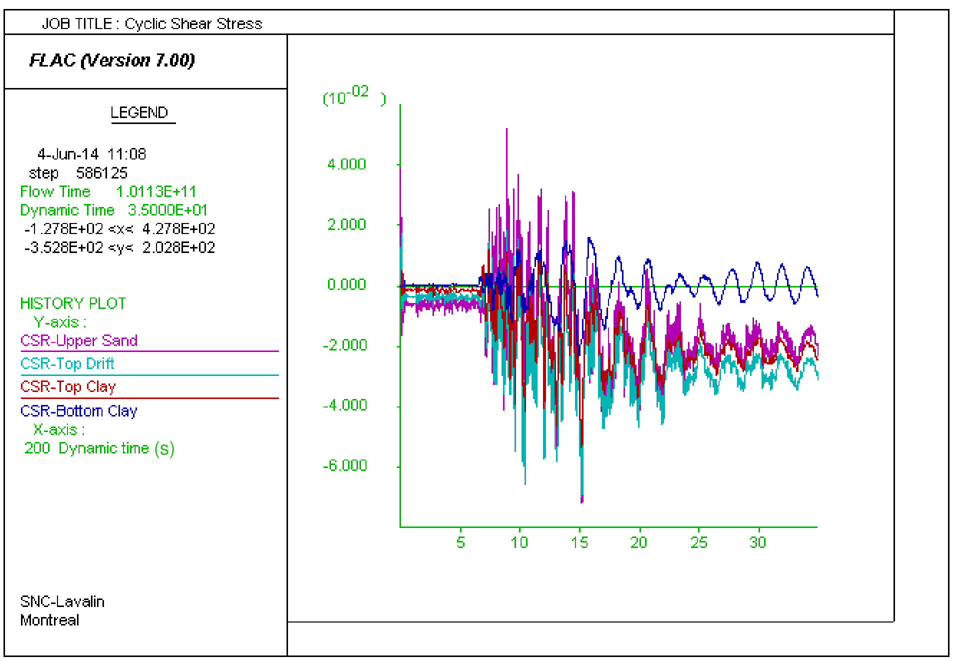

Figure G-11 - Sag16T – Cyclic Shear Stress (CSR) during Shaking at A, B, C and D

[1] $r_u = {\Delta\sigma'_{vo}}/{\sigma'_{vo}}$

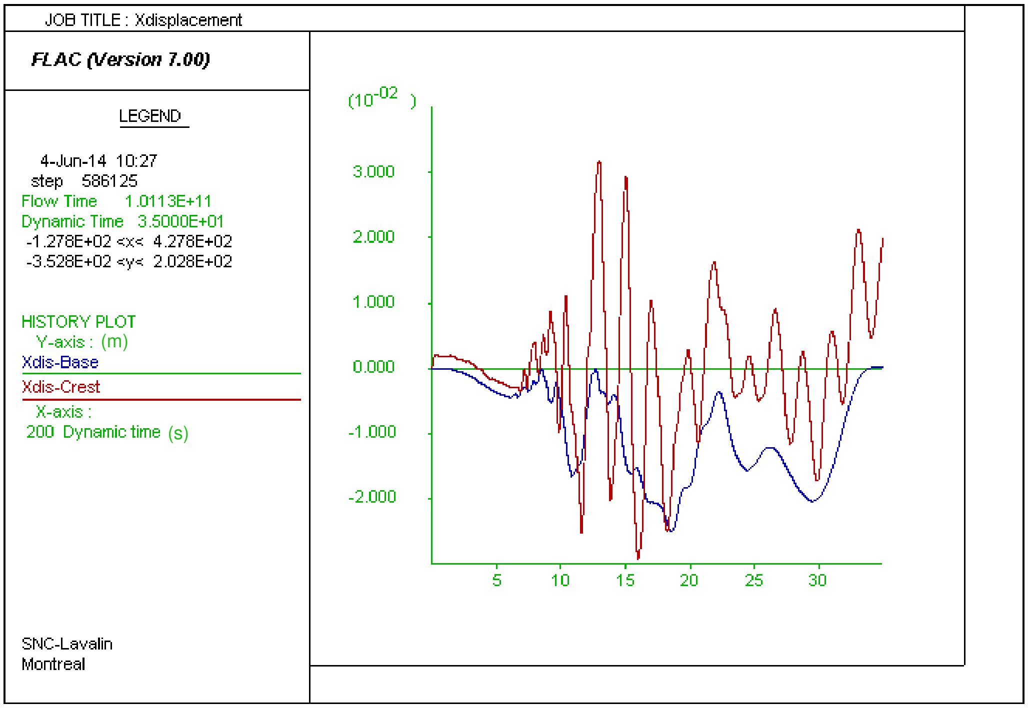

Figure G-12 - Sag16T – X-Displacement at Base and Crest during Shaking

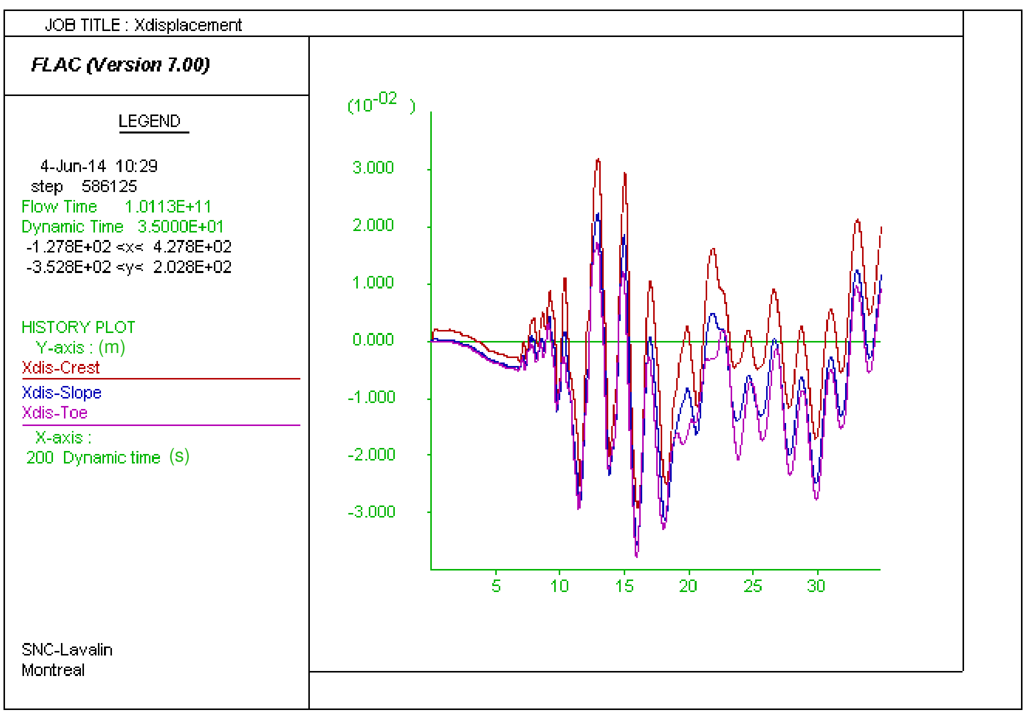

Figure G-13 - Sag16T – X-Displacement at Crest, Slope and Toe during Shaking

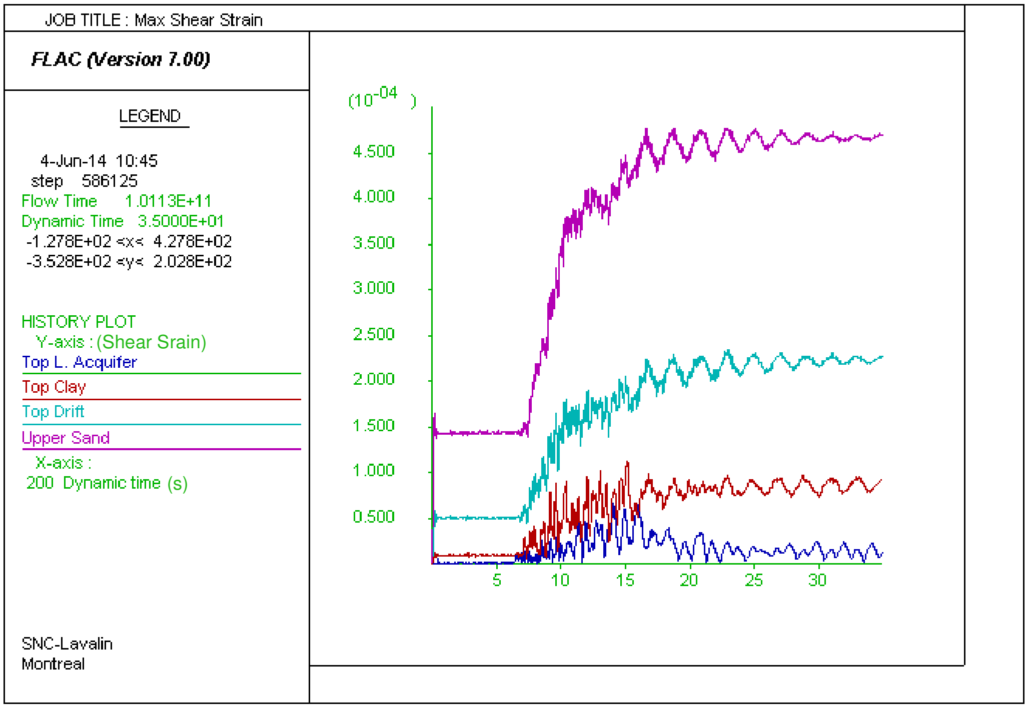

Figure G-14 - Sag16T – Shear Strain during Shaking at A, B, C and E

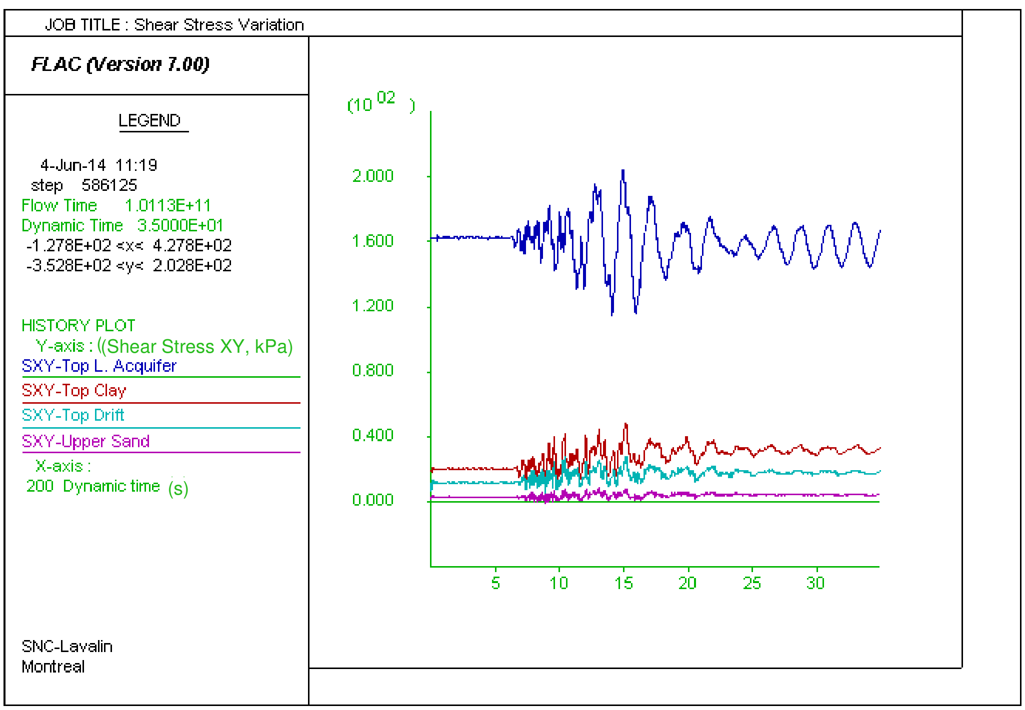

Figure G-15 - Sag16T –Shear Stress during Shaking at A, B, C and E

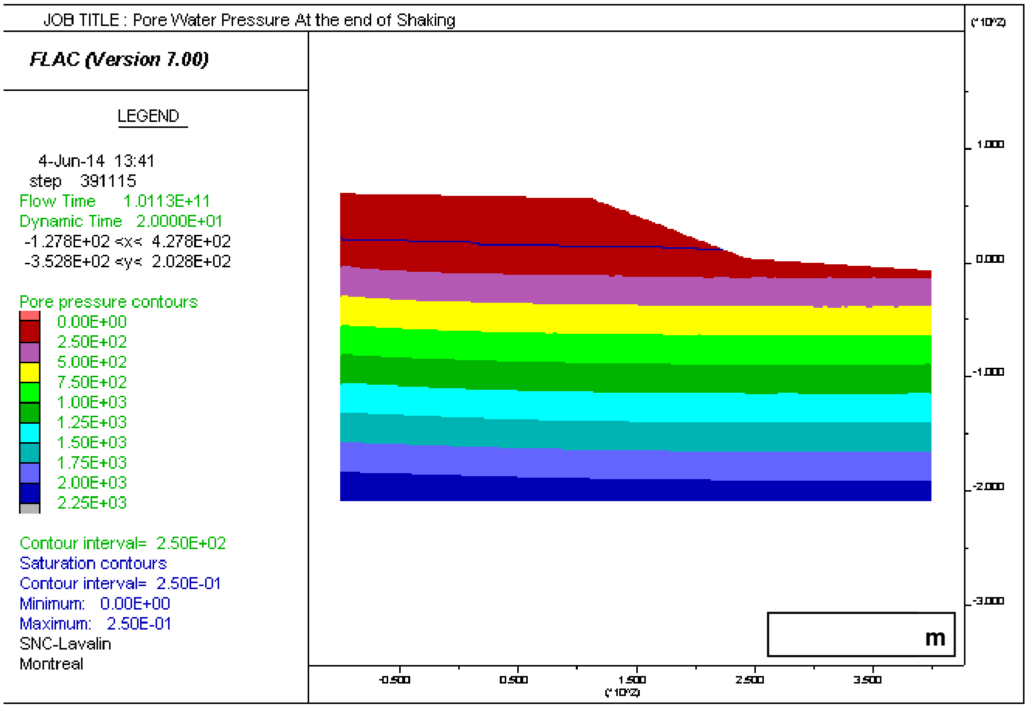

Figure G-16 - Nahanni-S2330 - Pore Water Pressure at the End of Shaking

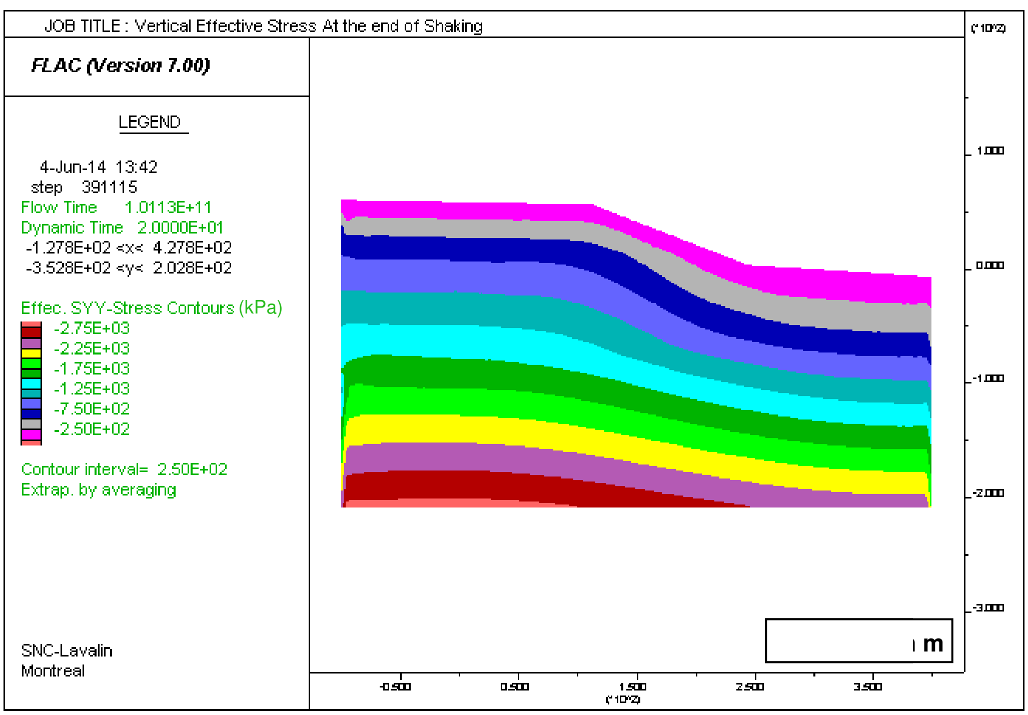

Figure G-17 - Nahanni-S2330 – Effective Vertical Stress at the End of Shaking

SNC·LAVALIN	NORTH SPUR STABILIZATION WORKS – DYNAMIC ANALYSIS STUDY – PHASE 2	Revision		Page
	Nalcor Doc. No. MFA-SN-CD-2800-GT-RP-0007-01	B2	Date	
	SLI Doc. No. 505573-3281-4GER-0005	01	08-Dec-2015	G-13

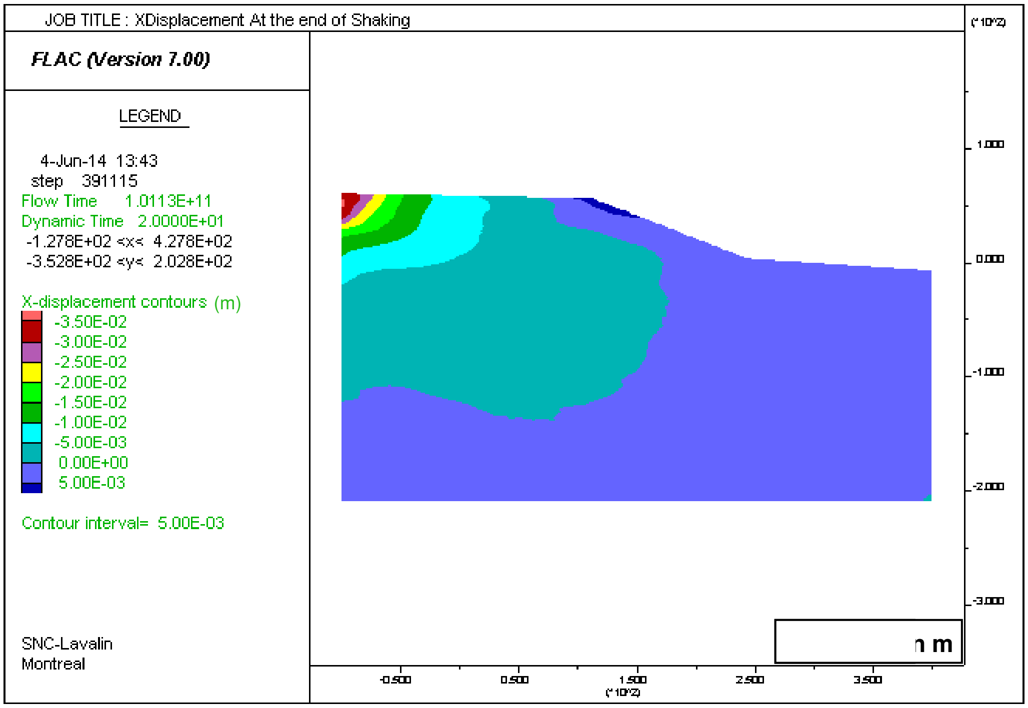

Figure G-18 - Nahanni-S2330 – X-Displacement at the End of Shaking

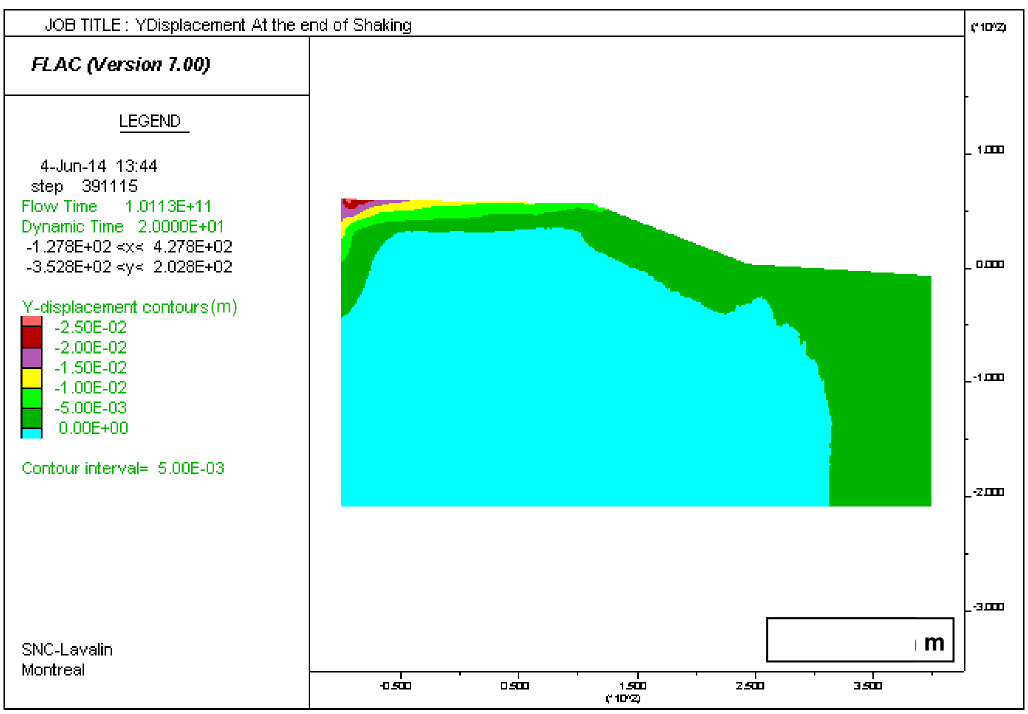

Figure G-19 - Nahanni-S2330 – Y-Displacement at the End of Shaking

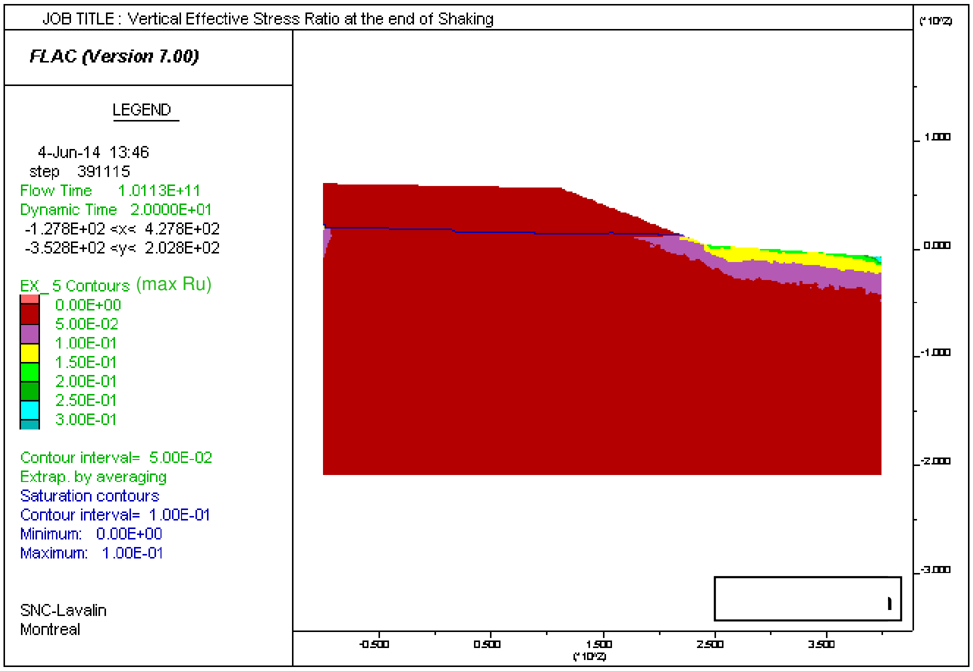

Figure G-20 - Nahanni-S2330 – Maximum Ru[2] at the End of Shaking

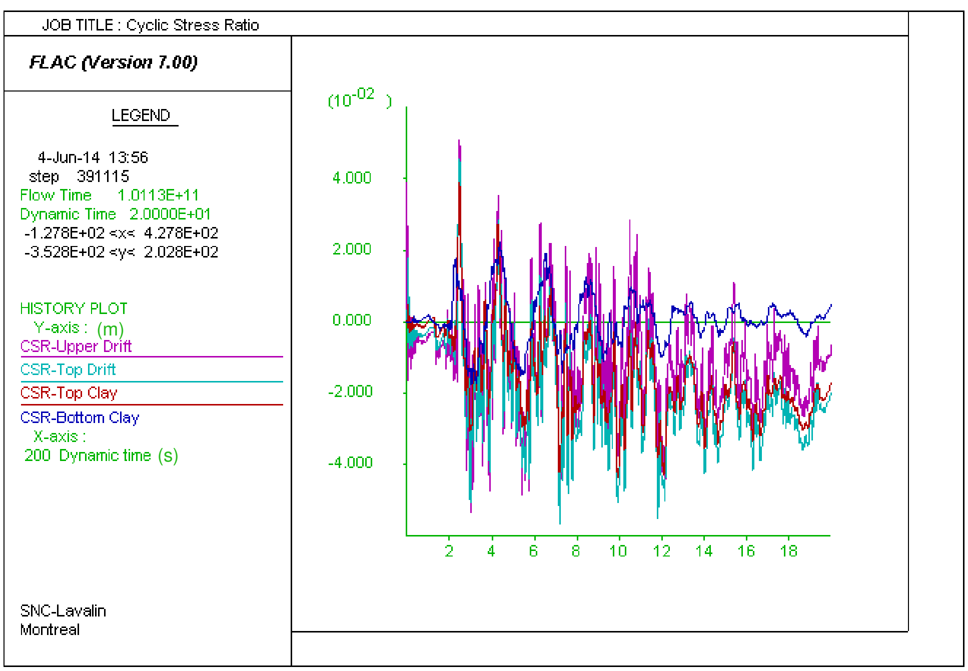

Figure G-21 - Nahanni-S2330 – Cyclic Shear Stress (CSR) during Shaking at A, B, C and D

$^2\ r_u = \Delta\sigma'_{vo}/\sigma'_{vo}$

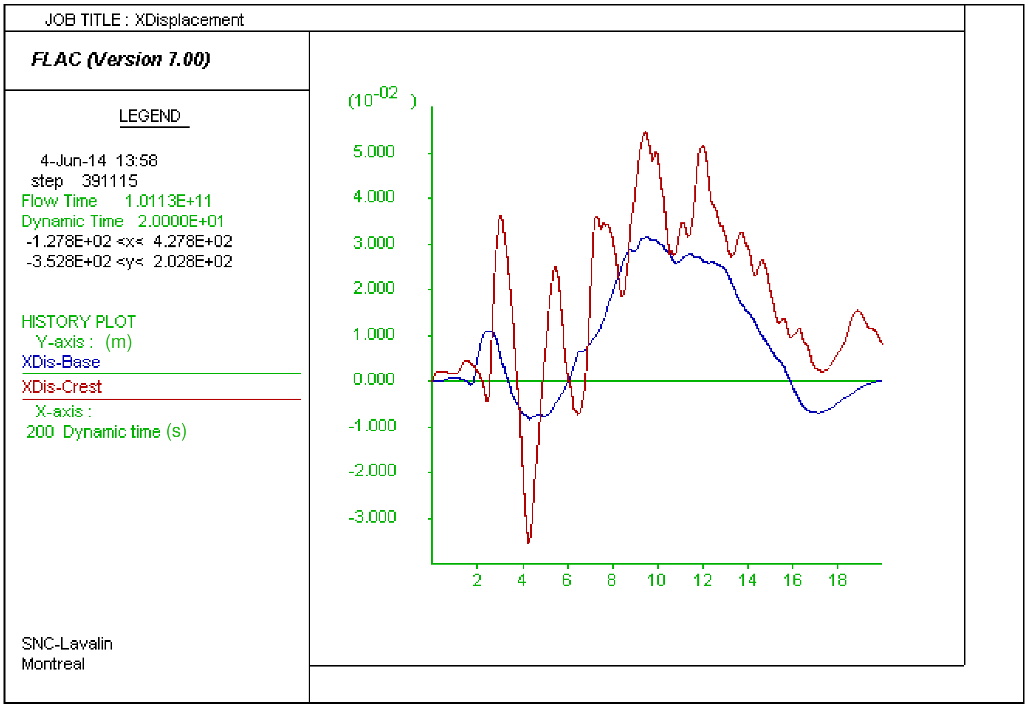

Figure G-22 - Nahanni-S2330 – X-Displacement at Base and Crest during Shaking

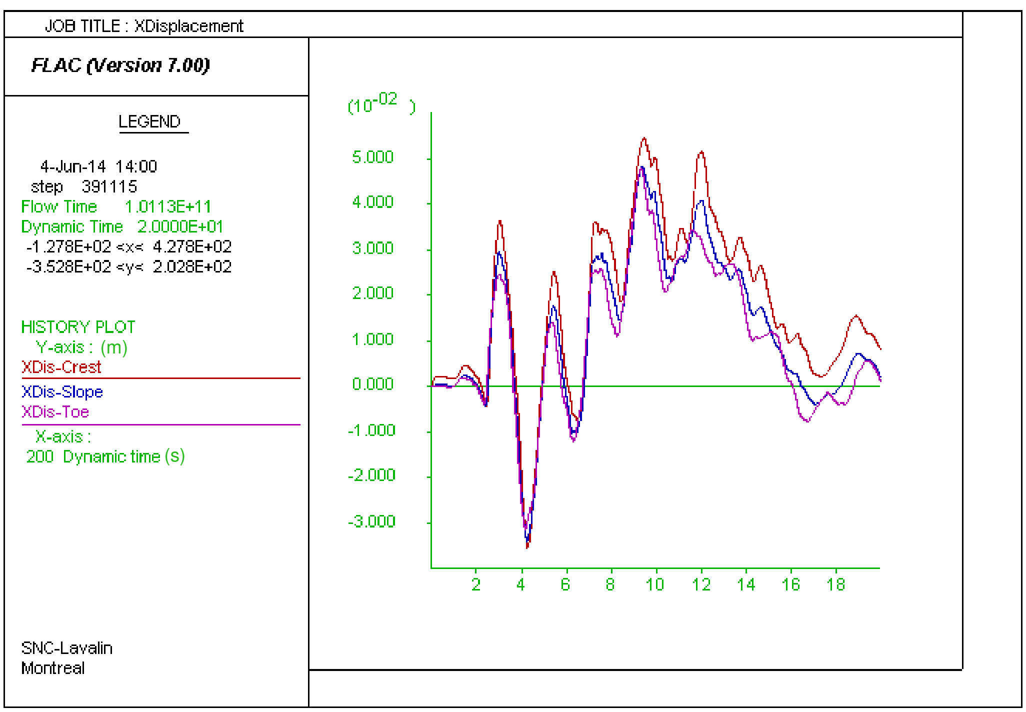

Figure G-23 - Nahanni-S2330 – X-Displacement at Crest, Slope and Toe during Shaking

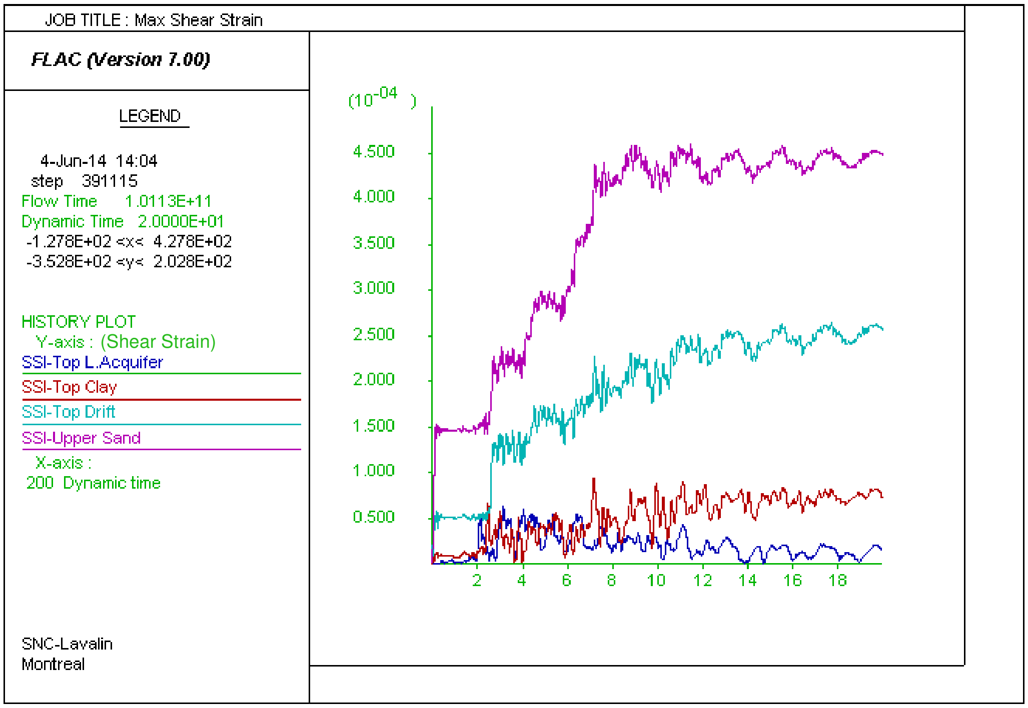

Figure G-24 - Nahanni-S2330 – Shear Strain during Shaking at A, B, C and E

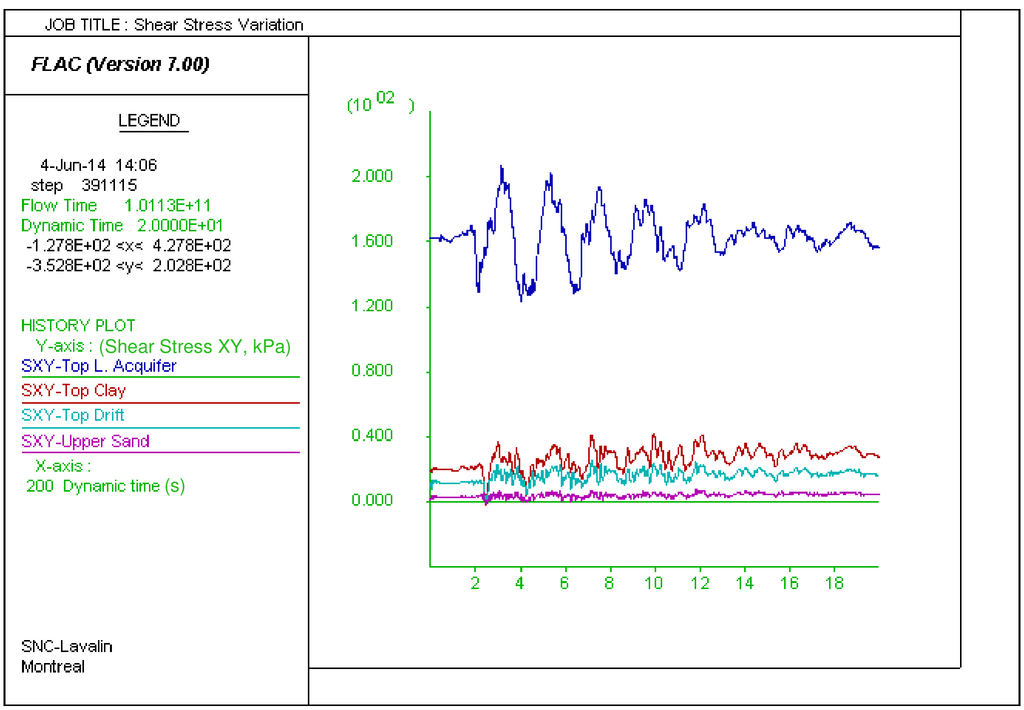

Figure G-25 - Nahanni-S2330 –Shear Stress during Shaking at A, B, C and E

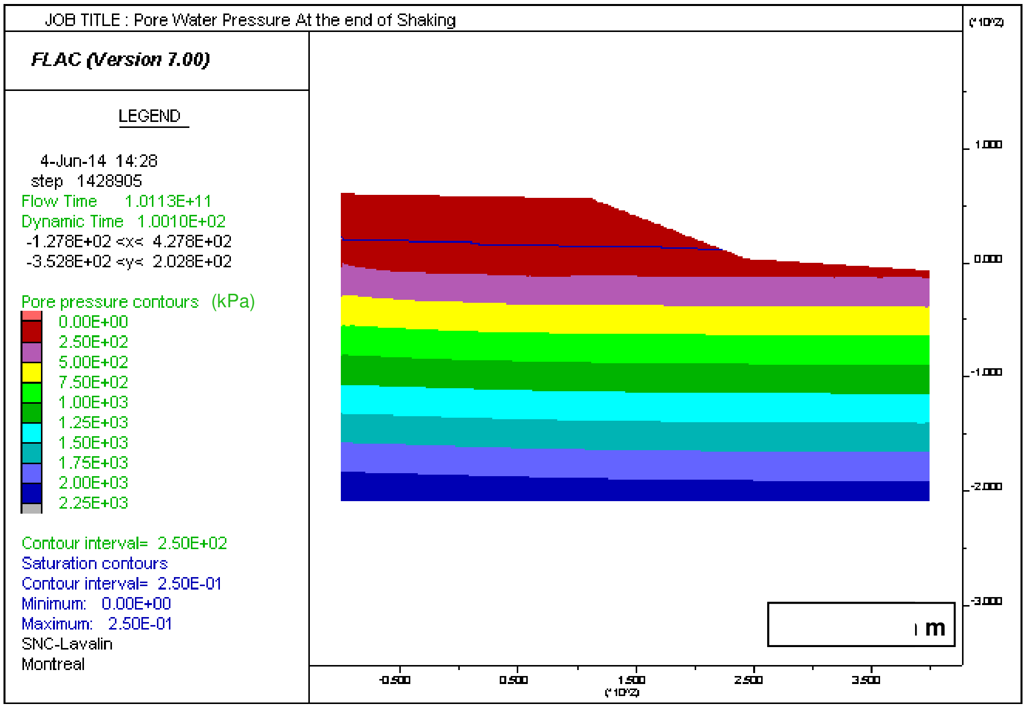

Figure G-26 - TAP035-N - Pore Water Pressure at the End of Shaking

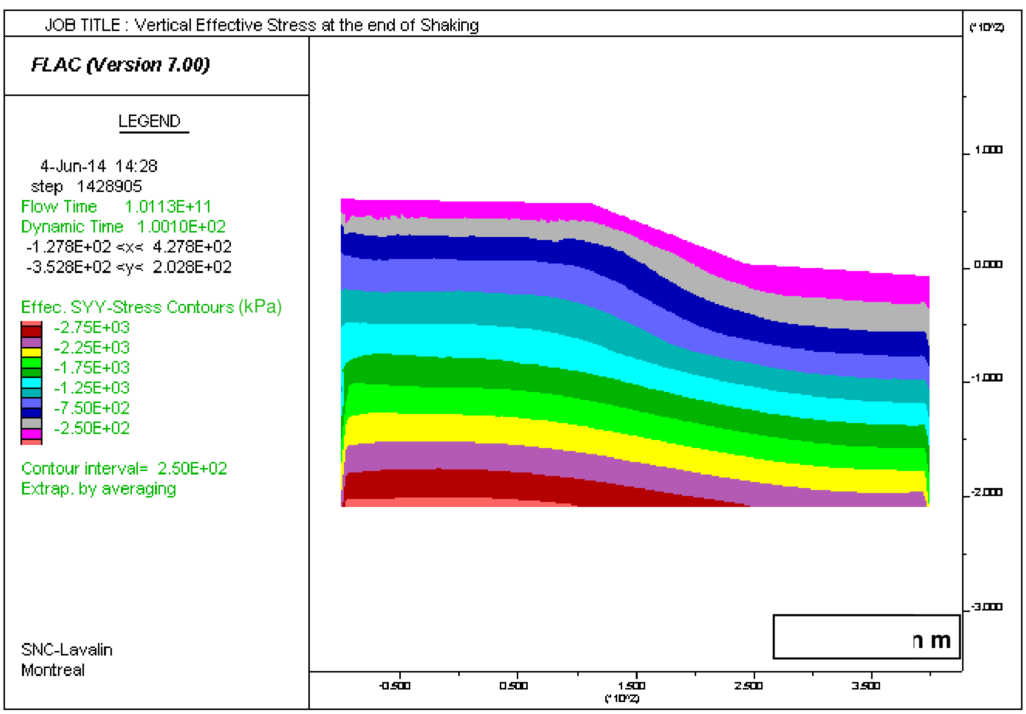

Figure G-27 - TAP035-N – Effective Vertical Stress at the End of Shaking

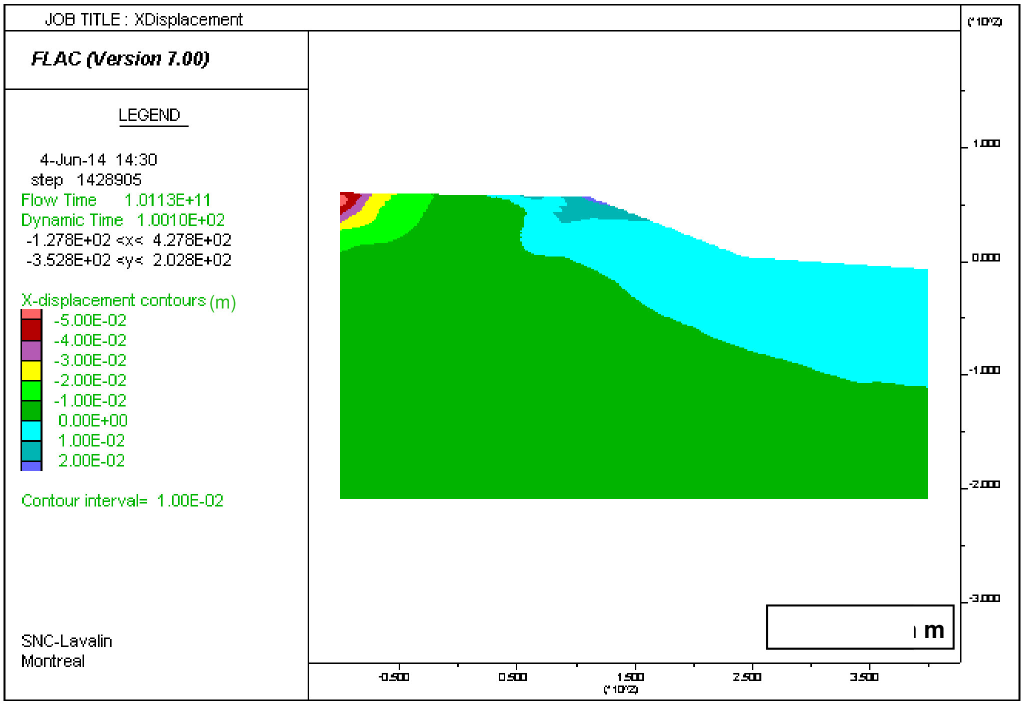

Figure G-28 - TAP035-N – X-Displacement at the End of Shaking

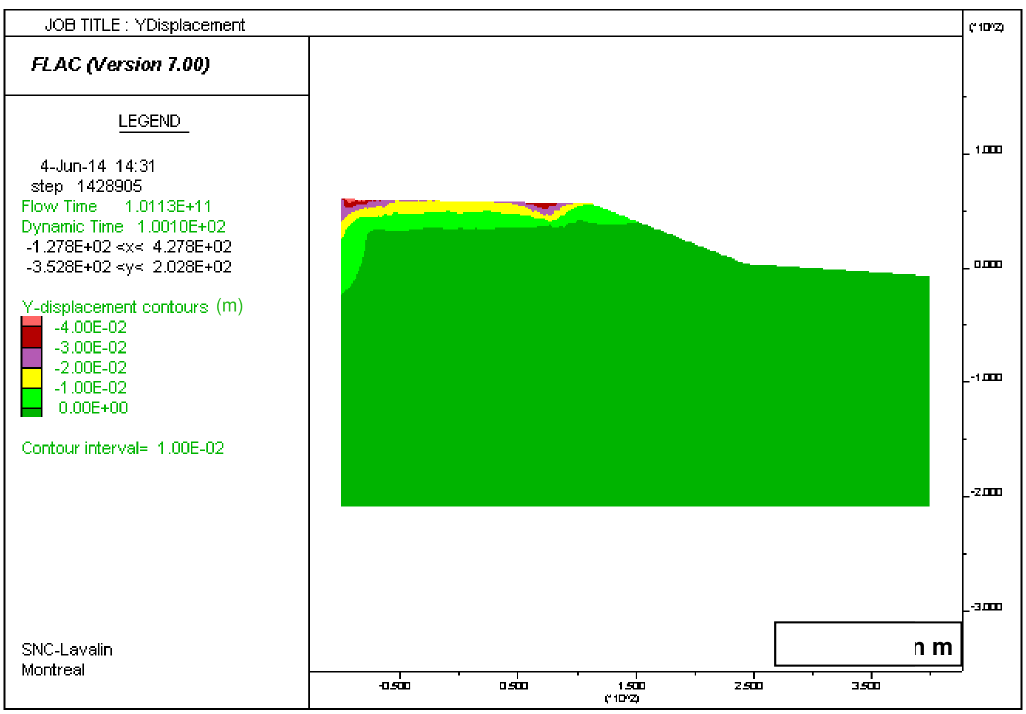

Figure G-29 - TAP035-N – Y-Displacement at the End of Shaking

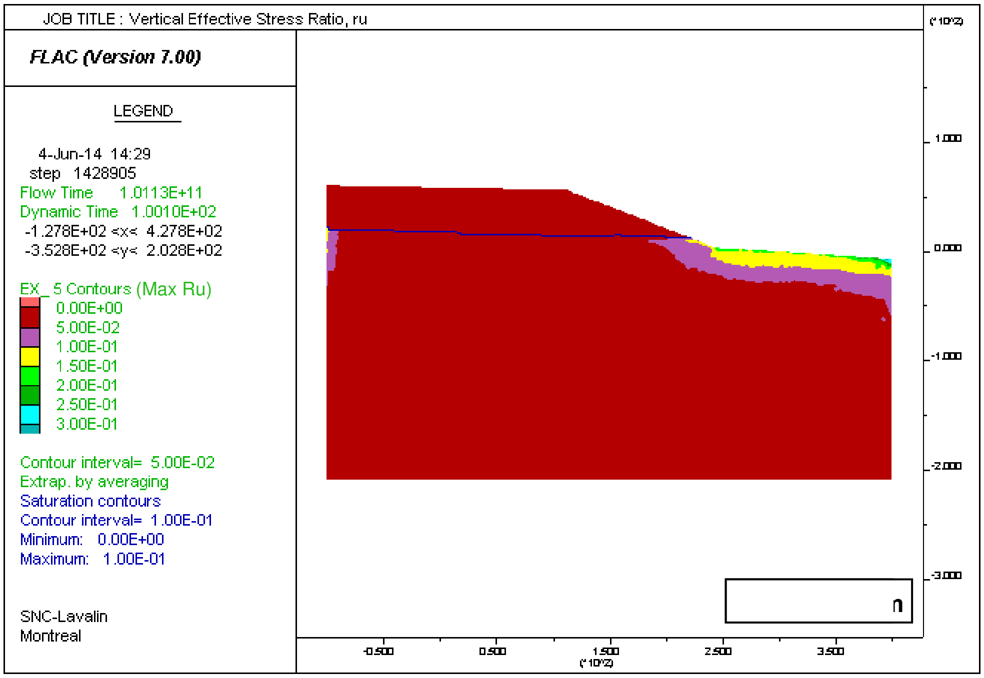

Figure G-30 - TAP035-N – Maximum Ru[3] at the End of Shaking

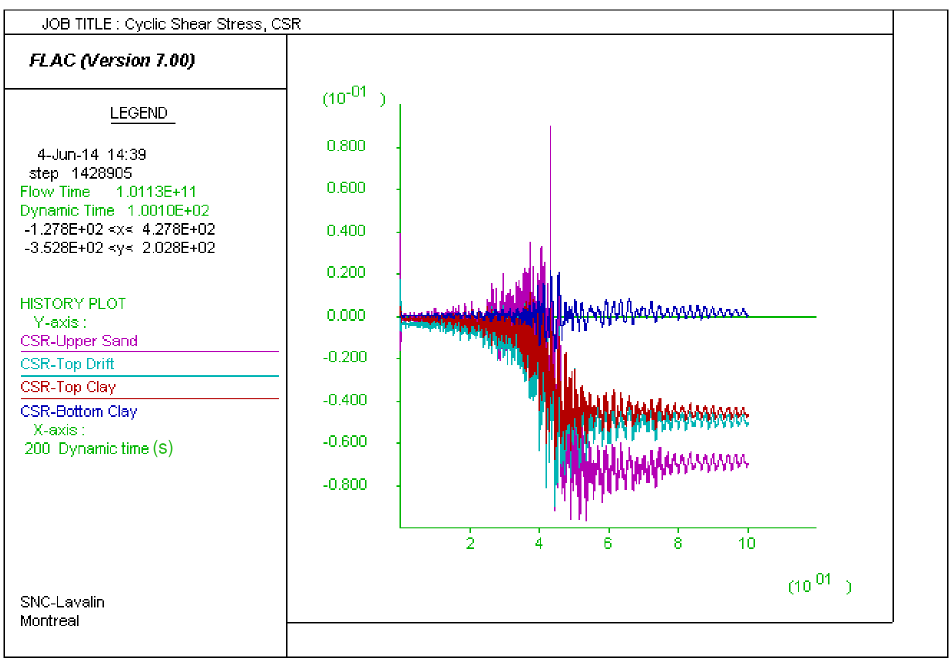

Figure G-31 - TAP035-N – Cyclic Shear Stress (CSR) during Shaking at A, B, C and D

3 $r_u = \Delta\sigma'_{vo} / \sigma'_{vo}$

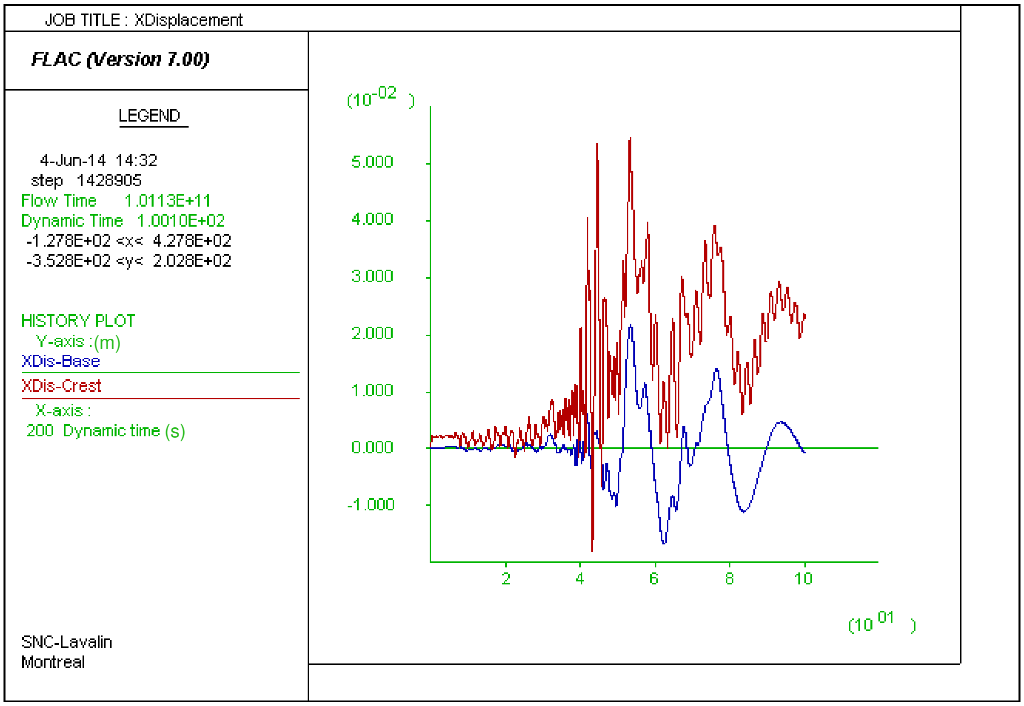

Figure G-32 - TAP035-N – X-Displacement at Base and Crest during Shaking

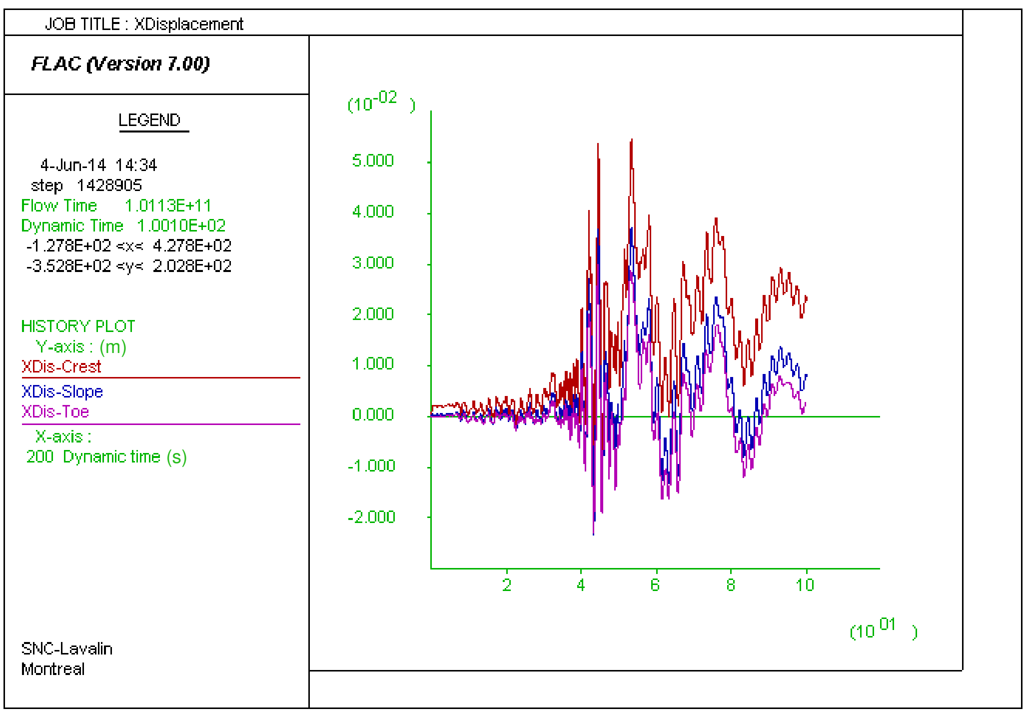

Figure G-33 - TAP035-N – X-Displacement at Crest, Slope and Toe during Shaking

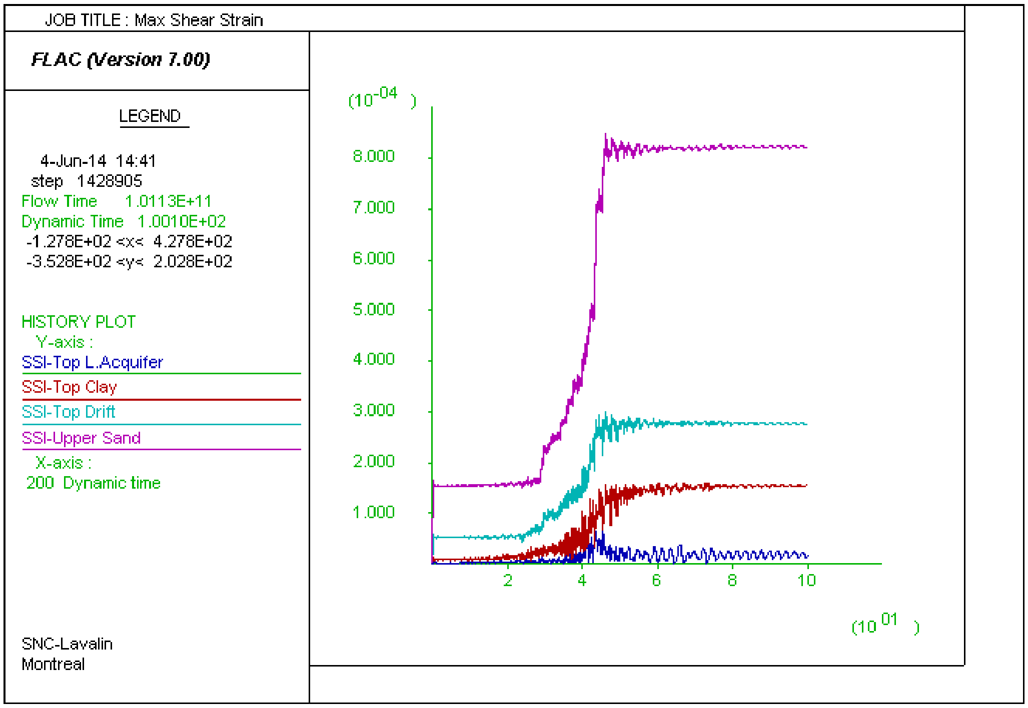

Figure G-34 - TAP035-N – Shear Strain during Shaking at A, B, C and E

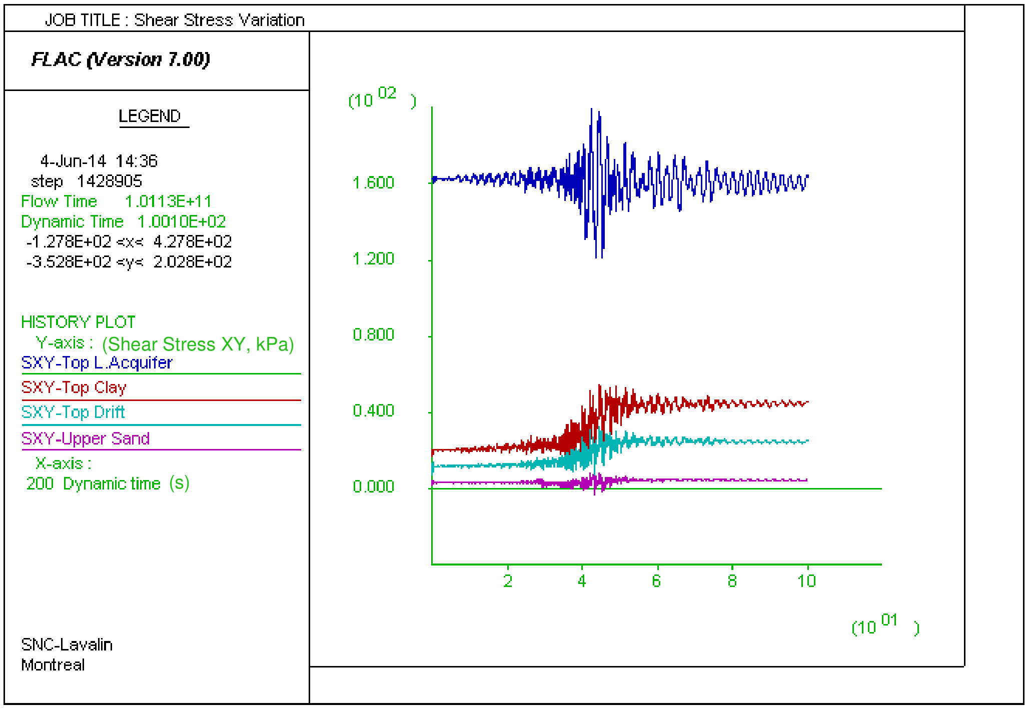

Figure G-35 - TAP035-N –Shear Stress during Shaking at A, B, C and E

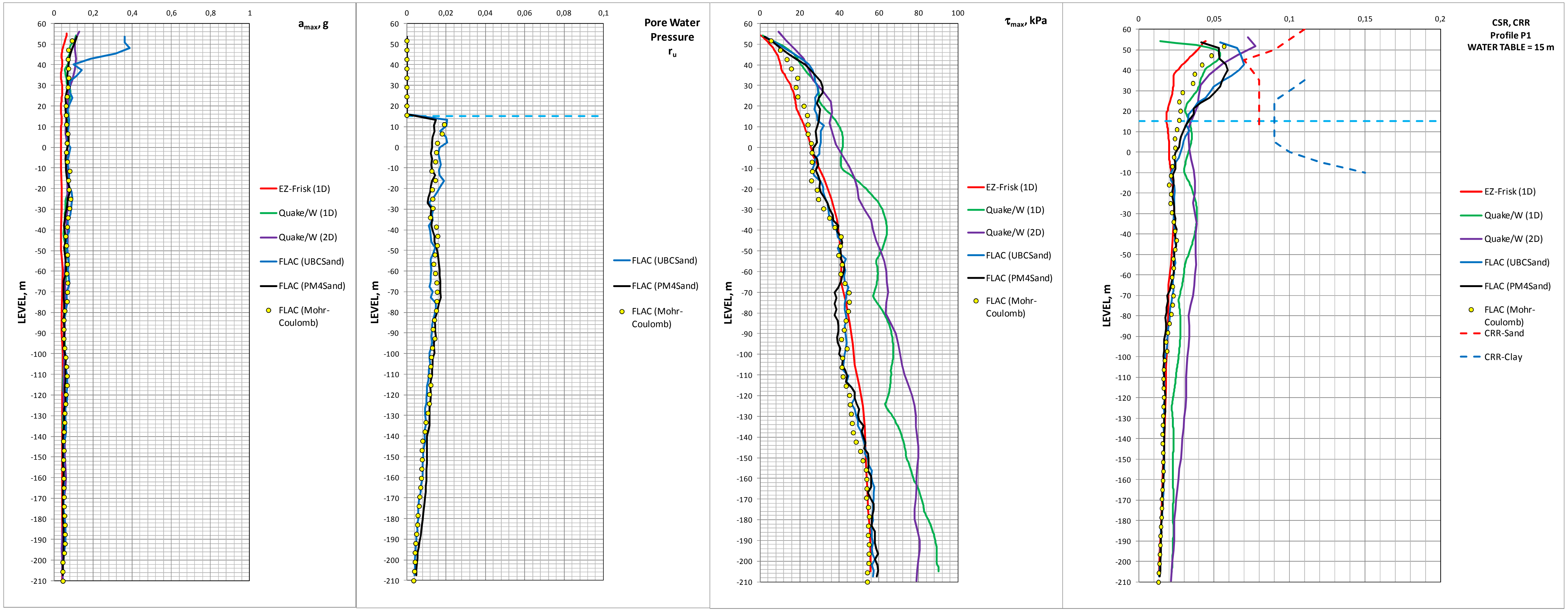

Figure G-36 – 1D and 2D Analyses for P1 Profile, Water Table at 15 m and Sag-16T Input Motion– Comparison